TUDelft

Delft University of Technology

Poison to Products

On harnessing the power of microorganisms to convert waste streams into new chemicals

Allaart, M.T.

Important note
To cite this publication, please use the final published version (if applicable).
Please check the document version above.

Poison to Products

On harnessing the power of microorganisms to convert waste streams into new chemicals

Maximilienne Toetie Allaart

POISON TO PRODUCTS

ON HARNESSING THE POWER OF MICROORGANISMS TO CONVERT WASTE STREAMS INTO NEW CHEMICALS

Dissertation

for the purpose of obtaining the degree of doctor
at Delft University of Technology
by the authority of the Rector Magnificus, prof. dr. ir. T.H.J.J. van der Hagen,
chair of the Board for Doctorates
to be defended publicly on
Wednesday 25 October 2023 at 15:00 o'clock

by

Maximilienne Toetie ALLAART

Master of Science in Life Science and Technology,
Delft University of Technology, The Netherlands
born in Amsterdam, The Netherlands

This dissertation has been approved by the promotors.

Composition of the doctoral committee:

Rector Magnificus,	chairperson
Dr. ir. R. Kleerebezem,	Delft University of Technology, *promotor*
Prof. dr. D.Z. Sousa,	Wageningen University and Research, *promotor*

Independent members:

Prof. dr. L.T. Angenent	University of Tübingen, Germany
Prof. dr. R. Ganigué	Ghent University, Belgium
Prof. dr. M. Suarez Diez	Wageningen University and Research
Prof. dr. ir. P. Daran-Lapujade	Delft University of Technology
Prof. dr. ir. M. Ottens,	Delft University of Technology, reserve member

Other member:

Dr. ir. M. Diender,	Wageningen University and Research

I write, erase, rewrite
Erase again, and then
A poppy blooms.

Katsushika Hokusai

CONTENTS

SUMMARY

One of the main challenges society currently deals with is the depletion of fossil fuels. To navigate this issue, we must embrace the concept of circularity and turn waste into a resource. Waste streams are omnifarious and their conversion into new chemical building blocks is not always trivial. Luckily, we can take a look at nature's problem solving skills to help us out. Because nature, in due time, always finds a solution and there is a (micro)organism for everything.

But.. we can also give nature a hand by simplifying the problem. The diversity and complexity of waste streams can be reduced by using gasification, where the waste is combusted at a high temperature with small amounts of oxygen. This yields syngas, a mixture consisting of mainly carbon monoxide, carbon dioxide and hydrogen gas. Syngas can be converted chemically into i.e. ethanol, but the success of this process highly depends on the ratios of CO, CO_2 and H_2 and the absence of impurities in the gas. Microorganisms can deal with much more variability, making them a promising biocatalyst for the conversion of syngas to chemical building blocks. Yet, we have to understand the microorganisms to be able to work together with them in combatting climate change.

The work in this thesis is aimed at increasing our understanding of two specific types of microorganisms that can help us to turn waste into new chemicals: syngas fermenting bacteria and chain elongating bacteria. Together, they can form a team that turns a C_1 molecule (carbon monoxide) all the way into a C_6 molecule (hexanoate). To make the team as effective as possible, we studied both team members in detail. The syngas fermenting bacterium we studied goes by the name *Clostridium autoethanogenum*, and is already being used at industrial scale by the company LanzaTech. For its chain-elongating counterpart, however, we used a mixed community of microorganisms that was specifically selected to perform chain elongation. We used this mixed community because the single, optimal partner for *C. autoethanogenum* has yet to be found.

It has been established previously, by other researchers, that producing a lot of hexanoate is easiest when you feed chain elongating organisms a substrate with a *high* ethanol-to-acetate ratio. *C. autoethanogenum* naturally produces ethanol and acetate, but usually in a *low* ethanol-to-acetate ratio. In **Chapter 2** we use a theoretical framework based on thermodynamics, as well as data from literature to understand what triggers *C. autoethanogenum* to make ethanol. We found that acetate conversion into ethanol is a stress response used to deal with a (too) high load of CO, which can be classified as overflow metabolism. We show that this behavior not only takes place when feeding CO alone, but also in the presence of both CO and H_2, underlining its relevance in syngas fermentation processes. The stress response can be induced by tuning the operational parameters of the bioreactor, such as the CO supply rate or the growth rate.

In **Chapter 3** we quantify this effect in the laboratory ourselves. We use a steady-state culture of *C. autoethanogenum* in a chemostat bioreactor and repeatedly disturb it for

periods of one hour with increasing amounts of CO in the inlet gas, up to a CO partial pressure of 1.2 atm. We see that ethanol production increases with increasing CO partial pressures, and at a p_{CO} of 0.6 atm or higher external acetate is even consumed to sustain higher ethanol production rates. This proves that the product spectrum of syngas fermentation can be directed by changing the operational conditions. Furthemore, the experimental method that we used allowed for the identification of the CO uptake rate at each CO partial pressure, directly via the off-gas measurements. We observed biomass-specific CO uptake rates of up to -119 ± 1 mmol$\cdot g_x^{-1} \cdot h^{-1}$, which is much higher than has previously been reported for this organism. The biomass-specific uptake rate is instrumental for obtaining an accurate mathematical description (or: kinetic model) of this microorganism, which in turn allows for more accurate bioprocess design.

Chapter 4 focusses on the chain-elongating counterpart of our syngas fermenter. *C. autoethanogenum* prefers to grow at a pH of 5 –5.5, and most chain elongators that have been described in literature rather grow at neutral pH ($\pm$ 7.0). This chapter revolves around this discrepancy. By using enrichment cultures in a sequencing batch bioreactor, we select for chain elongating microorganisms both at pH 7.0 and pH 5.5. In doing so, we establish that chain elongators can live at pH 5.5 and that a very comparable microbial community (on genus-level) develops at both pH. However, the behavior in the bioreactors was not the same. At lower pH, a significantly smaller fraction of the supplied ethanol was converted to hexanoate. Instead, more of the C_4 molecule butyrate was produced, likely because it is less toxic to the microorganisms than hexanoate. This means that pH is an important parameter to control the product spectrum of chain elongation and that establishing an effective microbial team for C_1-to-C_6 conversion likely requires more than finding microbes with the same preferred pH.

In **Chapter 5** we delve into the biochemistry of chain elongating microbes. They are known to be very flexible in their metabolism, and they can deal with a wide range of ethanol-to-acetate ratios. Theoretically, this ratio could even be infinite (i.e. feeding only ethanol), which would lead to the production of only hexanoate and no butyrate. We call this ethanol-only chain elongation. This is interesting from a fundamental as well as a process design perspective. Therefore, we test whether it is also possible in practice by using well-monitored batch experiments in bioreactors. We use different initial conditions: only ethanol, ethanol and a small amount of acetate and ethanol and a small amount of butyrate. We observe in the bioreactors that ethanol-only chain elongation is possible, but that it proceeds very slowly. Beside that, the microorganisms prefer the presence of either acetate or butyrate so much that they eventually start producing these compounds from ethanol themselves when they are not available. This behavior has never been observed before, nor was it regarded as possible.

In **Chapter 6** we present a dataset of well-controlled bioreactor experiments in 9 different initial conditions, including the experiments described in the previous chapter. This dataset can be used to refine the current mathematical description of chain elongating microbes. We describe the initial analysis of this dataset and how we assure its quality and usability for kinetic modelling using data reconciliation. With this reconciled dataset we test the accuracy of the currently available kinetic model. From this over-all analysis we set out the next steps for the formulation of a more accurate kinetic model of chain elongating microbes in the future.

Chapter 7 recapitulates the significant findings from this thesis, but more importantly provides a list of questions that still remain to be answered. These questions are grouped around three different themes to provide some structure: the inner world of microorganisms, the interactions between (communities of different) microorganisms and the design of efficient (new) bioprocesses for a more sustainable world. To conclude, I reflect on the societal role of a scientist.

SAMENVATTING

Een van de grootste maatschappelijke problemen op dit moment is dat fossiele brandstoffen niet onuitputtelijk beschikbaar zijn. Een circulaire economie biedt uitkomst voor dit probleem en vereist dat afvalstromen als grondstof worden gebruikt voor het maken van nieuwe producten en chemicaliën. Afvalstromen zijn echter vaak heterogeen en hun compositie is niet constant, waardoor hun conversie in nieuwe producten niet altijd triviaal is. Gelukkig kunnen we afkijken bij de natuur en haar manieren om complexe problemen op te lossen. Want de natuur vindt, met een beetje tijd, altijd een oplossing omdat er overal een (micro-)organisme voor bestaat!

We kunnen de natuur natuurlijk ook een handje helpen door het probleem wat te versimpelen. De diversiteit en complexiteit van afvalstromen kan gereduceerd worden met behulp van vergassing, waar het afval verbrand wordt met een kleine hoeveelheid zuurstof. Dit levert syngas op, een mix van grotendeels koolmonoxide, kooldioxide en waterstofgas. Syngas kan chemisch worden omgezet in bijvoorbeeld ethanol, maar de efficiëntie van die omzetting hangt sterk af van de ratio tussen CO, CO_2 en H_2 en de afwezigheid van andere moleculen in de syngasstroom. Micro-organismen zijn beter opgewassen tegen variabiliteit, waardoor ze een veelbelovende biocatalyst zijn voor het omzetten van syngas in nieuwe chemische bouwstenen. We moeten de microorganismen die hiertoe in staat zijn echter nog wel een stuk beter begrijpen voordat we met ze kunnen samenwerken tegen klimaatverandering.

Dit proefschrift is gericht op het uitbreiden van ons begrip van twee soorten microorganismen die ons kunnen helpen met het omzetten van afval in nieuwe chemicaliën: syngas fermenterende bacteriën en ketenverlengende bacteriën. Samen vormen zij een microbieel team dat C_1 moleculen (koolmonoxide) helemaal op kan bouwen tot C_6 moleculen (hexanoaat). Om dit team zo goed mogelijk te kunnen laten werken, hebben we eerst de twee individuele teamleden goed bestudeerd. De syngas-fermenterende bacterie die we hier bestuderen heet *Clostridium autoethanogenum* en wordt nu al gebruikt in industriële bioreactoren door het bedrijf LanzaTech. Om het ketenverlengende teamlid te bestuderen, gebruiken wij echter een mengcultuur van micro-organismen die we hier uitgeselecteerd hebben. We hebben deze mengcultuur gebruikt omdat de beste individuele partner voor *C. autoethanogenum* nog gevonden moet worden – wij proberen een stapje in de juiste richting te zetten.

Andere onderzoekers hebben laten zien dat het maken van veel hexanoaat het makkelijkst gaat als je ketenverlengers voert met een mengsel van veel ethanol en een beetje azijnzuur (een *hoge* ethanol:azijnzuur-verhouding). *C. autoethanogenum* produceert zowel ethanol als azijnzuur, maar normaliter met een *lage* ethanol:azijnzuur-verhouding. In **hoofdstuk 2** gebruiken wij theoretische kennis over de thermodynamica en data uit de reeds gepubliceerde literatuur om te begrijpen wanneer *C. autoethanogenum* veel ethanol maakt. We hebben gevonden dat azijnzuur kan worden omgezet in ethanol, en dat

dit een stressrespons is die door de microben gebruikt wordt om met een (te) hoge CO toevoer om te gaan. Dit gedrag hebben wij geclassificeerd als overflow metabolisme, een fenomeen wat in veel andere celtypen ook wordt waargenomen in stressvolle condities. We laten zien dat dit gedrag niet uniek is voor systemen waar alleen CO wordt gevoerd, maar dat het ook gebeurt wanneer er zowel CO als H_2 wordt gevoerd. Dit bevestigt dat deze stressrespons belangrijk is tijdens syngasfermentatie, en zelfs dat ze getriggerd kan worden door de condities in de bioreactor aan te passen, zoals de gascompositie en -voersnelheid of de groeisnelheid.

In **hoofdstuk 3** kwantificeren we het overflowgedrag in onze eigen bioreactor in het lab. We gebruiken een steady-state cultuur van *C. autoethanogenum* in een chemostaat-reactor die we steeds voor een periode van één uur verstoren met een toenemende hoeveelheid CO in de ingaande gasstroom, tot aan een CO partieeldruk van 1.2 atm. We zien dat de ethanolproductie toeneemt met toenemende CO-spanning, en dat bij p_{CO}'s van 0.6 atm en hoger azijnzuur wat aanwezig is in de vloeistof wordt omgezet naar ethanol. Dit bewijst dat het productspectrum van syngasfermentatie gestuurd kan worden door de operationele condities van de bioreactor te veranderen. Verder maakte de gebruikte experimentele methode het mogelijk om direct uit de gasmetingen de snelheid waarmee de micro-organismen CO consumeren af te leiden. We observeerden biomassa-specifieke CO opnamesnelheden tot -119 ± 1 mmol·g_x^{-1}·h^{-1}, wat significant hoger is dan eerder gerapporteerd voor dit organisme. De biomassa-specifieke opnamesnelheid is een belangrijke parameter voor de mathematische beschrijving (of: het kinetische model) van dit micro-organisme, aan de hand waarvan betere biotechnologische processen ontworpen kunnen worden.

Hoofdstuk 4 focust op de ketenverlengende teamspelers. Onze syngas-fermenteerder *C. autoethanogenum* groeit graag op een pH van 5 –5.5, maar de meeste individuele ketenverlengers die tot nu toe zijn beschreven groeien liever op neutrale pH ($\pm$ 7.0). Dit hoofdstuk draait om deze discrepantie. We gebruiken ophopingsculturen in bioreactoren die worden geopereerd als sequentiële batches om te selecteren voor ketenverleng-kampioenen op zowel pH 7.0 als 5.5. Hiermee bevestigen we dat ketenverlengers op beide pH-waarden goed kunnen overleven, en dat zeer vergelijkbare micro-organismen (op genus-niveau) beide bioreactoren bewonen. Het gedrag in de bioreactoren was echter niet hetzelfde. Bij een lagere pH wordt een significant kleinere fractie van de gevoerde ethanol omgezet naar hexanoaat. In plaats daarvan werd er meer van het C_4-molecuul boterzuur gevormd, waarschijnlijk omdat dat minder giftig voor de microben is dan hexanoaat. Dit betekent dat de pH een belangrijke parameter is om het productspectrum van ketenverlenging mee te controleren, en dat het vinden van een efficiënt microbieel team voor de omzetting van C_1 naar C_6 moleculen waarschijnlijk meer vereist dan slechts het vinden van micro-organismen met een vergelijkbare optimale pH.

In **hoofdstuk 5** duiken we in de biochemie van de ketenverlengers. Er is al bekend dat ketenverlengers een flexibel metabolisme hebben, en dat ze om kunnen gaan met een grote range aan ethanol:azijnzuur-verhoudingen. Theoretisch is het zelfs mogelijk dat deze verhouding oneindig is, oftewel dat er slechts ethanol gevoerd wordt, wat op papier leidt tot de productie van enkel hexanoaat (en geen boterzuur). Dit is zowel fundamenteel als uit procesoogpunt interessant. Daarom testen wij in bioreactoren die we met hoge resolutie in de gaten houden of de conversie van enkel ethanol in enkel hexanoaat

ook in de praktijk mogelijk is. We observeren in de bioreactoren dat dit inderdaad het geval is, maar dat de omzetting traag verloopt. Daarnaast hebben de micro-organismen een zodanige voorkeur voor de aanwezigheid van azijn- en/of boterzuur dat ze na enige tijd deze moleculen zelf beginnen te produceren uit ethanol. Dit gedrag is nog nooit eerder geobserveerd, en werd niet eens theoretisch voor mogelijk gehouden.

In **hoofdstuk 6** presenteren we een dataset met goed gecontroleerde bioreactorexperimenten in 9 verschillende startcondities. Deze dataset kan gebruikt worden voor het verfijnen van de huidige mathematische beschrijving van ketenverlengende micro-organismen. We beschrijven onze initiële analyse van deze dataset en hoe we de kwaliteit en betrouwbaarheid van de data waarborgen en optimaliseren. Met de geoptimaliseerde dataset testen we de nauwkeurigheid van het op dit moment beschikbare kinetische model, en zetten we de volgende stappen voor het genereren van een toekomstig beter model uiteen.

Hoofdstuk 7 recapituleert de significante ontdekkingen uit dit proefschrift en, veel belangrijker, voorziet de lezer van een overzicht van de vragen die nog niet beantwoord zijn met betrekking tot syngasfermentatie en ketenverlenging. Deze vragen zijn in drie subcategorieën verdeeld: hoe de innerlijke wereld van deze micro-organismen eruit ziet, de interacties in (gemeenschappen van) micro-organismen en het ontwerpen van (nieuwe) efficiënte biotechnologische processen. Tot slot reflecteer ik over de rol die wetenschappers hebben in de maatschappij.

Resumen

Uno de los problemas sociales actuales más grandes es el agotamiento de los combustibles fósiles. Podemos prevenir alguna de sus consecuencias mediante la transición hacia una economía circular, la cual exige el uso de residuos para la producción de nuevas sustancias químicas. Sin embargo, hay muchos residuos diferentes y su composición no siempre es igual, lo que complica su transformación en nuevos (bio)productos. Afortunadamente, tenemos un buen ejemplo en nuestro camino hacía una economía circular: la naturaleza. Ella, a su tiempo, tiene una solución para todos los problemas, probablemente porque hay un microorganismo solucionando cada uno de ellos.

También le podemos ayudar un poquito, especialmente si sabemos cómo simplificar el problema. La heterogeneidad de los residuos, por ejemplo, se puede reducir si aplicamos el proceso de gasificación. Eso quiere decir que se combustionan los residuos a una temperatura muy alta en presencia de poco oxígeno. El resultado: un flujo de gas que contiene sobre todo monóxido de carbono, dióxido de carbono e hidrógeno, conocido por el nombre de syngas. El syngas se puede convertir mediante métodos químicos en, por ejemplo, etanol, pero el proceso depende en gran medida de la proporción de CO, CO_2 y H_2 y la ausencia de otras moléculas en el gas. Los microorganismos se desenvuelven mejor con las variaciones típicas del syngas, por lo cual podemos usarlos como biocatalizadores para su valorización. Sólo nos falta un poco de conocimiento sobre los microorganismos para poder luchar con ellos contra el cambio climático.

La tesis que sujetas en tus manos se dedica exactamente a ello. Nos enfocamos en ampliar nuestra comprensión de dos microorganismos particulares: bacterias a las a que les gusta consumir syngas y las que pueden producir moléculas largas de carbono a partir de unas más pequeñas (llamémoslas 'alargadoras de cadenas'). Juntas, estas dos bacterias pueden alargar moléculas C_1 (CO) hasta convertirlas en moléculas C_6 (ácido hexanoico). Para poder escoger el mejor equipo bacteriano, empezamos estudiando cada miembro del equipo individualmente. El consumidor de syngas que hemos estudiado se llama *Clostridium autoethanogenum*, ya utilizado en bioreactores industriales por la empresa LanzaTech. Para estudiar la bacteria alargadora de cadenas seleccionamos cultivos mixtos de esas bacterias en nuestros bioreactores. Elegimos cultivos mixtos porque la pareja ideal concreta para *Clostridium autoethanogenum* aún no ha sido encontrada. ¡Quizás la seleccionamos en nuestros cultivos!

Se ha descrito que la producción del ácido hexanoico es bastante fácil cuando alimentas las alargadoras de cadenas con un sustrato con una proporción etanol:ácido acético *alta*. *Clostridium autoethanogenum* produce etanol y ácido acético, pero normalmente en una proporción *baja*. En el **Capítulo 2** usamos un marco teórico y datos de la literatura científica para entender cuándo *Clostridium autoethanogenum* produce etanol. Se descubre que la conversión de ácido acético en etanol es un marcador de estrés celular ya que las bacterias utilizan este mecanismo para detoxificar el CO, clasificando tal fi-

siología como metabolismo 'overflow'. Este tipo de metabolismo ocurre en muchos más tipos celulares como reacción al estrés. Mostramos que esta fisiología no solo ocurre cuando la bacteria crece en presencia de solo CO, pero también cuando hay CO_2 y H_2 en el biorreactor, indicando su importancia también en fermentaciones a escala industrial. Podemos controlar la fisiología mediante el modo de operación del biorreactor, por ejemplo cambiando la tasa de crecimiento o el contenido del gas en el biorreactor.

En el **Capítulo 3** se investiga el metabolismo 'overflow' en nuestros propios biorreactores. Se usa un cultivo continuo de *Clostridium autoethanogenum*, aumentando el contenido de CO del gas que entra en el biorreactor durante una hora, en repetidas ocasiones y hasta una presión de 1.2 atm de CO. Se observa que la producción de etanol aumenta cuando aumenta la presión parcial de CO. A partir de una presión parcial de 0.6 atm, se observa directamente cómo el consumo de ácido acético aumenta la producción de etanol. Estos resultados prueban que el modo de operación del biorreactor es fundamental para el control del producto que se produce durante la fermentación del syngas. Además, el método que se utiliza nos permite medir la velocidad del consumo de CO por las bacterias. Se pudo calcular una velocidad de -119 ± 1 mmol·g_x^{-1}·h^{-1}, que es notablemente más alta que las velocidades anteriormente publicadas. Tener un valor preciso de la velocidad con la que la biomasa consume CO es fundamental para el diseño de nuevos bioprocesos sostenibles.

El **Capítulo 4** se enfoca en las bacterias alargadoras de cadenas. Uno de los problemas a solucionar para conseguir un conjunto microbiano capaz de convertir el syngas en ácido hexanoico es la diferencia de pH en la que *Clostridium autoethanogenum* crece, pH 5 –5.5, en comparación con la mayoría de las alargadoras de cadenas, que crecen a un pH de $\pm$ 7.0. Utilizando enriquecimientos microbianos en biorreactores operados de forma secuencial se han seleccionado las mejores alargadoras de cadenas, a pH 7.0 y a pH 5.5. Con esto se muestra que las bacterias alargadoras de cadenas pueden vivir a un pH más bajo, y que las bacterias seleccionadas en ambas condiciones son similares (respecto a su género). Sin embargo, la fisiología observada es distinta. Las bacterias que crecen a pH 7.0 convierten una proporción mayor de etanol en ácido hexanoico, y en pH 5.5 hay más ácido butírico. Probablemente es porque el ácido butírico es menos tóxico para las células. Esto significa que el pH es un parámetro de control importante en este bioproceso, y que hay más problemas además del pH en la formación de un conjunto microbiano capaz de convertir el syngas en ácido hexanoico.

En el **Capítulo 5**, entramos en el maravilloso mundo bioquímico de los alargadoras de cadenas. Se conoce que tienen un catabolismo versátil y que se pueden alimentar con etanol y ácido acético en distintas proporciones. Teóricamente, tal proporción puede ser infinita, que quiere decir que podrían alimentarse solo de etanol. Eso dirigiría los organismos a la producción de sólo ácido hexanoico y nada de butírico. Visto desde una perspectiva tanto industrial como fundamental, es interesante. Es por eso, que investigamos si se podía observar tal proceso in vivo, utilizando experimentos en biorreactores operados como lotes individuales. Usamos diferentes condiciones iniciales: sólo etanol, etanol y una pequeña cantidad de ácido acético y etanol y una pequeña cantidad de ácido butírico. Se observó que la transformación de etanol en hexanoico ocurre, pero a baja velocidad. Además, los microorganismos tienen una fuerte preferencia por la presencia de acetato o butirato, al punto de que llegan a producir estos compuestos a partir

del etanol cuando no están disponibles de forma natural. Esto no había sido observado anteriormente, ni se pensaba que fuera posible.

En el **Capítulo 6** se presentan una serie de datos experimentales de bioreactores bien controlados operados bajo 9 condiciones iniciales diferentes, incluyendo los datos de los experimentos descritos en el capítulo 5. Esta serie de datos se puede utilizar para mejorar la descripción matemática de las bacterias alargadoras de cadenas. Se presenta el análisis de los datos y cómo nos aseguramos de su calidad y facilidad de uso a la hora de calibrar modelos cinéticos. Se aplican varias correcciones, por ejemplo por la evaporación del etanol del biorreactor durante los experimentos, para mejorar la usabilidad de los datos. Con los datos corregidos se comprueba la precisión del modelo cinético actual. Con esto, describimos los siguientes pasos en el desarrollo de un modelo mejor.

El **Capítulo 7** ofrece un resumen de los objetivos científicos de esta tesis y, más importante aún, enumera las preguntas que quedan por abordar. Estas preguntas tienen que ver con tres temas diferentes: el mundo interno de los organismos que estudiamos, las interacciones en comunidades microbianas y el diseño de (nuevos) bioprocesos sostenibles. Termino con una reflexión sobre el papel social de un(a) investigador(a) científica.

PREFACE

Microorganisms are fascinating.

That is one of the key messages of this thesis, as well as of many theses that have been written before this one and hopefully many many more to be written after this one. We have a myriad of things left to learn and explore and luckily many scientists dedicate their time and passion to uncovering the small and big details of the life that we cannot see. I try to do exactly that, too.

Personally, I tend to want to crawl into the skin (all right, the membranes, to be correct) of the bugs I study. I try to feel my way through what they are doing, especially when I don't understand what I am seeing very well yet. Then, sometimes much later and often with a little help from a friend comes reason. Reason helps me to articulate my gut feeling and put it to the test. This occasionally leads to frustration, yet much more often to wonderment.

Microorganisms are fascinating.

This thesis is the proof of my wonderment and where it has taken me in the past years. I hope I manage to share some of my fascination with you, dear reader.

Maxim Allaart
Delft, June 2023

ACKNOWLEDGEMENTS

I know this section usually comes at the end of a thesis, but I think that it is important to realize right from the start that this was by no means a solo effort. I am grateful to everyone that contributed directly or indirectly to this thesis and would like to thank many of you personally in the following dictionary of indispensable (groups of) people.

Robbert, **Baassie**, dankjewel, thank you, muchas gracias for supporting me through a whole rollercoaster of emotions. I have appreciated your direct (heh?!) style of feedback since the beginning of our journey, when I was still trying to make lactic acid. It is important for me that I can count on honesty and open communication, and you provided me with that. What I most appreciated, though, is that you always made me feel like you trusted me in what I was doing, and that there was always room for low-key interaction and a good laugh. These things have helped me greatly in developing the independent researcher in me.

Diana, your habit of spontaneously cheering me on from time to time has brought me lightness and confidence during my PhD, which is incredibly valuable to me. My favorite shared event during my PhD was the ICBM conference in Braga, where I was kindly adopted by you and the people from your group. You have created a wonderful atmosphere in the group, and also when I visited Wageningen I always felt so welcome. Thank you.

Mark, even though you were not directly involved in my project, your contribution is significant. The atmosphere you created in the group, your presence at Friday drinks and your lightning-fast responses to emails all reinforce the enjoyable working atmosphere at EBT.

My dear **students**, you all worked your assess off during your projects and taught me a great deal about myself and my microbes. Even if you don't see your work back in this thesis directly, you can be sure that it shaped my thinking and that it was essential for this book to reach its current form. For all of you: a little example of how you contributed exactly. **Mees**, you were dedicated and determined to do a good job, and thereby also challenged me. You were my first student and with that, you taught me how to be a supervisor instead of a pal. **Stef**, the speed of your brain amazed, inspired and amused me. You taught me how to pull you out of deep, deep rabbit holes of the internet and how to help someone (including myself) with structuring a story. **Ingo**, we amazingly had our first meeting on a Thursday, and on Friday we were already in the lab with our combined full-blown enthusiasm. You were (sometimes painfully) critical towards my methods in the lab, making my work better and more rigorous as you went. **Marjolein**, I was your fan since you first walked (or ran, since you never just walked in the hallways) into my office. Because we are very similar in some aspects, you provided me a mirror and helped me to get to know myself better. **Maaike**, you made it look so easy! You showed me that it is also okay to take my hands off off something close to my heart and

trust that someone else will take charge. **Harry**, you were so so precise in the lab! You taught me how to manage somebody else's stress levels (;)) and made it very easy for me to write chapter 3. **Elisabeth**, your thesis experience was not what we planned for AT ALL, but our interaction was always fun and pleasant. You taught me how to keep two people (you ánd myself) motivated in very harsh conditions. Thank you all.

To the **technical and safety staff**, our work would literally not be possible without you. **Dirk, Rob and Song**, thank you so much for all your efforts in getting the CO setup to work and Dirk, also for answering all the other questions (Can you explain me *again* how a backpressure valve works? How do I order a gas bottle? How do I attach a stirrer? How do I close this hole in my septum? - the candle solution was my personal favorite) I came to ask you. **Johan** and **Astrid**, for making sure and eventually trusting that me and my students were safe. **Zita** and **Ben**, for preventing the labs from becoming a jungle and for the dedication with the Nanopore. **Apilena, Jannie, Gea**, for the hugs, friendliness and help with exploded media vessels. **Dita**, **Martin, Cor, Carol, Patricia**, for making it possible to measure all that my heart desired.

Marina, the CO setups would have never worked without you. I am so grateful that you were there to share the struggles ánd the victories, to take a sample when I wasn't there and to discuss the weirdness of our microbe. Speaking of discussing weirdness, **Martijn**, I would have gone a bit mad without you I think. Thank you so much for replying to my (and my students') questions at all times, for coming over to Delft, for showing me how you do it in Wageningen and for giving me pre-culture after pre-culture. Luckily, when you took small steps out of the lab I could also count on **Ivette** for the pre-culture business. Muchas gracias. Both of you also proved to be excellent (conference) friends, and I hope we keep seeing each other! Or, of course, organizing conferences, maybe together with **Jules** again? I am super proud of our EMT conference and really loved the dynamics in our organizer-team.

My **officemates** were also quite indespensible on this journey. **Roel**, thank you for your hums and grumbles and your sharp eye, and **Michel** for your happy face in the mornings of my early PhD days. **Alba**, thank you for your laughter and for all the chats that helped me decompress and/or keep my Spanish up to date. **Jelmpie**, thank you for the weirdness, for idly listening to all my complaints and the sometimes much-needed problem solving, for the haikus and kai-hus and for being the number one fan of my dinosaurs. **Gerben**, thank you for your excitement and wonderment when we talked through many of the shenanigans of my microbes, for making my graphs more beautiful, for making data analysis a piece of cake and for all the other things you did along the way to make this job a little easier. This thesis would not have looked the same and I don't think I would have enjoyed making it as much without you. You make me a happy and more confident scientist.

David, **Sergio**, **Mariana**, **Chris**, **Nina**, **Ali**, **Lemin**, **Sam**, **Francesc**, **Rodoula**, **Stefan**, thank you for being my **EBT family** during this adventure, with all our Friday drinks, lunches, retreats, poledancing, games, escape rooms, volleybal or other injury-inducing sports, dinners with or without competitive element and laughter in any other situation. You all have a very special place in my heart and made work feel like home. I am very very grateful to have you in my life. Other old and new EBT friends: **Jure, Morez, Ingrid, Marta, Michele, Florence, Alberte, Ángel, Diana, Francesc, Hugo, Felipe, Shengle, Vik-**

1

INTRODUCTION

This chapter was written to introduce the topics of this dissertation to the general public. Therefore, the language used in this chapter is different from the language used in Chapters 2-6, each containing an academic introduction to their contents.

1.1. MICROORGANISMS AND THE DEFINITION OF CATABOLISM

HUMANS belong to a eukaryotic species that thrives on planet Earth. From our own perspective, we seem to be the most important species on Earth. However, we depend on many other organisms in many different ways. For example, we need plants and animals to feed ourselves. Most humans are aware that they need these other species to stay alive. This is relatively logical, as the species we eat are visible species that look different than we do. These visible differences originate from differences in our biological origin. Past events, such as endosymbiosis, natural selection and, simply, chance, have enabled an astonishing number of different kinds of species to develop. Species that we can see and species that we can only see with the appropriate tools. It might therefore be a little bit more complicated to imagine that we also depend on a tremendous number of organisms that we cannot see with the naked eye. A whole world of so-called microorganisms (microscopically small organisms) helps us to digest our food, protect our skin, keep our soils fertile, preserve food products, keep our water clean and help us with an unimaginable number of other processes.

The currently known biological diversity existing on Earth is represented by the phylogenetic tree of life, which spans both visible and invisible (to the naked eye, that is) domains of life. In 2011, it was estimated that there are approximately 8.7 million species on Earth [1]. However, the method used to estimate this number works rather poorly for some of the domains in the tree of life – especially the invisible ones. The number of bacterial species, for example, could not be estimated accurately. You will soon find out that some members of the bacterial domain of life are the protagonists in the stories to follow. But for now, five years after this prediction of $8.7 \cdot 10^6$ species, another study [2] predicted the number of microbial, invisible, species to be close to one trillion (10^{12}), which is clearly many orders of magnitude larger than anticipated earlier. Even more bafflingly, only approximately 10.000 of these species have been grown and studied in laboratories. So, there are not only many things we cannot see, but also many things we simply do not know yet.

Even for the species that we do know how to grow, or cultivate, in laboratories, there are many aspects that we do not yet know or understand. For example how exactly they consume their food, what their favorite conditions are to live in and how they collaborate with all the other organisms that they share their habitats with. This provides us with opportunities to learn. We can pursue learning new things just because it is cool and satisfying to learn new things, but also because it might somehow serve us. We'll get back to that in a bit.

First, we should dive into some of the basics. Some things we do understand. A good example of such a thing is that all organisms, whether they are microscopically small or not, need food. More specifically, we (being: organisms) need food because it gives us energy to:

   i. Keep ourselves alive
  ii. Reproduce ourselves

This is important, because both things are pivotal in the process of not going extinct as a species.

To get the energy out of our food, we essentially need to change its chemistry. The process of changing the chemistry of food to release energy from it is called catabolism. This originates from the Greek words $\kappa\alpha\tau\omega$ and $\beta\alpha\lambda\lambda\epsilon\iota\nu$, which mean 'downward' and 'throwing', respectively. Throwing something that is breakable in a downward direction usually leads to its shattering in to multiple, smaller pieces. Depending on the amount of force you throw with, of course. So, we kind of get an idea of what 'catabolism' means. Oxford Languages states the following definition of the word:

> *'The breakdown of complex molecules in living organisms to form simpler ones, together with the release of energy; destructive metabolism'*

All organisms use catabolism to generate energy and its antagonist, anabolism, to build molecules that they need to grow (i.e., build new cells). The inner workings of this are explained further in Box 1.1. All cells consist of the same molecules, like DNA, proteins, water and some fats to encapsulate everything. Interestingly, building these molecules can be powered by many, many different catabolic routes. This is because the energy that is released in catabolism is stored in a universal energy-carrying molecule: ATP. Storing energy like that makes the source of the energy is less important, just the availability of energy is what counts.

1.2. THE ROLE OF MICRO-LIFE IN ELEMENTAL CYCLES

Now let us look at some of these many different catabolic routes that microorganisms can use to generate energy to build things. Before we start, we must realize that life is made of a finite number of elements (fig. 1.1). Phew, at least we don't have an infinite number of options there. However, by making different combinations of different elements, even when following the basic rules of chemistry and physics, a tremendous number of different molecules can be formed. The elements represented in yellow and green exist in so many different molecular forms that can be converted into each other, that their turnover (on planet-scale!!) is often referred to as a cycle (fig. 1.2). This implies that both destruction and construction must be balanced to make sure we don't run out of one of the intermediates, which would result in the entire cycle running dry. Our planet and many of the organisms living on it do their utmost to keep these elemental cycles running nicely, but the fact of the matter is that human interventions have significantly shifted the balance of more than one of them.

Maybe, just maybe, if we understand that processes on our planet are supposed to be cyclical, it will become a little bit easier to actually contribute to this cyclical nature instead of creating chaos and imbalance. That's the dream.

To get some inspiration, let's zoom into those elemental cycles a little bit more. Processes of different natures lie at the basis of displacement of elements and their interconversion, ranging from weathering of rocks to the digestion of plant materials
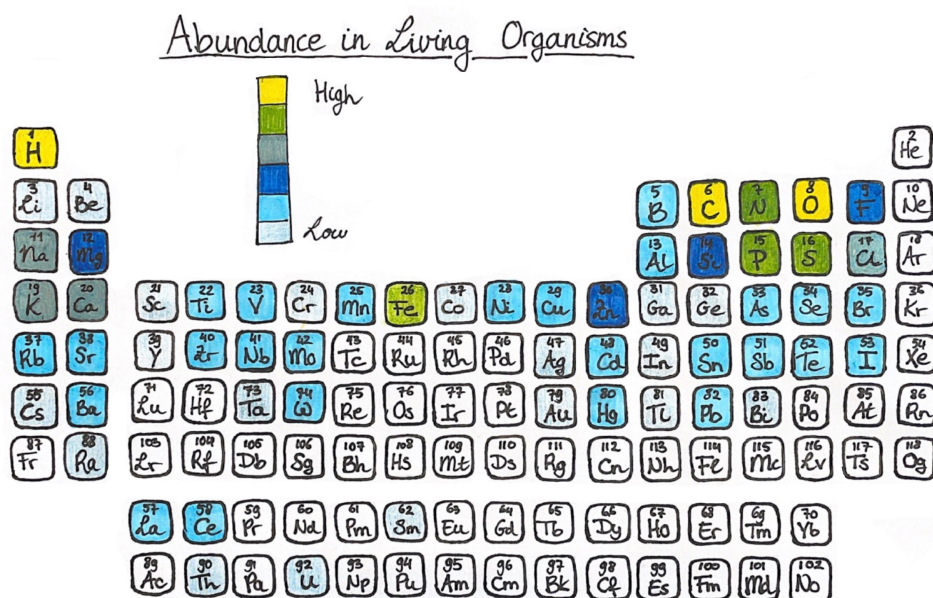
Figure 1.1: Periodic table of the elements. The color scale of the table indicates how prevalent atoms are in living organisms. It is important to know that this image was not made to be precisely quantitative and that it is not possible to summarize all the diversity of life in one color scale. This particular color scale was developed with general assumptions about cellular composition as well as the average composition of human cells and the nutrients essential for growing anaerobic bacteria in mind.

by animals. On the left side of fig. 1.2 we see a simplified representation of the global nitrogen cycle. As you can see, many little arrows indicate the interconversion of nitrogen species. It is not only important, but also fascinating to realize that the processes indicated by most of the little arrows are carried out by microorganisms. In other words, the availability of nitrogen in soils, which is indispensable for the growth of plants, depends completely on our invisible micro-friends. Even though catabolism often consists of a chain of multiple reactions, there even are microorganisms that have specialized in performing a single reaction, just to be able to do that one reaction phenomenally well.

Microorganisms are also responsible for key conversions in the other elemental cycles. Where plenty of microorganisms are specialists in a particular conversion or set of conversion of a single element, there are also microorganisms that have built their metabolism around various elements. These 'multidisciplinary microbes' play a key role in cleaning up our sewage water, for example. But for now, we will not get into that. For now, we will move our focus to the elemental poison of choice of this thesis: carbon. Looking at the scheme of the elemental cycle, we see that fixation of carbon dioxide into organic molecules happens via photosynthesis, which is carried out by plants. However, a big chunk of the atmospheric carbon that ends

up back in soils (20% of it, to be more or less precise) is actually fixed by bacteria, not by plants. It is all about teamwork. I have mentioned before that bacteria are the protagonists of this thesis. To be a bit more specific, the bacteria that can turn inorganic, gaseous carbon compounds (like CO_2) into organic molecules are one of the two lead characters in the story. "Why?", might you ask. Let's get into that!
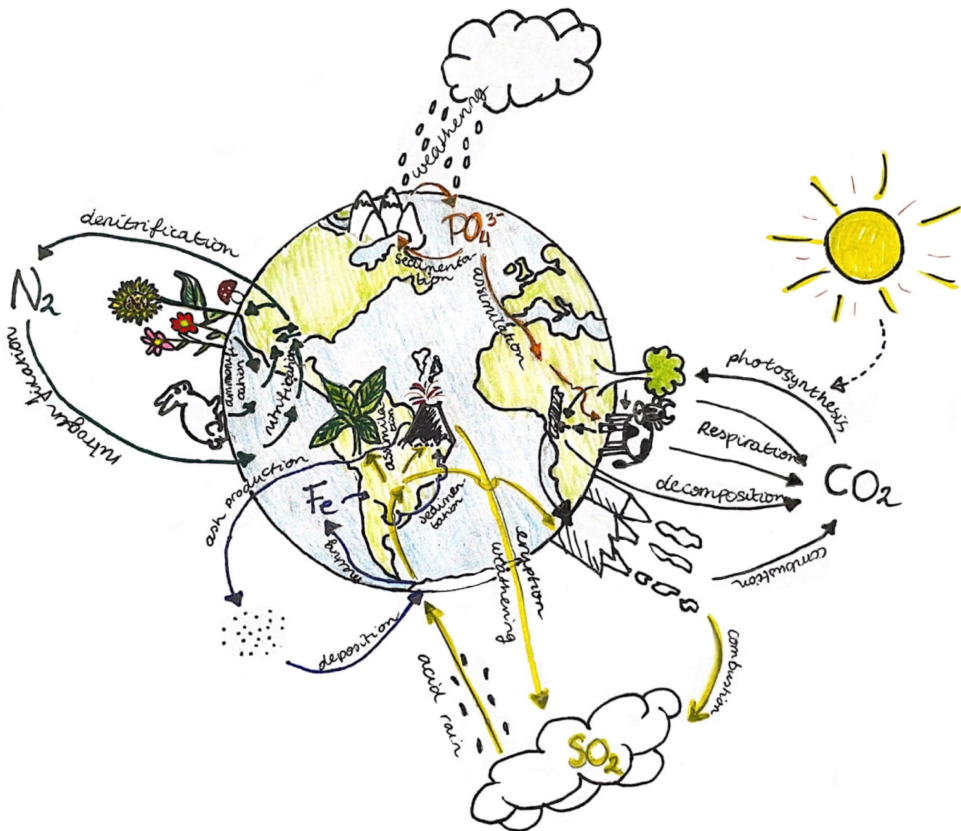
Figure 1.2: Schematic representation of the global elemental cycles of carbon, nitrogen, sulfur, phosphorus, and iron. The cycles are represented in a highly simplified manner, without explicit depiction of all intermediate molecules. This image is meant to illustrate the impressive number of crucial processes that proceed on our planet in for example soils, air and water bodies, often without us even noticing their mere existence.

1

Box 1.1. Thermodynamics and Catabolism

Metabolism is the overall chemical reaction of the cell, in which catabolism is the energy generating component and anabolism builds new cell material. They have in common that they are redox reactions, meaning that they rely on electrons transfer. What is an electron, you might ask? Well, it is one of the three main building blocks of an atom (fig. 1.1), beside protons and neutrons. Electrons are essential for the formation of molecules, as they can be shared among different atoms to form bonds between them. Their transfer is pivotal for chemical reactions to occur.

When we eat food we are actually doing chemistry. Let's simplify our digestive system a little bit, and assume that we essentially eat sugar (i.e. glucose) and break it down to CO_2. The difference between glucose and CO_2 is that glucose has a lot of electrons to give away, while CO_2 has none. This makes glucose an electron donor. But the electrons that glucose donates during its conversion to CO_2 cannot just spill out into the world: they have to be accepted by an electron acceptor. In fact, this is the reason we need oxygen to stay alive: oxygen is really good at accepting electrons.

Getting energy from combusting glucose to CO_2 is possible because *the laws of thermodynamics* dictate that it is. Without discussing the intricate details of thermodynamics, we can state that the energy liberated from a reaction depends on the amount of heat that is consumed or generated and the amount of either chaos or order created during this reaction. The universe in its entirety is always moving towards more chaos, so even reactions that might need heat to occur, could overall be energy-generating if they create a lot of chaos. In the case of glucose combustion, it's both: it releases heat and produces chaos because an organized, solid molecule is turned into many chaotic gaseous molecules. This means that plenty of ATP can be harvested.

Then, it is intriguing to realize that plants make the sugars we eat via CO_2 fixation. In other words: plants are doing the exact opposite of what we are doing, but still somehow get energy to grow! That sounds impossible, but plants have the enormous advantage of being green. In their green chlorophyll particles, they have the machinery to use sunlight as an energy source to turn the direction of the reaction around. This means that the energy stored in chemical bonds is not the only possible source of energy for organisms to grow on. Just imagine the realm of possibilities that this brings!

Glucose + 6 O₂ ⟷ 6 CO₂ + 6 H₂O
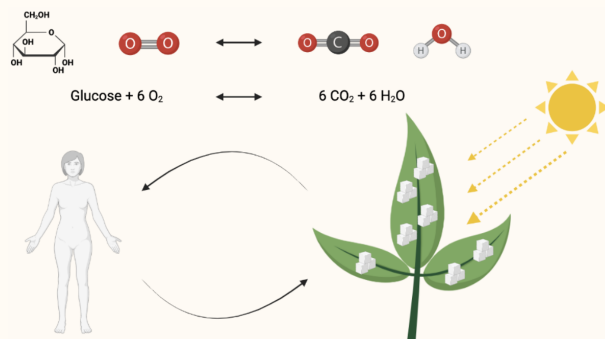
Figure 1.3: The same catabolic reaction running in opposite directions in different organisms. Figure generated using BioRender.Com

1.3. Harnessing the power of microorganisms to solve societal issues

So, we were talking about carbon, right? You might have heard that we, as a species living on this planet, have been inflicting a huge shift in the distribution of carbon over different reserves. To put it differently, we are well on track to exhaust the natural reserves of fossil fuels, which we have either burned upon formation of CO_2 or turned into products that we don't want to use anymore after a way too short while, resulting in enormous piles of trash. Good job, *Homo sapiens*! To thicken the plot a bit further, the fossil fuel reserves can be restored.

Naturally.

Without any effort.

But… it only works if you have lots and lots of time. The rate at which we are consuming fossil fuels is so many orders of magnitude larger than the rate of fossilization that restores the reserves, that we have introduced a conundrum. If we want to keep living our lives in the exact same way as we are doing now, that is.

Clearly, we must change something. As we have gotten used to having basically anything that we want at just a tap on a screen's distance, it is nearly unthinkable that we just stop consuming things that we don't actually need altogether. This means that we need to find alternative building blocks for making our favorite products to decrease or abolish our need for fossil fuels. But how?

Enter the whimsical world of microorganisms! Those 10.000 organisms that we have studied in our labs and those trillion(s?) that we have not yet met formally. I am convinced that they can do anything. Our task is merely to map what they can do and learn how to collaborate with them on the way to reaching, let's say, our Net Zero in 2050 goal. A nice strategy to work on this problem is to start seeing waste as a resource.

1.3.1. On how organisms harvest energy

Net Zero means that all our industrial processes should have an overall greenhouse gas emission of exactly nothing. This means that, for example, all the CO_2 that we are so frivolously exhausting in our fossil-powered industries should be captured or not emitted at all. From the waste-to-resource perspective, this means that CO_2 would then be our building block to make new chemicals. Ideally, we would use microorganisms to do so, but we have also learned that their survival depends on breaking molecules into smaller ones. CO_2 is a very small molecule, and it requires a lot of energy to break it apart into the atoms it consists of. That looks like another conundrum. Yet, we have paused earlier to recognize that ±20% of the carbon in soils ends up there due to CO_2 consuming microorganisms.

CO_2 consuming microorganisms...

Consuming CO_2 to do what!? If CO_2 can't be broken down but still any organism

needs catabolism to exist, how is it possible to eat CO_2?

Here comes one of the flaws of the terminology in (micro)biology: catabolism doesn't have to be destructive. Nature only dictates that catabolism should generate ATP, because ATP is the required currency for staying alive and building new cell material. ATP can be generated in two different ways, which we could classify as the straightforward way and the smart way if you would ask me. The straightforward way relies on the harvesting of energy that is contained in some of the chemical bonds in organic molecules. It is almost[1] as if the energy just comes spilling out if you break that bond. The smart way of ATP formation relies on one of the key rules of life, which is that things generally move to get closer to equilibrium (or to just create more chaos) [3, 4]. Following this line of thought, a cell can then deliberately create an imbalance to get something moving. In the case of the smart way of generating ATP, actual physical movement must be generated in a microscopically small motor called an ATPase (fig. 1.4). To do this, a chemical gradient of positively charged ions (often protons) is made, removing the inside relative to the outside of the cell further from equilibrium. The energy required for building up this chemical gradient can originate from all kinds of reactions happening in the cell that have an excess of free energy, for example electron transfer reactions (also see Box 1.2). So, this mini motor is used to turn chemical energy into mechanical energy back into chemical energy. Pretty ingenious if you'd ask me.
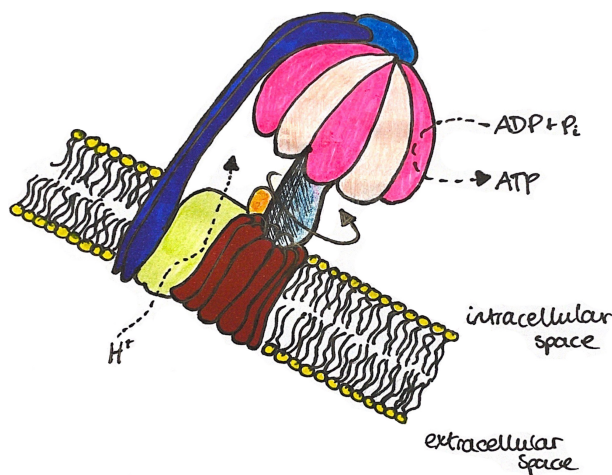
Figure 1.4: F_0F_1 ATPase, one of the molecular motors in cells that is being used for the generation of energy in the form of ATP. Chemical energy from a proton gradient is converted into mechanical energy that drives conformational changes in the protein complex, enabling the conversion of ADP and inorganic phosphate into ATP.

---

[1]Almost, but not entirely. Some kind of 'activation' of a molecule often precedes the release of the energy it contains. For example, a phosphate group can be bound to the molecule first, before that same phosphate group can be donated to ATP's low-energy brother ADP. The phosphate group takes the energy contained in the chemical bond with it and forms ATP.

Still, there is more to it. You might even be able to feel that building up this chemical gradient can't be for free. Indeed, it is not, and the mechanism to make it work in the bacteria that play the main part in this thesis, is something I personally like to describe as a microbe playing some internal ping-pong. The generally more accepted term, however, is 'electron bifurcation', which is explained in more (excruciating) detail in Box 1.2. For now, we should accept that being rather good at internal ping-pong is one of the things that enables some types of bacteria to eat CO_2 for a living.

1.3.2. Turning gaseous and toxic waste into small molecules

THE fundament of this thesis is that microorganisms can eat our waste gases. These microorganisms, as mentioned before, can live in soils and sediments [5, 6], but also in many other environments [7] such as animal [8, 9] or human [10] guts and hydrothermal vents [11]. They all exploit catabolism to stay alive and multiply, and as the laws of physics and thermodynamics allow multiple different combinations of atoms, they have different catabolic products which are very likely to be the resultant of the environment the microbes reside in.

Here, I focus on bacteria that cannot only eat CO_2, but also hydrogen gas (H_2) and carbon monoxide (CO). These three gases are the main constituents of syngas, a gaseous waste stream that can either originate directly from heavy industries like steel mills or from gasification of all kinds of solid waste. The species I work with is called *Clostridium autoethanogenum*, and it is special because it was isolated from a rabbit's gut, it basically eats poison and it can produce acetate, ethanol and some other products while doing so. These products are alluring when thinking about closed cycles, because we can use them for cleaning or fueling cars, for example. Different researchers have been studying this microbe [12–19], in part to figure out how best to use it in industry for converting toxic waste gas into bioethanol. It should be noted here that *C. autoethanogenum* generally likes producing acetate, so getting it to make ethanol requires some effort. **Chapter 2** of this thesis dives into the inner workings of the catabolism of *C. autoethanogenum*. By doing that, I aimed to gain perspective on the situations in which producing ethanol would make sense. In **Chapter 3** I looked for the maximal capacity of the microbe to take up CO, which is useful to know when you're designing an efficient industrial process, and verified whether the theory I proposed in **Chapter 2** also held true in my own bioreactor experiments.

1.3.3. Turning small molecules into larger ones

THE fact that we can make small, usable molecules from waste gases using a microbe that lives inside a rabbit is amazing. This, however, is not even close to the limit of what microbial life is capable of. In nature, microorganisms live in communities where the community members rely on each other for various reasons. With some understanding of what the different community members like to eat, for example, we can also construct our own microbial networks. In the context of syngas fermentation, microbial networks can be interesting to expand the range of products

1

that can be made without the need for genetic engineering [20]. Specifically, we can introduce a microorganism that can consume the products of *C. autoethanogenum* and turn them into longer molecules with other applications (feed additives, biofuel- and fragrance precursors, etc.). This process is called microbial chain elongation and is the subject of **Chapters 4**, **5** and **6**.

To make a working microbial network, the conditions in which the organisms thrive must be at least similar. Syngas fermenting microbes and chain-elongating microbes can live in similar environments, but often prefer slightly different specific cultivation conditions. We can tackle this problem in different ways. One of the options is to look for microbes in nature that can survive in the envisioned conditions. We can do this by doing an enrichment study, where we apply the conditions that we want and start with lots of different microbes. The ones that can survive the environment will stay alive, and the ones that positively thrive will, in time, become the dominant organism. Another option is to understand the consequences of cultivating a microbe in suboptimal conditions - then we can minimize these consequences using smart bioreactor design. **Chapter 4** aims at killing two birds with one stone: we enrich chain-elongating microbes at their preferred pH and at a supposedly suboptimal one to see if we 1) get a chain elongator that is better suited to live at suboptimal pH and 2) map the consequences of cultivating chain elongators at a suboptimal pH, as compared to their preferred pH.

To successfully control a bioreactor system, both at small but definitely at large scale, it is important to know the effect of different conditions on the operated system. This knowledge can be gained via trial-and-error, but it is much easier if the response of the microbes in various situations is carefully mapped and somewhat predictable. In **Chapter 5** we cultivate chain-elongating microbes in, for them, stringent conditions to map their resulting behavior. In **Chapter 6** we study them in some more different conditions and analyze all these sets of data together. We make an overview of our key observations, which can be translated into an improved mathematical description of chain-elongating microbes in the future, making their behavior more predictable.

1

Box 1.2. Electron Bifurcation

We have learned that ATP is the universal energy-carrying molecule in biology. Let's assume that a cell is like a house, and that ATP would be the gas that allows us to keep our house warm and cook our food. If that house would have only ATP as energy source, we would be living in the dark. To be able to switch on the lights, we also need electricity. Similarly, cells need another energy source to keep the show on the road: electrons. Sometimes, electrons are being liberated from a molecule. Other times, a molecule requires electron input. For the entire metabolic route to work, the number of liberated electrons and the number of required electrons must be balanced. To make this balancing act a little bit more doable, it is nice to be able to temporarily store the electrons that come out of certain reactions in a kind of battery. Then, that battery can be used to provide electrons to the reactions that require them. In biology, we call these batteries electron carriers. Intriguingly, there is not just a single type of electron carrier. This is, among other things, because some reactions require a lot of power input to make them possible, whereas others just need a little push. Similarly, your remote control can work fine on AAA batteries, but a Tesla car will most likely not move a centimeter if you use AAA batteries to try to make it work. The electron carriers that are important in this thesis (from least to most powerful) are called NAD(H), NADP(H) and ferredoxin. Cells, mainly the ones that live in the absence of oxygen, live in a world where energy is scarce. That is why they have evolved to use smart little tricks to:

    i. Harvest energy from reactions that are thermodynamically very favorable, but where ATP formation is not possible

    ii. Transfer electrons from one carrier to another without losing energy

These two tricks rely on the same principle: **electron bifurcation**. Simply put, it is a way to supercharge electrons. This means that low-power electrons, e.g. carried by NADH, can be turned into high-power electrons, e.g. carried by ferredoxin. The energy to do this can come from reactions that have an excess of energy, but the electron carriers can also share their energy among themselves (fig. 1.5).
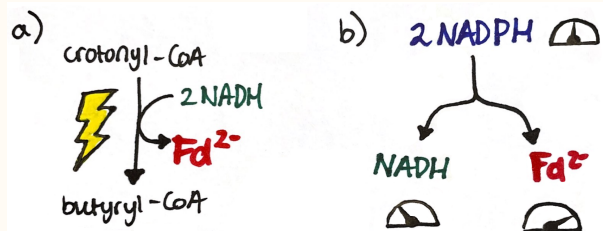
Figure 1.5: Electron bifurcating mechanisms where a). Energy is harvested from a thermodynamically very favorable reaction and b). The electrical potential of the electrons of NADPH is distributed to a weaker (NADH) and a stronger (ferredoxin) electron carrier, resulting in the conservation of the same overall potential.

1.4. PURE- VS. MIXED CULTURES

IN this thesis, we work with both pure cultures (i.e. single, known species) and mixed microbial cultures of microorganisms. I feel that there is a separation in the academic world between people working with pure cultures and people working with microbial communities. However, both cultivation approaches can teach us a great deal about life. Pure cultures have the advantage that they are often the pet organisms of other researchers as well. This means that a lot of information is available about the microbe and that there is plenty of other work to base your expectations on and compare your own work with. Factors contributing to noise in experimental data (unknown interactions between different microbes, competition for food, exchange of genetic information, etc.) are eliminated when working with pure cultures, which can make it easier to focus on a specific trait that you might want to uncover. Microbial communities, however, can show us the true potential that nature possesses. We can create an environment and select for whoever survives there, which can help us discover functionalities that we were not yet aware of. I see great potential in both types of research and am glad I got the opportunity to explore both worlds.

1.5. CURIOSITY-DRIVEN RESEARCH

I THINK that microbes play a key role in solving the problems that we have (created) as a society. To exploit all the potential that microbes harbor, I believe that understanding the fundamentals of their behavior is crucial. With this understanding, we will be able to rationally engineer industrial production systems that will allow us to prevent creating even more imbalances in our elemental cycles. In my project, sustainable production of biochemical building blocks was a clearly marked spot on the horizon. Having this spot is wonderful, even if it only were a way to explain what I work on to others. However, a marked spot on the horizon should not become a restraint. Big discoveries often originate from curiosity and serendipity. Working with bioreactors before starting this project has brought me many surprises and insights that were not pre-meditated. Therefore, even though meticulously planning out experimental work that should take about four years before you set foot in the lab is very well possible, I decided to allow myself room to explore some of the things I encountered along the way. In other words, the implicit aim of this thesis was to let amazement and curiosity rather than the spot on the horizon lead my way. The (more formally formulated) aim of this thesis, however, is as follows:

> *'Increasing our fundamental understanding of acetogens and chain-elongating microbes to pave the way towards their full-scale application in syngas bioconversion to biochemical building blocks'*

BIBLIOGRAPHY

[1]   C. Mora, D. P. Tittensor, S. Adl, A. G. B. Simpson, and B. Worm. "How Many Species Are There on Earth and in the Ocean?" In: *PLoS Biology* 9.8 (Aug. 2011). Ed. by G. M. Mace, e1001127. DOI: 10.1371/journal.pbio.1001127.

[2]   K. J. Locey and J. T. Lennon. "Scaling laws predict global microbial diversity". In: *Proceedings of the National Academy of Sciences* 113.21 (May 2016), pp. 5970–5975. DOI: 10.1073/pnas.1521291113.

[3]   D. A. Beard and H. Qian. "Relationship between Thermodynamic Driving Force and One-Way Fluxes in Reversible Processes". In: *PLoS ONE* 2.1 (Jan. 2007). Ed. by T. Secomb, e144. DOI: 10.1371/journal.pone.0000144.

[4]   S. Carnot. *Réflexions sur la puissance motrice du feu et sur les machines propres à développer cette puissance.* Paris: Bachelier, 1824.

[5]   M. V. Simankova, O. R. Kotsyurbenko, E. Stackebrandt, N. A. Kostrikina, A. M. Lysenko, G. A. Osipov, and A. N. Nozhevnikova. "*Acetobacterium tundrae* sp. nov., a new psychrophilic acetogenic bacterium from tundra soil". In: *Archives of Microbiology* 174.6 (Dec. 2000), pp. 440–447. DOI: 10.1007/s002030000229.

[6]   W. E. Balch, S. Schoberth, R. S. Tanner, and R. S. Wolfe. "*Acetobacterium*, a New Genus of Hydrogen-Oxidizing, Carbon Dioxide-Reducing, Anaerobic Bacteria". In: *International Journal of Systematic Bacteriology* 27.4 (Oct. 1977), pp. 355–361. DOI: 10.1099/00207713-27-4-355.

[7]   H. L. Drake, A. S. Gößner, and S. L. Daniel. "Old Acetogens, New Light". In: *Annals of the New York Academy of Sciences* 1125.1 (Mar. 2008), pp. 100–128. DOI: 10.1196/annals.1419.016.

[8]   J. Abrini, H. Naveau, and E.-J. Nyns. "*Clostridium autoethanogenum*, sp. nov., an anaerobic bacterium that produces ethanol from carbon monoxide". In: *Archives of Microbiology* 161 (1993).

[9]   R. S. Tanner, L. M. Miller, and D. Yang. "*Clostridium ljungdahlii* sp. nov., an Acetogenic Species in Clostridial rRNA Homology Group I". In: *International Journal of Systematic Bacteriology* 43.2 (1993).

[10] B. Kamlage, B. Gruhl, and M. Blaut. "Isolation and characterization of two new homoacetogenic hydrogen-utilizing bacteria from the human intestinal tract that are closely related to *Clostridium coccoides*". In: *Applied and Environmental Microbiology* 63.5 (May 1997), pp. 1732–1738. DOI: 10.1128/aem.63.5.1732-1738.1997.

[11] V. Svetlichny, T. Sokolova, M. Gerhardt, M. Ringpfeil, N. Kostrikina, and G. Zavarzin. "*Carboxydothermus hydrogenoformans* gen. nov., sp. nov., a CO-utilizing Thermophilic Anaerobic Bacterium from Hydrothermal Environments of Kunashir Island". In: *Systematic and Applied Microbiology* 14.3 (July 1991), pp. 254–260. DOI: 10.1016/S0723-2020(11)80377-2.

1

[12] E. Marcellin, J. B. Behrendorff, S. Nagaraju, S. DeTissera, S. Segovia, R. W. Palfreyman, J. Daniell, C. Licona-Cassani, L.-e. Quek, R. Speight, M. P. Hodson, S. D. Simpson, W. P. Mitchell, M. Köpke, and L. K. Nielsen. "Low carbon fuels and commodity chemicals from waste gases – systematic approach to understand energy metabolism in a model acetogen". In: *Green Chemistry* 18.10 (2016), pp. 3020–3028. DOI: 10.1039/C5GC02708J.

[13] J. K. Heffernan, V. Mahamkali, K. Valgepea, E. Marcellin, and L. K. Nielsen. "Analytical tools for unravelling the metabolism of gas-fermenting *Clostridia*". In: *Current Opinion in Biotechnology* 75 (June 2022), p. 102700. DOI: 10.1016/j.copbio.2022.102700.

[14] J. K. Heffernan, K. Valgepea, R. De Souza Pinto Lemgruber, I. Casini, M. Plan, R. Tappel, S. D. Simpson, M. Köpke, L. K. Nielsen, and E. Marcellin. "Enhancing CO_2-Valorization Using *Clostridium autoethanogenum* for Sustainable Fuel and Chemicals Production". In: *Frontiers in Bioengineering and Biotechnology* 8 (Mar. 2020), p. 204. DOI: 10.3389/fbioe.2020.00204.

[15] K. Valgepea, R. De Souza Pinto Lemgruber, T. Abdalla, S. Binos, N. Takemori, A. Takemori, Y. Tanaka, R. Tappel, M. Köpke, S. D. Simpson, L. K. Nielsen, and E. Marcellin. "H2 drives metabolic rearrangements in gas-fermenting *Clostridium autoethanogenum*". In: *Biotechnology for Biofuels* 11.1 (Dec. 2018), p. 55. DOI: 10.1186/s13068-018-1052-9.

[16] K. Valgepea, R. De Souza Pinto Lemgruber, K. Meaghan, R. W. Palfreyman, T. Abdalla, B. D. Heijstra, J. B. Behrendorff, R. Tappel, M. Köpke, S. D. Simpson, L. K. Nielsen, and E. Marcellin. "Maintenance of ATP Homeostasis Triggers Metabolic Shifts in Gas-Fermenting Acetogens". In: *Cell Systems* 4.5 (May 2017), 505–515.e5. DOI: 10.1016/j.cels.2017.04.008.

[17] F. Liew, A. M. Henstra, M. Köpke, K. Winzer, S. D. Simpson, and N. P. Minton. "Metabolic engineering of *Clostridium autoethanogenum* for selective alcohol production". In: *Metabolic Engineering* 40 (Mar. 2017), pp. 104–114. DOI: 10.1016/j.ymben.2017.01.007.

[18] L. A. De Lima, H. Ingelman, K. Brahmbhatt, K. Reinmets, C. Barry, A. Harris, E. Marcellin, M. Köpke, and K. Valgepea. "Faster Growth Enhances Low Carbon Fuel and Chemical Production Through Gas Fermentation". In: *Frontiers in Bioengineering and Biotechnology* 10 (Apr. 2022), p. 879578. DOI: 10.3389/fbioe.2022.879578.

[19] R. De Souza Pinto Lemgruber, K. Valgepea, R. Tappel, J. B. Behrendorff, R. W. Palfreyman, M. Plan, M. P. Hodson, S. D. Simpson, L. K. Nielsen, M. Köpke, and E. Marcellin. "Systems-level engineering and characterisation of *Clostridium autoethanogenum* through heterologous production of poly-3-hydroxybutyrate (PHB)". In: *Metabolic Engineering* 53 (May 2019), pp. 14–23. DOI: 10.1016/j.ymben.2019.01.003.

[20] M. Diender, A. J. M. Stams, and D. Z. Sousa. "Production of medium-chain fatty acids and higher alcohols by a synthetic co-culture grown on carbon monoxide or syngas". In: *Biotechnology for Biofuels* 9.1 (Dec. 2016), p. 82. DOI: 10.1186/s13068-016-0495-0.

2

OVERFLOW METABOLISM AT THE THERMODYNAMIC LIMIT OF LIFE: HOW CARBOXYDOTROPHIC ACETOGENS MITIGATE CARBON MONOXIDE TOXICITY

Maximilienne Toetie Allaart, Martijn Diender, Diana Z. Sousa, Robbert Kleerebezem

2

ABSTRACT

Carboxydotrophic metabolism is gaining interest due to its applications in gas fermentation technology, enabling the conversion of carbon monoxide to fuels and commodities. Acetogenic carboxydotrophs play a central role in current gas fermentation processes. In contrast to other energy-rich microbial substrates, CO is highly toxic, which makes it a challenging substrate to utilize. Instantaneous scavenging of CO upon entering the cell is required to mitigate its toxicity. Experiments conducted with Clostridium autoethanogenum *at different biomass specific growth rates show that elevated ethanol production occurs at increasing growth rates. The increased allocation of electrons towards ethanol at higher growth rates strongly suggests that* C. autoethanogenum *employs a form of overflow metabolism to cope with high dissolved CO concentrations. We argue that this overflow branch enables acetogens to efficiently use CO at highly variable substrate influxes by increasing the conversion rate almost instantaneously when required to remove toxic substrate and promote growth. In this perspective we will address the case study of* C. autoethanogenum *grown solely on CO and syngas mixtures to assess how it employs acetate reduction to ethanol as a form of overflow metabolism.*

2.1. INTRODUCTION

CARBON-fixating acetogenic species have been characterized to convert CO_2, H_2 and CO to predominantly acetate and ethanol using the Wood-Ljungdahl pathway (WLP) [2, 3]. This conversion contributes substantially to the global carbon cycle as autotrophic acetogens fix CO_2 into biologically available molecules. Additionally, these microorganisms provide us with a novel avenue for reducing greenhouse gas emissions and producing liquid fuels from gaseous waste streams such as syngas [4–6]. To steer industrial gas fermentation efficiently, mechanistic understanding of the factors driving cellular metabolism is required.

Among the different substrates for gas fermentation, carbon monoxide in particular proves to be a highly interesting substrate. It contains a substantial amount of energy in the form of low-redox-potential electrons ($E^{0'}$=-520 mV) that can be directly transferred to ferredoxin. Reduced ferredoxin can, among other things, be used for the generation of a cation gradient using the Rnf or Ech complex [7]. These complexes allow acetogens to harvest energy from catabolic reactions that proceed close to thermodynamic equilibrium [8]. In catabolic pathways, electrons from the substrate are transferred to electron carriers such as NAD(P)(H), FAD(H) or ferredoxin and reallocated to different electron accepting reactions. This facilitates the evolutionary development of a wide variety of catabolic pathways and products. Generally, the catabolic flux can be carried by I) a long, energy efficient pathway or by II) a shorter pathway with a lower ATP yield that can run at a higher overall rate [9, 10]. Shifts in cellular strategy as a function of the (imposed) growth rate have been observed in cell types of different branches of the phylogenetic tree and are characterized by the utilization of energy-inefficient pathways at high catabolic rates [9, 11, 12]. This phenomenon is referred to as overflow metabolism. Different hypotheses have been posed to explain this effect, such as efficient proteome allocation, limited space in the cell membrane or cytosol, maximization of the ATP flux rather than yield, an upper limit to Gibbs energy dissipation or the number of active constraints on growth [10, 11, 13–16]. Switching from balanced to overflow metabolism proceeds almost instantaneously, implying that the enzymes needed for both efficient and inefficient pathways must always be expressed [10, 17]. The capacity to shift between balanced metabolism and overflow metabolism is a trait that provides flexibility and resilience towards ever changing environmental conditions.

In summary, overflow metabolism is the exploitation of a short, energetically inefficient metabolic route even when available nutrient concentrations are not limiting growth. This mechanism is used to optimally use cellular resources with the aim of maximizing the biomass-specific growth rate. Growth on gaseous substrates (H_2/CO_2, CO) is typically associated with highly variable substrate influxes and it has been recognized that ethanol production in gas-fermenting organisms is controlled by redox and thermodynamics rather than gene or protein expression levels [18–20]. To assimilate these findings, we pose that the reduction of acetate to ethanol is a form of overflow metabolism during acetogenic gas fermentation. This hypothesis will be assessed using a case study of *Clostridium autoethanogenum*, a model organism for carbon monoxide fermentation, using literature and thermodynamic

analyses. We aim to solidify the theory by identifying overflow-related traits in other carboxydotrophic acetogens.

2

2.2. Carbon monoxide dehydrogenase is the first step in CO detoxification

Acetogenic catabolism is highly dependent on carbon monoxide-sensitive metalloenzymes such as NiFe- or FeFe-hydrogenases to form intermediates for growth and to maintain cellular redox balance [21–23]. Carbon monoxide is known to bind metal clusters in enzymes and inhibit binding of their native substrates [24]. Therefore, carbon monoxide toxicity should be mitigated efficiently by carboxydotrophic organisms to prevent the ferredoxin pool to become completely reduced, or key enzymes to get inhibited. Carbon monoxide is detoxified by the carbon monoxide dehydrogenase enzyme (CODH), which catalyzes the oxidation of CO to CO_2 upon reduction of ferredoxin at a high specific activity [25, 26]. The maximum rate of diffusion of CO into the cell is defined by the concentration gradient between intra- and extracellular CO. Estimating the CO turnover rate using previously reported CODH activities and the absolute quantification of CODH concentration in *C. autoethanogenum* [26, 27], we find that this number is in the same order of magnitude as the flux of CO diffusion into the cell in a CO-saturated broth [28] (for calculation, see Box 2.1). This suggests that CO is detoxified to CO_2 immediately upon entering the cell, limiting inhibitory effects of CO on metalloenzymes. However, the capacity of the CODH to rapidly oxidize CO, even when diffusion into the cell is maximal, causes highly variable incoming fluxes of reduced ferredoxin. If the electrons carried by reduced ferredoxin cannot be re-allocated equally fast, this could lead to a metabolic arrest. To understand the effects of fluctuating reduced ferredoxin formation rates and how they can be mitigated, the metabolism and physiology of carboxydotrophic acetogens has to be examined.

2.3. Higher dilution rates lead to higher ethanol production rates in *C. autoethanogenum*

C. autoethanogenum is an acetogen that employs the Wood-Ljungdahl pathway for carbon fixation. This pathway leads to the production of acetate and ethanol as main products. In light of the objective to convert waste gas into (bio)fuels, substantial efforts have been made to shift the product spectrum of *C. autoethanogenum* and closely related species towards ethanol production, for example through medium optimization, changing the ingas composition and metabolic engineering [29–31]. The biochemistry of the Wood-Ljungdahl pathway allows for the highest ATP yield when acetate is produced as final product, due to the combination of ATP conservation from a cation gradient and substrate-level phosphorylation. This makes diverting the acetyl-CoA flux away from acetate towards ethanol via metabolic engineering approaches inherently difficult. Acetate formation on the one hand, and the conversion of acetate to ethanol on the other can also be viewed as

two separate metabolic strategies. Acetate formation from CO via the WLP is the longer, more efficient, strategy ($Y_{ATP/CO}$ = 0.375 mol/mol$_{CO}$) and the independent reduction of acetate to ethanol using CO is the shorter, inefficient strategy ($Y_{ATP/CO}$ = 0.27 mol/mol$_{CO}$) (fig. 2.1, table 2.1). This perspective leads to the hypothesis that autotrophic acetogens, even though they operate their catabolism much closer to thermodynamic equilibrium than for example sugar fermenters or aerobic microorganisms, can exhibit overflow metabolism.
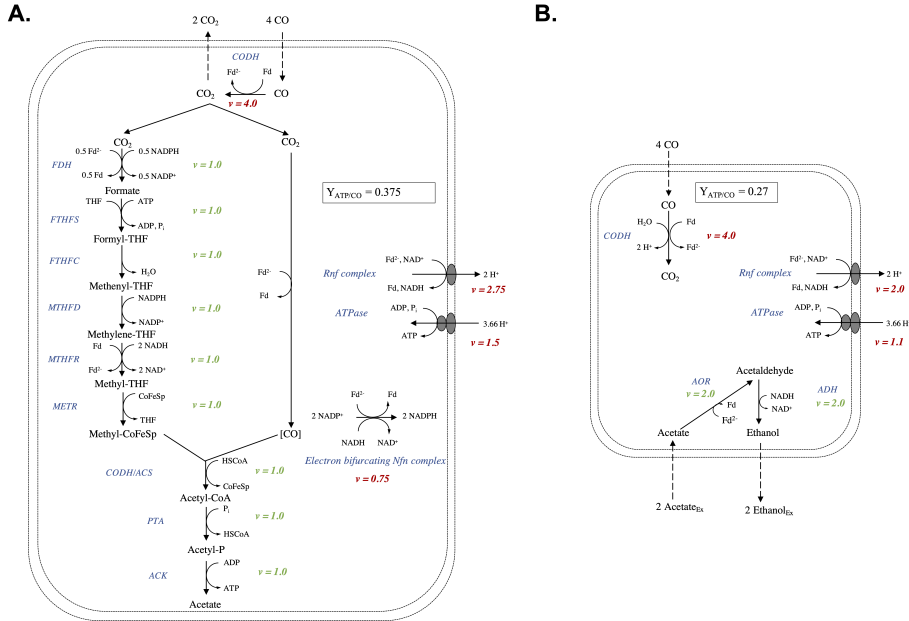
Figure 2.1: Energy-efficient (A) vs. energy-inefficient (B) CO catabolism in *Clostridium autoethanogenum* [3, 21, 23]. Energy-efficient CO fermentation leads to the production of acetate via the Wood-Ljungdahl or reductive acetyl-CoA pathway. Inefficient catabolism comprises the uptake of external acetate and reduction to ethanol with CO as electron donor. In both catabolic pathways, the electron bifurcating Rnf complex is pivotal for the harvesting of ATP through buildup of a proton gradient. The catabolic stoichiometries and fluxes through the enzymatic reactions in both A) and B) are represented per 4 mol of CO.

Independent CO-limited continuous cultivation studies show that at higher dilution rates and consequently higher growth rates (μ=D) more ethanol is produced (fig. 2.2). The dilution rate linearly correlated with the biomass-specific CO uptake rate, as increasing dilution rates were matched with an increased mass transfer rate by applying a faster stirring speed [32]. The authors note that 'These observations are not trivial as faster growth demands more energy while reduced products like ethanol [...] consume redox cofactors that acetogens could otherwise use for ATP generation'. Overflow metabolism provides a likely explanation for their observations. Beside this, transcriptome analysis reveals that the expression levels of the catabolic genes involved in production of both acetate and ethanol were expressed at similar

levels at different growth rates. However, higher transcript levels for genes involved in the synthesis of biomass and for the Rnf complex (used both in efficient and inefficient pathways) were found at higher growth rates [32]. The transcriptome data is in agreement with results reported in earlier studies, where catabolic transcript levels were also independent of growth conditions [19, 20]. This means that changes in product spectrum do not arise from changes in catabolic protein concentrations, but are driven by condition-imposed changes in metabolite levels.

Thus, the key characteristics of overflow metabolism are distinguished in continuous cultures of *C. autoethanogenum*:

1. The catabolic flux is increasingly diverted to an energy-inefficient pathway at increasing dilution rates (fig. 2.2)

2. No significant changes in transcriptome or proteome of the central carbon metabolism, including acetate conversion to ethanol, are observed at different growth rates but genes involved in biosynthesis are upregulated.

To expand our understanding of acetogen overflow metabolism on gaseous substrates, it should be noted that higher growth rates generally correspond to higher electron uptake rates. Inclusion of steady-state data obtained in chemostats fed with CO as well as H_2 by summing the biomass-specific CO and H_2 rates to an overall electron uptake rate ($q_{electron}$) also resulted in an apparent linear correlation between $q_{electron}$ and q_{EtOH} (fig. 2.2). This suggests that increased ethanol production generally allows for increased electron uptake rates. Like other types of overflow metabolism, acetate reduction to ethanol is thus exploited to sustain higher metabolic rates [10].

2.4. Theoretical pathway analysis – yield vs. rate trade-off

To understand the drivers of overflow metabolism, we can view the selection of the metabolic strategy as a yield vs. rate trade-off. The difference between energy-efficient and energy-inefficient metabolism is in fact the extent to which the free energy generated in a metabolic pathway can be harvested by the microorganism. Harvesting energy as ATP allows for re-allocation to other cellular processes such as growth and maintenance. However, dissipating free energy is required to enable flux in the process. In other words, energy dissipation generates driving force towards the production of a certain metabolite. As stated above, ethanol is used as an electron sink when the influx of electrons increases (fig. 2.2). As the production of ethanol requires the consumption of a reduced ferredoxin (fig. 2.1), less reduced ferredoxin will be available for the generation of a chemiosmotic gradient from which ATP can be harvested. Thus, on average more energy is dissipated per reaction step in ethanol formation and cells producing ethanol operate further away from the thermodynamic limit (table 2.1). Following the flux-force relationship, reactions that are further away from thermodynamic equilibrium generally proceed at a higher flux [14, 36, 37]. In acetogenic metabolism, imposing a higher electron flux in turn leads
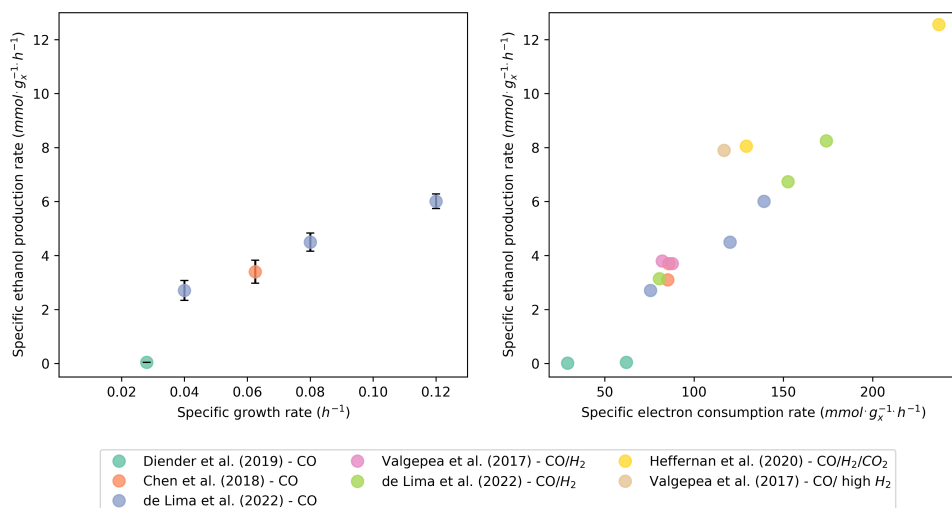
Figure 2.2: Dependency of the biomass-specific ethanol production rate (q_{EtOH}) on specific growth- and electron uptake rate of *C. autoethanogenum*. Panel A: q_{EtOH} data was obtained from three independent studies [32–34] and plotted as a function of the reported μ. All studies were performed in gas-liquid mass transfer-limited continuous cultures fed with CO as only carbon- and electron source, either in chemostat or in a bubble column. One study [34] was executed at higher pH than the other two studies (6.2 vs 5). Low pH is known to trigger solventogenesis [20], which may explain the slight diversion of q_{EtOH} in this study as compared to the trend through the other datasets. Panel B: chemostat studies fed with mixtures of CO, H_2 and CO_2 were compiled by plotting the electron uptake rate ($\sum(q_{CO} + q_{H_2}) \cdot 2$) versus the observed ethanol production rate. Seven different datasets of continuous cultures with *C. autoethanogenum* were included in this analysis [4, 31–35].

the system to move further away from thermodynamic equilibrium by diverting more of the incoming electrons to ethanol rather than acetate (fig. 2.2). Furthermore, it has been observed that chemostat cultures of *C. autoethanogenum* grown on H_2/CO_2 mixtures, the metabolism with the lowest energy dissipation, washed out when doubling the dilution rate from 0.02 h^{-1} to 0.04 h^{-1} whereas CO-fed cultures could be grown at up to 0.12 h^{-1} [4, 32]. These observations all confirm that there is a relationship between energy dissipation and flux [38]. Thus, the product spectrum of acetogenic syngas fermentation is subject to a rate vs. yield trade-off, which in essence is a trade-off between harvesting and dissipating Gibbs free energy. This complies with the conclusions in earlier work that stated that the metabolism of the acetogens *C. autoethanogenum* and *C. ljungdahlii* is not subject to transcriptional regulation [19, 20]. The outcome of the trade-off between dissipating and harvesting energy can therefore be controlled when imposing a certain amount of energy dissipation by imposing a certain flux. This can be achieved by controlling the biomass-specific growth rate or the biomass-specific electron uptake rate (fig. 2.2).

21

Table 2.1: Free energy change, ATP yield per mol of electron donor based on the enzymes depicted in Figure 1 and percentage of the free energy harvested in ATP.

Stoichiometry	ΔG^{01} [kJ/mol$_{Ed}$]	$Y_{ATP/Ed}$ [mol/mol$_{Ed}$]	$Y_{ATP,max}$ [mol/mol$_{Ed}$]	$\Delta G_{harvest}$ [kJ/mol$_{Ed}$]	no. reactions [-]	ΔG_{dis} [kJ/reaction]
$2CO_2+4H_2 \rightarrow C_2H_4O_2+2CO_2$	-13.8	0.240	0.31	78%	14	-0.9
$4CO+2H_2O \rightarrow C_2H_4O_2+2CO_2$	-33.8	0.375	0.75	50%	12	-5.6
$2CO+C_2H_4O_2 \rightarrow C_2H_6O+2CO_2$	-41.0	0.273	0.91	30%	4	-14.4

The ATP yield per electron donor was calculated assuming a Rnf complex stoichiometry of 1 H+ extruded per electron transferred and a H+/ATP stoichiometry of 3.66. To calculate the maximum ATP yield, it was assumed that 45 kJ of Gibbs free energy are required to produce 1 mole of ATP. The number of reactions was calculatedby counting the number of carbon molecule-altering biochemical steps and multiplying them by their respective fluxes.

2.5. EXPANDING THE HYPOTHESIS: CO OVERFLOW METABOLISM IN THE ACETOGEN ECOLOGICAL NICHE

Verification of the overflow hypothesis in other carboxydotrophic acetogens is limited by the lack of comparable cultivations described in literature. Few studies cultivate in chemostats fed with CO as only carbon- and energy source, let alone at different growth rates. However, careful examination of various sources does point at the exhibition of overflow metabolism in other species that are genetically highly similar to *C. autoethanogenum* and harbor the same set of enzymes for acetate and ethanol production [39–41]. First of all, ethanol has been proposed to be an overflow product of which the production is thermodynamically controlled in *C. ljungdahlii* [20] . This control is, however, linked to a certain critical concentration of acetic acid and reduced electron carriers inside the cell. Similarly, a genome-scale metabolic model of *C. ljungdahlii* predicts ethanol to be an overflow product [42]. In both studies, the experimental data to link overflow metabolism to growth- or electron uptake rate is lacking. In a batch bioreactor with *Clostridium sp. AWRP* decreasing the gas flow rate led to less ethanol and more acetate production, whereas increasing the stirring speed at the same gas flow rate led to acetate consumption and ethanol formation[40]. By controlling the gas flow rate and stirring speed both the mass transfer- and thereby the biomass-specific electron uptake rates are controlled. This is a clear indication that this species exploits overflow metabolism to manage increasing electron influxes. Even in batch bottle cultivations of *Clostridium carboxidivorans* a negative correlation between acetate concentration and agitation speed can be distinguished, whereas alcohol (ethanol, butanol and hexanol) concentrations keep increasing with increasing agitation [43].

More generally, organisms capable of growth on CO-rich gases have an additional electron sink beside acetate. For *C. autoethanogenum* and *C. ljungdahlii* this is ethanol formation [20, 42], whereas *C. carboxidivorans* can produce ethanol, butanol and hexanol [43, 44]. Furthermore, the well-studied thermophilic CO fermenter *Moorella thermoacetica* is capable of proton reduction to H_2 using electrons from CO, providing it with a non-organic electron sink [45]. Lastly, the gut bacterium *Eubacterium limosum* has been characterized to produce ethanol, butyrate and butanol from CO [46]. Interestingly, *Acetobacterium woodii* is only known to produce acetate and suffers from CO at increasing CO partial pressures [47]. The catabolic routes that these microorganisms employ for the reallocation of increased electron fluxes require organic acids as a precursor. Acetate is the product of their efficient catabolism, but other weak acids (i.e., butyrate, hexanoate) can originate from the fermentation of organic carbon sources. This gives a perspective on the ecological niche of CO-utilizing species, namely that organic acids are plentiful in their native environments. The abundance of CO-consuming acetogens in soils and the fact that *C. autoethanogenum* particularly was isolated from a rabbit gut confirms this perspective [28, 48]. Additionally, this suggests that higher concentrations of acetate boost the uptake capacity of CO consumers. Indeed, increased overflow product formation has been observed in different studies upon acetate supply [20, 23, 34, 46, 49, 50]. Besides an increased capacity for electron reallocation, overflow products

can be re-used when substrate is scarcer [51–53].

To provide a full picture of overflow metabolism in *C. autoethanogenum* and other CO-consuming acetogens, future experimental work should be directed at showing the effect of increasing CO supply at (very) low extracellular acetate concentrations. If the theory applies, the microorganisms will sustain lower biomass-specific CO uptake rates than when acetate is available in abundance.

2.6. Overflow metabolism is used to prevent over-reduction of electron carrier pools

To prevent toxicity effects of CO, carboxydotrophic microorganisms need reliable mechanisms to deal with variable substrate influxes. The high turnover rates of the CODH enzyme ensure low intracellular CO concentrations. However, the conversion of CO to CO_2 via the CODH also results in production of reduced ferredoxin. The rate of oxidation of CO therefore directly influences the redox state of the cell, as ferredoxin needs to be re-oxidized at an equally high rate to maintain cellular homeostasis. The primary mechanism for ferredoxin re-oxidation in carboxydotrophic acetogens is through the generation of a cation gradient via the Rnf complex or similar enzymes. This bifurcating enzyme transfers the electrons from reduced ferredoxin to NAD^+, generating NADH that again must be re-oxidized. NADH oxidation through acetate formation requires 12 enzymatic steps (table 2.1, whereas only 4 steps are employed in the acetate reduction to ethanol. Considering a situation where the CO influx is high, ethanol formation has the additional advantage of consuming a reduced ferredoxin for the formation of acetaldehyde. Thus, ethanol formation provides a route that contributes both to ferredoxin and NADH reoxidation and that requires few enzymes compared to acetate formation. If the enzymes for ethanol production would not be available, all the enzymes of the WLP would either have to be quickly upregulated to sustain a higher flux or always be highly expressed to be able to deal with changing conditions. Expressing only two additional enzymes (AOR and ADH) to increase the capacity of re-oxidizing electron carriers is more efficient from a resource allocation point of view. The continuous availability of the enzymes for acetate reduction to ethanol, despite non-solventogenic conditions [20] fits the theory that this pathway is used for overflow metabolism. Consistent presence of the machinery of this pathway allows to directly deal with sudden increases in CO supply and prevent over-reduction of the electron carrier pools. This is also reflected in the observation that start-up of CO-fed systems is easier when acetate or even other carboxylic acids are added to the culture medium [50, 54]. The overflow function of these enzymes is also supported by the observation that acetogens lacking the AOR enzyme, such as *A. woodii*, are prone to inhibition by CO as a substrate [47].

2.7. CONCLUDING REMARKS

Overflow metabolism is a mechanism for cellular resilience and most likely spans all branches of the phylogenetic tree of life. Here, we propose that overflow metabolism can also be observed in microorganisms that operate their catabolism close to thermodynamic equilibrium. The ecological niche of the microorganism could have a defining role in the actual physiology that is exploited in overflow conditions. Fundamental understanding of the drivers of product formation in CO-consuming acetogenic microorganisms allows for process optimization independent of complex and laborious genetic engineering approaches. More specifically, we propose that the product spectrum of gas fermentation can be controlled through controlling either the specific growth rate or the biomass-specific CO uptake rate in bioreactors.

2

Box 2.1. Cellular CODH capacity and CO diffusion into the cell

The orders of magnitude of the capacity of the CODH enzyme and the maximum rate of diffusion of CO into a cell give a clear perspective of the efficiency of the CODH enzyme for CO detoxification. These rates can be calculated from a number of biological and physicochemical parameters, respectively.

Calculating the activity of CODH

In this calculation, kinetic parameters and molecular weight (MW_{CODH}) reported for CODH2 of *Carboxidothermus hydrogenoformans* are used [26]. The concentration of CODH in *C. autoethanogenum* was quantified by [27]. The weight of a bacterial cell (m_{cell}) was assumed to be 1 picogram. The following parameters were used to calculate the CODH activity:

Parameter	Value	Unit
Specific activity	$2.3 \cdot 10^{-1}$	$mol_{CO} \cdot s^{-1} \cdot g_{CODHII}^{-1}$
c_{CODH}	$122 \cdot 10^{-9}$	$mol \cdot g_x^{-1}$
MW_{CODH}	$129 \cdot 10^{-3}$	$g_x \cdot mol^{-1}$

CODH activity = Specific activity x c_{CODH} x MW_{CODH} x m_{cell} = $3.63 \cdot 10^{-15}$ $mol \cdot s^{-1}$

Calculating the rate of CO diffusion into the cell

Here, the diffusion rate of CO into the cell was calculated at 25°C. It was assumed that the diffusion coefficient in the cell membrane is equal to the diffusion coefficient in water. Gas diffusion measurements in natural ester mixtures confirm that this assumption will give an estimate in the correct order of magnitude [55].

Parameter	Value	Unit
D_{CO}	$2.03 \cdot 10^{-9}$	$m^2 \cdot s^{-1}$
c_{CO}^*	$9.85 \cdot 10^{-4}$	$mol \cdot L^{-1}$
L_{cell}	$5 \cdot 10^{-6}$	m
D_{cell}	$5 \cdot 10^{-7}$	m
$D_{membrane}$	$75 \cdot 10^{-10}$	m

The diffusion flux can be calculated using Fick's law:

$$J = -D\frac{dc}{dx}$$

with $dc = c_{CO}^*$ (assuming the CO concentration in the cell is zero) and $dx = D_{membrane}$. Then:

$$J = 2.67 \cdot 10^{-4} mol \cdot m^{-2} \cdot s^{-1}$$

To convert this to the flux per cell, the surface area of the cell was calculated assuming the cell is a cylindrical rod. The diffusion flux was multiplied by the cell surface area, giving:

CO diffusion rate = $2.3 \cdot 10^{-15} mol \cdot s^{-1}$

BIBLIOGRAPHY

[1] M. T. Allaart, M. Diender, D. Z. Sousa, and R. Kleerebezem. "Overflow metabolism at the thermodynamic limit of life: How carboxydotrophic acetogens mitigate carbon monoxide toxicity". In: *Microbial Biotechnology* 16.4 (Apr. 2023), pp. 697–705. DOI: 10.1111/1751-7915.14212.

[2] H. G. Wood. "Life with CO or CO_2 and H_2 as a source of carbon and energy". In: *The FASEB Journal* 5.2 (Feb. 1991), pp. 156–163. DOI: 10.1096/fasebj.5.2.1900793.

[3] H. G. Wood, S. W. Ragsdale, and E. Pezacka. "The acetyl-CoA pathway of autotrophic growth". In: *FEMS Microbiology Letters* 39.4 (Oct. 1986), pp. 345–362. DOI: 10.1111/j.1574-6968.1986.tb01865.x.

[4] J. K. Heffernan, K. Valgepea, R. De Souza Pinto Lemgruber, I. Casini, M. Plan, R. Tappel, S. D. Simpson, M. Köpke, L. K. Nielsen, and E. Marcellin. "Enhancing CO_2-Valorization Using *Clostridium autoethanogenum* for Sustainable Fuel and Chemicals Production". In: *Frontiers in Bioengineering and Biotechnology* 8 (Mar. 2020), p. 204. DOI: 10.3389/fbioe.2020.00204.

[5] E. Marcellin, J. B. Behrendorff, S. Nagaraju, S. DeTissera, S. Segovia, R. W. Palfreyman, J. Daniell, C. Licona-Cassani, L.-e. Quek, R. Speight, M. P. Hodson, S. D. Simpson, W. P. Mitchell, M. Köpke, and L. K. Nielsen. "Low carbon fuels and commodity chemicals from waste gases – systematic approach to understand energy metabolism in a model acetogen". In: *Green Chemistry* 18.10 (2016), pp. 3020–3028. DOI: 10.1039/C5GC02708J.

[6] B. Molitor, H. Richter, M. E. Martin, R. O. Jensen, A. Juminaga, C. Mihalcea, and L. T. Angenent. "Carbon recovery by fermentation of CO-rich off gases – Turning steel mills into biorefineries". In: *Bioresource Technology* 215 (Sept. 2016), pp. 386–396. DOI: 10.1016/j.biortech.2016.03.094.

[7] W. Buckel and R. K. Thauer. "Flavin-Based Electron Bifurcation, A New Mechanism of Biological Energy Coupling". In: *Chemical Reviews* 118.7 (Apr. 2018), pp. 3862–3886. DOI: 10.1021/acs.chemrev.7b00707.

[8] K. Schuchmann and V. Müller. "Autotrophy at the thermodynamic limit of life: a model for energy conservation in acetogenic bacteria". In: *Nature Reviews Microbiology* 12.12 (Dec. 2014), pp. 809–821. DOI: 10.1038/nrmicro3365.

[9] E. Costa, J. Pérez, and J.-U. Kreft. "Why is metabolic labour divided in nitrification?" In: *Trends in Microbiology* 14.5 (May 2006), pp. 213–219. DOI: 10.1016/j.tim.2006.03.006.

[10] D. Molenaar, R. Van Berlo, D. De Ridder, and B. Teusink. "Shifts in growth strategies reflect tradeoffs in cellular economics". In: *Molecular Systems Biology* 5.1 (Jan. 2009), p. 323. DOI: 10.1038/msb.2009.82.

[11] M. Basan, S. Hui, H. Okano, Z. Zhang, Y. Shen, J. R. Williamson, and T. Hwa. "Overflow metabolism in Escherichia coli results from efficient proteome allocation". In: *Nature* 528.7580 (Dec. 2015), pp. 99–104. DOI: 10.1038/nature15765.

[12] M. V. Liberti and J. W. Locasale. "The Warburg Effect: How Does it Benefit Cancer Cells?" In: *Trends in Biochemical Sciences* 41.3 (Mar. 2016), pp. 211–218. DOI: 10.1016/j.tibs.2015.12.001.

[13] D. H. De Groot, C. Van Boxtel, R. Planqué, F. J. Bruggeman, and B. Teusink. "The number of active metabolic pathways is bounded by the number of cellular constraints at maximal metabolic rates". In: *PLOS Computational Biology* 15.3 (Mar. 2019). Ed. by V. Hatzimanikatis, e1006858. DOI: 10.1371/journal.pcbi.1006858.

[14] A. Flamholz, E. Noor, A. Bar-Even, W. Liebermeister, and R. Milo. "Glycolytic strategy as a tradeoff between energy yield and protein cost". In: *Proceedings of the National Academy of Sciences* 110.24 (June 2013), pp. 10039–10044. DOI: 10.1073/pnas.1215283110.

[15] A. Goel, T. H. Eckhardt, P. Puri, A. De Jong, F. Branco Dos Santos, M. Giera, F. Fusetti, W. M. De Vos, J. Kok, B. Poolman, D. Molenaar, O. P. Kuipers, and B. Teusink. "Protein costs do not explain evolution of metabolic strategies and regulation of ribosomal content: does protein investment explain an anaerobic bacterial Crabtree effect?: Protein costs and evolution of metabolic strategies". In: *Molecular Microbiology* 97.1 (July 2015), pp. 77–92. DOI: 10.1111/mmi.13012.

[16] B. Niebel, S. Leupold, and M. Heinemann. "An upper limit on Gibbs energy dissipation governs cellular metabolism". In: *Nature Metabolism* 1.1 (Jan. 2019), pp. 125–132. DOI: 10.1038/s42255-018-0006-7.

[17] F. J. Bruggeman, R. Planqué, D. Molenaar, and B. Teusink. "Searching for principles of microbial physiology". In: *FEMS Microbiology Reviews* 44.6 (Nov. 2020), pp. 821–844. DOI: 10.1093/femsre/fuaa034.

[18] J. L. Cotter, M. S. Chinn, and A. M. Grunden. "Influence of process parameters on growth of *Clostridium ljungdahlii* and *Clostridium autoethanogenum* on synthesis gas". In: *Enzyme and Microbial Technology* 44.5 (May 2009), pp. 281–288. DOI: 10.1016/j.enzmictec.2008.11.002.

[19] V. Mahamkali, K. Valgepea, R. De Souza Pinto Lemgruber, M. Plan, R. Tappel, M. Köpke, S. D. Simpson, L. K. Nielsen, and E. Marcellin. "Redox controls metabolic robustness in the gas-fermenting acetogen *Clostridium autoethanogenum*". In: *Proceedings of the National Academy of Sciences* 117.23 (June 2020), pp. 13168–13175. DOI: 10.1073/pnas.1919531117.

[20] H. Richter, B. Molitor, H. Wei, W. Chen, L. Aristilde, and L. T. Angenent. "Ethanol production in syngas-fermenting *Clostridium ljungdahlii* is controlled by thermodynamics rather than by enzyme expression". In: *Energy & Environmental Science* 9.7 (2016), pp. 2392–2399. DOI: 10.1039/C6EE01108J.

[21] J. Mock, Y. Zheng, A. P. Mueller, S. Ly, L. Tran, S. Segovia, S. Nagaraju, M. Köpke, P. Dürre, and R. K. Thauer. "Energy Conservation Associated with Ethanol Formation from H_2 and CO_2 in *Clostridium autoethanogenum* Involving Electron Bifurcation". In: *Journal of Bacteriology* 197.18 (Sept. 2015). Ed. by W. W. Metcalf, pp. 2965–2980. DOI: 10.1128/JB.00399-15.

[22] K. Schuchmann, N. P. Chowdhury, and V. Müller. "Complex Multimeric [FeFe] Hydrogenases: Biochemistry, Physiology and New Opportunities for the Hydrogen Economy". In: *Frontiers in Microbiology* 9 (Dec. 2018), p. 2911. DOI: 10.3389/fmicb.2018.02911.

[23] S. Wang, H. Huang, J. Kahnt, A. P. Mueller, M. Köpke, and R. K. Thauer. "NADP-Specific Electron-Bifurcating [FeFe]-Hydrogenase in a Functional Complex with Formate Dehydrogenase in *Clostridium autoethanogenum* Grown on CO". In: *Journal of Bacteriology* 195.19 (Oct. 2013), pp. 4373–4386. DOI: 10.1128/JB.00678-13.

[24] S. Menon and S. W. Ragsdale. "Unleashing Hydrogenase Activity in Carbon Monoxide Dehydrogenase/Acetyl-CoA Synthase and Pyruvate:Ferredoxin Oxidoreductase". In: *Biochemistry* 35.49 (Jan. 1996), pp. 15814–15821. DOI: 10.1021/bi9615598.

[25] S. W. Ragsdale. "Enzymology of the Wood-Ljungdahl Pathway of Acetogenesis". In: *Annals of the New York Academy of Sciences* 1125.1 (Mar. 2008), pp. 129–136. DOI: 10.1196/annals.1419.015.

[26] V. Svetlitchnyi, C. Peschel, G. Acker, and O. Meyer. "Two Membrane-Associated NiFeS-Carbon Monoxide Dehydrogenases from the Anaerobic Carbon-Monoxide-Utilizing Eubacterium *Carboxydothermus hydrogenoformans*". In: *Journal of Bacteriology* 183.17 (Sept. 2001), pp. 5134–5144. DOI: 10.1128/JB.183.17.5134-5144.2001.

[27] K. Valgepea, G. Talbo, N. Takemori, A. Takemori, C. Ludwig, V. Mahamkali, A. P. Mueller, R. Tappel, M. Köpke, S. D. Simpson, L. K. Nielsen, and E. Marcellin. "Absolute Proteome Quantification in the Gas-Fermenting Acetogen *Clostridium autoethanogenum*". en. In: *mSystems* 7.2 (Apr. 2022). Ed. by K. Faust, e00026–22. DOI: 10.1128/msystems.00026-22.

[28] J. Abrini, H. Naveau, and E.-J. Nyns. "*Clostridium autoethanogenum*, sp. nov., an anaerobic bacterium that produces ethanol from carbon monoxide". In: *Archives of Microbiology* 161 (1993).

[29] C.-M. Klask, N. Kliem-Kuster, B. Molitor, and L. T. Angenent. "Nitrate Feed Improves Growth and Ethanol Production of *Clostridium ljungdahlii* With CO_2 and H_2, but Results in Stochastic Inhibition Events". In: *Frontiers in Microbiology* 11 (May 2020), p. 724. DOI: 10.3389/fmicb.2020.00724.

[30] F. Liew, A. M. Henstra, M. Köpke, K. Winzer, S. D. Simpson, and N. P. Minton. "Metabolic engineering of *Clostridium autoethanogenum* for selective alcohol production". In: *Metabolic Engineering* 40 (Mar. 2017), pp. 104–114. DOI: 10.1016/j.ymben.2017.01.007.

[31] K. Valgepea, R. De Souza Pinto Lemgruber, K. Meaghan, R. W. Palfreyman, T. Abdalla, B. D. Heijstra, J. B. Behrendorff, R. Tappel, M. Köpke, S. D. Simpson, L. K. Nielsen, and E. Marcellin. "Maintenance of ATP Homeostasis Triggers Metabolic Shifts in Gas-Fermenting Acetogens". In: *Cell Systems* 4.5 (May 2017), 505–515.e5. DOI: 10.1016/j.cels.2017.04.008.

[32] L. A. De Lima, H. Ingelman, K. Brahmbhatt, K. Reinmets, C. Barry, A. Harris, E. Marcellin, M. Köpke, and K. Valgepea. "Faster Growth Enhances Low Carbon Fuel and Chemical Production Through Gas Fermentation". In: *Frontiers in Bioengineering and Biotechnology* 10 (Apr. 2022), p. 879578. DOI: 10.3389/fbioe.2022.879578.

[33] J. Chen, J. Daniell, D. Griffin, X. Li, and M. A. Henson. "Experimental testing of a spatiotemporal metabolic model for carbon monoxide fermentation with *Clostridium autoethanogenum*". In: *Biochemical Engineering Journal* 129 (Jan. 2018), pp. 64–73. DOI: 10.1016/j.bej.2017.10.018.

[34] M. Diender, I. Parera Olm, M. Gelderloos, J. J. Koehorst, P. J. Schaap, A. J. M. Stams, and D. Z. Sousa. "Metabolic shift induced by synthetic co-cultivation promotes high yield of chain elongated acids from syngas". In: *Scientific Reports* 9.1 (Dec. 2019), p. 18081. DOI: 10.1038/s41598-019-54445-y.

[35] K. Valgepea, R. De Souza Pinto Lemgruber, T. Abdalla, S. Binos, N. Takemori, A. Takemori, Y. Tanaka, R. Tappel, M. Köpke, S. D. Simpson, L. K. Nielsen, and E. Marcellin. "H2 drives metabolic rearrangements in gas-fermenting *Clostridium autoethanogenum*". In: *Biotechnology for Biofuels* 11.1 (Dec. 2018), p. 55. DOI: 10.1186/s13068-018-1052-9.

[36] D. A. Beard and H. Qian. "Relationship between Thermodynamic Driving Force and One-Way Fluxes in Reversible Processes". In: *PLoS ONE* 2.1 (Jan. 2007). Ed. by T. Secomb, e144. DOI: 10.1371/journal.pone.0000144.

[37] Y. Peng, H. Qian, D. A. Beard, and H. Ge. "Universal relation between thermodynamic driving force and one-way fluxes in a nonequilibrium chemical reaction with complex mechanism". In: *Physical Review Research* 2.3 (July 2020), p. 033089. DOI: 10.1103/PhysRevResearch.2.033089.

[38] J. Rodríguez, J. M. Lema, and R. Kleerebezem. "Energy-based models for environmental biotechnology". In: *Trends in Biotechnology* 26.7 (July 2008), pp. 366–374. DOI: 10.1016/j.tibtech.2008.04.003.

[39] S. D. Brown, S. Nagaraju, S. Utturkar, S. De Tissera, S. Segovia, W. Mitchell, M. L. Land, A. Dassanayake, and M. K\"{o}pke. "Comparison of single-molecule sequencing and hybrid approaches for finishing the genome of *Clostridium autoethanogenum* and analysis of CRISPR systems in industrial relevant *Clostridia*". In: *Biotechnology for Biofuels* 7.1 (Dec. 2014), p. 40. DOI: 10.1186/1754-6834-7-40.

[40] J. Lee, J. W. Lee, C. G. Chae, S. J. Kwon, Y. J. Kim, J.-H. Lee, and H. S. Lee. "Domestication of the novel alcohologenic acetogen *Clostridium* sp. AWRP: from isolation to characterization for syngas fermentation". In: *Biotechnology for Biofuels* 12.1 (Dec. 2019), p. 228. DOI: 10.1186/s13068-019-1570-0.

[41] J. S.-C. Liou, D. L. Balkwill, G. R. Drake, and R. S. Tanner. "*Clostridium carboxidivorans* sp. nov., a solvent-producing clostridium isolated from an agricultural settling lagoon, and reclassification of the acetogen *Clostridium scatologenes* strain SL1 as *Clostridium drakei sp. nov.*" In: *International Journal of Systematic and Evolutionary Microbiology* 55.5 (Sept. 2005), pp. 2085–2091. DOI: 10.1099/ijs.0.63482-0.

[42] J. K. Liu, C. Lloyd, M. M. Al-Bassam, A. Ebrahim, J.-N. Kim, C. Olson, A. Aksenov, P. Dorrestein, and K. Zengler. "Predicting proteome allocation, overflow metabolism, and metal requirements in a model acetogen". In: *PLOS Computational Biology* 15.3 (Mar. 2019). Ed. by C. Henry, e1006848. DOI: 10.1371/journal.pcbi.1006848.

[43] J. R. Phillips, H. K. Atiyeh, R. S. Tanner, J. R. Torres, J. Saxena, M. R. Wilkins, and R. L. Huhnke. "Butanol and hexanol production in *Clostridium carboxidivorans* syngas fermentation: Medium development and culture techniques". In: *Bioresource Technology* 190 (Aug. 2015), pp. 114–121. DOI: 10.1016/j.biortech.2015.04.043.

[44] K. M. Hurst and R. S. Lewis. "Carbon monoxide partial pressure effects on the metabolic process of syngas fermentation". In: *Biochemical Engineering Journal* 48.2 (Jan. 2010), pp. 159–165. DOI: 10.1016/j.bej.2009.09.004.

2

[45] D. R. Martin, L. L. Lundie, R. Kellum, and H. L. Drake. "Carbon monoxide-dependent evolution of hydrogen by the homoacetate-fermenting bacterium *Clostridium thermoaceticum*". In: *Current Microbiology* 8.6 (Nov. 1983), pp. 337–340. DOI: 10.1007/BF01573705.

[46] S. Park, M. Yasin, J. Jeong, M. Cha, H. Kang, N. Jang, I.-G. Choi, and I. S. Chang. "Acetate-assisted increase of butyrate production by *Eubacterium limosum* KIST612 during carbon monoxide fermentation". In: *Bioresource Technology* 245 (Dec. 2017), pp. 560–566. DOI: 10.1016/j.biortech.2017.08.132.

[47] J. Bertsch and V. Müller. "Bioenergetic constraints for conversion of syngas to biofuels in acetogenic bacteria". In: *Biotechnology for Biofuels* 8.1 (Dec. 2015), p. 210. DOI: 10.1186/s13068-015-0393-x.

[48] P. F. Levy, G. W. Barnard, D. V. Garcia-Martinez, J. E. Sanderson, and D. L. Wise. "Organic acid production from CO_2/H_2 and CO/H_2 by mixed-culture anaerobes". In: *Biotechnology and Bioengineering* 23.10 (Oct. 1981), pp. 2293–2306. DOI: 10.1002/bit.260231012.

[49] S. J. Kwon, J. Lee, and H. S. Lee. "Acetate-assisted carbon monoxide fermentation of *Clostridium* sp. AWRP". In: *Process Biochemistry* 113 (Feb. 2022), pp. 47–54. DOI: 10.1016/j.procbio.2021.12.015.

[50] H. Xu, C. Liang, X. Chen, J. Xu, Q. Yu, Y. Zhang, and Z. Yuan. "Impact of exogenous acetate on ethanol formation and gene transcription for key enzymes in *Clostridium autoethanogenum* grown on CO". In: *Biochemical Engineering Journal* 155 (Mar. 2020), p. 107470. DOI: 10.1016/j.bej.2019.107470.

[51] J. Bertsch, A. L. Siemund, F. Kremp, and V. Müller. "A novel route for ethanol oxidation in the acetogenic bacterium *Acetobacterium woodii* : the acetaldehyde/ethanol dehydrogenase pathway". In: *Environmental Microbiology* 18.9 (Sept. 2016), pp. 2913–2922. DOI: 10.1111/1462-2920.13082.

[52] B. Enjalbert, P. Millard, M. Dinclaux, J.-C. Portais, and F. Létisse. "Acetate fluxes in *Escherichia coli* are determined by the thermodynamic control of the Pta-AckA pathway". In: *Scientific Reports* 7.1 (Feb. 2017), p. 42135. DOI: 10.1038/srep42135.

[53] Z.-Y. Liu, D.-C. Jia, K.-D. Zhang, H.-F. Zhu, Q. Zhang, W.-H. Jiang, Y. Gu, and F.-L. Li. "Ethanol Metabolism Dynamics in Clostridium ljungdahlii Grown on Carbon Monoxide". In: *Applied and Environmental Microbiology* 86.14 (July 2020). Ed. by M. J. Pettinari, e00730–20. DOI: 10.1128/AEM.00730-20.

[54] J. M. Perez, H. Richter, S. E. Loftus, and L. T. Angenent. "Biocatalytic reduction of short-chain carboxylic acids into their corresponding alcohols with syngas fermentation". In: *Biotechnology and Bioengineering* 110.4 (Apr. 2013), pp. 1066–1077. DOI: 10.1002/bit.24786.

[55] W. Ye, J. Hao, Y. Chen, M. Zhu, Z. Pan, and F. Hou. "Difference Analysis of Gas Molecules Diffusion Behavior in Natural Ester and Mineral Oil Based on Molecular Dynamic Simulation". In: *Molecules* 24.24 (Dec. 2019), p. 4463. DOI: 10.3390/molecules24244463.

3

A NOVEL EXPERIMENTAL METHOD TO DETERMINE SUBSTRATE UPTAKE KINETICS OF GASEOUS SUBSTRATES APPLIED TO CARBON MONOXIDE-FERMENTING *Clostridium autoethanogenum*

Maximilienne Toetie Allaart, Harry Korkontzelos, Diana Z. Sousa, Robbert Kleerebezem

3

ABSTRACT

Syngas fermentation has gained momentum over the last decades. Cost-efficient design of industrial-scale bioprocesses is highly dependent on quantitative microbial growth data. Kinetic and stoichiometric models have been developed for syngas-converting microbes, but accurate experimental validation of the derived parameters is lacking. Here, we describe a novel experimental approach for measuring substrate uptake kinetics of gas-fermenting microbes, using the model microorganism Clostridium autoethanogenum. *One-hour disturbances of a steady-state chemostat bioreactor with increased CO partial pressures (up to 1.2 bar) allowed for measurement of biomass-specific CO uptake- and CO_2 production rates (q_{CO}, q_{CO_2}), using off-gas analysis. At a p_{CO} of 1.2 bar, a q_{CO} of -119 ± 1 $mmol \cdot g_x^{-1} \cdot h^{-1}$ was measured. This value is 1.8 to 3.5-fold higher than previously reported experimental and kinetic modelling results for syngas fermenters. Analysis of the catabolic flux distribution reveals a metabolic shift towards ethanol production at the expense of acetate at p_{CO} ≥ 0.6 atm, which is likely to be mediated by acetate availability and cellular redox state. The metabolic shift was characterized as acetogenic overflow metabolism. These results provide key mechanistic understanding of the factors steering the product spectrum of CO fermentation in* C. autoethanogenum *and emphasize the importance of dedicated experimental validation of kinetic parameters*

3.1. INTRODUCTION

O NE of the most important challenges of our society today is to effectively transition from a petrol-based to a circular economy. Reaching a circular economy requires waste streams to be perceived as resources. Gasification provides an avenue for the reuse of recalcitrant or non-biodegradable waste streams and yields carbon monoxide (CO)-rich syngas [1]. CO is a source of both carbon and energy that can be (biologically) assimilated into chemical building blocks. Another CO-rich waste stream is flue gas, which originates from steel processing [2]. This gas is currently detoxified by combustion, leading to approximately 3.9 billion tonnes of CO_2 emissions per year [3, 4]. Thus, for the transition to a bio-based society, a robust technology for the conversion of CO into chemical building blocks is needed.

Purely chemical gas conversion processes such as Fischer-Tropsch synthesis are sensitive to gas composition and impurities [5]. Therefore, novel technologies for syngas and flue gas conversion must be developed. Anaerobic acetogenic microorganisms are known to convert syngas constituents into products such as acetate and ethanol [6–9]. These organisms are less sensitive to changes in gas composition than metal catalysts and can withstand the presence of impurities like NH_3 and H_2S [10–12]. Additionally, processes with microbial catalysts are less energy-demanding because they can be operated at mild temperatures and pressures. Microbial conversions therefore provide interesting opportunities for valorisation of CO-rich gases [2, 13–15].

To enable the design of large-scale CO fermentation processes it is crucial to have a thorough understanding of the kinetics of microbial conversions [16]. However, there is currently a lack of kinetic information specifically related to syngas fermentation [17]. This knowledge gap can be attributed to the difficulty associated to measuring substrate concentrations accurately, as the substrate concentration in the broth is governed by both gas-liquid mass transfer of poorly soluble CO and microbial uptake rates. Consequently, classical batch bottle incubations are inadequate for kinetic characterization of gas fermenting microbes [18]. Therefore, previously reported kinetic parameters obtained in batch bottle experiments [19] are untrustworthy, as it is virtually impossible to determine whether the observed rates were limited by mass transfer, biological capacity, or inhibited by carbon monoxide. Furthermore, the pH, biomass-, substrate- and product concentrations are not constant over time in batch bottle incubations. All these factors affect gas-liquid mass transfer properties, which in turn influence the CO availability [20, 21].

Some of these limitations are overcome when using chemostat cultivation in bioreactors. Mathematical modelling studies using chemostat data for kinetic parameter estimation have also been conducted. Such studies estimated q_{CO}^{max}-values ranging between -37.5 and -46.3 mmol·g_X^{-1}·h^{-1} for different closely related *Clostridium* strains [22]. More recently, however, chemostat experiments were published in which a q_{CO} of ± -70 mmol·g_X^{-1}·h^{-1} was sustained [13]. These variations highlight the significant influence of input data on kinetic parameter estimation, and that steady-state data is not suited for characterization of substrate uptake kinetics. To obtain reliable models for bioprocess design, parameter estimation should be done in dynamic environments where q_{CO} can be directly inferred from the experimental

data. Cultivation in bioreactors with controllable gas-liquid mass transfer properties and online off-gas analysis is highly suitable for assessing the substrate uptake capacity of gas fermenting organisms [23]. Therefore, this work is aimed at the identification of q_{CO}^{max} of one of the model organisms for CO fermentation, *Clostridium autoethanogenum*, by using dynamic bioreactor experiments.

To study the CO uptake kinetics of *C. autoethanogenum*, we have used CO-grown chemostat cultures and exposed them to pulses of increasing CO partial pressures (p_{CO}) to identify the maximum substrate uptake rate. The pulse experiments were carried out for one hour to prevent significant growth of the microorganism. In this way, the immediate capacity of the microorganism to consume CO was assessed, rather than reaching a different steady state due to increased CO supply.

3.2. Materials and Methods

3.2.1. Cultivation media and pre-culturing

C. autoethanogenum DSM10061 was obtained as anaerobic pre-culture grown on fructose from colleagues at Wageningen University. Routine batch bottle cultivation was done in 100 mL serum bottles with a working volume of 50 mL. The mineral medium contained (per litre) 0.9 g NH$_4$Cl, 0.9 g NaCl, 0.2 g MgSO$_4$·7 H$_2$O, 0.75 g KH$_2$PO$_4$, 1.5 g K$_2$HPO$_4$, 0.02 g CaCl$_2$·2 H$_2$O, 0.5 mg Na-resazurin, 1 mL of SL-10 trace elements and 0.2 mL of alkaline trace elements. The SL-10 trace elements solution contained (in g·L^{-1}): FeCl$_2$·4 H$_2$O 1.5, FeCl$_3$·6 H$_2$O 2.5, ZnCl$_2$ 0.07, MnCl$_2$·4 H$_2$O 0.1, H$_3$BO$_3$ 0.006, CoCl$_2$·6 H$_2$O 0.19, CuCl$_2$·2 H$_2$O 0.002, NiCl$_2$·6 H$_2$O 0.024, Na$_2$MoO$_4$·2 H$_2$O 0.036 and 10 mL 25% HCl. The alkaline trace elements solution contained (in g·L^{-1}): NaOH 0.4, Na$_2$SeO$_3$ 0.017, Na$_2$WO·2 H$_2$O 1.03, Na$_2$MoO$_4$·2H$_2$O 0.024. After autoclaving, the headspace was exchanged with 100% CO and the headspace pressure was set to 1.5 bar. Before inoculation yeast extract (0.5 g·L^{-1}), B vitamins (2 mL·L^{-1}) and cysteine (0.75 g·L^{-1}) were added from sterile stock solutions. The B vitamin solution contained (in g·L^{-1}): biotin 0.02, nicotinamide 0.2, p-aminobenzoic acid 0.1, thiamine hydrochloride 0.2, Ca-pantothenate 0.1, pyridoxamine 0.5, cyanocobalamin 0.1, riboflavin 0.1.

Bioreactor cultivation was done using a chemically defined medium without yeast extract as described by Valgepea et al. (2017). The mineral medium contained per litre: 0.5 g MgSO$_4$·7 H$_2$O, 0.2 g NaCl, 0.1 g CaCl$_2$, 2.65 g NaH$_2$PO$_4$·2 H$_2$O, 0.5 g KCl, 2.5 g NH$_4$Cl, 0.017 g FeCl$_3$·6 H$_2$O, 0.5 mg Na-resazurin, 10 ml trace metal solution (TMS).The TMS contained per liter: 1.5 g trisodium nitrilotriacetate, 3 g MgSO$_4$·7 H$_2$O, 0.5 g MnSO$_4$·H$_2$O, 1 g NaCl , 0.667 g FeSO$_4$·7 H$_2$O, 0.2 g CoCl$_2$·6 H$_2$O, 0.2 g ZnSO$_4$·7 H$_2$O, 0.02 g CuCl$_2$·2 H$_2$O, 0.014 g Al$_2$(SO$_4$)$_3$·18 H$_2$O, 0.3 g H$_3$BO$_3$, 0.03 g NaMoO$_4$·2 H$_2$O, 0.02 g Na$_2$SeO$_3$, 0.02 g NiCl$_2$·6 H$_2$O and 0.02 g Na$_2$WO$_4$·2 H$_2$O. After sterilizing the medium at 121°C, it was stirred and sparged with N$_2$ for at least 24 hours to strip out the oxygen. Next, 0.5 g·L^{-1} of sterile L-cysteine-HCl·H$_2$O and 2 mL·L^{-1} concentrated filter-sterilized vitamin solution were added. The B vitamin solution contained per litre: 100 mg biotin, 100 mg folic acid, 50 mg pyridoxine hydrochloride, 250 mg thiamine-HCl·H$_2$O, 250 mg riboflavin, 250 mg nicotinic acid, 250 mg calcium pantothenate, 250 mg cyanocobalamin, 250 mg 4-aminobenzoic

acid and 250 mg thioctic acid. Moreover, 0.5 mL of 37% HCl was added per litre of medium to maintain sterility after cysteine and vitamin addition.

3.2.2. Chemostat cultivation

Chemostat cultivation was done in a glass jacketed 3 L bioreactor (Applikon, Delft, The Netherlands) with a working volume of 1.6 L. The bioreactor was inoculated with 100 mL of exponentially growing *C. autoethanogenum* culture (grown in batch bottles on CO, in medium containing yeast extract). CO supply was increased by increasing the stirring speed, gas flowrate and inlet gas composition until steady-state operational setpoints were reached. After reaching this, in- and effluent pumps were turned on to feed the reactor with chemically defined medium and control the dilution rate at 0.01 h^{-1}. The gas composition and sparging rate were controlled using separate mass flow controllers for CO and N_2 (Brooks Brooks Instruments, Hatfield, PA). The total gas flowrate was kept at 100 mL·min^{-1} at 1.0 atm and the reactor was fed with a 90%/10% mixture of N_2 and CO, respectively, during steady-state operation. The reactor was continuously agitated at a speed of 600 rpm using two equally spaced 6-bladed mechanical stirrers and pH was maintained at 5.5 ± 0.05 using 2 mol·L^{-1} NaOH (InControl, Applikon, The Netherlands). Reactor temperature was maintained at 37°C using a water jacket and a thermostat bath (E300, Lauda, Germany). To prevent culture broth evaporation, the off-gas was cooled using a cryostat set to 4.5°C.

3.2.3. CO pulse experiments

CO pulse experiments were carried out after steady state was reached. Due to a technical disturbance, two highly similar steady states were obtained. *C. autoethanogenum* was subjected to increased p_{CO} for one hour, after which the inlet gas was returned to the original settings (p_{CO} = 0.1 atm) (fig. 3.1). p_{CO} was increased with 0.05 atm increments up to p_{CO} = 1.0 atm and with 0.1 atm increments up to p_{CO} = 1.2 atm (table 3.1). Pulse experiments up to p_{CO} = 0.85 atm were carried out during Steady State I, as well as one of the four pulses at p_{CO} = 0.9 atm. The rest of the pulse experiments were carried out after reaching Steady State II. pH control was switched off during the pulses to prevent changes in CO_2 solubility from influencing the off-gas measurements. Pulses were carried out in biological duplicates, triplicates, or quadruplicates. Liquid samples were taken either right after termination of the pulse experiment (pulses of 80% CO and above), or when the off-gas measurements returned to the steady-state values. The optical density of the broth was measured to assess whether significant growth had taken place during the pulse experiment. If the optical density increased more than 5% compared to the steady-state value during a pulse experiment, the chemostat was left undisturbed for at least a day before administering the next pulse. The OD never increased more than 10% during a single pulse experiment, validating the use of the steady-state biomass concentration for calculation of the biomass-specific substrate uptake rate.
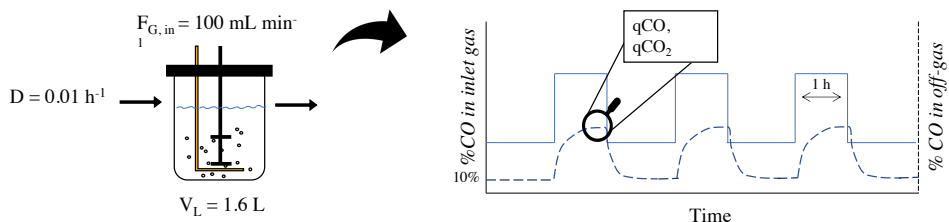
Figure 3.1: Schematic representation of the pulse experimentation method for direct measurement of the biomass-specific CO uptake- and CO_2 production rates.

3.2.4. ANALYTICAL METHODS

The off-gas composition of gas fermentation experiments was followed using an X-stream Enhanced XEGP Off-Gas Analyzer equipped with an infrared detector for CO and CO_2 (6 mm and 30 mm, respectively) measurement and a thermal conductivity detector for H_2 measurement (Emerson, The Netherlands). During pulse experiments with an inlet gas fraction of CO above 60%, the off-gas was diluted with 100 mL·min^{-1} N_2 gas to stay withing the measuring range of the off-gas analyser. Biomass concentrations were monitored both by measuring optical density (OD_{660}) and the amount of VSS in the broth using 100 mL effluent (APHA, 1999), calculated assuming a biomass molecular weight of 24.6 g·Cmol^{-1}. Both OD and VSS were always determined in duplicate. OD and VSS correlated linearly (VSS = 0.2935*OD_{660}). Acetate, lactate, formate, 2,3-butanediol and ethanol concentrations were determined using a Vanquish (Thermo Fisher Scientific, Massachuchets, USA) high performance liquid chromatography machine (HPLC) with an Aminex HPX-87H column (BioRad, USA) at 50°C coupled to a refractive index- and ultraviolet detector (Waters, USA). 1.5 mmol·L^{-1} phosphoric acid was used as eluent at 0.75 mL·min^{-1}. Biomass was removed from the reactor samples before storage or measuring fermentation products by filtration using a 0.22 μm membrane filter (Millipore, Millex-GV, Ireland).

3.2.5. DETERMINATION OF BIOMASS-SPECIFIC CO UPTAKE AND CO_2 PRODUCTION RATES

CO uptake and CO_2 production were calculated using gas- and liquid mass balances. First, the volumetric outflow of the reactor was calculated using the inert fraction (N_2) of the inlet gas as reference, assuming the gas phase was in steady state in the last 10 minutes of the pulse experiment:

$$\frac{dN_{N_2}}{dt} = F_{G,in} \cdot y_{in,N_2} - F_{G,out} \cdot y_{out,N_2} \tag{3.1}$$

$$y_{out,N_2} = 1 - y_{out,CO} - y_{out,CO_2} - y_{out,H_2} \tag{3.2}$$

For CO and CO_2 in the gas phase, mass transfer to and from the liquid, respectively, must be considered:

$$\frac{dN_i}{dt} = F_{G,in} \cdot y_{in,i} - F_{G,out} \cdot y_{out,i} \pm T_{N,i} \tag{3.3}$$

The general mass balance equation for a species in the liquid is as follows:

$$\frac{dM_i}{dt} = F_{L,in} \cdot c_{in,i} - F_{L,out} \cdot c_{out,i} + T_{N,i} + q_i \cdot C_x \cdot V_L \tag{3.4}$$

For CO, this equation can be simplified under the assumption that the in-and outflowing liquids contain negligible concentrations of CO:

$$\frac{dM_{CO}}{dt} = T_{N,CO} + q_{CO} \cdot C_x \cdot V_L \tag{3.5}$$

When stable off-gas values were measured during a pulse experiment, pseudo-steady state was assumed for CO due to which the $\frac{dM_{CO}}{dt}$ – term becomes zero. As CO is consumed, the value of q_{CO} will become negative.

CO_2 has a higher solubility than CO and therefore the concentration in the outflowing liquid cannot be neglected. The inflow concentration of CO_2 is negligible as the medium does not contain (bi)carbonate. All soluble CO_2 species (H_2CO_3, HCO_3^-, CO_3^{2-}) are included in the CO_2 terms in the balance equation to calculate the biomass-specific CO_2 production rate:

$$\frac{dM_{CO_2}}{dt} = F_{L,out} \cdot c_{out,CO_2} + T_{N,CO_2} + q_{CO_2} \cdot C_x \cdot V_L \tag{3.6}$$

CO_2 speciation is strongly affected by the increasing CO_2 partial pressure and the increasing pH during a CO pulse. Therefore, dissolved concentrations of CO_2 species (H_2CO_3, HCO_3^-, CO_3^{2-}) were calculated at each collected data point (1-minute intervals). It was assumed that the gas- and liquid phase were in equilibrium at each data point. The dissolved inorganic carbon concentration was calculated using the equilibrium constants for the different CO_2 species at 37°C as a function of the off-gas partial pressure and pH. The equilibrium assumption was verified by estimating the mass transfer rate in the bioreactor ($k_L a$) from the pulse data and estimating the dissolved CO_2 concentration required for the observed transfer rate. This concentration differed less than 10% from the maximum equilibrium concentration of CO_2, confirming that the system is near equilibrium and can therefor be assumed to be in full equilibrium. The increase in total CO_2-equivalents in the liquid was calculated through integration over the timespan of the pulse and used to correct the observed q_{CO_2} from the off-gas measurements.

3.2.6. FLUX DISTRIBUTION ANALYSIS

Assuming the carbon flux to biomass is negligible, the product spectrum of syngas fermentation can be inferred directly from the off-gas measurements. All carbon and electrons that enter the cell must be recovered in the products. Here, the considered compounds were CO, H_2, CO_2, acetate and ethanol. 2,3-BDO production

was neglected as this was never produced in quantifiable amounts in this study. Then, two balance equations describe the overall microbial conversion (eq. 7, 8). Three of the stoichiometric coefficients are needed as input and the other two can be calculated. Here, CO, H_2 and CO_2 are used as inputs, as they are continuously measured, to calculate ethanol and acetate. All fluxes are defined as positive, considering CO and H_2 as substrates and CO_2, acetate and ethanol as products. Since there is a stoichiometric coupling between substrates and products, biomass-specific rates can also be used as input to calculate the production rates. In that case $v_i = q_i$.

The balance equations for carbon and electrons (with inorganic carbon as reference oxidation state) are:

$$\frac{dC}{dt} = v_{CO} - v_{CO_2} - 2v_{ac} - 2v_{EtOH} \tag{3.7}$$

$$\frac{de^-}{dt} = 2v_{CO} - 2v_{H_2} - 8v_{ac} - 12v_{EtOH} \tag{3.8}$$

Additional to the distribution of excreted products, the flux distribution over key catabolic reactions was calculated to assess the effect of different feeding regimes on the energy conservation of the microorganism. With the biochemistry as represented in supplementary fig. 3.5, a script of intracellular balance equations was written in MATLAB R2020a to calculate the intracellular distribution of carbon and electrons, given a certain stoichiometry of CO, CO_2 and H_2. This was done using all steps of the catabolism that use redox carriers (NAD(H), NADP(H), Fd(2^-)). For a feasible overall stoichiometry, oxidation and reduction of each electron carrier must be balanced. This led to the derivation of the redox carrier balances, with the enzyme abbreviations as used in supplementary fig. 3.5:

$$\frac{dFd^{2-}}{dt} = v_{CODH} + 0.5v_{H_2} + v_{MTHFR} - v_{Rnf} - v_{AOR} - v_{Nfn} - 0.5v_{FDH} - v_{CODH/ACS} \tag{3.9}$$

$$\frac{dNADH}{dt} = v_{Rnf} + v_{ALDH} - v_{MTHFR} - v_{ADH} - v_{Nfn} \tag{3.10}$$

$$\frac{dNADPH}{dt} = 0.5v_{H_2} + 2v_{Nfn} - v_{MTHFD} - v_{FDH} \tag{3.11}$$

In this model, it was assumed that all CO entering the cell is oxidized upon generation of reduced ferredoxin ($v_{CO} = v_{CODH}$). To be able to solve the system, it was constrained so that no metabolites could accumulate intracellularly and that all ATP invested in the methyl branch of the Wood-Ljungdahl Pathway (WLP) was recuperated in the acetate kinase reaction. Lastly, an additional flux for acetate excretion (with no additional costs) was added as acetate can either be excreted or further reduced to acetaldehyde and ethanol.

The constraints were formulated as:

$$v_{FDH} = v_{MTHFD} \tag{3.12}$$

$$v_{MFTHD} = v_{MTHFR} \tag{3.13}$$

$$v_{CODH/ACS} = v_{FDH} \tag{3.14}$$

$$v_{ACK} = v_{Ac} + v_{AOR} \tag{3.15}$$

$$v_{AOR} = v_{ALDH} + v_{ADH} \tag{3.16}$$

$$v_{MTHFD} = v_{ACK} \tag{3.17}$$

This system of equations was solved using a least-squares nonlinear solver. The system proved to be robust: it was not sensitive to changes in initial values and the solution space did not have to be constrained for a correct solution to be obtained.

The biomass-specific ATP production rate (q_{ATP}) was calculated in steady-state by multiplying q_{Rnf} with the assumed H^+/ATP stoichiometry of *C. autoethanogenum* (supplementary fig. 3.5). Dividing the imposed steady-state growth rate in the chemostat ($\mu = 0.01$ h^{-1}) by q_{ATP} gives the molar growth yield on ATP (Y_{ATP}) [24]. Assuming that Y_{ATP} stays constant over the range of tested p_{CO}, the growth rate during a CO pulse was calculated by multiplying q_{ATP} with Y_{ATP}.

3.3. Results

3.3.1. Steady state chemostat operation

C. autoethanogenum was cultivated in a chemostat with a working volume of 1.6 L at a dilution rate of 0.01 h^{-1} and sparged with 100 mL·min^{-1} of 10% CO and 90% N$_2$ gas. Steady state was assumed when stable off-gas, biomass and product concentrations were measured for at least 2 volume exchanges. During CO pulse experiments, steady state was lost once due to technical problems. After restarting the system, a very similar steady state was reached with a slightly different biomass concentration. As the biomass concentration is pivotal for the accurate calculation of q_{CO}, these steady states are reported separately (table 3.1). Both steady states were characterized by a q_{CO} of ±-10 mmol · g$_x^{-1}$·h^{-1} and a q_{CO_2} of ± 6.2 mmol· g$_x^{-1}$·h^{-1}. The liquid product spectrum consisted of acetate and small amounts of ethanol. The biomass concentrations in Steady State I and II equalled 0.52±0.02 and 0.59±0.03 g·L^{-1}, respectively.

Table 3.1: Biological CO consumption and product formation rates and corresponding biomass concentrations in steady state chemostats. Steady state I and II were obtained in the same bioreactor with the same operational conditions. Standard deviations were calculated from gas- and liquid measurements before the steady state was disturbed with CO pulses.

		Steady State I	Steady State II
q_{CO}	$[mmol \cdot g_x^{-1} \cdot h^{-1}]$	-10.80 ± 0.54	-9.85 ± 0.46
q_{CO_2}	$[mmol \cdot g_x^{-1} \cdot h^{-1}]$	6.26 ± 0.35	6.16 ± 0.76
$q_{Acetate}$	$[mmol \cdot g_x^{-1} \cdot h^{-1}]$	1.86 ± 0.29	1.82 ± 0.09
$q_{Ethanol}$	$[mmol \cdot g_x^{-1} \cdot h^{-1}]$	0.21 ± 0.04	0.16 ± 0.02
C_x	$[g_x \cdot L^{-1}]$	0.52 ± 0.02	0.59 ± 0.03

3.3.2. CO uptake is limited by mass transfer rather than biological capacity

To assess the CO uptake capacity of *C. autoethanogenum*, the CO-concentration in the inlet gas was increased for a period of one hour. The rate of CO uptake depends on the mass transfer rate, which was manipulated by adjusting the inlet partial pressure of CO and the headspace pressure (supplementary table 3.1). The calculation of q_{CO} and q_{CO_2} was conducted from the data gathered in the last 10 minutes of the CO pulse (supplementary fig. 3.1). As the dynamics of the pulse experiments altered the speciation of inorganic carbon, dissolved inorganic carbon species were accounted for in the calculation of q_{CO_2}. In fig. 3.2, a clear correlation is depicted between p$_{CO}$ in the inlet gas and q_{CO} and q_{CO_2}. It was observed that q_{CO} decreased linearly up to -119 ± 1 mmol· g$_x^{-1}$·h^{-1} with increasing p$_{CO}$. This suggests that the biological conversion of CO is mass transfer limited over the entire range of tested p$_{CO}$. q_{CO_2} increases linearly up to a p$_{CO}$ of 1.0 atm, after which it plateaus at approximately 90 mmol· g$_x^{-1}$·h^{-1}. This might indicate that in the conditions with high p$_{CO_2}$, the microorganism metabolized CO at near-maximal

rates. Up to a p_{CO} of 0.45, trace amounts of hydrogen were measured in the reactor off-gas, but the biomass-specific hydrogen production rate decreased with increasing p_{CO} (supplementary fig. 3.2). The differences between the q_{CO} and q_{CO_2} profiles could be accounted to changes in metabolic strategy (fig. 3.2).
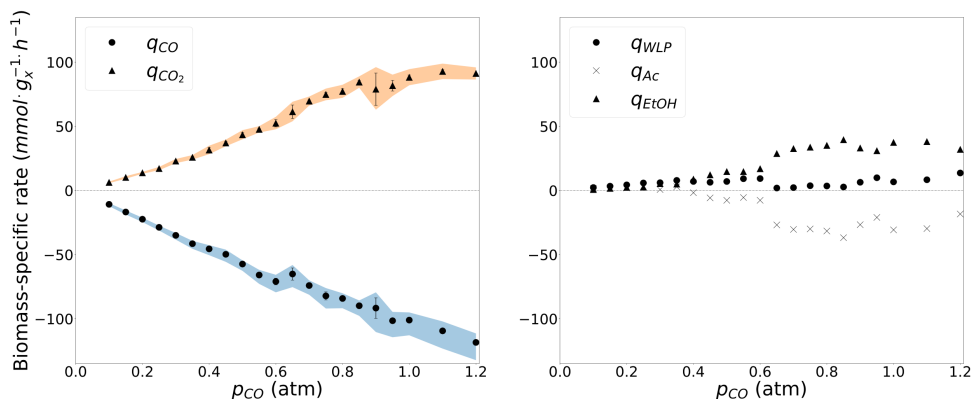
Figure 3.2: Biomass-specific fluxes during CO pulses. Left panel: CO uptake rate (q_{CO}) and CO_2 production rate (q_{CO_2}) as a function of the fraction of CO in the inlet gas. The biomass-specific rates were determined from two, three or four individual biological replicates and the standard deviation is depicted by the error bars. The shaded area shows the error range of the calculated rates based on the standard deviation in the steady-state biomass concentration and the standard deviations of the measurements. Right panel: Flux distribution analysis illustrating the relationship between CO partial pressure, the rate through central carbon metabolism (q_{WLP}) and the production rates of acetate (q_{Ac}) and ethanol (q_{EtOH}). The rates were calculated using q_{CO} and q_{CO_2}, considering that all carbon and electrons consumed by *C. autoethanogenum* must be recovered in the products and that oxidation and reduction of redox carriers in the metabolism must be balanced. Negative values for a biomass-specific rate indicate net consumption of a metabolite.

3.3.3. ACETATE CONSUMPTION FOR SUSTAINING INCREASED q_{CO} LEADS TO SHIFTS IN PRODUCT SPECTRUM

The effect of increasing CO uptake rates on the metabolism of *C. autoethanogenum* was assessed with a stoichiometric model of the central carbon metabolism. The measured q_{CO}, q_{CO_2} and q_{H_2} were used as input values to calculate the fluxes of product formation and through the WLP as shown in fig. 3.2 (right panel). A shift was observed from the formation of mainly acetate at a p_{CO} of 0.1 – 0.35 atm, to the formation of mainly ethanol up until a p_{CO} of 0.6 atm and significant net consumption of acetate for additional ethanol production at p_{CO} above 0.6 atm. The flux distribution analysis based on off-gas data was cross-verified with measurements of pH and metabolites in the culture broth (supplementary fig. 3.3), confirming that shifts in the catabolic strategy of *C. autoethanogenum* can be identified based solely on off-gas measurements. It is noteworthy that the overall rate through the WLP did not increase proportionally with increasing q_{CO}. Instead,

an increase in q_{CO} led to increasing q_{EtOH} and net acetate consumption at a p_{CO} above 0.6 atm. The highest observed q_{WLP} was 13.6 mmol· g_x^{-1}·h^{-1}. To investigate the effect of shifts in the product spectrum on energy conservation of *C. autoethanogenum*, the approximated growth rate and the relationship between q_{Rnf} and q_{CO} during the pulse experiments were analysed. The biomass yield on ATP (Y_{ATP}) was calculated from chemostat data (table 3.1) and equalled 2.6 g_x per mol ATP. The biomass-specific ATP production rate (q_{ATP}) during the pulse experiments was calculated by multiplying q_{Rnf}, following from the flux distribution analysis, with the assumed H^+/ATP stoichiometry of *C. autoethanogenum* (supplementary fig. 3.5).The growth rate (μ) was calculated assuming that Y_{ATP} is equal in chemostat and pulse conditions, following $\mu = Y_{ATP} \cdot q_{ATP}$ and was found to increase linearly with increasing p_{CO} (fig. 3.3, left panel). The rate of the Rnf complex relative to the CO uptake rate is a proxy for the ATP yield on CO during the pulse experiments and decreased with an increasing flux towards ethanol (supplementary fig. 3.3).
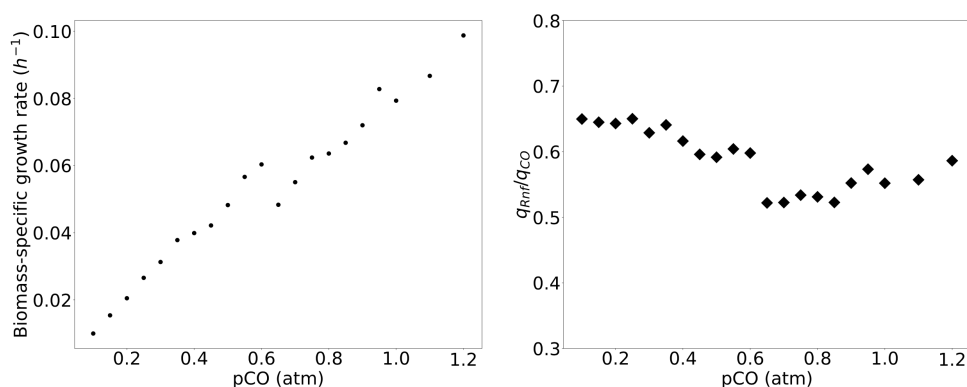
Figure 3.3: Estimated biomass-specific growth rate (μ, left) and the flux of the Rnf complex (q_{Rnf}) divided by the observed q_{CO} (right). The biomass-specific growth rate was estimated by using q_{Rnf} and the stoichiometries of the Rnf and ATPase complexes shown in fig. 3.2 to calculate the biomass-specific ATP production rate. The ATP production rate was multiplied by the biomass yield on ATP (Y_{ATP}) derived from steady-state data to obtain the biomass-specific growth rate. q_{Rnf}/q_{CO} gives a proxy for the ATP yield per mol of CO consumed.

3.4. DISCUSSION

In a gas-fed bioreactor, the substrate conversion rate can be limited either by the mass transfer rate or by the biological conversion rate. When the latter is the case, the concentration of substrate in the liquid will build up. So far, it has been widely accepted that build-up of CO in the liquid can lead to metabolic arrest. This occurs because CO binds to the active site of metalloenzymes, rendering them inactive [25, 26]. Various enzymes involved in the WLP rely on metal clusters. Consequently, a decrease in metabolic activity due to CO toxicity would result in reduced CO uptake rates, resulting in in noticeable changes in the off-gas profile These observations would indicate that the limit of the biomass-specific CO uptake rate (q_{CO}^{max}) has been reached. Interestingly, in our experiments, q_{CO} continued to increase over the entire range of CO partial pressures, up to -119±1 mmol·g_x^{-1}·h^{-1}. The increase in q_{CO} followed a linear trend with increasing p$_{CO}$, indicating that CO conversion was mass transfer limited over the entire experimental range. Thus, q_{CO}^{max} of *C. autoethanogenum* could not be identified in our bioreactor system. This contrasts with the study of Mann et al. [27], where a metabolic collapse of the closely relative species *Clostridium ljungdahlii* occurred due to CO accumulation in the liquid at a q_{CO} of -42 mmol·g_x^{-1}·h^{-1}. In their study, high mass transfer rates were maintained for a longer period compared to the experiments performed here. This shows that the time of exposure to elevated p$_{CO}$ could also affect microbial survival rates. Conducting CO pulse experiments of varying durations could provide valuable insights into the CO consumption capacity of *C. autoethanogenum* and warrant an interesting avenue for further investigation.

Our study proves the crucial need for dedicated and well-controlled experimental validation of key kinetic parameters and shows that the CO uptake capacity of *C. autoethanogenum* has been severely underestimated to date. The highest observed q_{CO} in this study is 2.5 – 3.5-fold higher than the q_{CO}^{max} reported in kinetic modelling studies that used only steady-state chemostat or batch bottle data for parameter estimation and 1.8-fold higher than the highest q_{CO} reported in literature for *C. autoethanogenum* [13, 19, 22]. Furthermore, it is not possible to verify whether mass transfer or biological capacity limited the CO conversion rate in previous studies. Our study shows that mass transfer limitation in the model systems likely lead to the prediction of lower values for q_{CO}^{max} than the q_{CO} of -119±1 mmol·g_x^{-1}·h^{-1} observed here. It is pivotal to obtain the actual q_{CO}^{max} of *C. autoethanogenum* to further improve the predictive power of kinetic models. Bioreactor systems with a different geometry or impeller type could be useful, as increased stirring rates also increase the mass transfer capacity of a bioreactor system [13, 23, 27–29]. In the bioreactor system used here, higher stirring speeds led to vortex formation around the impellers which was detrimental for the mass transfer rate (supplementary fig. 3.4). Alternatively, a pressurizable bioreactor system could be employed to further increase p$_{CO}$ and investigate its impact on q_{CO}, or higher q_{CO} could be achieved in a system operated at a lower biomass concentration.

When interpreting the results of this study, it should be considered that the bioreactor has been operated for five months, including one month recovery after a technical disturbance, under the pulse-feeding regime. Therefore, it cannot

be completely excluded that the culture has adapted to fluctuating conditions. Adjustments in the proteome are unlikely, as previous work has shown that protein expression did not change even in chemostat experiments where periodically highly fluctuating CO and H_2 uptake rates were observed [30]. Still, phenotype-altering mutations might accumulate in the genome during long-term exposure to fluctuating conditions [31]. It can, however, be argued that strains with such mutations resemble industrial workhorses, since microorganisms continuously experience fluctuating conditions in industrial-scale systems as well [32].

The combination of online off-gas measurements and flux distribution analysis provides a powerful means to monitor product distribution during CO fermentation, without the need for liquid measurements. This approach highlights the effectiveness of dynamic bioreactor experiments with online data analysis for studying microbial physiology, as also demonstrated in chapter 4 and [33]. In our study, we observed that for pulses up to a p_{CO} of 0.35, acetate was the main catabolic product. However, as the p_{CO} increased, larger amounts of ethanol were formed, at the expense of acetate present in the fermentation broth. This shift from net acetate production to net acetate consumption is noteworthy. Similar observations have been made before in *C. autoethanogenum* and other closely related *Clostridium* species [13, 27, 34, 35]. The observed changes in physiology are in line with the overflow hypothesis elaborated in chapter 2, stating that acetate reduction to ethanol is exploited to mitigate CO toxicity.

In the experiments performed here, we controlled the rate at which CO was supplied via the mass transfer rate. Through metabolic flux analysis, we observed that the flux through the WLP did not increase significantly beyond a p_{CO} of 0.6 atm. However, the increased CO uptake rate was compensated with higher rates of acetate reduction to ethanol. This is likely to be related to the redox state of the electron carriers and the fact that acetate was available in the cultivation broth [30, 36–39]. Effectively, the product spectrum changed as a function of the mass transfer rate. In other words, the product spectrum of CO fermentation can be controlled by controlling the CO uptake rate through the operational conditions of the bioreactor. This provides an appealing alternative to tedious genetic engineering strategies for improving ethanol production from CO-containing waste.

BIBLIOGRAPHY

[1] U. Arena. "Process and technological aspects of municipal solid waste gasification. A review". In: *Waste Management* 32.4 (Apr. 2012), pp. 625–639. DOI: 10.1016/j. wasman.2011.09.025.

[2] B. Molitor, H. Richter, M. E. Martin, R. O. Jensen, A. Juminaga, C. Mihalcea, and L. T. Angenent. "Carbon recovery by fermentation of CO-rich off gases – Turning steel mills into biorefineries". In: *Bioresource Technology* 215 (Sept. 2016), pp. 386–396. DOI: 10.1016/j.biortech.2016.03.094.

[3] I. E. Agency. *Iron and Steel Technology Roadmap - Towards more sustainable steelmaking.* 2020.

[4] W. S. Association. *World Steel in Figures.* 2022.

[5] M. E. Dry. "The Fischer–Tropsch process: 1950–2000". In: *Catalysis Today* (2002).

[6] J. Abrini, H. Naveau, and E.-J. Nyns. "*Clostridium autoethanogenum*, sp. nov., an anaerobic bacterium that produces ethanol from carbon monoxide". In: *Archives of Microbiology* 161 (1993).

[7] J. Lee, J. W. Lee, C. G. Chae, S. J. Kwon, Y. J. Kim, J.-H. Lee, and H. S. Lee. "Domestication of the novel alcohologenic acetogen *Clostridium* sp. AWRP: from isolation to characterization for syngas fermentation". In: *Biotechnology for Biofuels* 12.1 (Dec. 2019), p. 228. DOI: 10.1186/s13068-019-1570-0.

[8] P. F. Levy, G. W. Barnard, D. V. Garcia-Martinez, J. E. Sanderson, and D. L. Wise. "Organic acid production from CO_2/H_2 and CO/H_2 by mixed-culture anaerobes". In: *Biotechnology and Bioengineering* 23.10 (Oct. 1981), pp. 2293–2306. DOI: 10.1002/bit.260231012.

[9] A. L. Arantes, J. P. C. Moreira, M. Diender, S. N. Parshina, A. J. M. Stams, M. M. Alves, J. I. Alves, and D. Z. Sousa. "Enrichment of Anaerobic Syngas-Converting Communities and Isolation of a Novel Carboxydotrophic *Acetobacterium wieringae* Strain JM". In: *Frontiers in Microbiology* 11 (Jan. 2020), p. 58. DOI: 10.3389/fmicb.2020.00058.

[10] A. Ahmed and R. S. Lewis. "Fermentation of biomass-generated synthesis gas: Effects of nitric oxide". In: *Biotechnology and Bioengineering* 97.5 (Aug. 2007), pp. 1080–1086. DOI: 10.1002/bit.21305.

[11] C.-M. Klask, N. Kliem-Kuster, B. Molitor, and L. T. Angenent. "Nitrate Feed Improves Growth and Ethanol Production of *Clostridium ljungdahlii* With CO_2 and H_2, but Results in Stochastic Inhibition Events". In: *Frontiers in Microbiology* 11 (May 2020), p. 724. DOI: 10.3389/fmicb.2020.00724.

[12] A. Rückel, J. Hannemann, C. Maierhofer, A. Fuchs, and D. Weuster-Botz. "Studies on Syngas Fermentation With *Clostridium carboxidivorans* in Stirred-Tank Reactors With Defined Gas Impurities". In: *Frontiers in Microbiology* 12 (Apr. 2021), p. 655390. DOI: 10.3389/fmicb.2021.655390.

[13]   L. A. De Lima, H. Ingelman, K. Brahmbhatt, K. Reinmets, C. Barry, A. Harris, E. Marcellin, M. Köpke, and K. Valgepea. "Faster Growth Enhances Low Carbon Fuel and Chemical Production Through Gas Fermentation". In: *Frontiers in Bioengineering and Biotechnology* 10 (Apr. 2022), p. 879578. DOI: 10.3389/fbioe.2022.879578.

[14]   J. K. Heffernan, K. Valgepea, R. De Souza Pinto Lemgruber, I. Casini, M. Plan, R. Tappel, S. D. Simpson, M. Köpke, L. K. Nielsen, and E. Marcellin. "Enhancing CO_2-Valorization Using *Clostridium autoethanogenum* for Sustainable Fuel and Chemicals Production". In: *Frontiers in Bioengineering and Biotechnology* 8 (Mar. 2020), p. 204. DOI: 10.3389/fbioe.2020.00204.

[15]   K. Valgepea, R. De Souza Pinto Lemgruber, T. Abdalla, S. Binos, N. Takemori, A. Takemori, Y. Tanaka, R. Tappel, M. Köpke, S. D. Simpson, L. K. Nielsen, and E. Marcellin. "H2 drives metabolic rearrangements in gas-fermenting *Clostridium autoethanogenum*". In: *Biotechnology for Biofuels* 11.1 (Dec. 2018), p. 55. DOI: 10.1186/s13068-018-1052-9.

[16]   B. Wett, M. Schoen, P. Phothilangka, F. Wackerle, and H. Insam. "Model based design of an agricultural biogas plant – application of Anaerobic Digestion Model No.1 for an improved 4 chamber scheme". In: *Water Science and Technology* 50.10 (2007), pp. 21–28.

[17]   J. K. Heffernan, V. Mahamkali, K. Valgepea, E. Marcellin, and L. K. Nielsen. "Analytical tools for unravelling the metabolism of gas-fermenting *Clostridia*". In: *Current Opinion in Biotechnology* 75 (June 2022), p. 102700. DOI: 10.1016/j.copbio.2022.102700.

[18]   E. Sipkema, W. De Koning, K. Ganzeveld, D. Janssen, and A. Beenackers. "Experimental pulse technique for the study of microbial kinetics in continuous culture". In: *Journal of Biotechnology* 64.2-3 (Oct. 1998), pp. 159–176. DOI: 10.1016/S0168-1656(98)00076-5.

[19]   M. Mohammadi, A. R. Mohamed, G. D. Najafpour, H. Younesi, and M. H. Uzir. "Kinetic Studies on Fermentative Production of Biofuel from Synthesis Gas Using *Clostridium ljungdahlii*". In: *The Scientific World Journal* 2014 (2014), pp. 1–8. DOI: 10.1155/2014/910590.

[20]   J. L. Cotter, M. S. Chinn, and A. M. Grunden. "Influence of process parameters on growth of *Clostridium ljungdahlii* and *Clostridium autoethanogenum* on synthesis gas". In: *Enzyme and Microbial Technology* 44.5 (May 2009), pp. 281–288. DOI: 10.1016/j.enzmictec.2008.11.002.

[21]   L. Puiman, M. P. Elisiário, L. M. Crasborn, L. E. Wagenaar, A. J. Straathof, and C. Haringa. "Gas mass transfer in syngas fermentation broths is enhanced by ethanol". In: *Biochemical Engineering Journal* 185 (July 2022), p. 108505. DOI: 10.1016/j.bej.2022.108505.

[22]   E. M. Medeiros, J. A. Posada, H. Noorman, and R. M. Filho. "Dynamic modeling of syngas fermentation in a continuous stirred-tank reactor: Multi-response parameter estimation and process optimization". In: *Biotechnology and Bioengineering* 116.10 (Oct. 2019), pp. 2473–2487. DOI: 10.1002/bit.27108.

[23]   K. Novak, C. S. Neuendorf, I. Kofler, N. Kieberger, S. Klamt, and S. Pflügl. "Blending industrial blast furnace gas with H2 enables *Acetobacterium woodii* to efficiently co-utilize CO, CO_2 and H_2". In: *Bioresource Technology* 323 (Mar. 2021), p. 124573. DOI: 10.1016/j.biortech.2020.124573.

[24] A. H. Stouthamer and C. Bettenhaussen. "Utilization of energy for growth and maintenance in continuous and batch cultures of microorganisms". In: *Biochimica et Biophysica Acta* 301 (1973).

[25] S. Menon and S. W. Ragsdale. "Unleashing Hydrogenase Activity in Carbon Monoxide Dehydrogenase/Acetyl-CoA Synthase and Pyruvate:Ferredoxin Oxidoreductase". In: *Biochemistry* 35.49 (Jan. 1996), pp. 15814–15821. DOI: 10.1021/bi9615598.

[26] K. Schuchmann, N. P. Chowdhury, and V. Müller. "Complex Multimeric [FeFe] Hydrogenases: Biochemistry, Physiology and New Opportunities for the Hydrogen Economy". In: *Frontiers in Microbiology* 9 (Dec. 2018), p. 2911. DOI: 10.3389/fmicb.2018.02911.

[27] M. Mann, K. Miebach, and J. Büchs. "Online measurement of dissolved carbon monoxide concentrations reveals critical operating conditions in gas fermentation experiments". In: *Biotechnology and Bioengineering* 118.1 (Jan. 2021), pp. 253–264. DOI: 10.1002/bit.27567.

[28] K. Valgepea, R. De Souza Pinto Lemgruber, K. Meaghan, R. W. Palfreyman, T. Abdalla, B. D. Heijstra, J. B. Behrendorff, R. Tappel, M. Köpke, S. D. Simpson, L. K. Nielsen, and E. Marcellin. "Maintenance of ATP Homeostasis Triggers Metabolic Shifts in Gas-Fermenting Acetogens". In: *Cell Systems* 4.5 (May 2017), 505–515.e5. DOI: 10.1016/j.cels.2017.04.008.

[29] M. Hermann, A. Teleki, S. Weitz, A. Niess, A. Freund, F. R. Bengelsdorf, and R. Takors. "Electron availability in CO_2 , CO and H_2 mixtures constrains flux distribution, energy management and product formation in *Clostridium ljungdahlii*". In: *Microbial Biotechnology* 13.6 (Nov. 2020), pp. 1831–1846. DOI: 10.1111/1751-7915.13625.

[30] V. Mahamkali, K. Valgepea, R. De Souza Pinto Lemgruber, M. Plan, R. Tappel, M. Köpke, S. D. Simpson, L. K. Nielsen, and E. Marcellin. "Redox controls metabolic robustness in the gas-fermenting acetogen *Clostridium autoethanogenum*". In: *Proceedings of the National Academy of Sciences* 117.23 (June 2020), pp. 13168–13175. DOI: 10.1073/pnas.1919531117.

[31] H. Ingelman, J. K. Heffernan, A. Harris, S. D. Brown, A. Y. Saqib, M. J. Pinheiro, L. A. De Lima, K. R. Martinez, R. A. Gonzalez-Garcia, G. Hawkins, J. Daleiden, L. Tran, H. Zeleznik, R. O. Jensen, V. Reynoso, S. D. Simpson, M. Köpke, E. Marcellin, and K. Valgepea. *Autotrophic adaptive laboratory evolution of the acetogen Clostridium autoethanogenum delivers the gas-fermenting strain LAbrini with superior growth, products, and robustness.* preprint. Bioengineering, Jan. 2023. DOI: 10.1101/2023.01.28.526018.

[32] L. Puiman, E. Almeida Benalcázar, C. Picioreanu, H. J. Noorman, and C. Haringa. "Downscaling Industrial-Scale Syngas Fermentation to Simulate Frequent and Irregular Dissolved Gas Concentration Shocks". In: *Bioengineering* 10.5 (Apr. 2023), p. 518. DOI: 10.3390/bioengineering10050518.

[33] G. R. Stouten, S. Douwenga, C. Hogendoorn, and R. Kleerebezem. *System characterization of dynamic biological cultivations through improved data analysis.* preprint. Microbiology, May 2021. DOI: 10.1101/2021.05.14.442977.

[34] K. M. Hurst and R. S. Lewis. "Carbon monoxide partial pressure effects on the metabolic process of syngas fermentation". In: *Biochemical Engineering Journal* 48.2 (Jan. 2010), pp. 159–165. DOI: 10.1016/j.bej.2009.09.004.

3

[35] J. R. Phillips, H. K. Atiyeh, R. S. Tanner, J. R. Torres, J. Saxena, M. R. Wilkins, and R. L. Huhnke. "Butanol and hexanol production in *Clostridium carboxidivorans* syngas fermentation: Medium development and culture techniques". In: *Bioresource Technology* 190 (Aug. 2015), pp. 114–121. DOI: 10.1016/j.biortech.2015.04.043.

[36] M. Diender, I. Parera Olm, M. Gelderloos, J. J. Koehorst, P. J. Schaap, A. J. M. Stams, and D. Z. Sousa. "Metabolic shift induced by synthetic co-cultivation promotes high yield of chain elongated acids from syngas". In: *Scientific Reports* 9.1 (Dec. 2019), p. 18081. DOI: 10.1038/s41598-019-54445-y.

[37] H. Richter, B. Molitor, H. Wei, W. Chen, L. Aristilde, and L. T. Angenent. "Ethanol production in syngas-fermenting *Clostridium ljungdahlii* is controlled by thermodynamics rather than by enzyme expression". In: *Energy & Environmental Science* 9.7 (2016), pp. 2392–2399. DOI: 10.1039/C6EE01108J.

[38] S. Schulz, B. Molitor, and L. T. Angenent. "Acetate augmentation boosts the ethanol production rate and specificity by *Clostridium ljungdahlii* during gas fermentation with pure carbon monoxide". In: *Bioresource Technology* 369 (Feb. 2023), p. 128387. DOI: 10.1016/j.biortech.2022.128387.

[39] H. Xu, C. Liang, X. Chen, J. Xu, Q. Yu, Y. Zhang, and Z. Yuan. "Impact of exogenous acetate on ethanol formation and gene transcription for key enzymes in *Clostridium autoethanogenum* grown on CO". In: *Biochemical Engineering Journal* 155 (Mar. 2020), p. 107470. DOI: 10.1016/j.bej.2019.107470.

[40] J. Bertsch and V. Müller. "Bioenergetic constraints for conversion of syngas to biofuels in acetogenic bacteria". In: *Biotechnology for Biofuels* 8.1 (Dec. 2015), p. 210. DOI: 10.1186/s13068-015-0393-x.

[41] J. Mock, Y. Zheng, A. P. Mueller, S. Ly, L. Tran, S. Segovia, S. Nagaraju, M. Köpke, P. Dürre, and R. K. Thauer. "Energy Conservation Associated with Ethanol Formation from H_2 and CO_2 in *Clostridium autoethanogenum* Involving Electron Bifurcation". In: *Journal of Bacteriology* 197.18 (Sept. 2015). Ed. by W. W. Metcalf, pp. 2965–2980. DOI: 10.1128/JB.00399-15.

[42] S. Wang, H. Huang, J. Kahnt, A. P. Mueller, M. Köpke, and R. K. Thauer. "NADP-Specific Electron-Bifurcating [FeFe]-Hydrogenase in a Functional Complex with Formate Dehydrogenase in *Clostridium autoethanogenum* Grown on CO". In: *Journal of Bacteriology* 195.19 (Oct. 2013), pp. 4373–4386. DOI: 10.1128/JB.00678-13.

[43] H. G. Wood, S. W. Ragsdale, and E. Pezacka. "The acetyl-CoA pathway of autotrophic growth". In: *FEMS Microbiology Letters* 39.4 (Oct. 1986), pp. 345–362. DOI: 10.1111/j.1574-6968.1986.tb01865.x.

3.5. SUPPLEMENTARY MATERIALS

Table S 3.1: Conditions during pulse experimentation. To maintain a constant inlet gas flow rate ($F_{G,in}$) of 100 mL·min^{-1} a supply of N_2 was introduced. Additionally, a N_2 flow in the off-gas was used to dilute the bioreactor off-gas to values within the measuring range of the off-gas analyzer

p_{CO} [atm]	CO flow [mL·min^{-1}]	N_2 flow inlet [mL·min^{-1}]	N_2 flow off-gas [mL·min^{-1}]	Overpressure [atm]	No. replicates [−]
0.15	15	85	0	-	4
0.20	20	80	0	-	4
0.25	25	75	0	-	4
0.30	30	70	0	-	4
0.35	35	65	0	-	4
0.40	40	60	0	-	4
0.45	45	55	0	-	4
0.50	50	50	0	-	4
0.55	55	45	0	-	3
0.60	60	40	100	-	3
0.65	65	35	100	-	4
0.70	70	30	100	-	2
0.75	75	25	100	-	3
0.80	80	20	100	-	3
0.85	85	15	100	-	3
0.90	90	10	100	-	4
0.95	95	5	100	-	2
1.00	100	0	100	-	3
1.10	100	0	100	0.1	2
1.20	100	0	100	0.2	2

3
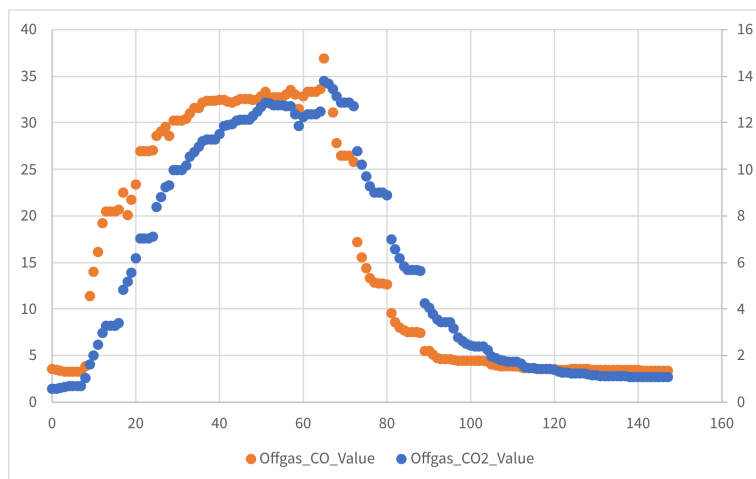
Figure S 3.1: Raw off-gas data during a pulse experiment with 90% CO in the inlet gas. Reactor off-gas was diluted to stay within the measuring range of the off-gas analyzer. Biomass-specific rates are calculated from the part of the curve where CO and CO_2 values both have stabilized, which is between minute 50 and 60. Outlier points were removed before calculation.
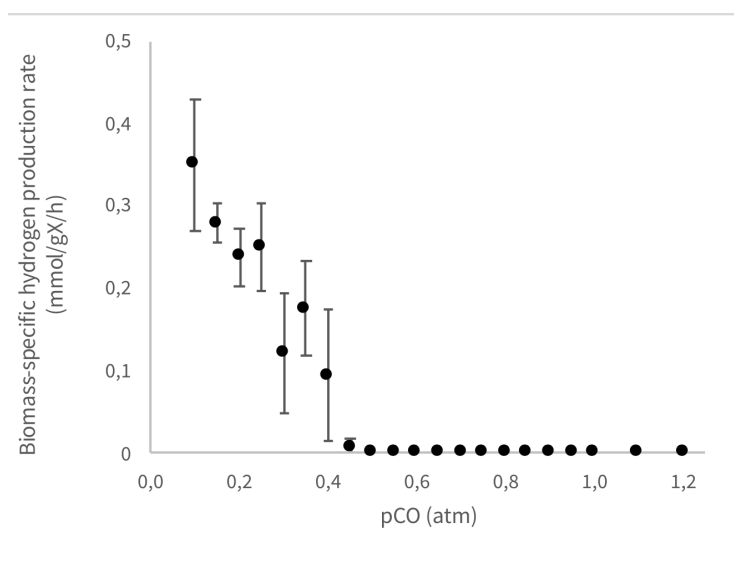
Figure S 3.2: Biomass-specific hydrogen production rate as a function of the carbon monoxide partial pressure. The biomass-specific rates (non-zero) were determined from four individual biological replicates and the standard deviation is depicted by the error bars.
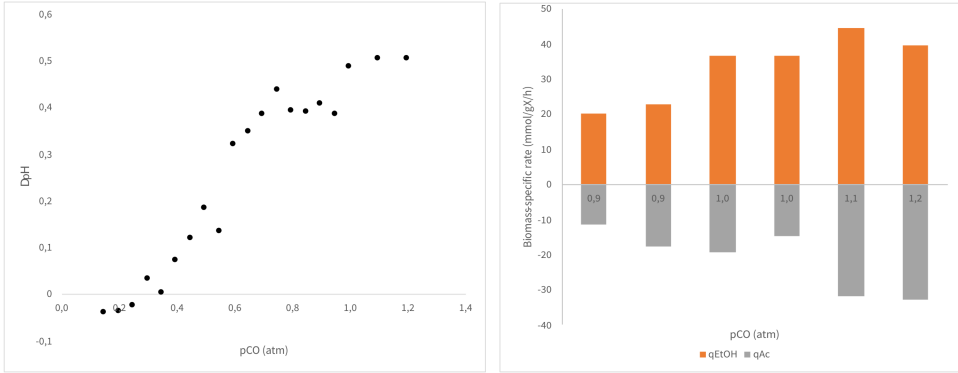
Figure S 3.3: Measured changes in pH and actual biomass-specific ethanol and acetate range during pulse experiments. The actual biomass-specific ethanol and acetate rates were calculated comparing liquid concentration measurements of right before and right after (t = 60 min) a pulse experiment. Sampling right after a single pulse experiment was done from p_{CO} of 0.85 and higher. Before that, samples were taken after the system had returned to steady-state off-gas values, which gives a less reliable measurement of the rates during the pulse.
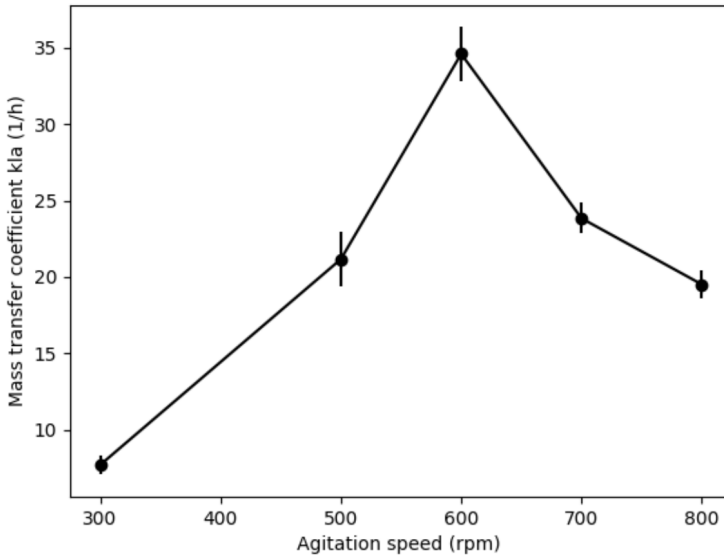
Figure S 3.4: Mass transfer coefficient (k_La) as a function of the agitation speed in the bioreactor system used in this study. The k_La was determined by on-line measurement of the dissolved oxygen (DO) in time after switching a completely anaerobic system to sparging with compressed air at 100 mL·min^{-1}

3
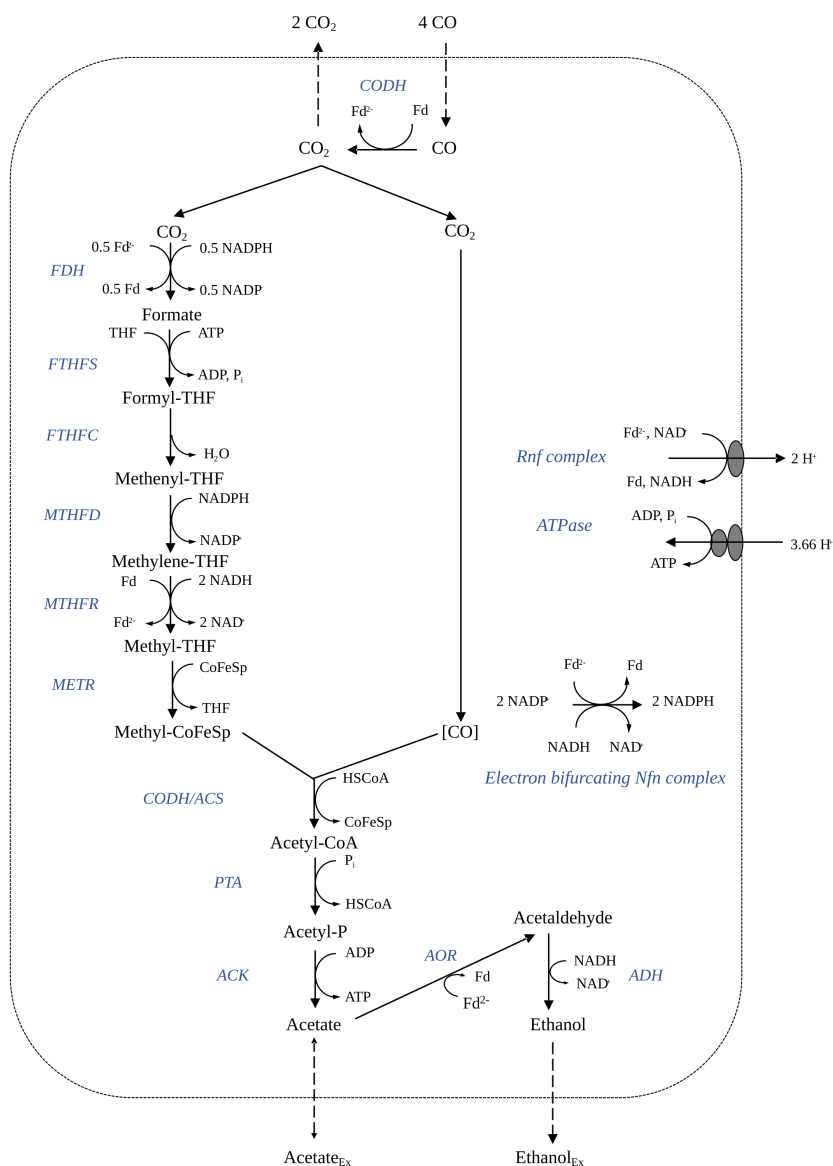
Figure S 3.5: Schematic representation of the enzymatic steps in the central carbon metabolism, the Wood-Ljungdahl pathway (WLP), of *C. autoethanogenum* [40–43]. The electron bifurcating Rnf complex is pivotal for the harvesting of ATP through build-up of a proton gradient.

4

PRODUCT INHIBITION AND PH INFLUENCE STOICHIOMETRY AND KINETICS OF CHAIN-ELONGATING COMMUNITIES IN SEQUENCING BATCH BIOREACTORS

Maximilienne Toetie Allaart, Gerben Roelandt Stouten, Diana Z. Sousa, Robbert Kleerebezem

ABSTRACT

Anaerobic microbial communities can produce carboxylic acids of medium chain length (e.g. hexanoate, octanoate) by elongating short-chain fatty acids through reversed β-oxidation. Ethanol is a common electron donor for this process. The influence of environmental conditions on the stoichiometry and kinetics of ethanol-based chain elongation remains elusive. Here, a sequencing batch bioreactor setup with high-resolution off-gas measurements was used to identify the physiological characteristics of chain-elongating microbial communities enriched on acetate and ethanol at pH 7.0±0.2 and 5.5±0.2. Operation at both pH-values led to the development of communities that were highly enriched (>50%, based on 16S rRNA gene amplicon sequencing) in Clostridium kluyveri *related species. At both pH-values, stably performing cultures were characterized by incomplete substrate conversion and decreasing biomass-specific hydrogen production rates during an operational cycle. The process stoichiometries obtained at both pH-values were different: at pH 7.0, 71±6% of the consumed electrons were converted to hexanoate, compared to only 30±5% at pH 5.5. Operating at pH 5.5 led to a decrease in the biomass yield, but a significant increase in the biomass-specific substrate uptake rate, suggesting that the organisms employ catabolic overcapacity to deal with energy losses associated to product inhibition. These results highlight that chain-elongating conversions rely on a delicate balance between substrate uptake- and product inhibition kinetics.*

4

4.1. INTRODUCTION

I N the transition from a petroleum-based to a bio-based society, the microbial production of chemicals from renewable resources has gained significant interest. Medium-chain carboxylic acids (MCCAs) are an example of native microbial products that can be generated from (complex) substrates, ranging from organic to gaseous waste streams [2–7]. Hexanoic acid, a six-carbon MCCA, can be used as antimicrobial agent replacing antibiotics in animal feed [8], as corrosion inhibitor, and as precursor for flavors, fragrances, solvents and fuels [9].

Hexanoic acid is naturally produced in different types of microbial ecosystems [10–12] by elongating short-chain carboxylic acids using ethanol or lactate as electron donor through reversed β-oxidation [13]. Chain-elongating organisms compete for substrate with acetoclastic methanogens, syntrophic ethanol oxidizers and sulfate reducing organisms and provide substrate to, for example, homoacetogens, syntrophic butyrate oxidizing organisms and hydrogenotrophic methanogens [14, 15]. By tuning the operational parameters in a bioreactor, the competition between these organisms can be controlled. In this way, mixed microbial communities of chain elongators can be enriched in non-sterile environments [16].

The biochemistry of the model organism for chain elongation, *Clostridium kluyveri*, was unraveled using whole-genome sequencing [17] and efforts were made to quantify the kinetic properties of this organism [18]. The stoichiometry of the process and the flexibility of chain-elongating metabolism were assessed through thermodynamic analyses [14, 19] and experiments with different substrates in different ratios [20, 21]. Despite these efforts, several aspects of the quantitative description of the chain elongation process remain to be elucidated. For example, the effect of pH on inhibition by weak acids is not reflected in the available kinetic model, nor is the effect of different electron donor versus electron acceptor ratios on the observed stoichiometries and rates. All in all, various of the fundamental aspects of chain elongation remain to be uncovered.

Fundamental insights are key in overcoming the challenges, such as steering the product spectrum and efficiently balancing integrated production- and extraction processes, in the exploitation of chain-elongating organisms for the production of biochemicals. Nevertheless, a large part of the scientific literature published in recent years has been focused on process intensification [20, 22, 23] and the application of chain elongation in the conversion of real waste streams [24–26]. This focus on the overall process results in the analysis of conversions at the reactor level, and the effects on the kinetic properties of the microorganisms involved are often overlooked. Therefore, an experimental setup in which process parameters and microbial conversions can be closely monitored and controlled is required to generate a comprehensive image of microbial behavior.

We have successfully operated sequencing batch bioreactors (SBRs) with a suspended microbial community converting acetate and ethanol to butyrate and hexanoate at pH 7.0 and pH 5.5, gaining insight in the effects of product inhibition on chain-elongating microorganisms. These findings pave the way towards in-depth understanding of the microbial physiology of chain elongators, which increases the amount of control we can exert on MCCA-producing mixed cultures.

4.2. MATERIALS AND METHODS

4.2.1. REACTOR OPERATION

The enrichments were carried out in glass jacketed 2 L bioreactors (Applikon, The Netherlands) with a working volume of 1 L. The bioreactors were operated in sequencing batch mode, with a and a solids- and hydraulic retention time (SRT, HRT) of 1 day and a cycle time of 12 hours. Each cycle, 50% of the volume of the bioreactor was exchanged for 50 g of nutrient stock solution and 400 g of demineralized water. One hour after the start of the effluent phase a 50 g pulse of carbon solution was fed, dosing 125.5 mmol ethanol and 21.1 mmol acetate to the reactor in each cycle. This equaled an ethanol-to-acetate ratio of 6:1 in the bioreactor feed. A relatively high concentration of ethanol versus acetate was reported to positively influence hexanoate production [27] and a 6:1 ratio enabled both butyrate and hexanoate formation at pH 5.5 and 7.0 [11]. Therefore, this feeding regime was chosen to allow for the characterization of the effect of both butyrate and hexanoate on chain-elongating communities at different pH values. Anaerobic conditions were ensured by continuously sparging the reactors with a mixture N_2 and CO_2 (95:5vol%) at a rate of 46.6 mL min^{-1} (MX44, DASGIP, Germany). As CO_2 is required for growth of *C. kluyveri* [28], CO_2 was continuously sparged through the culture broth in non-limiting amounts. The headspace gas was continuously recirculated through the broth using a gas recirculation pump. To improve the quality of the gas data, the reactors were operated at 0.1 bar overpressure. The suspended culture was taken out of the reactors weekly for biofilm removal from the reactor walls. The reactors were continuously agitated at a speed of 400 rpm (SC4, DASGIP, Germany) using mechanical stirrers. Reactor temperature was maintained at 34°C using a water jacket and a thermostat bath (E300, Lauda, Germany). To prevent culture broth evaporation, the off-gas was cooled using a cryostat set to 5°C. Reactor pH was maintained at 5.5±0.2 or 7.0±0.2 using 1 mol·L^{-1} NaOH and 1 mol·L^{-1} HCl solutions. The pumps for feeding, effluent removal and pH control were controlled as described elsewhere, as well as the methods for data acquisition [29]. The reactors were inoculated with a chain-elongating community enriched from anaerobic digester sludge (Harnaschpolder, The Netherlands) for approximately three months with the same feeding regime and the same enrichment medium as described here. During the enrichment of the inoculum for the bioreactors operated here, the pH could not be controlled at a single value due to electrical interference with the pH measurement. This led to a pH fluctuating between values of approximately 5.0 - 7.5 in the initial enrichment stage.

4.2.2. Enrichment medium

An adapted *Clostridium kluyveri* medium was used as enrichment medium. The carbon- and nutrient source solutions were prepared separately as 10x concentrated stocks. The carbon stock solution contained 2.6 M ethanol and 0.44 M potassium acetate and the nutrients stock contained 67.6 mM KH_2PO_4, 93.5 mM NH_4Cl, 4.1 mM $MgSO4·7\ H_2O$, 5.9 mM $MgCl_2·6\ H_2O$, 20 mL of alkaline trace elements solution, 20 mL of SL-10 trace elements solution and 20 mL of B vitamin solution. The alkaline trace elements solution contained (in $g·L^{-1}$): NaOH 0.4, Na_2SeO_3 0.017, $Na_2WO_4·2\ H_2O$ 1.03, $Na_2MoO_4·2\ H_2O$ 0.024. The SL-10 trace elements solution contained (in $g·L^{-1}$): $FeCl_2·4\ H_2O$ 1.5, $FeCl_3·6\ H_2O$ 2.5, $ZnCl_2$ 0.07, $MnCl_2·4\ H_2O$ 0.1, H_3BO_3 0.006, $CoCl_2·6\ H_2O$ 0.19, $CuCl_2·2\ H_2O$ 0.002, $NiCl_2·6\ H_2O$ 0.024, $Na_2MoO_4·2\ H_2O$ 0.036 and 10 mL 25% HCl. The B vitamin solution contained (in $g·L^{-1}$): biotin 0.02, nicotinamide 0.2, p-aminobenzoic acid 0.1, thiamine hydrochloride 0.2, Ca-pantothenate 0.1, pyridoxamine 0.5, cyanocobalamine 0.1, riboflavin 0.1. From cycle 45 onwards, 50 mM 2-bromoethanesulfonate (BES) (TCI, Tokyo, Japan) was added to the 10x concentrated medium.

4.2.3. Analytical methods

The in- and off-gas composition of the reactors were measured using mass spectrometry (PRIMA BT Benchtop, Thermo Scientific, UK). pH values were stored and acid- and base dosage were monitored using an integrated revolution counter (MP8, DASGIP, Germany). Biomass concentrations were monitored both by measuring optical density (OD_{660}) and the amount of VSS in the broth using 150 mL effluent (APHA, 1999), calculated assuming a biomass molecular weight of 24.6 $g·Cmol^{-1}$. Technical replicates of both OD and VSS measurements were always performed. End of cycle acetate concentrations were determined using high performance liquid chromatography (HPLC) using an Aminex HPX-87H column (BioRad, USA) at 59°C coupled to an refractive index- and ultraviolet detector at 210 nm (Waters, USA). 1.5 $mmol·L^{-1}$ phosphoric acid was used as eluent. Biomass was removed from the reactor samples by centrifugation and filtration using a 0.22 μm membrane filter (Millipore, Millex-GV, Ireland). Ethanol, butyrate and hexanoate concentrations were analysed using gas chromatography (GC). GC was performed using a Trace 1300 machine (Thermo Scientific, USA) equipped with an injector maintained at 180°C, a carbowax polyethylene glycol column of 20 m × 0.18 mm (Agilent, USA), using a temperature gradient from 50°C to 180°C over 24 minutes. Helium was used as carrier gas and fermentation substrates and products were detected using a flame ionization detector set at 200°C. Iso-hexanoic acid was used as internal standard and samples were acidified using pure formic acid (Sigma Aldrich, US). The analytical methods allowed for the measurement of longer- and odd-chain carboxylic acids, but these were not detected. Biochemical conversion profiles during an operational cycle were obtained by taking hourly liquid samples. Biomass growth was monitored by measuring OD_{660} in duplicate, substrate consumption and product formation were measured using HPLC and GC after biomass removal using a 0.22 μm membrane filter. Online data was acquired during cycle measurements as described above.

4.2.4. MICROBIAL COMMUNITY ANALYSIS

Enrichment cultures were analyzed microscopically weekly (Axioplan 2 imaging, Zeiss, Germany). The microbial community composition was analyzed using en-of-cycle cell pellets of 4 mL samples. DNA was extracted from the cell pellets using the PowerSoil microbial extraction kit (Qiagen Inc., Germany) following manufacturer's instructions. The DNA-content of the extracts was quantified using a Qubit 4 (Thermo Fisher Scientific, U.S.A.) to confirm sufficient DNA was extracted for analysis. The samples were sent to Novogene Ltd. (Hongkong, China) for amplicon sequencing of the V3-V4 region of the 16S-rRNA gene (position 341-806) on an Illumina paired-end platform. After sequencing, the raw reads were quality filtered, chimeric sequences were removed and OTUs were generated on the base of >97% identity. Subsequently, the representative sequence for each OTU was annotated using the GreenGene Database. microbial community analysis was performed by Novogene using Mothur & Qiime software (V1.7.0). For phylogenetic determination the most recent SSURef database from SILVA (http://www.arb-silva.de/) was used. The sequences have been stored in the 4TU research database and can be found under the DOI: 10.4121/14394578.

4.2.5. PARAMETER ESTIMATION

The carbon- and electron balances were calculated using the gas productivities and end-of-cycle product and residual substrate concentrations. As the SBRs were operated at an exchange ratio of 0.5, and in case of steady state operational performance, 50% of the substrates and products amounts present at the end of a cycle correspond to the initial amounts of the next cycle (steady state assumption). The average biomass, hexanoate and hydrogen yields on ethanol were calculated using the amount of ethanol consumed and the amount of biomass (according to VSS measurements), hexanoate or hydrogen produced in a cycle. As 50% of the culture broth is removed every 12 h, the biomass duplicates within this time during stable bioreactor operation. Therefore, the average growth rate (μ) during one cycle can be estimated directly using the steady assumption, the exchange ratio and the cycle time. From the average growth rate (μ) and the biomass yield on ethanol ($Y_{X/EtOH}$) the average biomass specific ethanol uptake rate (q_{EtOH}) can directly be estimated according to $q_{EtOH} = \mu / Y_{X/EtOH}$. The standard deviations in the calculated (q_{EtOH}) values were determined with error propagation.

4.2.6. MODELING BIOREACTOR-SPECIFIC GAS PRODUCTIVITY

The actual bioreactor-specific respiration rates of H_2, N_2, O_2, CO_2, CH_4 were reconstructed from the off-gas composition measurements by modeling them in a physicochemical model that mimics the operated bioreactors. In order to do this, a Particle Filter state estimation method [30] was used. The main physicochemical processes, which include inorganic carbon speciation, gas mixing in the bulk liquid and head space, delays and non-equilibrium phase transfer rates, are incorporated in a model that allows for rate estimation using measured off-gas and pH data for calibration of the modeled respiration rates. For details, see [30] and section 4.5.

4.3. RESULTS

4.3.1. DEVELOPMENT OF MICROBIAL COMMUNITY STRUCTURE AND FUNCTIONALITY

Two bioreactors were operated for 48 days in sequencing batch mode at pH 7.0 ± 0.2 and pH 5.5 ± 0.2. In each operational cycle of 12 h, a substrate pulse of 125 mmol ethanol and 21 mmol acetate was dosed. Both reactors were inoculated with a culture that already exhibited chain-elongating activity. Chain-elongating activity is associated with hydrogen formation and the consumption of small amounts of CO_2. The composition of the off-gas and dosage of base were analyzed on-line, which allowed for continuous monitoring of H_2 and ch4 formation and CO_2 consumption. Furthermore, dissolved substrate and product concentrations at the end of an operational cycle were frequently measured throughout the enrichment to determine the change in product spectrum and extent of substrate consumption.

In both reactors, H_2 was detected in the off-gas and butyrate and hexanoate were measured in the liquid product spectrum (fig. 4.1). This confirmed that chain-elongating conversions took place in both conditions. Beside hydrogen, methane was also produced in the initial phase of both enrichments without BES addition (fig. 4.1), indicating that methane-producing biological conversions took place alongside chain elongation. A simultaneous decrease in net hydrogen productivity and increase in methane productivity and CO_2 consumption was observed at pH 7.0. This showed that at least a part of the methane production originates from hydrogenotrophic methanogenesis. At pH 5.5, the simultaneous slight increase in CO_2 consumption and methane production also suggested the presence of hydrogenotrophic methanogens. In order to solely study the characteristics of chain elongation and ensure comparability between the two systems, methanogens were inhibited in both reactors from cycle 45 onward by adding 5 mM of BES to the medium. Gas productivities stabilized within 10 cycles after BES addition and methane production was effectively suppressed (fig. 4.1). From cycle 60 onward the fractions of butyrate and hexanoate also stabilized (fig. 4.1). This confirmed a steady functional performance of the microbial community, consisting of only chain-elongating conversions.

16S rRNA gene amplicon sequencing data showed that *Clostridium sensu strictu 12* was the predominant genus at both pH (fig. 4.2). OTUs of >97% identity with the *C. kluyveri* 16S rRNA gene sequence consequently constituted more than 50% of the total number of reads and *C. kluyveri* was the only species of the *Clostridium* genus that was identified in the microbial community. This indicated that strong enrichment of *C. kluyveri* was maintained in both bioreactors. The presence of *Methanobacterium* coincided with periods of methane formation at both pH-values.
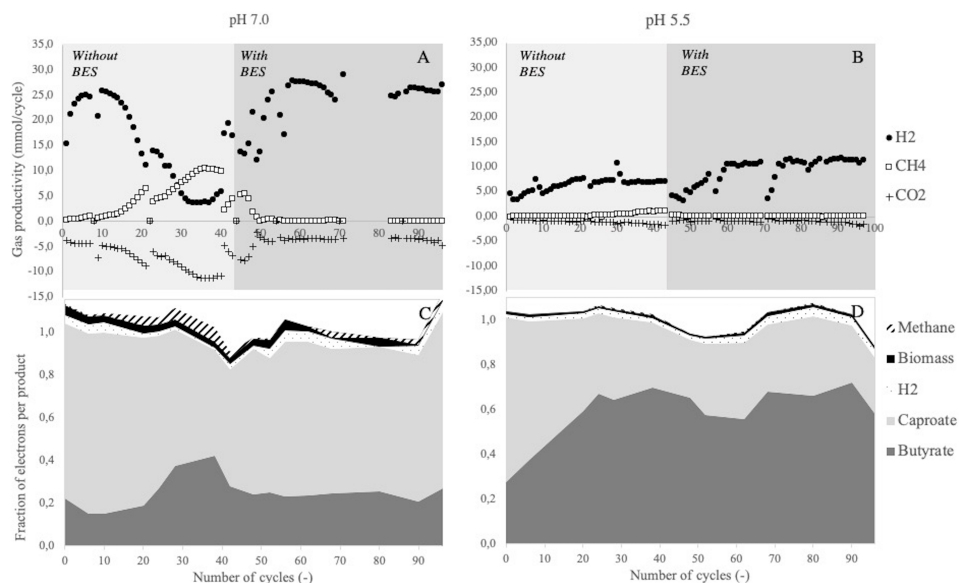
Figure 4.1: Gas productivities (mmol) per cycle (A,B) and distribution of consumed electrons over the fermentation products (C,D) over time in SBRs at different pH. A single spike of BES was given to the enrichment at pH 7.0 in cycle 40, from cycle 45 onward both enrichments were continuously supplemented with BES. Due to a technical error, gas data of the enrichment at pH 7.0 is missing between cycle 72 and 82. Sudden drops in hydrogen production at pH 5.5 are due to reactor cleaning, after which the biological activity recovers within 4 cycles.

Table 4.1: Average stoichiometric and kinetic properties of chain-elongating communities in SBRs at different pH during stable operation[a]

	pH 7.0	pH 5.5
Ethanol consumption (%)	47 ± 4	25 ± 3
Acetate consumption (%)	79 ± 3	66 ± 4
Electrons converted to hexaoate (%)	71 ± 6	30 ± 5
EtOH:H$_2$ ratio[b] (mol·mol^{-1})	3.0 ± 0.3	3.5 ± 0.2
Donor:Acceptor consumption ratio (mol·mol^{-1})	1.9 ± 0.1	2.1 ± 0.2
$Y_{X/EtOH}$ (Cmol·mol^{-1})	0.11 ± 0.02	0.05 ± 0.01
q_{EtOH} (mol·Cmol^{-1}·h^{-1})	0.54 ± 0.08	1.12 ± 0.13

[a]Only data between cycle 60 and cycle 96 is included in these calculations.

[b]Electron acceptor consumption was calculated as the summed consumption of acetate and butyrate.
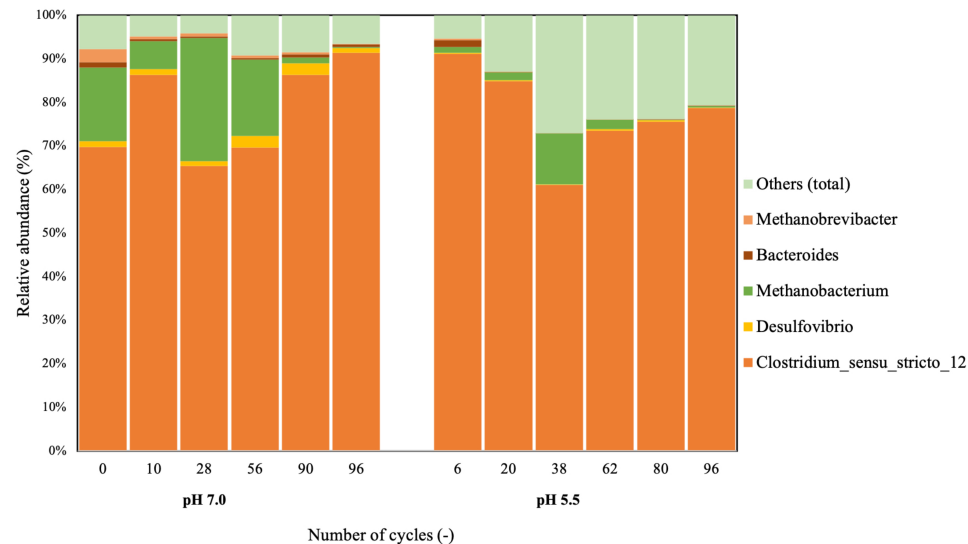
Figure 4.2: Taxonomic distribution of the microbial communities at pH 7.0 and 5.5. 16S rRNA amplicon sequencing was used to assess the community composition. All samples had a similar number of total reads. OTUs constituting less than 3% of the community were grouped under "Others." On the x-axis, the number of cycles after which the sample was taken from the bioreactor is displayed for each sample.
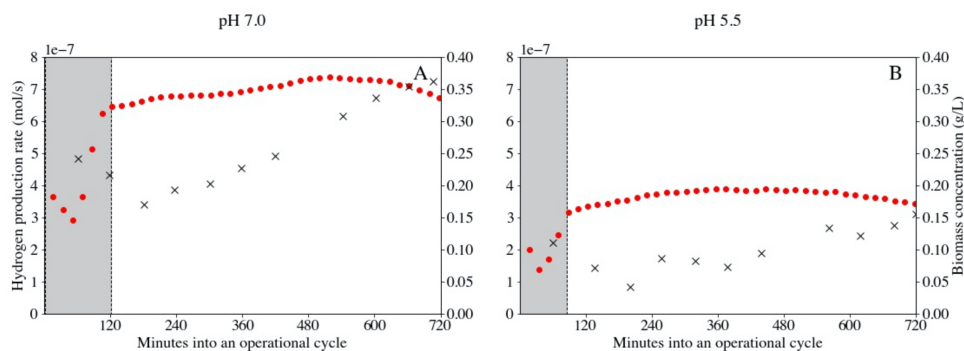
Figure 4.3: Bioreactor-specific hydrogen production rates (•) and biomass concentrations (×) at pH 7.0 (A) and pH 5.5 (B) during operational cycle 92. The physicochemical (abiotic) behavior of the reactor was modeled in order to accurately predict the biological activity responsible for the observed gas profiles. Areas shaded in gray indicate the initiation of a new cycle and its associated uncertainty in measurements due to a temporarily changing physiochemistry. This uncertainty is mainly related to incorrect prediction of CO_2 speciation. The period of uncertainty is shorter at pH 5.5 (90 min versus 120 min) as less CO_2 dissolves at this pH.

4.3.2. Stoichiometric and kinetic properties of chain-elongating communities at different pH

Stably performing chain-elongating communities were established at both pH-values from cycle 60 onward. In both enrichments, high residual ethanol concentrations at the end of the cycle were observed. Residual acetate was also measured in both conditions (table 4.1 and supplementary table 4.1). This showed that high residual ethanol concentrations were not related to acetate limitation. At pH 7.0, the consumed acetate and ethanol were converted to mainly hexanoate, comprising 71 ± 6% of the electrons found in fermentation products (table 4.1). Enriching at a pH of 5.5 led to a butyrate-dominated product spectrum (fig. 4.1 and table 4.1).

Chain-elongating organisms couple the oxidation of ethanol to acetate to the reductive elongation of acids in the reversed $\beta-$oxidation. The electron bifurcating reduction of crotonyl-CoA to butyryl-CoA discursively allows the release of the electrons originating from ethanol as hydrogen. Therefore, the ethanol- to-hydrogen ratio is a proxy for the metabolic proportion between ethanol oxidation and reversed $\beta-$oxidation through which metabolic flexibility can be identified. The canonical stoichiometry, in which 6 ethanol and 4 acetate are converted to 5 butyrate and 2 hydrogen, assumes a ratio of 1:5 between ethanol oxidation and reversed $\beta-$oxidation, resulting in the consumption of 3 ethanol per hydrogen formed. At pH 7.0, this canonical stoichiometry was observed (table 4.1). At pH 5.5, 3.5 ± 0.2 mol of ethanol were consumed per hydrogen formed. Concomitantly, the relative consumption of electron donor over electron acceptor increased to 2.1 ± 0.2 mol electron donor per mol electron acceptor at pH 5.5 (table 4.1). The consumption ratios of electron donor over electron acceptor are in the range of the ratios observed in acetate-limited chemostats of *C. kluyveri* (1.7-2.3 mol·mol^{-1}) by Kenealy & Waselefsky [21]. Changes in the ethanol-to-hydrogen ratio confirm that the stoichiometry of chain elongation is not fixed [19].

The average growth rate in both bioreactors was 0.058 h^{-1}, as imposed by the exchange ratio of 0.5 and the cycle time of 12 h. With this average growth rate and the initial and final substrate- and biomass concentrations (section 4.5), the biomass yield on ethanol and the average biomass-specific ethanol uptake rate could be calculated. The culture at pH 5.5 exhibited a lower biomass yield on ethanol, but a significantly higher biomass-specific substrate uptake rate (table 2.1). This indicates that the substrate requirements for maintenance are higher at low pH.

4.3.3. On-line gas analysis for kinetic bottleneck identification

The hydrogen concentration in the bioreactor off-gas is a measure of the biomass-specific catabolic rate if the catabolic stoichiometry is fixed. Therefore, the off-gas measurements were used in combination with a Particle Filter state estimation to calculate the overall hydrogen production rate in the two bioreactors over time. The Particle Filter could reconstruct the hydrogen production rates except for the period of volume exchange (section 4.5). In fig. 4.3 the biomass concentrations and hydrogen production rates during a representative operational cycle (cycle 92) are

presented. At this time the reactor performance was stable and biomass duplicated during each operational cycle at both pH-values. The overall hydrogen production rate did not double accordingly. In fact, a near-horizontal profile was obtained in the hydrogen production rate in both conditions. It was ruled out that nutrient limitation caused this behavior (data not shown). Thus, the biomass- specific catabolic flux decreases approximately 50% throughout an operational cycle both at pH 7.0 and at pH 5.5. This indicates that the ratio between substrate and product has a pronounced effect on the biomass-specific rate.

4

4.4. DISCUSSION

4.4.1. SBR ENRICHMENT OF CHAIN-ELONGATING MICROBIAL COMMUNITIES

In this work we have shown that SBR cultivation is suitable for enriching chain-elongating communities at pH 5.5 and pH 7.0. Although taxonomically similar microbial communities developed in both enrichments, significant differences were observed in microbial functionality. In both bioreactors, an average growth rate of 0.058 h^{-1} was imposed through the cycle length and exchange ratio. This growth rate is independent of the biomass concentration. As both communities reached a pseudo steady state, differences in biomass concentration are therefore related to compound concentrations and cultivation conditions. Here, it was found that changing the pH significantly affects the product ratios, biomass yield and catabolic rates.

4.4.2. WEAK ACID UNCOUPLING CAUSES DECREASED BIOMASS YIELD ON ETHANOL

In absence of product inhibition, enrichments in SBRs select for maximal growth rates and full substrate consumption. In this study, stably performing microbial communities were enriched in SBR systems but substrate limitation was never encountered. Therefore, it is likely that the functional differences observed between between the two enrichments were related to the inhibitory effects of the fermentation products. Two main mechanisms of toxicity of the elongated products can be distinguished [11, 18, 31]. First of all, protonated short- and medium chain carboxylic acids induce ATP consumption for the extrusion of protons and dissociated acids [32]. This is referred to as weak acid uncoupling. The effect of weak acid uncoupling is equal for butyric and hexanoic acid due to their very similar dissociation constants (pKa). Secondly, medium chain carboxylic acids can dissolve in the cell membrane both in their protonated and unprotonated forms and interfere with membrane integrity and fluidity [33]. This increases uncoupling effects by increasing membrane permeability and inherently reducing cellular efficiency [8]. Decreasing the culture pH increases the relative amounts of protonated acids and thereby amplifies weak acid uncoupling. At pH 5.5, a significantly lower biomass yield was obtained than at pH 7.0 (table 2.1). The biomass yield on ethanol at pH 7.0 of 0.11 ± 0.02 Cmol$_x$·mol^{-1} was comparable to earlier reported biomass yields at neutral pH of 0.11 Cmol$_x$·mol^{-1} [18] and 0.07−0.13 Cmol$_x$·mol^{-1} [21]. The yield at pH 5.5 (0.05 ± 0.01 Cmolx·mol^{-1}) was closer to the yield of 0.06 Cmol$_x$·mol^{-1} reported by [34] in batch experiments with uncontrolled pH. The decrease in biomass yield is therefore likely to be related to toxicity through weak acid uncoupling.

4.4.3. HEXANOIC ACID TOXICITY STEERS THE BALANCE BETWEEN SUBSTRATE CONSUMPTION AND PRODUCT INHIBITION

If weak acid uncoupling was the only mechanism of toxicity at play, both butyrate and hexanoate would cause a similar additional burden to the cells. The shift from

hexanoate to butyrate production at pH 5.5 was therefore either arbitrary, or related to another mechanism of MCCA toxicity as the elongation of butyrate to hexanoate retains the same amount ofacid equivalents. We hypothesize that the change in product spectrum is a protection mechanism against additional energy losses due to hexanoate dissolution in the cell membrane. In *Saccharomyces cerevisiae*, carboxylic acid toxicity was found to increase with increasing carbon chain length when comparing hexanoic, caprylic and decanoic acid [35]. Likewise, decanoic acid becomes completely inhibitory at half the inhibitory concentration of hexanoic and caprylic acid in *Escherichia coli* [36]. Furthermore, the inhibitory concentration of hexanoate is much lower than the inhibitory concentration of butyrate at neutral pH [18]. This confirms that hexanoate, even in its dissociated form, has a stronger inhibitory effect than butyrate, likely related to the carbon chain length. Experimental validation is required to further elucidate the effect of the different mechanisms of toxicity of hexanoate on the product distribution in chain-elongating communities.

By exchanging 50% of the culture broth with fresh medium at the beginning of an operational cycle, product and biomass concentrations are halved. The inhibitory effects of chain elongation products are therefore reduced. Throughout the cycle the product and biomass concentrations increased, which resulted in decreasing biomass-specific catabolic rates. This was reflected in largely stable hydrogen production rates during each operational cycle, despite strongly varying biomass concentrations (fig. 4.3). Various studies have shown that growth- and production rates are linearly affected by hexanoic acid toxicity, whereas butyric acid has a toxicity limit [18, 36, 37]. Therefore, the decreasing biomass-specific catabolic rate likely depended largely on the hexanoic acid concentration. Stable hydrogen production rates and incomplete substrate conversion at both pH confirmed that there is a delicate balance between substrate consumption and product inhibition. The apparent steady states were therefore governed by both the imposed retention time and the actual substrate and product concentrations. High concentrations of MCCAs impeded full substrate consumption and additional biomass growth. This underlines the relevance of bioreactor systems with integrated product removal for reaching complete substrate conversion and high MCCA production rates [23].

4.4.4. CATABOLIC OVERCAPACITY IS A STRATEGY FOR DEALING WITH PRODUCT TOXICITY

As both enriched cultures performed stably, the stoichiometric and kinetic parameters can be compared. The more stringent environment at pH 5.5 led to a decrease in biomass yield and a shift in product spectrum. Surprisingly, the biomass-specific ethanol consumption rate was twice as high. This implies that (1) a higher catabolic capacity is needed at pH 5.5 and that (2) this available capacity could not be invested in increasing the growth rate at pH 7.0. Possibly, a higher catabolic rate could not effectuate a higher growth rate at pH 7.0 because the culture was already growing at μ^{max}. However, the average growth rate in our systems was 0.058 h^{-1}, which is significantly lower than μ^{max} values reported in literature (0.1 – 0.24 h^{-1}) for *C. kluyveri* but comparable to growth rates (0.05 – 0.09 h^{-1}) of

communites enriched from anaerobic digester sludge in batch bottles [11, 12, 18]. Alternatively, faster growth might have been inhibited by relatively large amounts of fermentation products, leading to a trade-off between additional energy generation and maintaining endurable product concentrations. Considering the higher extent of weak acid uncoupling at mildly acidic pH, the higher catabolic flux might have been exploited for balancing increased non-growth-related ATP demands. A similar effect was seen when propionic acid was added to a culture of *Leptospirillum ferrooxidans* [38]. A flexible q_s^{max} might therefore be employed as a microbial strategy for dealing with product inhibition.

4.4.5. SBRs as a tool for microbial community characterization

Both SBR and chemostat systems have been used as a tool for studying mixed culture physiology and for creating a selective pressure toward certain characteristics [29, 39–41]. In the absence of storage polymers, SBR cultivation leads to a selective pressure on growth rate, whereas chemostat cultivation selects for substrate affinity. Even though both cultivation strategies provide insightful data, this work once again shows that SBRs prove to be more suitable for kinetic parameter identification of microbial communities [42]. Furthermore, when operating an SBR the effects of a perturbation become clear almost instantaneously. In future work, this allows the identification of the response of an established culture on changing process conditions, which is valuable for the generation of models upon which process design strategies can be based. Finally, every cycle in a functionally and taxonomically stable SBR is a biological replicate, improving the statistical significance of a stable culture. SBR cultivation can therefore be used to shed light on various aspects of chain-elongating communities. For instance, the interactions between chain-elongating organisms and methanogens have been studied to a limited extent and the effect of methanogen presence on chain elongator performance has not been quantified [43]. SBR cultivation would allow to identify the effect of the presence of methanogens in the microbial community on chain-elongating activity. Furthermore, growth rate-based selective pressure could lead to alternative strategies to prevent competition for substrate, while simultaneously allowing high-rate MCCA production. Alternatively, integrated SBR systems could be used for the optimization of process intensification strategies, such as in-line product extraction [2, 24] and simultaneous syngas fermentation and chain elongation [3].

In conclusion, SBR studies prove to be valuable for both fundamental characterization of microbial communities and for studying process optimization strategies. Beside substrate uptake kinetics, SBRs can be used to increase our fundamental understanding of the effect of product toxicity and changing ethanol-to-acetate ratios on chain-elongating organisms in dynamic environments. Omics techniques in combination with metabolic modeling could be used to identify labor division in microbial communities fed with a complex substrate and gain a deeper understanding of the effect of environmental conditions on the metabolic flux though microbial communities [44]. Lastly, integrated reactor setups can be exploited for testing the industrial potential of different cultivation strategies.

BIBLIOGRAPHY

[1] M. T. Allaart, G. R. Stouten, D. Z. Sousa, and R. Kleerebezem. "Product Inhibition and pH Affect Stoichiometry and Kinetics of Chain Elongating Microbial Communities in Sequencing Batch Bioreactors". In: *Frontiers in Bioengineering and Biotechnology* 9 (June 2021), p. 693030. DOI: 10.3389/fbioe.2021.693030.

[2] M. T. Agler, C. M. Spirito, J. G. Usack, J. J. Werner, and L. T. Angenent. "Chain elongation with reactor microbiomes: upgrading dilute ethanol to medium-chain carboxylates". In: *Energy & Environmental Science* 5.8 (2012), p. 8189. DOI: 10.1039/c2ee22101b.

[3] M. Diender, I. Parera Olm, M. Gelderloos, J. J. Koehorst, P. J. Schaap, A. J. M. Stams, and D. Z. Sousa. "Metabolic shift induced by synthetic co-cultivation promotes high yield of chain elongated acids from syngas". In: *Scientific Reports* 9.1 (Dec. 2019), p. 18081. DOI: 10.1038/s41598-019-54445-y.

[4] M. Diender, A. J. M. Stams, and D. Z. Sousa. "Production of medium-chain fatty acids and higher alcohols by a synthetic co-culture grown on carbon monoxide or syngas". In: *Biotechnology for Biofuels* 9.1 (Dec. 2016), p. 82. DOI: 10.1186/s13068-016-0495-0.

[5] R. Ganigué, P. Sánchez-Paredes, L. Bañeras, and J. Colprim. "Low Fermentation pH Is a Trigger to Alcohol Production, but a Killer to Chain Elongation". In: *Frontiers in Microbiology* 7 (May 2016). DOI: 10.3389/fmicb.2016.00702.

[6] S. Ge, J. G. Usack, C. M. Spirito, and L. T. Angenent. "Long-Term *n*-Caproic Acid Production from Yeast-Fermentation Beer in an Anaerobic Bioreactor with Continuous Product Extraction". In: *Environmental Science & Technology* 49.13 (July 2015), pp. 8012–8021. DOI: 10.1021/acs.est.5b00238.

[7] K. J. J. Steinbusch, H. V. M. Hamelers, C. M. Plugge, and C. J. N. Buisman. "Biological formation of caproate and caprylate from acetate: fuel and chemical production from low grade biomass". In: *Energy & Environmental Science* 4.1 (2011), pp. 216–224. DOI: 10.1039/C0EE00282H.

[8] A. P. Desbois. "Potential Applications of Antimicrobial Fatty Acids in Medicine, Agriculture and Other Industries". In: *Recent Patents on Anti-Infective Drug Discovery* 7.2 (June 2012), pp. 111–122. DOI: 10.2174/157489112801619728.

[9] M. T. Agler, B. A. Wrenn, S. H. Zinder, and L. T. Angenent. "Waste to bioproduct conversion with undefined mixed cultures: the carboxylate platform". In: *Trends in Biotechnology* 29.2 (Feb. 2011), pp. 70–78. DOI: 10.1016/j.tibtech.2010.11.006.

[10] H. A. Barker and S. M. Taha. "*Clostridium kluyverii*, an Organism Concerned in the Formation of Caproic Acid from Ethyl Alcohol". In: *Journal of Bacteriology* 43.3 (Mar. 1942), pp. 347–363. DOI: 10.1128/jb.43.3.347-363.1942.

[11] P. Candry, S. Huang, J. M. Carvajal-Arroyo, K. Rabaey, and R. Ganigue. "Enrichment and characterisation of ethanol chain elongating communities from natural and engineered environments". In: *Scientific Reports* 10.1 (Feb. 2020), p. 3682. DOI: 10.1038/s41598-020-60052-z.

[12] P. J. Weimer and D. M. Stevenson. "Isolation, characterization, and quantification of *Clostridium kluyveri* from the bovine rumen". In: *Applied Microbiology and Biotechnology* 94.2 (Apr. 2012), pp. 461–466. DOI: 10.1007/s00253-011-3751-z.

[13] C. M. Spirito, H. Richter, K. Rabaey, A. J. Stams, and L. T. Angenent. "Chain elongation in anaerobic reactor microbiomes to recover resources from waste". In: *Current Opinion in Biotechnology* 27 (June 2014), pp. 115–122. DOI: 10.1016/j.copbio.2014.01.003.

[14] W. D. A. Cavalcante, R. C. Leitão, T. A. Gehring, L. T. Angenent, and S. T. Santaella. "Anaerobic fermentation for n-caproic acid production: A review". In: *Process Biochemistry* 54 (Mar. 2017), pp. 106–119. DOI: 10.1016/j.procbio.2016.12.024.

[15] G. Muyzer and A. J. M. Stams. "The ecology and biotechnology of sulphate-reducing bacteria". In: *Nature Reviews Microbiology* 6.6 (June 2008), pp. 441–454. DOI: 10.1038/nrmicro1892.

[16] R. Kleerebezem and M. C. Van Loosdrecht. "Mixed culture biotechnology for bioenergy production". In: *Current Opinion in Biotechnology* 18.3 (June 2007), pp. 207–212. DOI: 10.1016/j.copbio.2007.05.001.

[17] H. Seedorf, W. F. Fricke, B. Veith, H. Brüggemann, H. Liesegang, A. Strittmatter, M. Miethke, W. Buckel, J. Hinderberger, F. Li, C. Hagemeier, R. K. Thauer, and G. Gottschalk. "The genome of *Clostridium kluyveri*, a strict anaerobe with unique metabolic features". In: *Proceedings of the National Academy of Sciences* 105.6 (Feb. 2008), pp. 2128–2133. DOI: 10.1073/pnas.0711093105.

[18] P. Candry, T. Van Daele, K. Denis, Y. Amerlinck, S. J. Andersen, R. Ganigué, J. B. A. Arends, I. Nopens, and K. Rabaey. "A novel high-throughput method for kinetic characterisation of anaerobic bioproduction strains, applied to *Clostridium kluyveri*". In: *Scientific Reports* 8.1 (June 2018), p. 9724. DOI: 10.1038/s41598-018-27594-9.

[19] L. T. Angenent, H. Richter, W. Buckel, C. M. Spirito, K. J. J. Steinbusch, C. M. Plugge, D. P. B. T. B. Strik, T. I. M. Grootscholten, C. J. N. Buisman, and H. V. M. Hamelers. "Chain Elongation with Reactor Microbiomes: Open-Culture Biotechnology To Produce Biochemicals". In: *Environmental Science & Technology* 50.6 (Mar. 2016), pp. 2796–2810. DOI: 10.1021/acs.est.5b04847.

[20] C. M. Spirito, A. M. Marzilli, and L. T. Angenent. "Higher Substrate Ratios of Ethanol to Acetate Steered Chain Elongation toward *n*-Caprylate in a Bioreactor with Product Extraction". In: *Environmental Science & Technology* 52.22 (Nov. 2018), pp. 13438–13447. DOI: 10.1021/acs.est.8b03856.

[21] W. R. Kenealy and D. M. Waselefsky. "Studies on the substrate range of *Clostridium kluyveri*; the use of propanol and succinate". In: *Archives of Microbiology* 141.3 (Apr. 1985), pp. 187–194. DOI: 10.1007/BF00408056.

[22] T. Grootscholten, K. Steinbusch, H. Hamelers, and C. Buisman. "Chain elongation of acetate and ethanol in an upflow anaerobic filter for high rate MCFA production". In: *Bioresource Technology* 135 (May 2013), pp. 440–445. DOI: 10.1016/j.biortech.2012.10.165.

[23] L. A. Kucek, C. M. Spirito, and L. T. Angenent. "High n-caprylate productivities and specificities from dilute ethanol and acetate: chain elongation with microbiomes to upgrade products from syngas fermentation". In: *Energy & Environmental Science* 9.11 (2016), pp. 3482–3494. DOI: 10.1039/C6EE01487A.

4

[24] S. Gildemyn, B. Molitor, J. G. Usack, M. Nguyen, K. Rabaey, and L. T. Angenent. "Upgrading syngas fermentation effluent using *Clostridium kluyveri* in a continuous fermentation". In: *Biotechnology for Biofuels* 10.1 (Dec. 2017), p. 83. DOI: 10.1186/s13068-017-0764-6.

[25] D. Vasudevan, H. Richter, and L. T. Angenent. "Upgrading dilute ethanol from syngas fermentation to n-caproate with reactor microbiomes". In: *Bioresource Technology* 151 (Jan. 2014), pp. 378–382. DOI: 10.1016/j.biortech.2013.09.105.

[26] Q. Wu, X. Feng, W. Guo, X. Bao, and N. Ren. "Long-term medium chain carboxylic acids production from liquor-making wastewater: Parameters optimization and toxicity mitigation". en. In: *Chemical Engineering Journal* 388 (May 2020), p. 124218. DOI: 10.1016/j.cej.2020.124218.

[27] Y. Liu, F. Lü, L. Shao, and P. He. "Alcohol-to-acid ratio and substrate concentration affect product structure in chain elongation reactions initiated by unacclimatized inoculum". In: *Bioresource Technology* 218 (Oct. 2016), pp. 1140–1150. DOI: 10.1016/j.biortech.2016.07.067.

[28] N. Tomlinson and H. Barker. "Carbon dioxide and acetate utilization by *Clostridium kluyveri*". In: *Journal of Biological Chemistry* 209.2 (Aug. 1954), pp. 585–595. DOI: 10.1016/S0021-9258(18)65485-7.

[29] G. R. Stouten, C. Hogendoorn, S. Douwenga, E. S. Kilias, G. Muyzer, and R. Kleerebezem. "Temperature as competitive strategy determining factor in pulse-fed aerobic bioreactors". In: *The ISME Journal* 13.12 (Dec. 2019), pp. 3112–3125. DOI: 10.1038/s41396-019-0495-8.

[30] G. R. Stouten, S. Douwenga, C. Hogendoorn, and R. Kleerebezem. *System characterization of dynamic biological cultivations through improved data analysis.* preprint. Microbiology, May 2021. DOI: 10.1101/2021.05.14.442977.

[31] M. Roghair, T. Hoogstad, D. P. Strik, C. M. Plugge, P. H. Timmers, R. A. Weusthuis, M. E. Bruins, and C. J. N. Buisman. "Controlling Ethanol Use in Chain Elongation by CO_2 Loading Rate". In: *Environmental Science & Technology* 52.3 (Feb. 2018), pp. 1496–1505. DOI: 10.1021/acs.est.7b04904.

[32] A. A. Herrero. "End-product inhibition in anaerobic fermentations". In: *Trends in Biotechnology* 1.2 ().

[33] L. R. Jarboe, L. A. Royce, and P. Liu. "Understanding biocatalyst inhibition by carboxylic acids". In: *Frontiers in Microbiology* 4 (2013). DOI: 10.3389/fmicb.2013.00272.

[34] R. K. Thauer, K. Jungermann, H. Henninger, J. Wenning, and K. Decker. "The Energy Metabolism of *Clostridium kluyveri*". In: *European Journal of Biochemistry* 4.2 (Apr. 1968), pp. 173–180. DOI: 10.1111/j.1432-1033.1968.tb00189.x.

[35] P. Liu, A. Chernyshov, T. Najdi, Y. Fu, J. Dickerson, S. Sandmeyer, and L. Jarboe. "Membrane stress caused by octanoic acid in *Saccharomyces cerevisiae*". In: *Applied Microbiology and Biotechnology* 97.7 (Apr. 2013), pp. 3239–3251. DOI: 10.1007/s00253-013-4773-5.

[36] L. A. Royce, P. Liu, M. J. Stebbins, B. C. Hanson, and L. R. Jarboe. "The damaging effects of short chain fatty acids on *Escherichia coli* membranes". In: *Applied Microbiology and Biotechnology* 97.18 (Sept. 2013), pp. 8317–8327. DOI: 10.1007/s00253-013-5113-5.

4

[37] M. Roghair, Y. Liu, J. C. Adiatma, R. A. Weusthuis, M. E. Bruins, C. J. N. Buisman, and D. P. B. T. B. Strik. "Effect of n-Caproate Concentration on Chain Elongation and Competing Processes". In: *ACS Sustainable Chemistry & Engineering* 6.6 (June 2018), pp. 7499–7506. DOI: 10.1021/acssuschemeng.8b00200.

[38] R. Kleerebezem and M. C. Van Loosdrecht. "Thermodynamic and kinetic characterization using process dynamics: Acidophilic ferrous iron oxidation by *Leptospirillum ferrooxidans*". In: *Biotechnology and Bioengineering* 100.1 (May 2008), pp. 49–60. DOI: 10.1002/bit.21745.

[39] M. F. Temudo, R. Kleerebezem, and M. Van Loosdrecht. "Influence of the pH on (open) mixed culture fermentation of glucose: A chemostat study". In: *Biotechnology and Bioengineering* 98.1 (Sept. 2007), pp. 69–79. DOI: 10.1002/bit.21412.

[40] M. F. Temudo, T. Mato, R. Kleerebezem, and M. C. M. Van Loosdrecht. "Xylose anaerobic conversion by open-mixed cultures". In: *Applied Microbiology and Biotechnology* 82.2 (Feb. 2009), pp. 231–239. DOI: 10.1007/s00253-008-1749-y.

[41] J. L. Rombouts, E. M. M. Kranendonk, A. Regueira, D. G. Weissbrodt, R. Kleerebezem, and M. C. M. Loosdrecht. "Selecting for lactic acid producing and utilising bacteria in anaerobic enrichment cultures". In: *Biotechnology and Bioengineering* 117.5 (May 2020), pp. 1281–1293. DOI: 10.1002/bit.27301.

[42] M. Strous, J. J. Heijnen, J. G. Kuenen, and M. S. M. Jetten. "The sequencing batch reactor as a powerful tool for the study of slowly growing anaerobic ammonium-oxidizing microorganisms". In: *Applied Microbiology and Biotechnology* 50.5 (Nov. 1998), pp. 589–596. DOI: 10.1007/s002530051340.

[43] P. Candry and R. Ganigué. "Chain elongators, friends, and foes". In: *Current Opinion in Biotechnology* 67 (Feb. 2021), pp. 99–110. DOI: 10.1016/j.copbio.2021.01.005.

[44] M. J. Scarborough, C. E. Lawson, J. J. Hamilton, T. J. Donohue, and D. R. Noguera. "Metatranscriptomic and Thermodynamic Insights into Medium-Chain Fatty Acid Production Using an Anaerobic Microbiome". In: *mSystems* 3.6 (2018).

4

4.5. SUPPLEMENTARY MATERIALS

Table S 4.1: Average steady state substrate and product concentrations at the start and end of the cycle and final biomass concentrations and hydrogen production. End of cycle concentrations were measured in the fermentation broth and cycle start concentrations were calculated taking into account the exchange ratio of 0.5. The measurements from samples in the operational cycles between 60 and 100 were taken to calculate the average start and end concentrations, as the systems performed stably during this period of time. Carbon- and electron balances were calculated assuming a normalized stoichiometry of $C_{1.0}H_{1.8}O_{0.5}N_{0.2}$ for biomass.

	pH 7.0 *start*	pH 7.0 *end*	pH 5.5 *start*	pH 5.5 *end*
Concentration (mmol·L^{-1})				
Ethanol	172	93 ± 11	201	150 ± 9
Acetate	24	6 ± 3	25	7 ± 3
Butyrate	12	25 ± 5	24	48 ± 6
Hexanoate	25	49 ± 2	7	14±3
Biomass		18.0 ± 2.4		5.2 ± 0.4
Hydrogen produced (mmol)		25.5		14.2 ± 1
Balances				
Carbon		106%		104%
Electrons		102%		100%

4.5.1. BIOLOGICAL RESPIRATION RATE DETERMINATION

For reconstruction of the biological respiration rates in a physicochemical model, boundaries have to be set for the rate at which the biological rate can change within a certain unit of time. These boundaries ensure that the obtained parameters are in a biologically relevant range and are therefore dependent on the system that is being studied. Here, fermentative organisms that do not fix nitrogen were studied. Therefore, the maximum change in the biological nitrogen respiration rate equals zero. Methanogenic organisms were present in such low abundance during stable bioreactor operation that the methane respiration rate, and the change therein, was at least an order of magnitude smaller than the hydrogen respiration rate. At pH 5.5 a significantly lower biomass concentration was observed, lowering the total biological capacity in the system. The process covariance was limited accordingly. Finally, CO_2 dissolution is limited at pH 5.5. Due to this change in physicochemical behavior, the maximum change in biological respiration rate of CO_2 was assumed to decrease twofold more than the other biological rates at this pH. The process covariance matrix (mol^2·s^{-2}), determining how fast the biological respiration rates can change, was defined as follows:

$$w_{k,pH7.0} = \mathscr{N}\left(\begin{pmatrix}0\\0\\0\\0\end{pmatrix}, diag\begin{pmatrix}1\\1\\1\\1\end{pmatrix} \cdot \begin{pmatrix}0\\2\cdot 10^{-9}\\2\cdot 10^{-9}\\2\cdot 10^{-9}\end{pmatrix}\right) \tag{4.1}$$

$$w_{k,pH5.5} = \mathscr{N}\left(\begin{pmatrix}0\\0\\0\\0\end{pmatrix}, diag\begin{pmatrix}1\\1\\1\\1\end{pmatrix} \cdot \begin{pmatrix}0\\1\cdot 10^{-9}\\5\cdot 10^{-10}\\1\cdot 10^{-10}\end{pmatrix}\right) \tag{4.2}$$

With wk representing the covariance matrix for nitrogen, hydrogen, carbon dioxide, and methane uptake rates. As the internal state estimation of the biological system is based on measurement data, the uncertainty in these measurements has to be taken into account in order to determine the accurate range of the estimation of the internal state at each timepoint. The uncertainty of the measurement depends on the accuracy of the mass spectrometer, which is different for the different gaseous species that are measured. The noise covariance for the off-gas (H_2, N_2, CO_2, CH_4) measurements (expressed as ppm^2) is expressed in the covariance matrix of the measurements:

$$v_{k,pH5.5} \sim \mathscr{N}\left(\begin{pmatrix}0\\0\\0\\0\end{pmatrix}, diag\begin{pmatrix}1\\1\\1\\1\end{pmatrix} \cdot \begin{pmatrix}30000\\2500\\2500\\250\end{pmatrix}\right) \tag{4.3}$$

With vk representing the covariance of head space gas mole fraction (N_2(g), H_2(g), CO_2(g), CH_4(g).
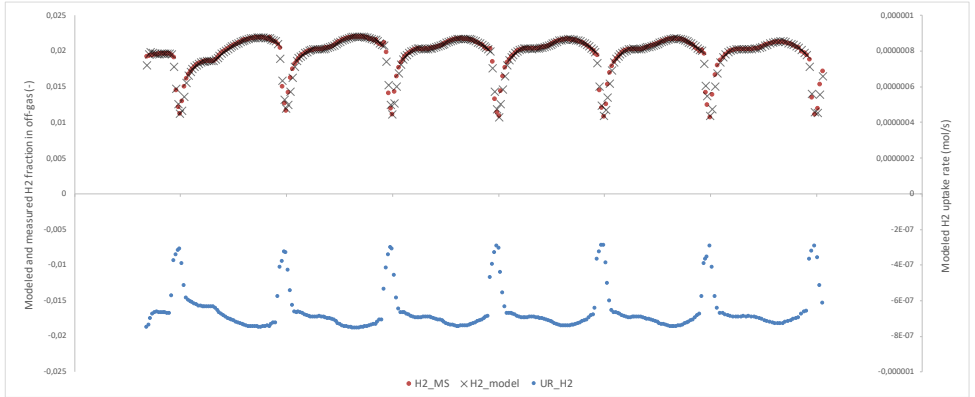
Figure S 4.1: Measured (red dots) and modeled (grey crosses) off-gas fraction of hydrogen and resulting hydrogen uptake rate (blue dots) in $mol\cdot s^{-1}$ of cycle 90-96 of the enrichment at pH 7.0. A negative uptake rate represents a positive production rate.

5

CHAIN-ELONGATING MICROORGANISMS METABOLIZE ETHANOL IN THE ABSENCE OF SHORT-CHAIN FATTY ACIDS

Maximilienne Toetie Allaart, Martin Pabst, Mees Fox, Ingo Nettersheim, Diana Z. Sousa, Robbert Kleerebezem

---

5

ABSTRACT

Hexanoate is a valuable chemical that is produced by microorganisms that can convert short-chain- to medium-chain fatty acids through a process called chain elongation. These microorganisms usually produce mixtures of butyrate and hexanoate from ethanol and acetate, but direct conversion of ethanol to hexanoate is theoretically possible. Steering microbial communities to ethanol-only chain elongation to hexanoate circumvents the need for acetate addition and simplifies product separation. The biological feasibility of ethanol elongation to hexanoate was validated in batch bioreactor experiments with a C. kluyveri-*dominated enrichment incubated with ethanol, acetate- and butyrate in different ratios. Frequent liquid sampling combined with high-resolution off-gas measurements allowed to monitor metabolic behavior. In experiments with an initial ethanol-to-acetate ratio of 6:1, acetate depletion occurred after ±35 hours of fermentation, which triggered a metabolic shift to direct conversion of ethanol to hexanoate despite the availability of butyrate (±10 mM). When only ethanol and no external electron acceptor was supplied, stable ethanol to hexanoate conversion could be maintained until 10-15 mM of hexanoate was produced. After this, transient production of either acetate and butyrate or butyrate and hexanoate was observed, requiring a putative reversal of the Rnf complex. This was not observed before acetate depletion or in presence of low concentrations (10-15 mM) of butyrate, suggesting a stabilizing or regulatory role of butyrate or butyrate-related catabolic intermediates. This study sheds light on previously unknown versatility of chain-elongating microbes and provides new avenues for optimizing (waste) bioconversions for hexanoate production.*

5.1. INTRODUCTION

MICROBIAL chain elongation is the anaerobic conversion of short-chain fatty acids (SCFAs) to medium-chain fatty acids (MCFAs) using ethanol or lactate as electron donor [1–3]. Chain elongation has gained momentum over the past two decades, as it can be used to convert a broad range of (organic) waste streams to biochemical building blocks like butyrate, hexanoate and octanoate [4–8]. Especially hexanoate has gained significant interest as a product of microbial chain elongation, both for its properties as antimicrobial agent, food and feed additive and biofuel precursor, and for its market value [9, 10].

Microbial communities are good catalysts for waste-to-value conversions. They allow digestion of complex waste streams through complementary functionalities in the microbiome and resilience to changes in operational parameters (temperature, influent composition etc.) due to functional redundancies. Furthermore, high costs for maintaining aseptic environments are omitted [9, 11]. Therefore, improving the understanding of the mechanisms that drive the physiology of chain-elongating communities is important for industrial process development [12].

In the case of chain elongation with ethanol as electron donor, the thermodynamically unfavorable ethanol oxidation (EO, eq. (5.1)) is coupled to reversed β-oxidation (RBO) of a SCFA (eq. (5.2) – acetate). Furthermore, electron bifurcation in RBO leads to the production of reduced ferredoxin, which is required for hydrogen formation [13, 14]. To enable the production of two H_2 from EO, at least two RBO cycles should run to provide sufficient reduced ferredoxin. Experimentally, however, EO and RBO are often observed to be coupled in a 1:5 ratio (eqs. (5.3) and (5.4)) [15, 16]. This facilitates the production of more reduced ferredoxin, which is used by the proton translocating Rnf complex to build up a chemiosmotic gradient from which additional ATP can be harvested. In fact, cellular redox balance can theoretically also be maintained when RBO operates independent of EO, rendering flexibility in their actual stoichiometric coupling [17].

$$Ethanol \rightarrow Acetate + H^+ + 2H_2 \tag{5.1}$$

$$\Delta G^{01} = +41.5 kJ/mol$$

$$Ethanol + Acetate \rightarrow Butyrate \tag{5.2}$$

$$\Delta G^{01} = -38.7 kJ/mol$$

$$6 Ethanol + 4 Acetate \rightarrow 5 Butyrate + H^+ + 2H_2 + H_2O \tag{5.3}$$

$$\Delta G^{01} = -183.6 kJ/mol$$

$$6 Ethanol + 5 Butyrate \rightarrow 5 Hexanoate + Acetate + H^+ + 2H_2 + H_2O \qquad (5.4)$$
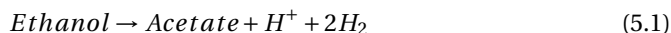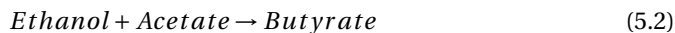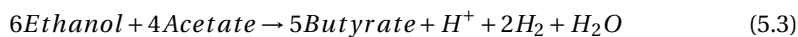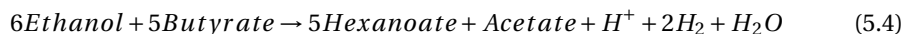
$$\Delta G^{01} = -184.6 kJ/mol$$

Even though the stoichiometric coupling of EO and RBO is flexible, few studies quantify the employed stoichiometry of chain elongators. Instead, a focus on the treatment of specific waste streams, process intensification or product spectrum control is distinguished in the literature on chain elongation [17–22].

Understanding the conditions that trigger different stoichiometric couplings between EO and RBO enables product spectrum control. For example, the elongation of ethanol to hexanoate without external electron acceptor is biochemically balanced (eq. (5.5) and fig. 5.1). Interestingly, conversion of ethanol to hexanoate in the absence of acetate and butyrate has been observed by Smith et al. [23], but this conversion has gained little to no attention afterwards. However, other authors reported an absolute requirement of acetate for the elongation of ethanol to butyrate and hexanoate [24, 25]. The discrepancy between these results makes it unclear whether and in which conditions ethanol can be converted to hexanoate in absence of acetate or butyrate as electron acceptor:

$$3 Ethanol \rightarrow Hexanoate + H^+ + 2H_2 + H_2O \qquad (5.5)$$
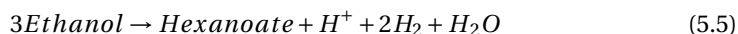
$$\Delta G^{01} = -67.9 kJ/mol$$

We theorize that the elongation of ethanol to hexanoate is the metabolic extreme of chain-elongating catabolism. This conversion encompasses a 1:2 stoichiometric ratio between EO and RBO and elongates internally generated acetate and butyrate subsequently to hexanoate. This can theoretically happen even in the complete absence of external electron accepting SCFAs. We therefore hypothesize that this stoichiometry will be exploited under electron acceptor limitation. In this work, we investigate the effect of omitting electron accepting SCFAs (acetate and butyrate) on the physiology and stoichiometry of chain-elongating microorganisms. Inocula were taken from an active sequencing batch bioreactor (SBR) performing ethanol-based chain elongation as described in chapter 4, grown in medium with only ethanol, medium with ethanol and acetate in a 6:1 ratio and medium with ethanol and butyrate in a 20:1 ratio. In the ethanol-only experiment the proteome was analyzed at time points where metabolic switching occurred.
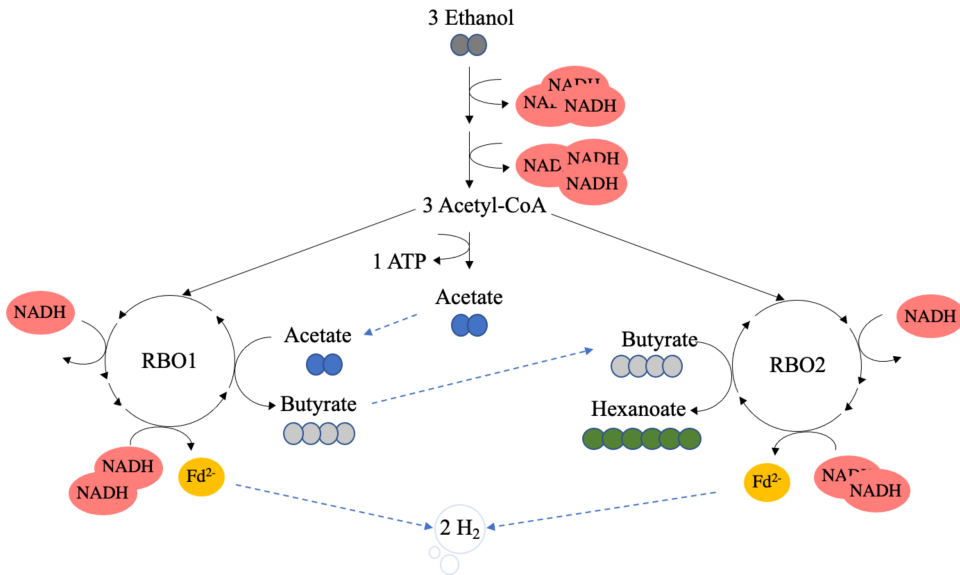
Figure 5.1: Schematic representation of the pathway for chain elongation of ethanol to hexanoate in the absence of external electron acceptor. In this stoichiometry ethanol oxidation and reversed β-oxidation are coupled in a 1:2 ratio, and acetate is subsequently elongated to butyrate and hexanoate. Energy conservation only happens via substrate-level phosphorylation, not via harvesting of proton motive force generated via the Rnf complex.

5

5.2. MATERIALS AND METHODS

5.2.1. SBR OPERATION

The microbial community was enriched at pH 7.0±0.2 in a glass jacketed 2 L bioreactor (Applikon, Delft, The Netherlands) with 1 L working volume as described in chapter 4. In short, an anaerobic SBR was inoculated with anaerobic sludge (Harnaschpolder, The Netherlands) and operated with a cycle time of 12 hours. Each cycle 50% of the fermentation broth (0.5 L) was exchanged for fresh medium and 125.5 mmol ethanol and 21.1 mmol acetate were added to the reactor in each cycle. The nutrient stock was the same as used in chapter 4, with the exception of the 2-BES concentration which was 10 instead of 5 mM. Anaerobic conditions were ensured by continuously sparging the reactors with 50±5 mL·min^{-1} (MX44, DASGIP, Germany) of N_2/CO_2 (95:5vol%). CO_2 was supplied to meet the anabolic requirements [26]. The headspace gas was continuously recirculated through the broth using a gas recirculation pump and the reactor was operated at 0.1 bar overpressure. The reactor was continuously agitated at a speed of 400 rpm (SC4, DASGIP, Germany) using mechanical stirrers. Temperature was maintained at 34°C using a water jacket and a thermostat bath (E300, Lauda, Germany). To prevent culture broth evaporation, the off-gas was cooled using a cryostat set to 5°C. After 249 operational cycles, glycerol stocks (50%) of the enriched culture were stored at -20°C for two months, after which the enrichment was re-started for continuation of this work. The cultivation medium was described in detail in chapter 4

5.2.2. BATCH CHAIN ELONGATION EXPERIMENTS

Batch experiments were carried out in in a 2 L bioreactor with the same initial working volume, temperature, pH and sparging as the enrichment reactor. The amounts of substrates added to the bioreactor in each experiment are summarized in table 5.1. The batch experiments were inoculated with 100 mL culture of the stable enrichment reactor, which contained approximately 10 mM ethanol, 0.5 mM acetate, 2.0 mM butyrate and 4.0 mM hexanoate. 90 g of 10x concentrated nutrient stock solution was added to each batch experiment to enable exponential growth. To ensure anaerobic conditions before initiation of the batch experiment, the carbon source and inoculum were added when no more oxygen was measured in the off-gas. Of all batch experiments a biological replicate was performed. The replicate of experiment 2 was performed with minimal sampling to confirm that sampling has a negligible effect on the biological conversions. Highly similar hydrogen profiles (supplementary fig. 5.1), fermentation times and final substrate- and product concentrations confirm biological replicability and negligibility of sampling effects. The replicates of experiment 3 showed very comparable physiologies until 100 hours of cultivation, after which no more hexanoate accumulated in replicate II and the decrease in ethanol concentration was most likely a result of evaporation (supplementary fig. 5.2). After the experiment we discovered that the gas recirculation machine of replicate II was malfunctioning which probably led to oxygen contamination in the reactor, most likely after ±100 hours of cultivation. Therefore, the data of replicate II is not presented in the Results section.

Table 5.1: Added amounts of susbtrate in batch chain elongation experiments.

Experiment no.	Acetate (mmol)	Ethanol (mmol)	Butyrate (mmol)	Hexanoate (mmol)
1	0	250	0	0
2	41	242	0	0
3	0	300	0	0

5.2.3. Analytical methods

The off-gas composition (N_2, CO_2, H_2, O_2, CH_4) of the reactors was measured using mass spectrometry (PRIMA BT Benchtop, Thermo Scientific, UK). Acid- and base dosage were monitored using an integrated revolution counter (MP8, DASGIP, Germany). Biomass concentrations (supplementary fig. 5.4) were monitored both by measuring optical density at 660 nm (OD_{660}) and the amount of volatile suspended solids (VSS) using 150 mL culture broth (APHA, 1999), calculated assuming a biomass molecular weight of 24.6 g $Cmol^{-1}$. After re-start of the enrichment, the cell pellets were washed with PBS before drying as the remaining supernatant after centrifuging interfered with correct biomass determination. The biomass measurements of the first batch experiment were corrected using the concentrations of butyrate and hexanoate and an assumed remaining supernatant volume of 5 mL. Technical duplicates of OD and VSS measurements were always performed. Ethanol, acetate, butyrate and hexanoate concentrations were determined using either high performance liquid chromatography (HPLC) or gas chromatography (GC). Biomass was removed from the reactor samples by centrifugation and filtration using a 0.22 μm membrane filter (Millipore, Millex-GV, Ireland). HPLC was performed using an Aminex HPX-87H column (BioRad, USA) at 59°C coupled to an ultraviolet detector at 210 nm (Waters, USA) with 1.5 mmol L^{-1} phosphoric acid as eluent. GC was performed using a Trace 1300 machine (Thermo Scientific, USA) equipped with an injector maintained at 180°C and a carbowax polyethylene glycol column of 20 m x 0.18 mm (Agilent, USA). A temperature gradient was used from 50°C to 180°C over 24 minutes. Helium was used as carrier gas and fermentation substrates and products were detected using a flame ionization detector set at 200°C. Iso-hexanoic acid was used as internal standard and samples were acidified using pure formic acid (Sigma Aldrich, US).

5.2.4. Microbial community analysis

The microbial community composition in the enrichment reactor was analyzed using amplicon sequencing of the 16S rRNA gene as described in [27] to confirm culture stability over time. The sequences have been stored in the 4TU research database and can be found under the DOI `10.4121/f74b503a-81d5-4187-b696-ba9c8133d2a3`. Furthermore, de novo composition analysis was performed from the proteome data at two different timepoints in the enrichment, which confirmed that the community was highly enriched in chain-elongating *C. kluyveri* (supplementary fig. 5.5).

5.2.5. PROTEOMICS SAMPLE PREPARATION

Protein extraction from chain-elongating microbial community pellets (250 μL cell pellet slurry of pellets from 50 mL culture broth) was performed in solution (protocol adapted from [28]. In short, the pellet slurries were resuspended in 250 μL 50 mM triethylammonium bicarbonate (TEAB) (Merck Sigma, Cat. No. T7408) containing 1% (w/w) NaDOC and 250 μ L B-PER™ Bacterial Protein Extraction Reagent (Thermo Fisher, cat no. 78243). Cells were lysed by glass bead beating and vortexing 6 times for 1.5 min alternated with 0.5 min rest on ice. The samples were kept in a thermoshaker for 3 minutes at 80°C and 1000 rpm and placed in an ultrasonic bath for 10 minutes for protein extraction. The proteins were precipitated by adding Trichloroacetic (TCA) solution 6.1N (Sigma Aldrich, T0699) in a 1:4 ratio to the supernatant and vortexing. Samples were incubated for 30 minutes at 4°C and spun down for 15 minutes at 14.000 rcf for precipitation. The protein pellet was washed with ice-cold acetone and resuspended in 6 M Urea (cat no. U5128, Sigma-Aldrich) in 200 mM ammonium bicarbonate. The extracted proteins were reduced by addition of 10 mM DTT (Merck Sigma, Cat. No. 43815) and incubated for 1 h at 37°C and 300 rpm in an Eppendorf ThermoMixer. Subsequently, the proteins were alkylated for 30 minutes at room temperature in the dark by addition of 20 mM iodoacetamide (Merck Sigma, I1149). Proteolytic digestion was performed using Sequencing Grade Trypsin (Promega, Cat. No. V5111), 1:100 enzyme to protein ratio (v/v) and incubated at 37°C and 300 rpm overnight. Solid phase extraction was performed with an Oasis HLB 96-well μElution plate (Waters, Milford, USA, Cat. No. 186001828BA). Eluates were dried using a SpeedVac vacuum concentrator. Dried peptides were resuspended in 3% ACN / 0.01% TFA prior to MS-analysis.

5.2.6. WHOLE CELL LYSATE SHOTGUN PROTEOMICS

An aliquot of approx. 250 ng protein digest per sample was analysed in triplicates using a one-dimensional shotgun proteomics approach [29]. Briefly, the samples were analysed using a nano-liquid-chromatography system consisting of an EASY nano-LC 1200 equipped with an Acclaim PepMap RSLC RP C18 separation column (50 μm x 150 mm, 2 μm), and an QE plus Orbitrap mass spectrometer (Thermo Fisher Scientific, Germany). The flow rate was maintained at 350 nL/min over a linear gradient from 5% to 25% solvent B over 88 minutes, and finally to 55% B over 60 minutes. Data were acquired from 0 to 175 min. Solvent A was H_2O containing 0.1% formic acid, and solvent B consisted of 80% acetonitrile in H_2O and 0.1% formic acid. The Orbitrap was operating in data dependent acquisition mode measuring peptide signals form 385–1250 m/z at 70 K resolution with a max IT of 75 ms and an AGC target of 3^6. The top 10 signals were isolated at a window of 2.0 m/z and fragmented using a NCE of 28. Fragments were acquired at 17 K resolution with a max IT of 75 ms and an AGC target of 2^5. Unassigned, singly and >6 times charged mass peaks were excluded from fragmentation.

5.2.7. Database searching

Mass spectrometric raw data were deposited in the PRIDE partner repository under accession number PXD040972 and first analysed using the NovoBridge pipeline [30] to estimate the microbial composition of the enrichment. Protein reference sequences at the genus level covering the major taxa were further retrieved from UniprotKB to confirm the taxonomic (protein) composition and to investigate overall metabolic changes. A focused analysis was further performed using the reference proteome of the major taxon *Clostridium kluyveri* (strain ATCC 8527/DSM 555/NCIMB 10680). Database searching was performed using PEAKS X (Bioinformatics Solutions Inc., Canada) allowing for 20 ppm parent ion and 0.02 m/z fragment ion mass error, 3 missed cleavages, carbamidomethylation as fixed and methionine oxidation and N/Q deamidation as variable modifications. Peptide spectrum matches were filtered for 1% false discovery rate and protein identifications with ≥ 2 unique peptides were accepted as significant.

5.2.8. Label free quantification

Label free quantification was performed using the PEAKS Q module (Bioinformatics Solutions Inc., Canada). A comparison of the protein expression level between conditions was performed on identified peptide spectra filtered for 1% false discovery rate, a mass error equal or less to 10 ppm and a maximum retention time shift between runs of 5 minutes. The significance of protein abundance changes within the groups (conditions) was determined using ANOVA. Considered proteins required at least 2 unique peptide identifications per protein sequence. The fold-change of protein levels obtained from PEAKSQ between the different samples was visualized with heatmaps using the seaborn package in Python 3.0.

5.2.9. Carbon- and electron recovery and ethanol evaporation measurements

To confirm the validity of the measurements, carbon- and electron recoveries were calculated over the batch experiments. The bioreactor volume was corrected for sampling, considering a sample volume of 3 or 4 mL per sample, and base addition. Additionally, the amounts of substrates and products removed with sampling were accounted for. The recovery of carbon and electrons was calculated by adding the amount of C/e- in the reactor at the final experimental timepoint and the removed amounts (via sampling and hydrogen removal with sparging) by the amount of C/e- in the reactor at t0. Generally, recoveries are considered reliable when they are between 90-110%. In the batch experiments, both carbon and electron recoveries were lower than 90%, especially for long batches. No significant unidentified peaks were found in the HPLC spectra. To test the significance of ethanol evaporation in the used setup, an abiotic test with the cultivation broth was carried out (fig. 5.2), which showed that ethanol evaporation cannot be disregarded in this system. We assume that the carbon- and electron gaps in the batches are due to ethanol evaporation, as their order of magnitude matches the rate at which ethanol evaporated in the abiotic test.

5.3. RESULTS

5.3.1. CHAIN-ELONGATING MICROORGANISMS ELONGATE ETHANOL IN THE ABSENCE OF EXTERNAL ELECTRON ACCEPTOR

To investigate the metabolic flexibility of chain-elongating microorganisms for survival with ethanol as only carbon- and energy source, an enriched chain-elongating community was inoculated in a batch bioreactor with mineral medium containing 250 mmol ethanol in duplicate. The inoculum contained small amounts of acetate, butyrate and hexanoate (supplementary table 4.1), but the resulting concentration of electron accepting SCFAs was negligible compared to the available amount of ethanol (fig. 5.2). First, it should be noted that the biological duplicates did not show identical physiologies after first phase. In the initial phase of both duplicates, ethanol was converted to hexanoate upon evolution of hydrogen gas following the stoichiometry in eq. 5. This conversion continued for approximately 100 and 200 hours, respectively, after which 10-15 mM of hexanoate had accumulated. The conversion of ethanol to hexanoate could not be maintained until ethanol exhaustion. In both biological replicates a switch to a different, seemingly faster, catabolism was observed onwards. In one of the replicates (fig. 5.2, left panel), the stoichiometric shift led to simultaneous accumulation of acetate, butyrate and hydrogen and a complete halt to hexanoate formation. In the other replicate (fig. 5.2, right panel) butyrate, hexanoate and hydrogen accumulated simultaneously. These stoichiometries occurred transiently. In replicate I, canonical chain elongation of the accumulated acetate and butyrate occurred in the third phase of the experiment, resulting in hexanoate formation until all ethanol was consumed. In replicate II ethanol elongation to hexanoate was resumed until ethanol was exhausted.

5.3.2. COMMUNITY COMPOSITION AND PROTEOME DURING ETHANOL-ONLY CHAIN ELONGATION

To assess whether the observed physiologies correlated with shifts in community composition or relative protein expression levels, 16S rRNA gene amplicon sequencing and comparative metaproteomics were performed on replicate II of the ethanol-only batch experiment. Both methods indicated approx. 80–90% enrichment of the *Clostridium* genus and confirmed *Clostridium kluyveri* as the major taxon (supplementary fig. 5.5). *Desulfovibrio* became more abundant during the experiment (up to approx. 15% based on protein biomass). Even though enzymes for sulfate reduction with ethanol or hydrogen as electron donor were detected, the net influence of sulfate reducing metabolisms on the overall stoichiometry was neglected due to minimal sulfate availability in the medium. Syntrophic ethanol oxidation and methane production were also excluded as no methane was measured in the off-gas in any of the replicates. Thus, the observed physiologies were all attributed to chain-elongating organisms. Therefore, the relative log2 fold-changes in protein levels of the community were mapped to the reference genome of the major taxon (*Clostridium kluyveri*) to ensure high annotation accuracy.

The relative protein levels of central carbon metabolism proteins were analyzed at the start of phase II (t1) and III (t2) compared to the inoculum (t0) (supplementary
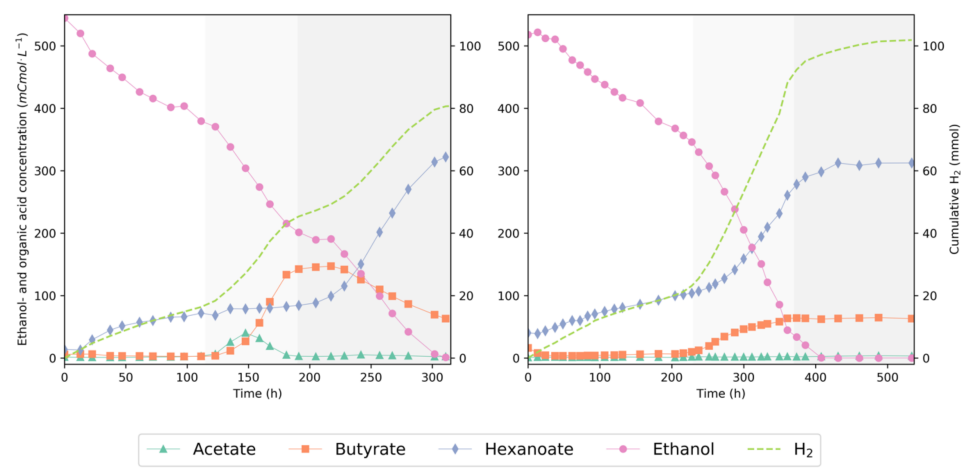
Figure 5.2: Ethanol-only batch experiment replicate I (A) and II (B). The replicates show different biochemical conversion profiles of ethanol. 100 mL of an active chain-elongating community was incubated in a batch bioreactor with 250 mM ethanol in duplicate. Different phases in the experiment are distinguished with different shades of background color. Solid lines are linear interpolations between the data points.

fig. 5.6). The proteome reflected that acetate kinase (ack) and cat3, which catalyzes the final transferase reaction of RBO, were more abundant in phases II and III. Increased abundance of acetate kinase indicates increased importance of ethanol oxidation to acetate in the applied conditions. Correspondingly, the levels of (several) alcohol dehydrogenases (aldh) and of phosphotransacetylase (pta) were also increased in phase II and III. Furthermore, increased amounts of the NADH dehydrogenase domain of the Rnf complex (RnfC) were distinguished (supplementary fig. 5.6). However, due to the membrane-integral or -associated nature of the Rnf subunits, quantitative conclusions on Rnf levels could not be drawn [31].

5.3.3. ETHANOL CHAIN ELONGATION IN THE PRESENCE OF ACETATE

In this experiment, the influence of acetate availability on the stoichiometry and rate of chain elongation was assessed by supplying ethanol and acetate in a 6:1 ratio. Three phases were distinguished in the experiment. The initial phase was characterized by exponential growth and exponentially increasing hydrogen production. In the second phase, growth became linear until acetate was depleted. Hexanoate production was favored over butyrate production during this phase. In the third phase of the experiment acetate was limiting. Butyrate did not get consumed completely and stayed constant at 9.8±0.7 mM. Ethanol was consumed upon hexanoate and hydrogen formation. Furthermore, the EtOH:H_2 ratio decreased substantially during this experimental phase, confirming a change in the catabolic stoichiometry to a 1:2 ratio between EO:RBO (fig. 5.3).
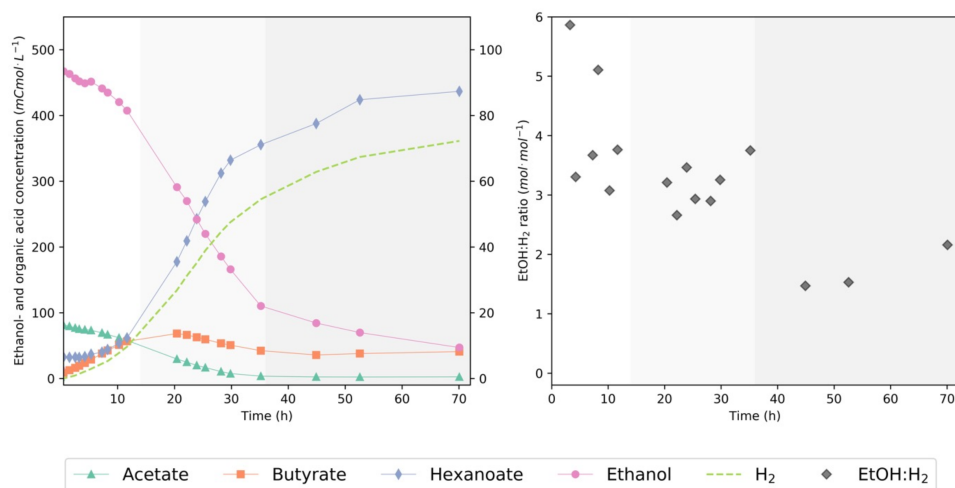
Figure 5.3: Biochemical conversion profiles (A) and EtOH:H$_2$ ratios (B) during ethanol chain elongation in presence of acetate. 100 mL of an active chain-elongating community was incubated in a batch bioreactor with 242 mM ethanol and 41 mM acetate. Different phases in the experiment are distinguished with different shades of background color. EtOH:H$_2$ ratios were calculated using the point-wise difference between consumed ethanol and produced hydrogen, outliers due to unreliable ethanol measurements were removed. Solid lines are linear interpolations between the data points.

5.3.4. ETHANOL CHAIN ELONGATION IN THE PRESENCE OF BUTYRATE

To assess the effect of butyrate availability on ethanol metabolism, a third experiment was performed with a 20:1 initial ethanol:butyrate ratio. The added butyrate concentration was 15 mM, which is in the order of magnitude of the concentrations at which butyrate consumption ceased in replicate II of the ethanol only batch and the ethanol + acetate batch. In this experiment, initial consumption of butyrate upon formation of hexanoate was observed, after which the stoichiometry changed to ethanol elongation to hexanoate, as reflected in Figure 4A and B. The EtOH:H$_2$ ratio during ethanol elongation to hexanoate was 1.9±0.7 mol mol-1, which is slightly higher than the expected ratio of 1.5 (fig. 5.1 and eq. (5.5)). This could be attributed to an overestimation of the ethanol consumption due to evaporation of ethanol during the experiment (supplementary fig. 5.2). After ±260 hours of cultivation, ethanol was not fully depleted but the H$_2$ fraction in the off-gas had dropped an order of magnitude. Therefore, it was assumed that there was no more metabolic activity.

The ethanol consumption rate in the presence of acetate (Phase I + II) was ±5 mmol·h^{-1}, where it was consumed at a rate of ±0.7-0.9 mmol·h^{-1} in absence of acetate in the ethanol-only experiments (not accounting for ethanol evaporation). The average ethanol consumption rate in the presence of small amounts of butyrate was ±0.8 mmol·h^{-1}. This rate is comparable to the ethanol consumption rate in the

absence of electron accepting SCFAs. Ethanol conversion in the presence of acetate was, thus, much faster than ethanol conversion in the absence of acetate.
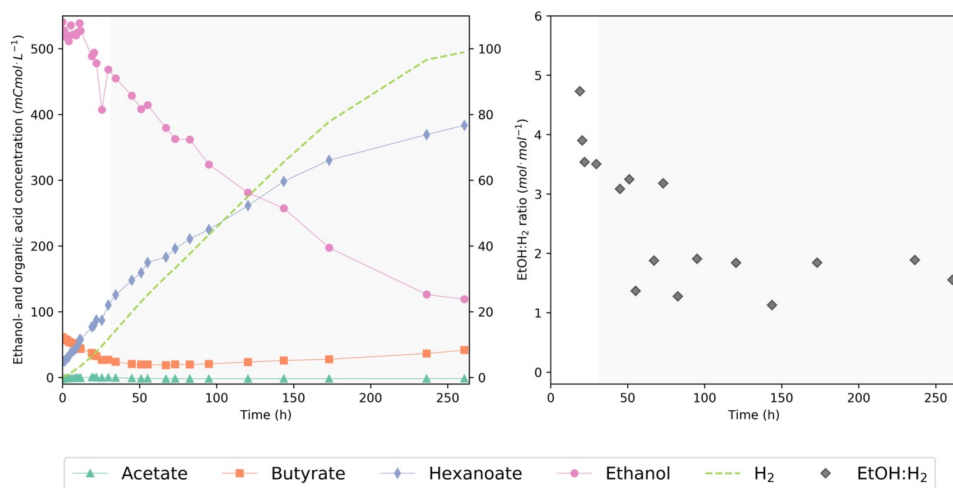

Figure 5.4: Biochemical conversion profiles (A) and EtOH:H$_2$ ratios (B) during ethanol chain elongation in presence of butyrate. 100 mL of an active chain-elongating community was incubated in a batch bioreactor with 300 mM ethanol and 15 mM butyrate. Different phases in the experiment are distinguished with different shades of background color. EtOH:H$_2$ ratios were calculated using the point-wise difference between consumed ethanol and produced hydrogen. Due to fluctuating ethanol measurements in the first 21 hours, the EtOH:H$_2$ ratio in this phase was calculated from t=0 to t=19 and from t=0 to t=20.5 with the initial concentration of ethanol as reference. Solid lines are linear interpolations between the data points.

5.4. Discussion

In this study, the effect of omitting electron-accepting SCFAs (acetate and butyrate) on the physiology and stoichiometry of chain-elongating microorganisms was assessed. Our results show that chain-elongating microbial communities can grow under electron acceptor limitation by elongating ethanol to hexanoate, rendering a 1:2 coupling of EO:RBO. However, this stoichiometry could not be maintained until ethanol depletion and a switch to simultaneous production of an acetate-butyrate or butyrate-hexanoate mixture from ethanol was observed. Low concentrations (10-15 mM) of butyrate prevented this transient physiology from occurring.
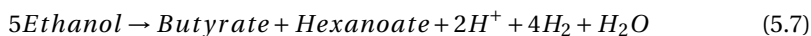
Various studies have shown that the supplied ratio of ethanol versus acetate strongly impacts the product spectrum of chain elongation [18, 32, 33]. Feeding more ethanol directs the product spectrum towards longer-chain products. However, the catabolic stoichiometry of the microbial communities subjected to high ethanol:acetate ratios was not assessed before. Here, we show that acetate limitation induces hexanoate production via EO and RBO in a 1:2 stoichiometry. The ethanol uptake rate was 6x lower when electron acceptor (acetate or butyrate) limitation was imposed. This could explain why previous studies with shorter incubation times reported no metabolic activity in the absence of acetate [25, 34].

Furthermore, our data strongly suggest that ethanol conversion to hexanoate in the absence of an external electron acceptor is unstable and can trigger a transient change in reaction stoichiometry leading to electron acceptor production. A possible explanation is that in absence of butyrate the intracellular concentration of butyryl-CoA becomes too low to render the condensation to 3-keto-hexanoyl-CoA feasible, triggering a metabolic shift towards transient butyrate production. This might explain that the presence of small amounts of butyrate (10-15 mM) stabilized ethanol to hexanoate conversion according to eq. (5.5), without net consumption of butyrate. Intracellular metabolomics of chain-elongating cultures in different conditions could shed light on the influence of metabolite levels on the observed stoichiometries and rates in chain-elongating processes [35]. However, a lack of commercially available standards for many of the intermediates of RBO impedes investigation of potential regulatory mechanisms in chain-elongating microbes.

A 1:2 stoichiometric coupling between EO and RBO was considered the extreme of ethanol-based chain elongation, but the organic acid production from ethanol observed here requires an EO:RBO ratio above 1:2. EO generates 2 moles of NADH ($\Delta E^{0'}$ (NADH/NAD+) = -320 mV), which, in principle, does not provide enough reductive power for hydrogen ($\Delta E^{0'}$ ($H_2/2H^+$) = -414 mV) formation. This is overcome by the electron bifurcating reaction in RBO, which lifts the electrons from NADH to ferredoxin ($\Delta E^{0'}$ (Fd^{2-}/Fd) $\approx$ -500 mV). In the case of an EO:RBO ratio higher than 1:2, a different mechanism for NADH consumption and Fd^{2-} formation must have been employed to maintain the cellular redox balance. We suggest that reversal of the Rnf complex enabled the production of organic acids from ethanol. In this scenario, a chemiosmotic gradient over the membrane ($\Delta\psi$) is built up by investing ATP conserved in EO and used to power the reduction of ferredoxin with NADH (fig. 5.5). Bidirectionality of the Rnf complex has not been assessed in chain-elongating organisms, but has been demonstrated in other

(an)aerobic organisms [31, 36–39].

The net ATP gain of EO with reversed Rnf activity is zero (fig. 5.5). Coupling it to RBO can relieve this energetic constraint by reducing the ATP requirements for ferredoxin reduction by the Rnf complex. In the ethanol-only experiment, simultaneous production of either acetate/butyrate or butyrate/hexanoate was observed. Potential catabolic stoichiometries that could underly these physiologies are shown in eq. (5.6) and eq. (5.7), respectively.

$$3 Ethanol + H_2O \rightarrow Acetate + Butyrate + 2H^+ + 4H_2 \qquad (5.6)$$

$$5 Ethanol \rightarrow Butyrate + Hexanoate + 2H^+ + 4H_2 + H_2O \qquad (5.7)$$

Verification of these stoichiometries with the experimental data is not trivial as the observed physiologies were transient and multiple stoichiometric couplings between EO and RBO render a redox balanced metabolism. Furthermore, the amounts of hydrogen evolved did not match the proposed stoichiometries exactly. This could also indicate that another electron sink was exploited, such as sulfate reduction or nitrogen fixation to NH_3 via the nitrogenase enzyme, of which two subunits were more abundant under electron acceptor limitation. Physiological studies, for example under complete soluble nitrogen limitation or with nitrogenase-deficient mutants could elucidate the role of nitrogen fixation in chain-elongating organisms.
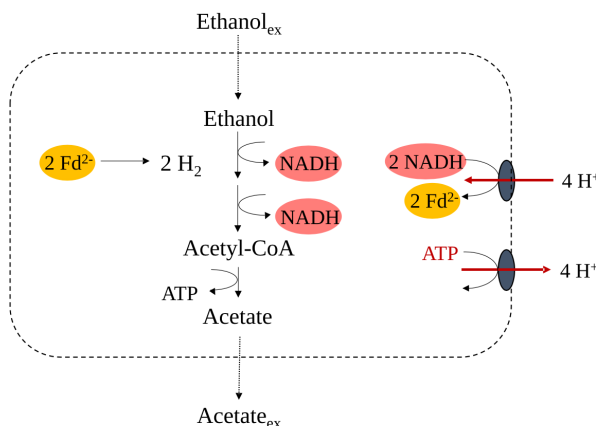
Figure 5.5: Ethanol oxidation and active export of protons via the ATPase. The reversal of the electron bifurcating Rnf complex drives the reduction of Fd, enabling hydrogen production. Rnf and ATPase stoichiometries based on [17]

Lastly, the ethanol-only experiments strongly suggest that the same mechanistic change does not consequently result in the same physiology [40]. Electron acceptor limitation proved to be stringent for the chain-elongating microbial community and different metabolic tricks are effective for overcoming this stringency. It is remarkable that hexanoate production ceased in only one of the two replicates. The cease in hexanoate production could be explained if different enzymes catalyze the

initiation or the entire second cycle of RBO. *C. kluyveri* possesses two non-identical sets of the same RBO enzymes and three different thiolase enzymes [41], but their individual functionalities have not been thoroughly studied. To do so, knock-out studies with pure cultures of *C. kluyveri* are needed. This requires a genetic toolbox for *C. kluyveri*, which is not available to date and provides an interesting target for future work.

5

BIBLIOGRAPHY

[1]   K. J. J. Steinbusch, H. V. M. Hamelers, C. M. Plugge, and C. J. N. Buisman. "Biological formation of caproate and caprylate from acetate: fuel and chemical production from low grade biomass". In: *Energy & Environmental Science* 4.1 (2011), pp. 216–224. DOI: 10.1039/C0EE00282H.

[2]   C. M. Spirito, H. Richter, K. Rabaey, A. J. Stams, and L. T. Angenent. "Chain elongation in anaerobic reactor microbiomes to recover resources from waste". In: *Current Opinion in Biotechnology* 27 (June 2014), pp. 115–122. DOI: 10.1016/j.copbio.2014.01.003.

[3]   W. D. A. Cavalcante, R. C. Leitão, T. A. Gehring, L. T. Angenent, and S. T. Santaella. "Anaerobic fermentation for n-caproic acid production: A review". In: *Process Biochemistry* 54 (Mar. 2017), pp. 106–119. DOI: 10.1016/j.procbio.2016.12.024.

[4]   D. Vasudevan, H. Richter, and L. T. Angenent. "Upgrading dilute ethanol from syngas fermentation to n-caproate with reactor microbiomes". In: *Bioresource Technology* 151 (Jan. 2014), pp. 378–382. DOI: 10.1016/j.biortech.2013.09.105.

[5]   S. Ge, J. G. Usack, C. M. Spirito, and L. T. Angenent. "Long-Term *n*-Caproic Acid Production from Yeast-Fermentation Beer in an Anaerobic Bioreactor with Continuous Product Extraction". In: *Environmental Science & Technology* 49.13 (July 2015), pp. 8012–8021. DOI: 10.1021/acs.est.5b00238.

[6]   Q. Mariën, B. Ulčar, J. Verleyen, B. Vanthuyne, and R. Ganigué. "High-rate conversion of lactic acid-rich streams to caproic acid in a fermentative granular system". In: *Bioresource Technology* 355 (July 2022), p. 127250. DOI: 10.1016/j.biortech.2022.127250.

[7]   D. Arslan, K. Steinbusch, L. Diels, H. De Wever, H. Hamelers, and C. Buisman. "Selective carboxylate production by controlling hydrogen, carbon dioxide and substrate concentrations in mixed culture fermentation". In: *Bioresource Technology* 136 (May 2013), pp. 452–460. DOI: 10.1016/j.biortech.2013.03.063.

[8]   X.-R. Pan, L. Huang, X.-Z. Fu, Y.-R. Yuan, H.-Q. Liu, W.-W. Li, L. Yu, Q.-B. Zhao, J. Zuo, L. Chen, and P. K.-S. Lam. "Long-term, selective production of caproate in an anaerobic membrane bioreactor". In: *Bioresource Technology* 302 (Apr. 2020), p. 122865. DOI: 10.1016/j.biortech.2020.122865.

[9]   M. T. Agler, B. A. Wrenn, S. H. Zinder, and L. T. Angenent. "Waste to bioproduct conversion with undefined mixed cultures: the carboxylate platform". In: *Trends in Biotechnology* 29.2 (Feb. 2011), pp. 70–78. DOI: 10.1016/j.tibtech.2010.11.006.

[10]   A. P. Desbois. "Potential Applications of Antimicrobial Fatty Acids in Medicine, Agriculture and Other Industries". In: *Recent Patents on Anti-Infective Drug Discovery* 7.2 (June 2012), pp. 111–122. DOI: 10.2174/157489112801619728.

[11]   R. Kleerebezem and M. C. Van Loosdrecht. "Mixed culture biotechnology for bioenergy production". In: *Current Opinion in Biotechnology* 18.3 (June 2007), pp. 207–212. DOI: 10.1016/j.copbio.2007.05.001.

[12]   P. Candry and R. Ganigué. "Chain elongators, friends, and foes". In: *Current Opinion in Biotechnology* 67 (Feb. 2021), pp. 99–110. DOI: 10.1016/j.copbio.2021.01.005.

[13]   F. Li, J. Hinderberger, H. Seedorf, J. Zhang, W. Buckel, and R. K. Thauer. "Coupled Ferredoxin and Crotonyl Coenzyme A (CoA) Reduction with NADH Catalyzed by the Butyryl-CoA Dehydrogenase/Etf Complex from *Clostridium kluyveri*". In: *Journal of Bacteriology* 190.3 (Feb. 2008), pp. 843–850. DOI: 10.1128/JB.01417-07.

[14]   W. Buckel and R. K. Thauer. "Flavin-Based Electron Bifurcation, A New Mechanism of Biological Energy Coupling". In: *Chemical Reviews* 118.7 (Apr. 2018), pp. 3862–3886. DOI: 10.1021/acs.chemrev.7b00707.

[15]   H. A. Barker, M. D. Kamen, and B. T. Bornstein. "The Synthesis of Butyric and Caproic Acids from Ethanol and Acetic Acid by *Clostridium kluyveri*". In: *Proceedings of the National Academy of Sciences* 31.12 (Dec. 1945), pp. 373–381. DOI: 10.1073/pnas.31.12.373.

[16]   R. K. Thauer, K. Jungermann, H. Henninger, J. Wenning, and K. Decker. "The Energy Metabolism of *Clostridium kluyveri*". In: *European Journal of Biochemistry* 4.2 (Apr. 1968), pp. 173–180. DOI: 10.1111/j.1432-1033.1968.tb00189.x.

[17]   L. T. Angenent, H. Richter, W. Buckel, C. M. Spirito, K. J. J. Steinbusch, C. M. Plugge, D. P. B. T. B. Strik, T. I. M. Grootscholten, C. J. N. Buisman, and H. V. M. Hamelers. "Chain Elongation with Reactor Microbiomes: Open-Culture Biotechnology To Produce Biochemicals". In: *Environmental Science & Technology* 50.6 (Mar. 2016), pp. 2796–2810. DOI: 10.1021/acs.est.5b04847.

[18]   L. A. Kucek, C. M. Spirito, and L. T. Angenent. "High n-caprylate productivities and specificities from dilute ethanol and acetate: chain elongation with microbiomes to upgrade products from syngas fermentation". In: *Energy & Environmental Science* 9.11 (2016), pp. 3482–3494. DOI: 10.1039/C6EE01487A.

[19]   Y. Liu, F. Lü, L. Shao, and P. He. "Alcohol-to-acid ratio and substrate concentration affect product structure in chain elongation reactions initiated by unacclimatized inoculum". In: *Bioresource Technology* 218 (Oct. 2016), pp. 1140–1150. DOI: 10.1016/j.biortech.2016.07.067.

[20]   M. Roghair, D. P. Strik, K. J. Steinbusch, R. A. Weusthuis, M. E. Bruins, and C. J. Buisman. "Granular sludge formation and characterization in a chain elongation process". In: *Process Biochemistry* 51.10 (Oct. 2016), pp. 1594–1598. DOI: 10.1016/j.procbio.2016.06.012.

[21]   Q. Wu, X. Feng, W. Guo, X. Bao, and N. Ren. "Long-term medium chain carboxylic acids production from liquor-making wastewater: Parameters optimization and toxicity mitigation". en. In: *Chemical Engineering Journal* 388 (May 2020), p. 124218. DOI: 10.1016/j.cej.2020.124218.

[22]   S. Crognale, C. M. Braguglia, A. Gallipoli, A. Gianico, S. Rossetti, and D. Montecchio. "Direct Conversion of Food Waste Extract into Caproate: Metagenomics Assessment of Chain Elongation Process". In: *Microorganisms* 9.2 (Feb. 2021), p. 327. DOI: 10.3390/microorganisms9020327.

[23]   G. M. Smith, B. W. Kim, A. A. Franke, and J. D. Roberts. "13C NMR studies of butyric fermentation in *Clostridium kluyveri*." In: *Journal of Biological Chemistry* 260.25 (Nov. 1985), pp. 13509–13512. DOI: 10.1016/S0021-9258(17)38751-3.

5

[24]   B. Bornstein and H. Barker. "The energy metabolism of *Clostridium kluyveri* and the synthesis of fatty acids". In: *Journal of Biological Chemistry* 172.2 (Feb. 1948), pp. 659–669. DOI: 10.1016/S0021-9258(19)52752-1.

[25]   P. J. Weimer and D. M. Stevenson. "Isolation, characterization, and quantification of *Clostridium kluyveri* from the bovine rumen". In: *Applied Microbiology and Biotechnology* 94.2 (Apr. 2012), pp. 461–466. DOI: 10.1007/s00253-011-3751-z.

[26]   N. Tomlinson and H. Barker. "Carbon dioxide and acetate utilization by *Clostridium kluyveri*". In: *Journal of Biological Chemistry* 209.2 (Aug. 1954), pp. 585–595. DOI: 10.1016/S0021-9258(18)65485-7.

[27]   M. T. Allaart, G. R. Stouten, D. Z. Sousa, and R. Kleerebezem. "Product Inhibition and pH Affect Stoichiometry and Kinetics of Chain Elongating Microbial Communities in Sequencing Batch Bioreactors". In: *Frontiers in Bioengineering and Biotechnology* 9 (June 2021), p. 693030. DOI: 10.3389/fbioe.2021.693030.

[28]   M. Pabst, D. S. Grouzdev, C. E. Lawson, H. B. C. Kleikamp, C. De Ram, R. Louwen, Y. M. Lin, S. Lücker, M. C. M. Van Loosdrecht, and M. Laureni. "A general approach to explore prokaryotic protein glycosylation reveals the unique surface layer modulation of an anammox bacterium". In: *The ISME Journal* 16.2 (Feb. 2022), pp. 346–357. DOI: 10.1038/s41396-021-01073-y.

[29]   M. Den Ridder, E. Knibbe, W. Van Den Brandeler, P. Daran-Lapujade, and M. Pabst. "A systematic evaluation of yeast sample preparation protocols for spectral identifications, proteome coverage and post-isolation modifications". In: *Journal of Proteomics* 261 (June 2022), p. 104576. DOI: 10.1016/j.jprot.2022.104576.

[30]   H. B. Kleikamp, M. Pronk, C. Tugui, L. Guedes Da Silva, B. Abbas, Y. M. Lin, M. C. Van Loosdrecht, and M. Pabst. "Database-independent de novo metaproteomics of complex microbial communities". In: *Cell Systems* 12.5 (May 2021), 375–383.e5. DOI: 10.1016/j.cels.2021.04.003.

[31]   E. Biegel, S. Schmidt, J. M. González, and V. Müller. "Biochemistry, evolution and physiological function of the Rnf complex, a novel ion-motive electron transport complex in prokaryotes". In: *Cellular and Molecular Life Sciences* 68.4 (Feb. 2011), pp. 613–634. DOI: 10.1007/s00018-010-0555-8.

[32]   C. M. Spirito, A. M. Marzilli, and L. T. Angenent. "Higher Substrate Ratios of Ethanol to Acetate Steered Chain Elongation toward *n*-Caprylate in a Bioreactor with Product Extraction". In: *Environmental Science & Technology* 52.22 (Nov. 2018), pp. 13438–13447. DOI: 10.1021/acs.est.8b03856.

[33]   S. Joshi, A. Robles, S. Aguiar, and A. G. Delgado. "The occurrence and ecology of microbial chain elongation of carboxylates in soils". In: *The ISME Journal* 15.7 (July 2021), pp. 1907–1918. DOI: 10.1038/s41396-021-00893-2.

[34]   P. Candry, T. Van Daele, K. Denis, Y. Amerlinck, S. J. Andersen, R. Ganigué, J. B. A. Arends, I. Nopens, and K. Rabaey. "A novel high-throughput method for kinetic characterisation of anaerobic bioproduction strains, applied to *Clostridium kluyveri*". In: *Scientific Reports* 8.1 (June 2018), p. 9724. DOI: 10.1038/s41598-018-27594-9.

[35]   J. K. Heffernan, V. Mahamkali, K. Valgepea, E. Marcellin, and L. K. Nielsen. "Analytical tools for unravelling the metabolism of gas-fermenting *Clostridia*". In: *Current Opinion in Biotechnology* 75 (June 2022), p. 102700. DOI: 10.1016/j.copbio.2022.102700.

5

[36] P.-L. Tremblay, T. Zhang, S. A. Dar, C. Leang, and D. R. Lovley. "The Rnf Complex of *Clostridium ljungdahlii* Is a Proton-Translocating Ferredoxin:NAD $^+$ Oxidoreductase Essential for Autotrophic Growth". In: *mBio* 4.1 (Mar. 2013). Ed. by D. K. Newman, e00406–12. DOI: 10.1128/mBio.00406-12.

[37] M. Kuhns, D. Trifunović, H. Huber, and V. Müller. "The Rnf complex is a Na+ coupled respiratory enzyme in a fermenting bacterium, *Thermotoga maritima*". In: *Communications Biology* 3.1 (Aug. 2020), p. 431. DOI: 10.1038/s42003-020-01158-y.

[38] M. Schmehl, A. Jahn, M. Schnppler, M. Marxer, J. Oelze, and W. Klipp. "Identification of a new class of nitrogen fixation genes in Rhodobacter capsulatus: a putative membrane complex involved in electron transport to nitrogenase". In: *MGG Molecular & General Genetics* 241.5-6 (1993), pp. 602–615.

[39] L. Westphal, A. Wiechmann, J. Baker, N. P. Minton, and V. Müller. "The Rnf Complex Is an Energy-Coupled Transhydrogenase Essential To Reversibly Link Cellular NADH and Ferredoxin Pools in the Acetogen *Acetobacterium woodii*". In: *Journal of Bacteriology* 200.21 (Nov. 2018). Ed. by W. W. Metcalf. DOI: 10.1128/JB.00357-18.

[40] M. Hecker and U. Völker. "General stress response of *Bacillus subtilis* and other bacteria". In: *Advances in Microbial Physiology*. Vol. 44. Elsevier, 2001, pp. 35–91. DOI: 10.1016/S0065-2911(01)44011-2.

[41] H. Seedorf, W. F. Fricke, B. Veith, H. Brüggemann, H. Liesegang, A. Strittmatter, M. Miethke, W. Buckel, J. Hinderberger, F. Li, C. Hagemeier, R. K. Thauer, and G. Gottschalk. "The genome of *Clostridium kluyveri*, a strict anaerobe with unique metabolic features". In: *Proceedings of the National Academy of Sciences* 105.6 (Feb. 2008), pp. 2128–2133. DOI: 10.1073/pnas.0711093105.

5

5.5. SUPPLEMENTARY MATERIALS
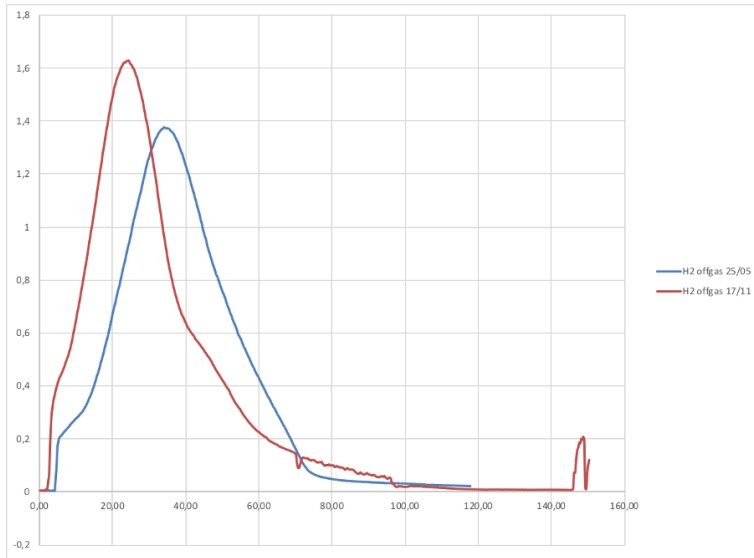
Figure S 5.1: Raw hydrogen profiles of both biological replicates of the Ethanol + Acetate batch experiment (experiment 2). Differences in the peak time and height were attributed to slight differences in the activity of the inoculum. More importantly, the cumulative amounts of hydrogen produced, the total fermentation time and the shapes of the curves are similar. This confirms the replicability of the batch experiment.
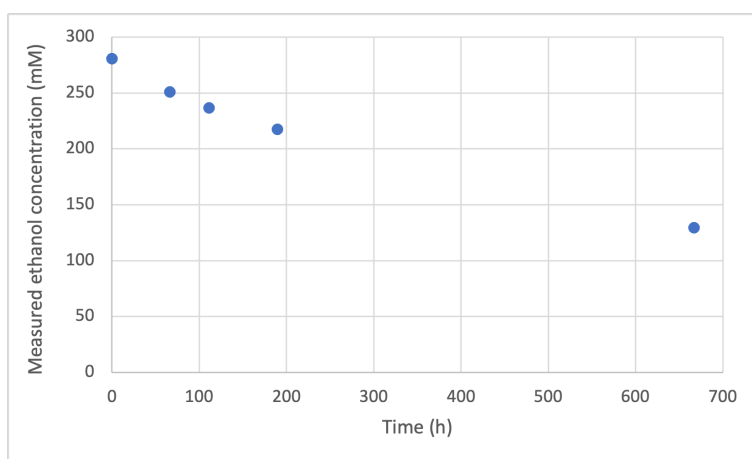
Figure S 5.2: Abiotic bioreactor experiment for quantification of ethanol evaporation during long-term batch experiments. The experiment was carried out in the same bioreactor configuration as the batch experiments, with the same reactor volume, stirring and gas flow rates. Ethanol concentration was measured using HPLC.
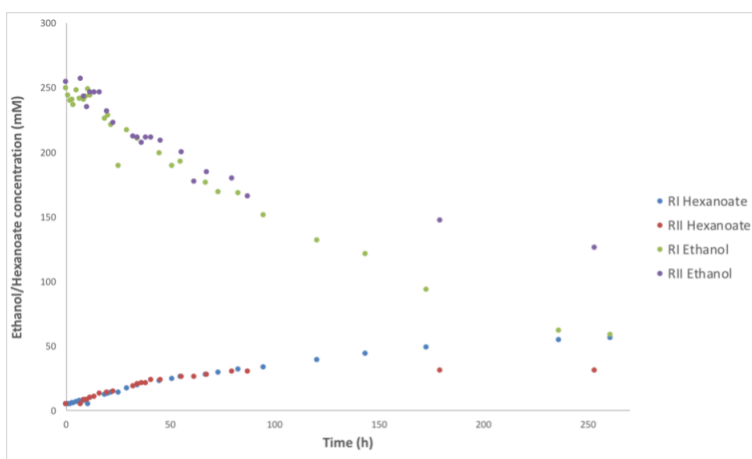
Figure S 5.3: Ethanol and hexanoate profiles of both biological replicates of the Ethanol + Butyrate batch experiment (experiment 3). Highly replicable data was obtained up until approximately 100 hours of cultivation, after which metabolic activity ceased in replicate II. We hypothesize this was related to oxygen contamination.
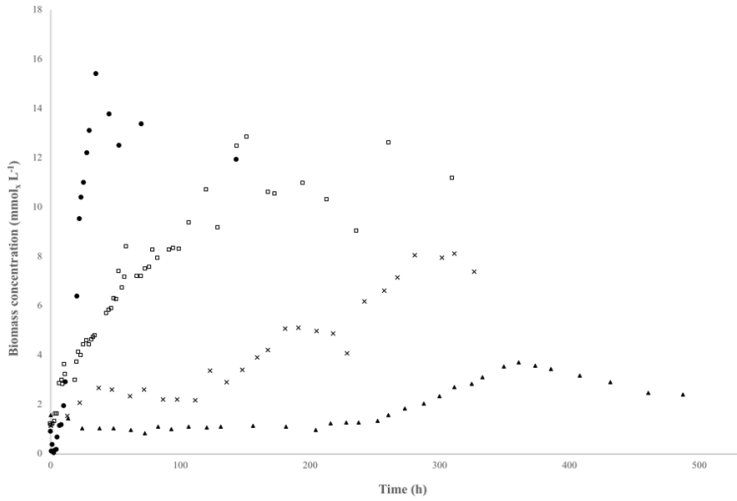
Figure S 5.4: Biomass concentration in time during the different batch experiments.
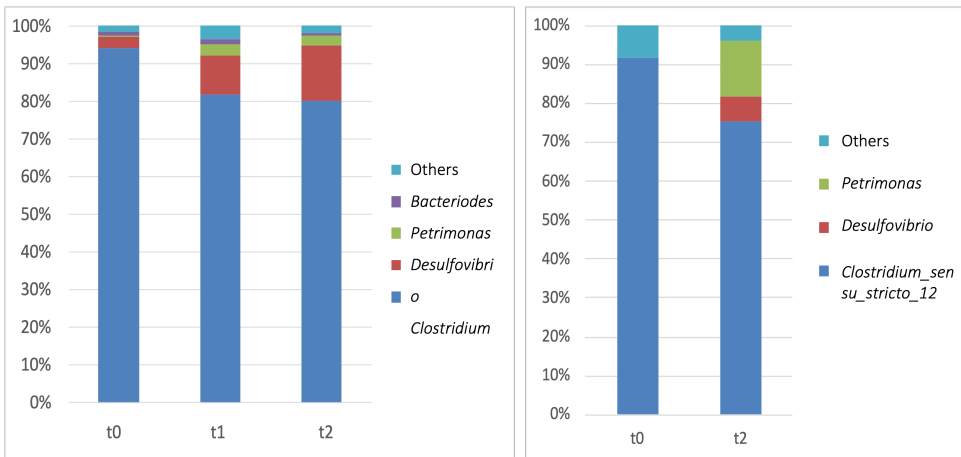
Figure S 5.5: Estimation of the microbial composition using metaproteomics (left, protein biomass) and 16S rRNA gene amplicon sequencing (right, 16S rRNA) of the chain-elongating microbial community in the ethanol-only batch experiment.

Figure S 5.6: Heatmap of the log2 fold-change in protein levels of central carbon metabolism proteins and other specific proteins of interest. The log2 fold-change was calculated by taking the 2-base logarithm of the protein counts normalized to the number of protein counts in de inoculum. All changes were statistically significant ($p < 0.03$).

6

TOWARDS KINETIC MODELLING OF CHAIN-ELONGATING MICROORGANISMS

Maximilienne Toetie Allaart, Gerben Roelandt Stouten, Maaike Remeijer, Ingo Nettersheim, Mees Fox, Diana Z. Sousa, Robbert Kleerebezem

This chapter provides valuable additional experimental data and considerations regarding a mechanistic model of chain-elongating microorganisms and serves as a foundation for a future manuscript.

ABSTRACT

Chain-elongating microbial communities are used in the valorization of different types of waste streams into antimicrobials, food and feed additives and biofuel precursors. Stoichiometric and kinetic models are available of these microorganisms, but both fail to fully represent the potential that they possess. Stoichiometric models reflect the characteristic metabolic versatility of the organisms but are generally not suited to study behavior in dynamic conditions. Kinetic models do describe physiology in dynamic conditions, but the models available for chain-elongating microbes do not include their flexible metabolism. This chapter presents a dataset of batch experiments with enrichments of chain-elongating microbes in well-controlled bioreactors with 9 different initial conditions to study the mechanisms that underlie their physiology. From this data, we deduce that chain elongator physiologies are highly reproducible and that H_2 production is a key indicator for the overall chain elongation rate in all conditions tested here. Furthermore, our data shows no clear preference for the consumption of acetate or butyrate as electron acceptor. Yet, acetate was consumed completely in most conditions, whereas the butyrate concentration stabilized between 5-15 mM in various experiments despite ethanol still being available. Instead of fully consuming butyrate, the microorganisms shifted to the elongation of ethanol to hexanoate, which comprises a different stoichiometric coupling between ethanol oxidation and reversed β-oxidation. This indicates the importance of including stoichiometric flexibility in a kinetic model describing chain-elongating microbes. Lastly, we observed hexanoate concentrations higher than the previously reported toxicity limit for a pure culture of C. kluyveri, *indicating that enrichments of chain elongators might be better adapted to high hexanoate concentrations than pure cultures are. We show that the currently available kinetic model fails to represent our experimental data well, highlighting the need for an improved kinetic model. Our datasets are suitable for parameter identification, but we have not yet succeeded to capture the complexity observed in our experiments in a newly formulated model. This chapter therefore provides a framework for data handling and reconciliation, resulting in a reconciled dataset that can be readily used for future model parameterization. Furthermore, we discuss the mechanisms that must be included in a future model, which include stoichiometric variability, product inhibition, and transport of substrates and products over the cell membrane. In summary, this chapter provides an excellent basis for future development of an improved kinetic model of chain-elongating microorganisms.*

6.1. Introduction

C HAIN elongating microorganisms were first isolated in Delft in 1942 [1], after which their metabolism and physiology were studied sporadically in the second half of the 20th century [2–6]. In recent years they have re-gained scientist' interest for their capacity to elongate short-chain fatty acids (i.e. acetate and butyrate) to medium-chain fatty acids (i.e. hexanoate and octanoate) in the presence of an electron donor like ethanol. This conversion enables the valorization of different types of waste streams, such as brewery wastewater [7], syngas fermentation effluents [8] and food waste [9, 10] into antimicrobials, food and feed additives and biofuel precursors using microbial communities [11, 12].

To design efficient bioprocesses for waste valorization, a fundamental understanding of the microorganisms responsible for the conversion is crucial. Experimental data serves as the basis for developing computational models, which are used by researchers and bioprocess engineers to predict microorganisms' behavior under various conditions. Generally, two different types of models are used when studying and predicting microbial behavior: stoichiometric and kinetic models. Genome-scale stoichiometric models represent the potential of a microorganism based on the genome sequence and available annotations, by mapping all the reactions it can catalyze. Condensed metabolic models reflect our understanding of the most important pathways and provide a good alternative to highly complex genome-scale models. Stoichiometric models can be used to study which metabolic routes are feasible for the conversion of substrates, using flux balance analysis and an optimization target [13]. Kinetic models, on the other hand, treat the microorganism more as a black box and are used to describe process dynamics rather than metabolic potential. Furthermore, they allow for the description of empirically discovered physiological characteristics, such as the affinity for substrates and inhibition by either substrates or products and how they affect the conversion rates in the system. Purely stoichiometric models fail to represent such complex interactions. Therefore, kinetic models are crucial for process design, as both biomass-specific- and overall process rates represent the technical limits of the process and thereby determine reactor configuration, throughput, and sizing.

Several models, both stoichiometric and kinetic, have been developed to describe chain-elongating microorganisms to date [14–17]. First, a stoichiometric model was published that displays that the catabolism of chain elongators is balanced for different stoichiometric couplings between ethanol oxidation (EO) and reversed β-oxidation (RBO) [14]. Cavalcante et al. (2017) published a kinetic model including biomass formation and a Monod inhibition term accounting for undissociated hexanoic acid toxicity, and a fixed overall stoichiometry between EO and RBO that has been unraveled based on the genome and biochemistry of key enzymes [18–20]. The parameters in this model were estimated from steady-state data published by Kenealy & Waselefsky (1985). However, estimating stoichiometric and kinetic parameters from steady-state data with the objective to predict physiologies in dynamic conditions is not ideal. This problem was addressed by Candry et al. (2018), who used dynamic experiments in 96-well plates for parameter identification. Furthermore, they identified the mechanisms of toxicity of butyrate and hexanoate

and included the appropriate equations in the model.

Yet, in chapter 5 we provide data demonstrating that chain-elongating microbes do not have a fixed catabolic stoichiometry. We observed a change in the EO:RBO proportion under acetate limitation, and even transient accumulation of acetate and butyrate under severe electron acceptor limitation. These physiologies cannot be represented by the currently available kinetic models that do assume a fixed stoichiometric coupling between EO and RBO. This means that there are ample opportunities for improvements in the model formulation, but also for the methods used to gather experimental data. The model of Candry et al. (2018) has for example been parameterized using experiments conducted in uncontrolled environments (i.e. without pH control and in small volumes where evaporation of the broth can become significant), without monitoring e.g. H_2 formation. Additionally, care must be taken when using experimental data for model parameterization. For example, sampling interferes with the biological process, biological replicates are never identical, and analytical methods come with an inherent error range. This should all be taken into account to enable the estimation of biologically valid parameters as well as their confidence intervals.

Here, we perform batch experiments with a chain-elongating microbial community in 9 different initial conditions in bioreactors with pH and temperature control and continuous on-line monitoring of the off-gas composition. Highly complex behavior was observed in these experiments, and we have not yet succeeded in translating this complexity into a new kinetic model of chain-elongating microbes. Yet, we develop a framework for data analysis and reconciliation and use the reconciled data to assess the accuracy of the kinetic model developed by Candry et al. (2018) to identify mechanisms that lack in this description of chain elongators. From this analysis, we deduce the essential components of an updated kinetic model and describe the next steps that should be taken in the future development of a new kinetic model of chain-elongating microorganisms.

6.2. MATERIALS AND METHODS

6.2.1. BIOREACTOR EXPERIMENTS

Batch experiments with different initial conditions have been performed in 2L jacketed bioreactors with a working volume of 1L, controlled at pH 7.0 ± 0.2 and 34 °C. The reactors were inoculated with 100 mL of a chain-elongating culture highly enriched in *Clostridium kluyveri* (described in chapters 4 and 5). Different initial experimental conditions were used to assess the variability in chain-elongating physiologies (table 6.1). The cultivation medium has been described in chapters 4 and 5.

Table 6.1: Overview of performed experiments and the amounts of ethanol and organic acids added initially. The three datasets presented in chapter 5 are included in this study as well.

Experiment no.	Acetate (mmol)	Ethanol (mmol)	Butyrate (mmol)	Hexanoate (mmol)	Description
1	41	242	0	0	6:1 - EtOH:Ac
2	41	242	0	40	Hexanoate toxicity
3	41	242	100	0	Butyrate toxicity
4-5	0	300	15	0	Butyrate availability
6-7	70	250	70	0	Electron acceptor preference
8-9	0	250	0	0	EtOH-only
10-11	225	225	0	0	1:1 –EtOH:Ac
12-14	75	225	0	0	3:1 –EtOH:Ac
15-16	18.75	225	0	0	12:1 –EtOH:Ac

6.2.2. ANALYTICAL METHODS

The analytical methods used for online and offline data collection and analysis have been described in chapters 4 and 5. In short, the off-gas composition (N_2, CO_2, H_2, O_2, CH_4) of the reactors was measured using mass spectrometry (MS). As methanogenesis is chemically inhibited in our bioreactors through the addition of 2-bromoethanesulfonate, no methane production is foreseen (in analogy to observations in chapters 4 and 5). Still, the measurement of mass fragments of mass 15, which is normally used for the detection of methane, is left on during the batch experiments. Ethanol ionization leads to the formation of a mass fragment ($[CH_3^+]$) of mass 15. Detection and quantification of ethanol evaporation could therefore be performed using the MS signal at mass 15. A separate abiotic experiment was performed over a period of 30 days to assess the evaporation kinetics and to verify the quantification of evaporated ethanol (fig. 5.2). Biomass concentrations were monitored using OD_{660} measurements during the experiments and TSS/VSS measurements at the end of the experiments. Ethanol, acetate, butyrate and hexanoate concentrations were determined using either high performance liquid chromatography (HPLC) or gas chromatography (GC). For GC measurements,

samples were diluted 20x with MilliQ water containing iso-hexanoic acid as internal standard and acidified with 10 μL of pure formic acid.

6.2.3. DATA HANDLING AND RECONCILIATION

The experimental data was stored in individual Excel files in the same format for each replicate, including all relevant metadata. The experimental data is accessible in the 4TU database (https://data.4tu.nl/private_datasets/ QlALTQ7PcpdwoL3uRY1PBzoG_JVRK-hhl-iLELTMZe0). Each experimental file contains 1) the online measured values for off-gas composition, pH, acid and base dose monitors, scale input data, 2) the offline measured values for OD_{660}, ethanol, acetate, butyrate, hexanoate, and the sample volumes, 3) metadata overview of the experiment including the starting concentrations of the experiment, gas composition of the in-gas, and operational conditions. Carbon and electron balances were calculated by dividing the total carbon or electrons at a certain timepoint by the initial amount added to the bioreactor, considering substrate- and products removal through sampling, the actual reactor volume at each sampling point as a function of sampling and acid- and/or base addition, and ethanol evaporation. More specifically, the total amount of carbon or electrons was separated into either present in the reactor, sampled, or removed via the off-gas. The cumulative amounts of H_2 and ethanol removed from the reactor via the off-gas at each sample timepoint were extracted from the online data. For each sampled timepoint, the total amount of carbon or electrons was calculated by multiplying the compound concentrations by the current reactor volume and subsequently multiplying compounds in the reactor, removed via sampling and removed via off-gas by their number of carbon or electrons in the compound. The initial amounts of carbon/electrons added to the bioreactor were used as reference, and the amounts present at each sample time were divided by this reference value. This resulted in a scalar of values, where 1 indicates a fully closed balance at a specific timepoint.

H_2 measurements that were outside the expected range were corrected using a scaling factor calculated from the EtOH:Ac 1:1 experiment. The ratio between the final amounts of H_2 produced between the replicates in this experiment was calculated, and this was used as a rescaling factor for the H_2 measurements in the EtOH:Ac 1:1 experiment - replicate II, the EtOH:Ac 3:1 experiment and the EtOH:Ac 12:1 experiment. After correcting the H_2 data, the carbon- and electron balances were rescaled separately to 100%. These reconciled values were obtained by dividing the measured concentrations at each timepoint by the value in the scalar of the carbon- or electron balance at that timepoint. To calculate the confidence of the reconciled values, the scalar values were represented as a value between 0 and 1. This means that for points where the balance was > 1, the reciprocal value ($1/x$) was taken as the confidence of the reconciled values at that timepoint.

6.2.4. MODEL ACCURACY ASSESSMENT

The model as published in Candry et al. (2018) was reproduced in Python for model verification. Model predictions were made using the initial conditions in

each experiment and compared to the reconciled datasets. The initial biomass concentration in each experiment was multiplied with an activity score between 0 and 1 (in practice, activity scores between 0.15 and 0.5 were used). This prevented that the initial modeled rates differed significantly from the observed rates.

6

6.3. Results and Discussion

Batch bioreactor experiments were performed in nine different initial conditions to monitor the physiology of chain-elongating microorganisms. Below, we analyze the raw concentration profiles of the experiments summarized in table 6.1. We compare the replicates to assess the reproducibility and reliability of the experimental data. In chapter 5, the initial analysis of the ethanol-only, butyrate availability and EtOH:Ac - 6:1 experiments has already been presented. This analysis revealed that the theoretical flexibility in the biochemistry of chain elongation [14] is also observed experimentally, leading to differences for example in the observed EtOH:H_2 ratio upon electron acceptor limitation. This shows that incorporating the metabolic flexibility into a refined kinetic model is essential to accurately represent chain-elongating physiologies in a wide range of operational conditions.

6.3.1. Electron acceptor preference

To determine the preference of chain-elongating microbes for acetate or butyrate as electron acceptor, equimolar amounts of acetate and butyrate were supplied to an enrichment of chain-elongating microorganisms. fig. 6.1 shows the conversion profiles in mCmol· L^{-1}. Hexanoate was the main product detected during this experiment, and the H_2 profile closely follows the shape of the hexanoate curve. The net conversion rates of acetate and butyrate are similar, and both substrates had not completely been consumed when ethanol became limiting. This indicates that diauxic growth was not the mechanism defining whether acetate or butyrate consumption takes place. Furthermore, the acetate and butyrate curves largely followed the same dynamics. This indicates that the net conversion rates of both compounds were similar, suggesting that there was no clear preference for acetate or butyrate as electron acceptor.

It is important to mention that the data form the electron acceptor preference experiment was highly reproducible. In this experiment, more fluctuations were observed in the measurements of the dissolved compounds as compared to the other experiments. The main difference was that the dissolved species were measured using GC instead of HPLC in this experiment. GC measurements are more error-prone, as they required dilution, full acidification of the sample and the addition of an internal standard. In each of these sample processing steps a small measurement error could have been introduced. Samples analyzed using HPLC were injected directly to the column without any alterations to the sample. Thus, a larger inherent error range should be attributed to the datapoints in this experiment for parameter fitting procedures to prevent that the observed variability is wrongfully ascribed to biological activity.

6.3.2. Ethanol:Acetate 1:1

When ethanol and acetate were supplied in an equimolar ratio (fig. 6.2), ethanol was the first substrate to become limiting, while ± 100 mM of acetate remained at the end of the experiment. Butyrate was the main product, and the H_2 profile follows the shape of the butyrate curve even though there is also net hexanoate formation.
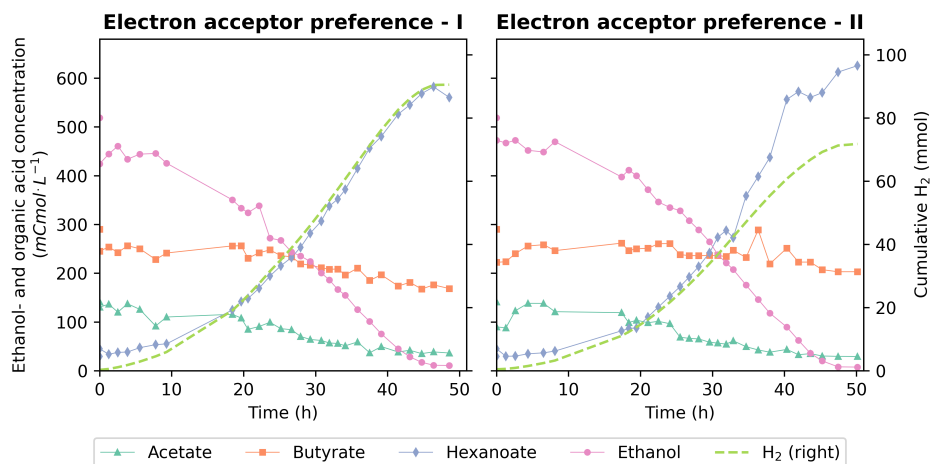
Figure 6.1: Electron acceptor preference. 100 mL of an active chain-elongating community was incubated in a batch bioreactor with 250 mmol ethanol, 70 mmol acetate and 70 mmol butyrate. Liquid measurements were done using gas chromatography. The cumulative hydrogen production was calculated from the off-gas measurements. Biological replicates were inoculated one hour after each other. The solid lines are linear interpolations between the data points.

Both replicates behaved analogously, beside the fact that the overall conversion rate appeared to be slightly higher towards the end in replicate II, leading to a shorter total fermentation time. Potentially, the inoculum needs to acclimatize when transferred from the SBR to the batch bioreactor. As biomass growth is exponential, a small difference in initial acclimatization time before the biomass is fully active can lead to a significant difference in total fermentation time. When modelling chain elongation, the acclimatization time of the inoculum might be an important parameter to consider, depending on the reactor operation. For parameter fitting in this study, the initial biomass activity could for example be a variable that is fitted for each individual experimental dataset. As all experiments were inoculated with the same amount of inoculum, the inoculum can be given an activity score between 0 and 1 to account for the variability in activity.

Another notable difference between the two replicates was the final amount of hydrogen produced. The hydrogen curves in both replicates closely mirrored the shape of the butyrate production profile. However, in replicate II, there was nearly half the amount of hydrogen produced compared to the end of the experiment in replicate I. The total amount of net produced acids was the same in both replicates, and net acid- and hydrogen production are biochemically coupled (section 6.3.7. This means that the amount of hydrogen produced in replicate I is conform our expectations, and in replicate II it is not. This might have a technical or a biological origin. Biological conversions that lead to H_2 consumption include homoacetogenesis, hydrogenotrophic methanogenesis and sulfate reduction with

H_2 as electron donor. Methanogenesis was inhibited by adding 10 mM 2-BES to the medium. Furthermore, no significant difference in CO_2 consumption between replicate I and II was measured and the amount of sulfate in the medium would only allow for the consumption of ± 2 mmol H_2 if all available sulfate would be fully reduced. Hence, it is not possible to completely disregard the involvement of H_2-consuming metabolisms. However, it is highly unlikely that they occurred to a significant extent, enough to account for the disparity in H_2 production between replicate I and II.

Therefore, a technical issue rather than a biological difference likely caused the aberrant measurements in replicate II. Technical issues that might cause this could range from small H_2 gas leaks from the bioreactor system or the tubing transporting the gas to the mass spectrometer to filament deterioration of the mass spectrometer hampering accurate measurement. It was excluded that differences in gas flow-rate through the bioreactor caused this difference by verifying the gas flowrate into and out of the reactor using water displacement. Data reconciliation of the H_2 measurements could be possible by using the acid:H_2 stoichiometry or by directly rescaling the H_2 in replicate II to be equal to the amount produced in replicate I. Furthermore, two clear outliers in ethanol- and butyrate concentrations were observed in replicate II. These outliers must be reconciled before parameter fitting procedures.

Figure 6.2: EtOH:Ac 1:1. 100 mL of an active chain-elongating community was incubated in a batch bioreactor with 225 mmol ethanol and 225 mmol acetate. Liquid measurements were done using HPLC. The cumulative hydrogen production was calculated from the off-gas measurements. Biological replicates were inoculated fifteen minutes after each other. The solid lines are linear interpolations between the data points.
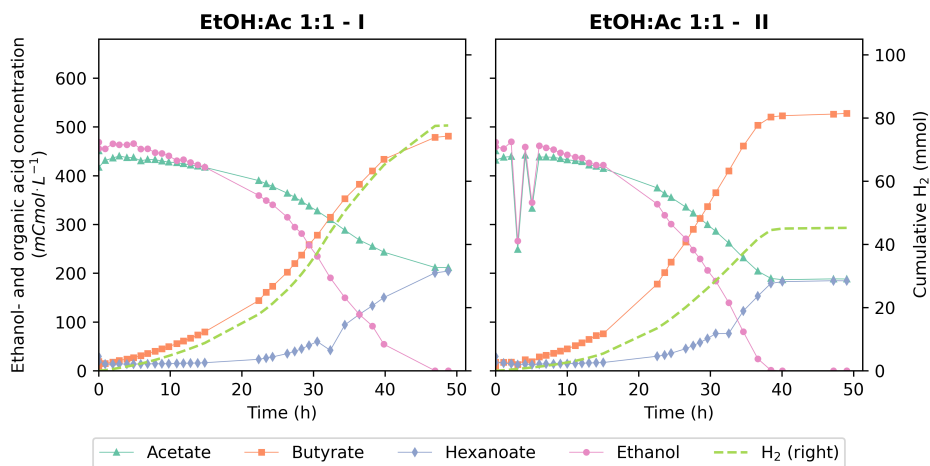
6.3.3. ETHANOL:ACETATE 3:1

fig. 6.3 shows the conversion profiles of ethanol and acetate supplied in a 3:1 molar ratio into butyrate, hexanoate and hydrogen in triplicate. These profiles show that the physiology was highly reproducible, even if the replicates were not performed in parallel. Before acetate became limiting, net butyrate production was observed in all replicates. Hexanoate production started after 10-15 mM of butyrate had accumulated, even though 3-6 mM of butyrate was already present from the start of the experiment due to transfer from the inoculum. This shows that it is not likely that the affinity for butyrate is high enough to effectuate elongation to hexanoate at concentrations below ±10 mM. The hydrogen profiles first followed the curve of butyrate production, but after ±25 hours its shape resembled the hexanoate curve more. This highlights that the main product was butyrate until acetate became limiting, when hexanoate became the main product. Likely, this is related to the fact that $C_{Acetate} > C_{Butyrate}$ until ±12 hours. Following Michaelis-Menten kinetics, a higher substrate concentration leads to a higher overall rate. All three replicates produced a total of 40-50 mmol of H_2, resulting in an overall EtOH:H_2 ratio of around 5 where a ratio close to 3 is expected in these conditions (chapter 5). Further analysis of the acid production (or base dosage) versus H_2 production should reveal whether this can be attributed to a difference in the catabolic stoichiometry or a measurement error as observed in Ethanol:Acetate 1:1, replicate II. Additionally, the outliers in the organic acid concentrations should be addressed in the data reconciliation.
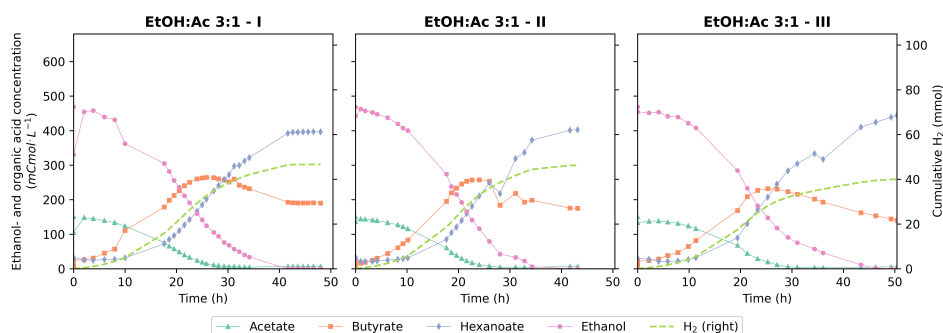
Figure 6.3: EtOH:Ac 3:1. 100 mL of an active chain-elongating community was incubated in a batch bioreactor with 225 mmol ethanol and 75 mmol acetate. Liquid measurements were done using HPLC. The cumulative hydrogen production was calculated from the off-gas measurements. Biological replicate 1 and 2 were inoculated one day after each other, biological replicate 3 was performed one month later. The solid lines are linear interpolations between the data points.

6.3.4. Ethanol:Acetate 12:1

When ethanol and acetate were supplied in a 12:1 ratio, the conversion profiles could be separated into two phases: a highly dynamic phase (0 – 50 h) in which highly similar conversion profiles were obtained, and a phase with less dynamics when electron accepting SCFAs were limiting (50 – 390 h). The full experiment as well as the dynamic phase are represented in fig. 6.4. In the dynamic phase, we observed an initial increase in butyrate concentrations until acetate became limiting. After this, butyrate was consumed to a concentration of 5-10 mM. This is comparable to the residual butyrate concentrations in the experiments in chapter 5.

After the dynamic phase, replicate I showed a short cease in activity represented by the flat cumulative H_2 profile and then slowly started producing butyrate. Replicate II tended more towards ethanol-only hexanoate production, which seized after ± 200 h. In the last ± 50 hours very slow accumulation of butyrate was also observed. The conditions in the second period of the 12:1 experiment were comparable to the conditions investigated in chapter 5, where it has been established that severe electron acceptor limitation leads to unstable behavior. Therefore, it should be considered to only use the first 50 hours of this dataset for model calibration. Furthermore, the total H_2 produced is just over 35 mmol for both experiments, which is lower than in most experiments performed here. Further analysis of the acid production (or base dosage) versus H_2 production should reveal whether this can be attributed to a difference in the biological process or a measurement error, as observed in Ethanol:Acetate 1:1, replicate II.
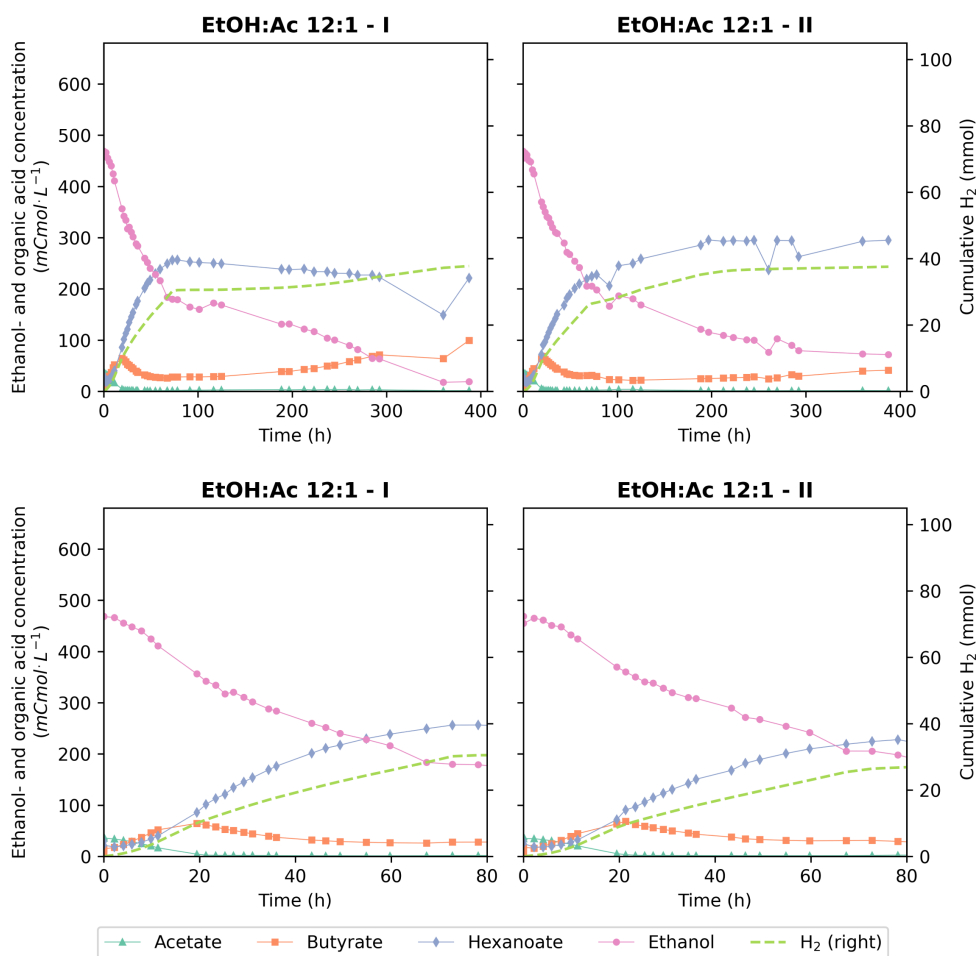
Figure 6.4: EtOH:Ac 12:1. 100 mL of an active chain-elongating community was incubated in a batch bioreactor with 225 mmol ethanol and 18.75 mmol acetate. Liquid measurements were done using HPLC. The cumulative hydrogen production was calculated from the off-gas measurements. Biological replicates were inoculated at the same time. The solid lines are linear interpolations between the data points. The top plots show the full experiment and the bottom plots zoom into the first 80 hours of the experiment.
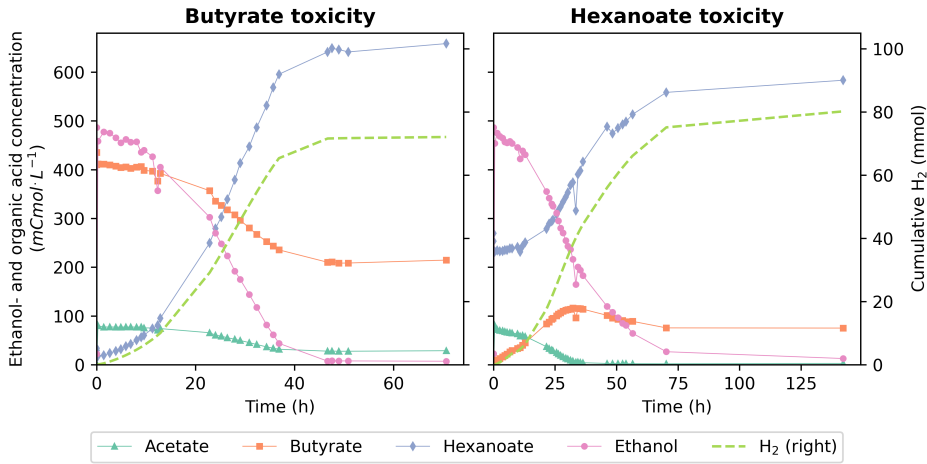
6.3.5. Butyrate and hexanoate toxicity

In the previous sections it has been established that chain-elongating physiologies are highly reproducible, except when ethanol is supplied as the sole carbon- and electron source. In this study, two experiments (experiment 2 and 3) were not performed in a biological replicate, and one experiment (experiment 1, figs. 5.1 and 5.3) was performed in duplicate but only one of the duplicates was sampled at a high frequency. Because of the demonstrated reproducibility of the physiologies in other conditions, we assume that the data of experiment 1, 2 and 3 (fig. 6.5) can also be used for kinetic model validation and re-calibration.

Candry et al. (2018) reported a toxicity limit for butyrate of 124.7 ± 5.7 mM. In the butyrate toxicity experiment, we used an initial butyrate concentration in the same order of magnitude to assess its effect on the behavior of our chain-elongating community. We observed no apparent inhibition due to the high initial butyrate concentration. All ethanol was consumed within 55 hours. The final hexanoate concentration was 110 mM, the highest concentration observed in the entire dataset presented here, and higher than the inhibition concentration measured by Candry et al. (2018). Furthermore, this is one of the few conditions where acetate was not completely consumed. This was likely due to a significantly higher driving force for hexanoate production during the entire experiment, as $C_{Butyrate}$ exceeds $C_{Acetate}$ at all time points.

In the hexanoate toxicity experiment the effect of the presence of hexanoate at approximately half the inhibition concentration of 91 mM [15] was assessed. In the EtOH:Ac 6:1 experiment (fig. 5.3), acetate became limiting after ±35 hours. At this point in the 6:1 experiment, the butyrate concentration was ±11 mM, the hexanoate concentration ±59 mM and ±55 mmol H_2 had been produced, and ±55 mM of ethanol remained. In the hexanoate toxicity experiment, acetate became limiting after the same amount of time, but the butyrate concentration at that point was ±29 mM, the hexanoate concentration ±65 mM and ±44 mmol H_2 had been produced and ±100mM of ethanol remained. Butyrate thus accumulated to a higher concentration in the presence of hexanoate, and the ethanol conversion rate was lower. This might be related to hexanoate toxicity and a lower overall driving force for hexanoate production.

6.3.6. Carbon- and electron balances

For the calculation of the carbon- and electron balances, the measured concentrations were recalculated to total amounts using the actual reactor volume corrected for sampling and acid/base addition and normalized to the total amount of carbon added to the reactor at t0. The electron balances including the contribution of electrons removed through sampling and ethanol evaporation are shown in fig. 6.6. The carbon balances can be found in Supplementary fig. 6.1. For experiments with a long runtime (EtOH:Ac 12:1, Butyrate availability and EtOH only) ethanol evaporation becomes significant. The balances in all datasets close between 90-110%, which is considered reliable. This means that in principle all datasets can be used for model calibration after reconciling the data to 100% C- and e-recovery.

Figure 6.5: Butyrate and hexanoate toxicity. 100 mL of an active chain-elongating community was incubated in a batch bioreactor with 242 mmol ethanol, 41 mmol acetate and 40 mmol hexanoate or 242 mmol ethanol, 41 mmol acetate and 100 mmol butyrate, respectively. Liquid measurements were done using HPLC. The cumulative hydrogen production was calculated from the off-gas measurements. The solid lines are linear interpolations between the data points.

Reconciliation prevents inaccuracies in parameter estimation due to the inherent standard deviations of the measurements used to monitor biological systems.

113
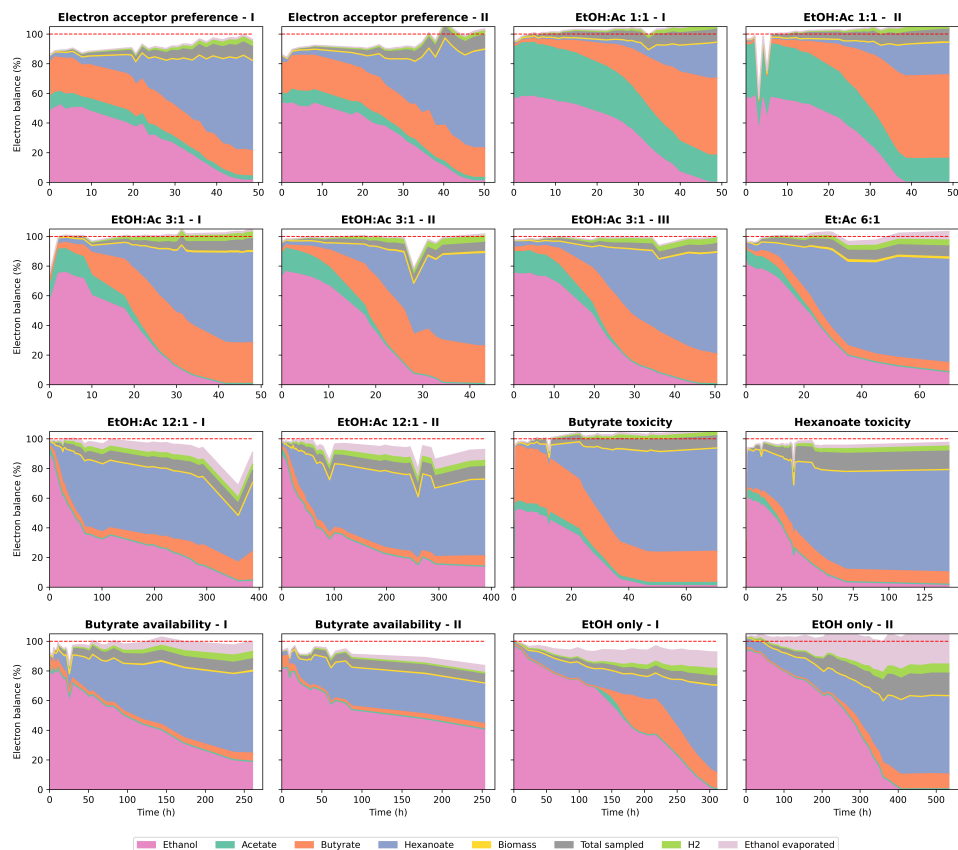
Figure 6.6: Normalized electron distribution. The electron distribution was calculated and normalized considering the removal of substrates and products and the volume changes through sampling and acid/base addition. Ethanol evaporation was calculated using data from an abiotic ethanol evaporation test and the mass 15 signal data from the MS. The red dashed line is drawn at 100%, indicating a fully closed balance.

6.3.7. HYDROGEN PRODUCTION VERSUS BASE CONSUMPTION

When considering the biochemistry of RBO and EO as separate, internally biochemically balanced processes, it can be deduced that the production of hydrogen is directly related to the oxidation of ethanol to acetate. This is the only process in which net electron release occurs. In RBO, an ethanol-moiety (γ = 12) is fused with acetate (γ = 8) to form butyrate (γ = 20), or an ethanol-moiety (γ = 12) is fused with butyrate (γ = 20) to form hexanoate (γ = 32), which both are electron balanced. Similarly, RBO is charge balanced, as an acid is being exchanged for another acid in a 1:1 ratio. Therefore, also all net acid production in a chain-elongating bioreactor is associated with EO activity. Following the stoichiometry of EO, the molar ratio between H_2 and acid production (or: base consumption) should be 2. Small deviations from this ratio could be attributed for example to electron requirements for growth. Large deviations are more likely to be due to technical aberrations and should be corrected in the data reconciliation. In a pH-controlled system with continuous off-gas measurements this ratio can be verified (fig. 6.7).

Online acid and base dose monitors were used to reconstruct the base profiles during the experiments. The profiles show that the H_2 measurements deviate from the 2 H_2 to 1 base equivalent for experiments EtOH:Ac 1:1 – replicate II, EtOH:Ac 3:1 – replicates I, II, and III, and EtOH:Ac 12:1 – replicates I and II. This confirmed our suspicion that the H_2-measurements in these experiments were faulty. The method for correcting this data is described in section 6.3.9.

6.3.8. GROWTH PROFILES

Kinetic models rely on the biomass concentration for the calculation of the overall conversion rate of a certain compound. In the experiments performed here, hydrogen production is a good proxy for the overall biological activity in the bioreactor. To assess whether the biological activity is correlated with the amount of biomass in the bioreactor, the H_2 production and biomass (OD_{660}) were plotted together as a function of time.

fig. 6.8 shows that biomass growth and the cumulative H_2 profiles follow similar trends. This indicates that the biological activity is indeed directly related to the total biomass concentration. However, direct ethanol elongation to hexanoate is not always associated with biomass growth. Furthermore, the availability of SCFAs appears instrumental for the biomass to grow, as reflected in the significantly lower final biomass concentrations in the EtOH:Ac 12:1, Butyrate availability and EtOH only experiments. These results suggest that varying catabolic stoichiometries come with varying catabolic ATP yields, affecting the overall capacity for biomass growth.

6
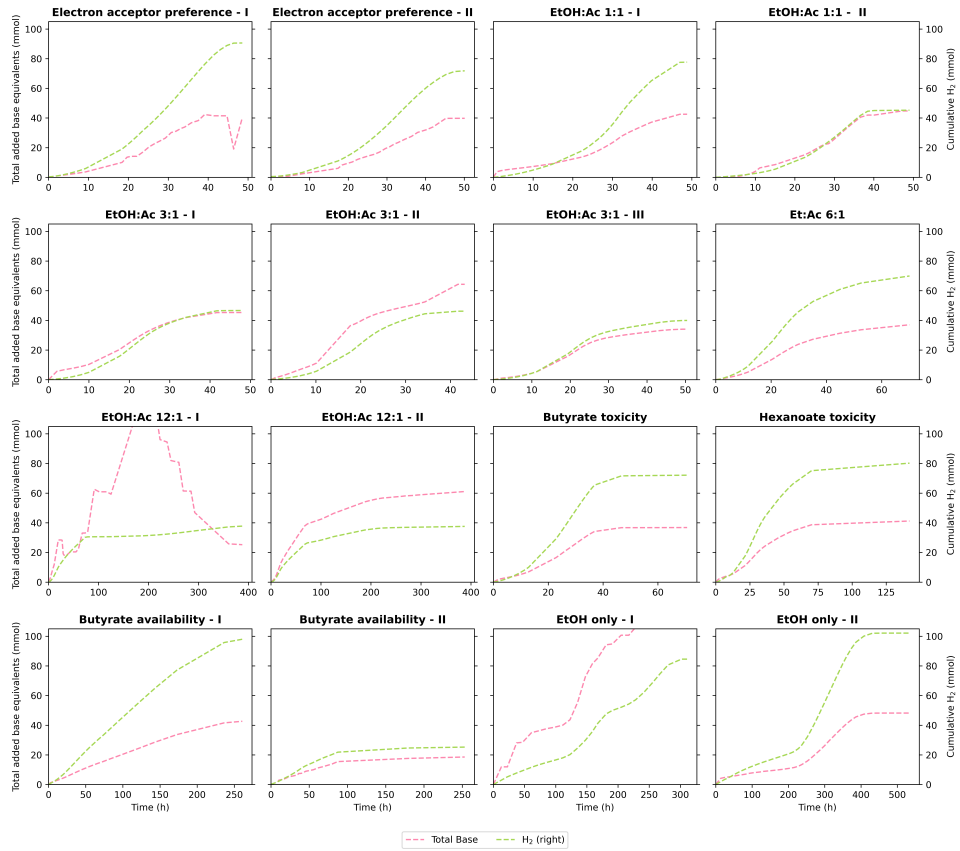
Figure 6.7: Base consumption vs. H_2 production. The net base consumption and cumulative hydrogen production as derived from the online data is plotted against time. If acid dosage occurred, this was subtracted from the base dosage to get the net total base consumption.
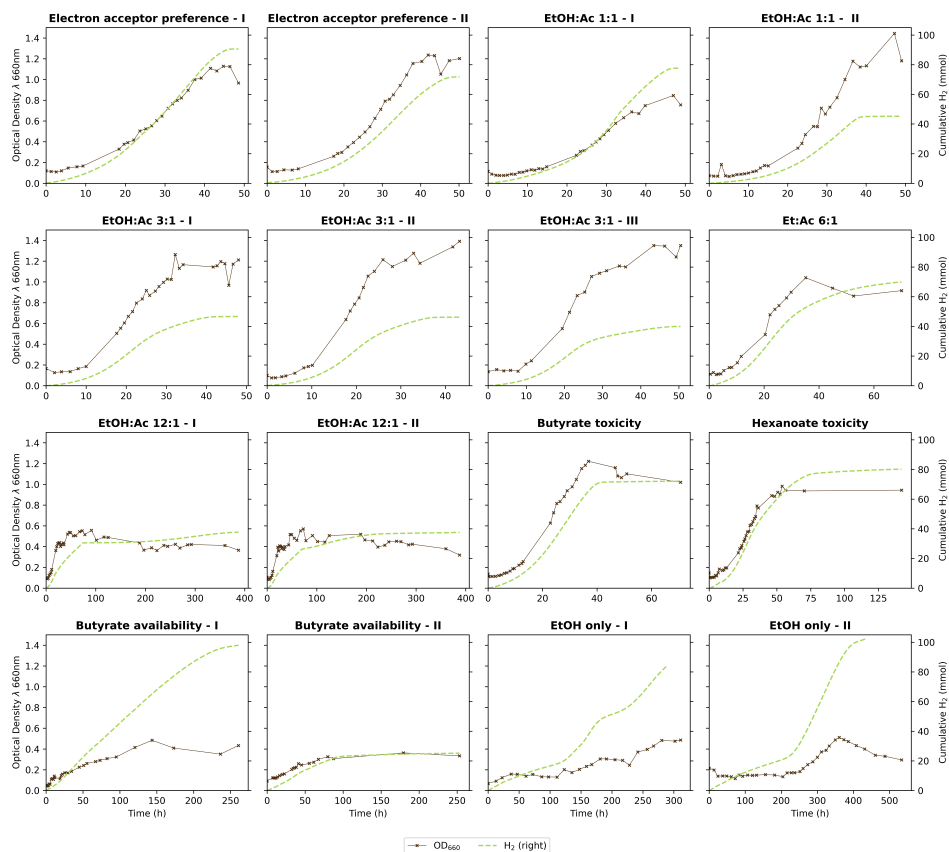
Figure 6.8: Biomass concentration vs. H$_2$ production. The raw biomass measurements (OD$_{660}$) and cumulative hydrogen production over time are visualized for all experiments.

6.3.9. DATA RECONCILIATION

Before assessing the accuracy of the Candry model, the experimental data generated here was reconciled. First, the aberrant H_2 measurements were corrected. The EtOH:Ac 1:1 experiment provides a basis for H_2 corrections, as replicate I performed as expected and replicate II did not. The ratio between the final amounts of H_2 produced between these experiments was calculated, and this was used as a rescaling factor for the H_2 measurements in 1:1 replicate II, the 3:1 and the 12:1 experiments. After this, the carbon- and electron balances were rescaled to 100% (fig. 6.9, S6.2). This is necessary because models yield closed carbon- and electron balances. If model parameters would be fitted from datasets with balances that are not fully closed, even if their deviations fall in a biologically acceptable range, this will skew the model towards accounting for these errors and make finding a perfect fit mathematically impossible. fig. 6.9 shows that balance rescaling effectively corrected for outlier measurements, which now fit better in the overall conversion profiles of the experiments. The black line in the figures indicates the confidence of the set of reconciled datapoints at a specific sampling time. Outlier measurement points have a lower confidence, whereas points that had an electron balance close to 100% already before data reconciliation have a high confidence. The confidence of the datapoints can be used as weighing factor during model fitting.

6
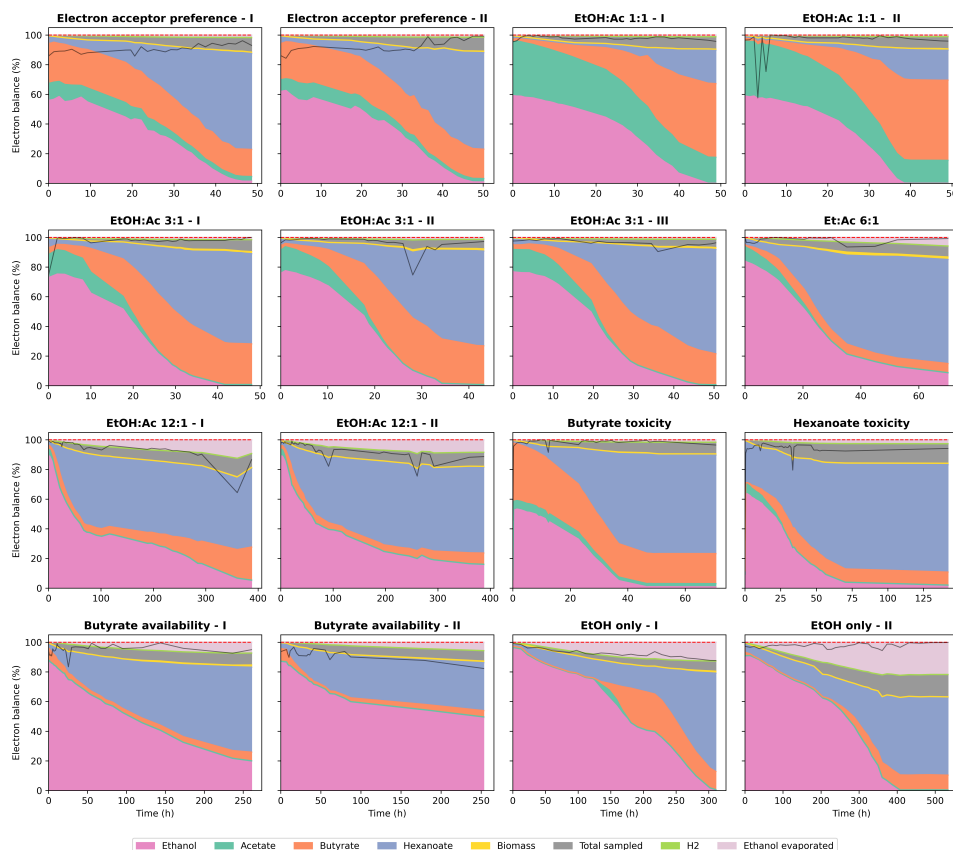
Figure 6.9: Reconciled electron distribution. The electron distribution was rescaled to get a 100% closed electron balance after correcting for aberrant H_2 profiles. The red dashed line is drawn at 100%, indicating a fully closed balance. The black solid line indicates the confidence of the data at each reconciled measurement point. Points where outliers used to be have a lower confidence, whereas points that had an electron balance close to 100% before data reconciliation have a high confidence.

6.3.10. Model accuracy assessment

Here, the potential of the available kinetic model to represent the physiologies observed in our experiments was assessed. The model was reproduced as described in Candry et al. (2018) and simulations were run with the initial conditions in our experiments as input values. As we observed poor fits with a starting biomass concentration of 1 mCmol· L^{-1}, we introduced an activity parameter, that effectively reduced the initial biomass concentration for the model. This was the single fitting parameter we used to improve the output of the model. A biological explanation for a lower activity could be due to adaptations of the biomass to substrate concentrations, which aligns with often observed initial dips in OD_{660}. In practice, the activity parameter ranged between 0.15 and 0.5 to yield best fitting substrate conversion profiles.

fig. 6.10 shows the model predictions and our reconciled measurement data. For the experiments with multiple replicates, the reconciled data of the replicate with the highest confidence (fig. 6.9) was displayed. The estimation of the overall conversion rates of the Candry model is relatively accurate for almost half of the conditions. This is reflected by the good overlap between the modelled and the observed ethanol conversion profiles in the 3:1, 6:1 and electron acceptor preference experiments, as well as the initial parts of the 12:1 and the butyrate availability experiments. Also, the final amounts of produced H_2 are predicted relatively well in the Electron acceptor preference, 1:1, 3:1, 6:1 and Butyrate toxicity experiments.

Yet, the comparison between model prediction and experimental data also revealed targets for model improvement. First, the model cannot predict the physiologies we observed under SCFA limitation. This is reflected by the flat lines of the model predictions in the 12:1, Butyrate availability and EtOH-only experiments. The failure to predict the experimentally observed physiologies is due to the fixed stoichiometries that are assumed for both butyrate and hexanoate production in the Candry model. In an improved model, the rates of RBO and EO should be modelled separately to be able to account, for instance, for direct ethanol to hexanoate conversion (chapter 5). Second, in the experiments where the initial EtOH:Ac ratio was above 6, the predicted consumption profiles of acetate and butyrate are far from the experimental observations, except for the electron acceptor preference experiment. This led to an overestimation of hexanoate production and an underestimation of butyrate production during the experiments. Experimentally, an increase followed by a decrease in butyrate concentration was often observed, whereas the model predicted a slighter increase followed by a largely stable butyrate concentration. Furthermore, butyrate was never fully consumed in the experiments, but rather stabilized around 10 mM when acetate became limiting. This is not reflected by the model, which predicts complete consumption of both acetate and butyrate when ethanol is still available. This indicates that an important biological mechanism is lacking in the model equations.

Lastly, hexanoate toxicity occurs at a lower concentration in the model than the concentrations attained in some of our experiments. This, combined with the characteristic overestimation of the hexanoate production rate, led to a premature predicted cease in biological activity in the hexanoate toxicity experiment.
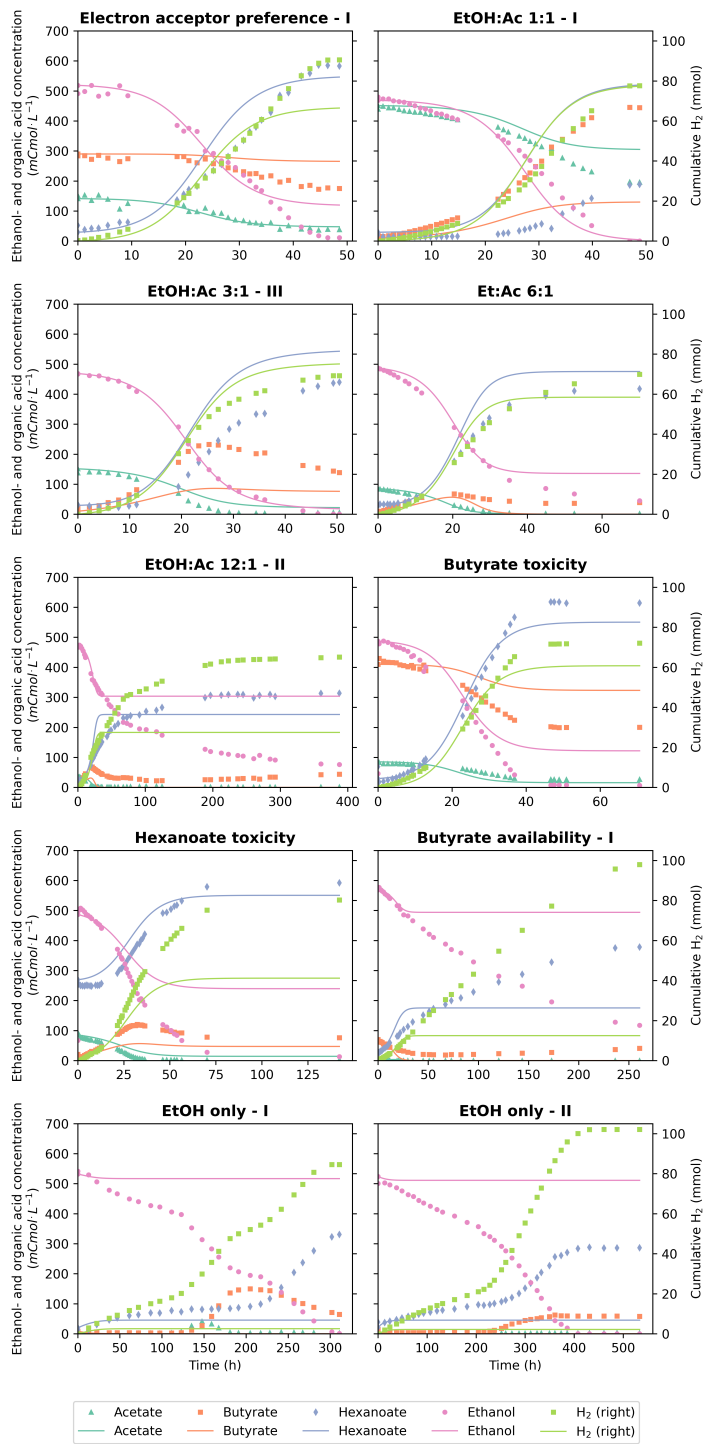
Figure 6.10: Model accuracy assessment. The currently available model (lines) was used to simulate the putative physiologies in the conditions tested here. Our datasets with the highest confidence in each tested condition are plotted (symbols) in the same figures. 121

6.3.11. TOWARDS IMPROVED KINETIC MODEL DEVELOPMENT

This chapter presents a dataset of reliable experiments with chain-elongating microbes that, especially after the corrections and reconciliation described above, is well-suited for the calibration of a new kinetic model of chain-elongating microbes. While analyzing the experimental data, several interesting observations have been made, for example the characteristic residual amount of butyrate in various experiments, switching of the catabolic stoichiometry, higher hexanoate concentrations than the reported toxicity limit, substrate conversion not coupled to growth, etcetera. All these observations must be translated into a new model, which is not a trivial task. The sections below will discuss the aspects that must be considered when formulating the new model.

DATA WEIGHTS AND KINETIC PARAMETER ERROR RANGES

In our dataset the measurements are not uniformly spread in time, which affects the parameter fitting of a model. Models use an objective function, often a weighted sum of squared errors (WSSE) to converge towards an optimal fit comprising a set of parameters. Three factors should be considered in the weighing of measurement points. First, the points that are further spaced out need to be assigned a higher relative weight to ensure they have a comparable influence on the fitting process [21, 22]. Second, the weight of a measurement point should be related to the confidence in the measurement, which is derived from the carbon and electron balance (as described in section 6.3.9). Third, the relative error and standard deviation based on the absolute value of the measurement and measurement method affects the weight of error, for example 5 mCmol difference in predicted and measured biomass should lead to a larger error than 5 mCmol difference for ethanol. These weighing factors are essential to allow fitting of the entire dynamics of the experiments. A second important aspect of parameter fitting is a sensitivity analysis. The confidence intervals of the parameters should be calculated based on the measurement errors and the variations between biological replicates.

STOICHIOMETRIC VARIABILITY

We have established that EO and RBO are two separate processes that can proceed individually or simultaneously and even at different rates without being strictly stoichiometrically coupled. The trade-off between these two 'internal' stoichiometries should be reflected in an improved kinetic model. The difference between these two stoichiometries lies in the way that energy is harvested. EO leads to ATP conservation via substrate-level phosphorylation, whereas with RBO cells rely solely on the proton gradient built up by the Rnf complex to conserve ATP. This proton gradient, however, might also be needed for transport mechanisms over the cell membrane, which will be discussed below. Rates for both processes should be derived in a kinetic model instead of fixing a stoichiometry for ethanol/acetate or ethanol/butyrate consumption. Furthermore, an overall biomass yield must be calculated based on the contribution of both stoichiometries to the overall rate, and their respective ATP yields. An estimate of the ATP requirements for growth can then

be used to convert the overall ATP yield into an overall biomass yield on substrate. From the data presented here, we can conclude that in the tested conditions, EO and RBO always occur simultaneously, which suggests that ethanol oxidation is not inhibited by the presence of acetate even though EO is a thermodynamically constrained reaction. In chapter 5 we showed that the rate of RBO seemingly depends on the availability of SCFAs. This leads to the hypothesis that the rate of EO is the 'base' rate of chain elongators. The factors that influence this rate could be inferred from the experiments where ethanol conversion to hexanoate takes place under electron acceptor limitation. Ethanol conversion rates higher than this 'base' rate can then be attributed to RBO activity.

Product inhibition

For modelling product inhibition, it should be noted that different mechanisms must be considered to adequately identify the rate-limiting step in the process. The first mechanism to consider is the overall driving force for product formation. When the concentration of butyrate or hexanoate is high, the driving force of RBO1 or RBO2, respectively, is reduced. Low concentrations of acetate or butyrate, respectively, have a similar effect. This might, following the flux-force relationship, lead to a lower observed rate of this pathway [23, 24]. Care should be taken that a low rate due to a low driving force is not misclassified as product toxicity, the second mechanism that can limit the substrate conversion rate. This could be done by reformulating the Monod-term for substrate uptake to a term that uses the substrate over product ratio, for example. The work by Candry et al. (2018) shows a clear linear decrease in growth rate in the presence of increasing amounts of hexanoate, meaning that the thermodynamic driving force for a certain pathway is not the only factor constraining the overall substrate conversion rate. Hexanoate buildup affects the integrity of the cell membrane, which leads to lower cellular efficiency. Hexanoate toxicity should thus be explicitly modelled, but the inhibition concentration is likely higher for well-acclimatized microbial communities, as hexanoate concentrations above the toxicity limit reported by Candry et al. (2018) were observed in the experiments performed here. Toxicity effects were not observed in presence of ± 100 mM butyrate, which indicates that the toxicity limit model chosen by Candry et al. (2018) is likely an adequate way of representing butyrate toxicity. Yet, acetate was not fully consumed in presence of this high butyrate concentration, whereas the Candry model did predict it would be. This highlights the relevance of an affinity term that also incorporates the product concentration to calculate the reaction rate.

Transport mechanisms over the cell membrane

For a kinetic model that includes a flexible catabolic stoichiometry, the assumption of a constant biomass yield on ethanol is not valid. Therefore, an accurate estimate of the biomass yield must be made for the conditions at hand, which depends on the net ATP yield. This net yield does not only depend on the active catabolism, but also on the import/export costs of substrates and products. Ethanol can be assumed to enter the cell passively, as it is a small, uncharged molecule. Acetate, butyrate and hexanoate transport, however, can occur via different mechanisms – depending

on intracellular and extracellular concentrations, as shown in Supplementary fig. 6.3 and discussed in the supplementary materials. These mechanisms will have different impacts on the net ATP yields of chain elongation. As chain elongators have a limited amount of ATP available ($Y_{ATP/EtOH} \leq 0.5$), it is likely that the transport of substrates and products is optimized for the lowest possible ATP costs. In most of the experiments, either acetate or butyrate are available in excess, which yields a chemical gradient where the intracellular concentration of these molecules is lower than their extracellular concentration. By using an acid/acid antiporter, this gradient could be used for the export of hexanoate against its concentration gradient. Potentially, the residual butyrate concentrations that we observed in various experiments are related to this type of product export, if the intracellular butyrate concentration is indeed significantly lower than the extracellular concentration. In the absence of a beneficial acetate and butyrate chemical gradient, the cells might utilize proton symport and active transport to export hexanoate against its concentration gradient. This would result in a significant ATP investment for the cells, which could be related to the reduction in biomass production we observed during direct ethanol elongation to hexanoate. Ideally, a newly formulated model would calculate the approximate ATP requirements for transport, given the concentrations at hand. This would require an estimation of the intracellular concentrations, which can be made using equilibrium thermodynamics.

Questions that remain to be addressed

In this work, it has been established that EO and RBO occur simultaneously following different stoichiometric couplings. This leads to the hypothesis that these stoichiometries can also run completely independently of each other. RBO likely does have a positive effect on the thermodynamics of EO, where the bottleneck lies in the formation of hydrogen from NADH. Presumably the NADH/NAD+ ratio in the cell shifts due to for example the electron bifurcating activity associated to RBO, which might make hydrogen formation thermodynamically feasible. The driving force for RBO, on the other hand, is not necessarily increased when EO is also taking place, given that ethanol and SCFAs are supplied in excess. In various conditions tested here, RBO could have theoretically run without EO being active, but this was not observed. Future work can be aimed at unraveling whether both EO and RBO can in fact run independently of each other. For EO, this implies that conditions in which H_2 formation from NADH is feasible (i.e $pH_2 < 3.2$ kPa) must be maintained [25]. Potentially, high bioreactor sparging rates could be used to achieve this, but this more likely requires the introduction of a H_2-consuming syntrophic partner. Activity of RBO alone might be observed in conditions of severe ethanol limitation and abundance of acetate (and butyrate). This can be achieved in a fed-batch bioreactor system where acetate is supplied in excess (± 250 mM) and ethanol is fed extremely slowly (1-10 mmol·h^{-1}).

6.4. CONCLUSIONS

Chain-elongating microbes are versatile organisms that can be exploited to produce interesting chemicals from waste streams. The experiments performed in this thesis shed new light on their metabolic potential with the experimental validation of the capacity to directly elongate ethanol to hexanoate and to transiently accumulate electron accepting short-chain fatty acids. The development of an updated kinetic model is of key importance to turn this new knowledge into a rigorous mathematical description that is useful for the design of new bioprocesses. The inherent errors associated with biological experimentation should be acknowledged and reconciled as much as possible before model parameterization to provide model users with a reliable parameter set including parameter confidence intervals. This chapter describes a framework for data processing through which a dataset suited for parameter estimation was obtained. The experiments performed in this chapter show that H_2 production is a key indicator of the activity of chain elongators, and that high-resolution monitoring of the gas productivity is therefore invaluable when studying these microbes. Furthermore, the presented experimental data shows that several mechanisms, including stoichiometric variability, product inhibition, and transport of substrates and products over the cell membrane must be included in a newly formulated model.

6

BIBLIOGRAPHY

[1] H. A. Barker and S. M. Taha. "*Clostridium kluyverii*, an Organism Concerned in the Formation of Caproic Acid from Ethyl Alcohol". In: *Journal of Bacteriology* 43.3 (Mar. 1942), pp. 347–363. DOI: 10.1128/jb.43.3.347-363.1942.

[2] H. A. Barker, M. D. Kamen, and B. T. Bornstein. "The Synthesis of Butyric and Caproic Acids from Ethanol and Acetic Acid by *Clostridium kluyveri*". In: *Proceedings of the National Academy of Sciences* 31.12 (Dec. 1945), pp. 373–381. DOI: 10.1073/pnas.31.12.373.

[3] W. R. Kenealy and D. M. Waselefsky. "Studies on the substrate range of *Clostridium kluyveri*; the use of propanol and succinate". In: *Archives of Microbiology* 141.3 (Apr. 1985), pp. 187–194. DOI: 10.1007/BF00408056.

[4] G. M. Smith, B. W. Kim, A. A. Franke, and J. D. Roberts. "13C NMR studies of butyric fermentation in *Clostridium kluyveri*." In: *Journal of Biological Chemistry* 260.25 (Nov. 1985), pp. 13509–13512. DOI: 10.1016/S0021-9258(17)38751-3.

[5] R. K. Thauer, K. Jungermann, H. Henninger, J. Wenning, and K. Decker. "The Energy Metabolism of *Clostridium kluyveri*". In: *European Journal of Biochemistry* 4.2 (Apr. 1968), pp. 173–180. DOI: 10.1111/j.1432-1033.1968.tb00189.x.

[6] N. Tomlinson and H. Barker. "Carbon dioxide and acetate utilization by *Clostridium kluyveri*". In: *Journal of Biological Chemistry* 209.2 (Aug. 1954), pp. 585–595. DOI: 10.1016/S0021-9258(18)65485-7.

[7] S. Ge, J. G. Usack, C. M. Spirito, and L. T. Angenent. "Long-Term *n*-Caproic Acid Production from Yeast-Fermentation Beer in an Anaerobic Bioreactor with Continuous Product Extraction". In: *Environmental Science & Technology* 49.13 (July 2015), pp. 8012–8021. DOI: 10.1021/acs.est.5b00238.

[8] D. Vasudevan, H. Richter, and L. T. Angenent. "Upgrading dilute ethanol from syngas fermentation to n-caproate with reactor microbiomes". In: *Bioresource Technology* 151 (Jan. 2014), pp. 378–382. DOI: 10.1016/j.biortech.2013.09.105.

[9] S. Crognale, C. M. Braguglia, A. Gallipoli, A. Gianico, S. Rossetti, and D. Montecchio. "Direct Conversion of Food Waste Extract into Caproate: Metagenomics Assessment of Chain Elongation Process". In: *Microorganisms* 9.2 (Feb. 2021), p. 327. DOI: 10.3390/microorganisms9020327.

[10] A. Regueira, R. Turunen, K. Vuoristo, M. Carballa, J. Lema, J. Uusitalo, and M. Mauricio-Iglesias. "Model-aided targeted volatile fatty acid production from food waste using a defined co-culture microbial community". In: *Science of The Total Environment* 857 (Jan. 2023), p. 159521. DOI: 10.1016/j.scitotenv.2022.159521.

[11] M. T. Agler, B. A. Wrenn, S. H. Zinder, and L. T. Angenent. "Waste to bioproduct conversion with undefined mixed cultures: the carboxylate platform". In: *Trends in Biotechnology* 29.2 (Feb. 2011), pp. 70–78. DOI: 10.1016/j.tibtech.2010.11.006.

[12]   A. P. Desbois. "Potential Applications of Antimicrobial Fatty Acids in Medicine, Agriculture and Other Industries". In: *Recent Patents on Anti-Infective Drug Discovery* 7.2 (June 2012), pp. 111–122. DOI: 10.2174/157489112801619728.

[13]   F. Santos, J. Boele, and B. Teusink. "A Practical Guide to Genome-Scale Metabolic Models and Their Analysis". en. In: *Methods in Enzymology*. Vol. 500. Elsevier, 2011, pp. 509–532. DOI: 10.1016/B978-0-12-385118-5.00024-4.

[14]   L. T. Angenent, H. Richter, W. Buckel, C. M. Spirito, K. J. J. Steinbusch, C. M. Plugge, D. P. B. T. B. Strik, T. I. M. Grootscholten, C. J. N. Buisman, and H. V. M. Hamelers. "Chain Elongation with Reactor Microbiomes: Open-Culture Biotechnology To Produce Biochemicals". In: *Environmental Science & Technology* 50.6 (Mar. 2016), pp. 2796–2810. DOI: 10.1021/acs.est.5b04847.

[15]   P. Candry, T. Van Daele, K. Denis, Y. Amerlinck, S. J. Andersen, R. Ganigué, J. B. A. Arends, I. Nopens, and K. Rabaey. "A novel high-throughput method for kinetic characterisation of anaerobic bioproduction strains, applied to *Clostridium kluyveri*". In: *Scientific Reports* 8.1 (June 2018), p. 9724. DOI: 10.1038/s41598-018-27594-9.

[16]   W. D. A. Cavalcante, R. C. Leitão, T. A. Gehring, L. T. Angenent, and S. T. Santaella. "Anaerobic fermentation for n-caproic acid production: A review". In: *Process Biochemistry* 54 (Mar. 2017), pp. 106–119. DOI: 10.1016/j.procbio.2016.12.024.

[17]   W. Zou, G. Ye, J. Zhang, C. Zhao, X. Zhao, and K. Zhang. "Genome-scale metabolic reconstruction and analysis for *Clostridium kluyveri*". In: *Genome* 61.8 (Aug. 2018). Ed. by D. Scofield, pp. 605–613. DOI: 10.1139/gen-2017-0177.

[18]   W. Buckel and R. K. Thauer. "Energy conservation via electron bifurcating ferredoxin reduction and proton/Na+ translocating ferredoxin oxidation". en. In: *Biochimica et Biophysica Acta (BBA) - Bioenergetics* 1827.2 (Feb. 2013), pp. 94–113. DOI: 10.1016/j.bbabio.2012.07.002.

[19]   F. Li, J. Hinderberger, H. Seedorf, J. Zhang, W. Buckel, and R. K. Thauer. "Coupled Ferredoxin and Crotonyl Coenzyme A (CoA) Reduction with NADH Catalyzed by the Butyryl-CoA Dehydrogenase/Etf Complex from *Clostridium kluyveri*". In: *Journal of Bacteriology* 190.3 (Feb. 2008), pp. 843–850. DOI: 10.1128/JB.01417-07.

[20]   H. Seedorf, W. F. Fricke, B. Veith, H. Brüggemann, H. Liesegang, A. Strittmatter, M. Miethke, W. Buckel, J. Hinderberger, F. Li, C. Hagemeier, R. K. Thauer, and G. Gottschalk. "The genome of *Clostridium kluyveri*, a strict anaerobe with unique metabolic features". In: *Proceedings of the National Academy of Sciences* 105.6 (Feb. 2008), pp. 2128–2133. DOI: 10.1073/pnas.0711093105.

[21]   P. Loskot, K. Atitey, and L. Mihaylova. "Comprehensive Review of Models and Methods for Inferences in Bio-Chemical Reaction Networks". en. In: *Frontiers in Genetics* 10 (June 2019), p. 549. DOI: 10.3389/fgene.2019.00549.

[22]   S. Kleinstein, D. Bottino, A. Georgieva, R. Sarangapani, and G. Lett. "Nonuniform Sampling for Global Optimization of Kinetic Rate Constants in Biological Pathways". en. In: *Proceedings of the 2006 Winter Simulation Conference*. Monterey, CA, USA: IEEE, Dec. 2006, pp. 1611–1616. DOI: 10.1109/WSC.2006.322934.

[23]   D. A. Beard and H. Qian. "Relationship between Thermodynamic Driving Force and One-Way Fluxes in Reversible Processes". In: *PLoS ONE* 2.1 (Jan. 2007). Ed. by T. Secomb, e144. DOI: 10.1371/journal.pone.0000144.

6

[24] Y. Peng, H. Qian, D. A. Beard, and H. Ge. "Universal relation between thermodynamic driving force and one-way fluxes in a nonequilibrium chemical reaction with complex mechanism". In: *Physical Review Research* 2.3 (July 2020), p. 033089. DOI: 10.1103/PhysRevResearch.2.033089.

[25] H.-J. Seitz, B. Schink, and R. Conrad. "Thermodynamics of hydrogen metabolism in methanogenic cocultures degrading ethanol or lactate". en. In: *FEMS Microbiology Letters* 55.2 (Oct. 1988), pp. 119–124. DOI: 10.1111/j.1574-6968.1988.tb13918.x.

[26] S. Benito-Vaquerizo, M. Diender, I. Parera Olm, V. A. Martins Dos Santos, P. J. Schaap, D. Z. Sousa, and M. Suarez-Diez. "Modeling a co-culture of *Clostridium autoethanogenum* and *Clostridium kluyveri* to increase syngas conversion to medium-chain fatty-acids". In: *Computational and Structural Biotechnology Journal* 18 (2020), pp. 3255–3266. DOI: 10.1016/j.csbj.2020.10.003.

6

6.5. Supplementary Materials
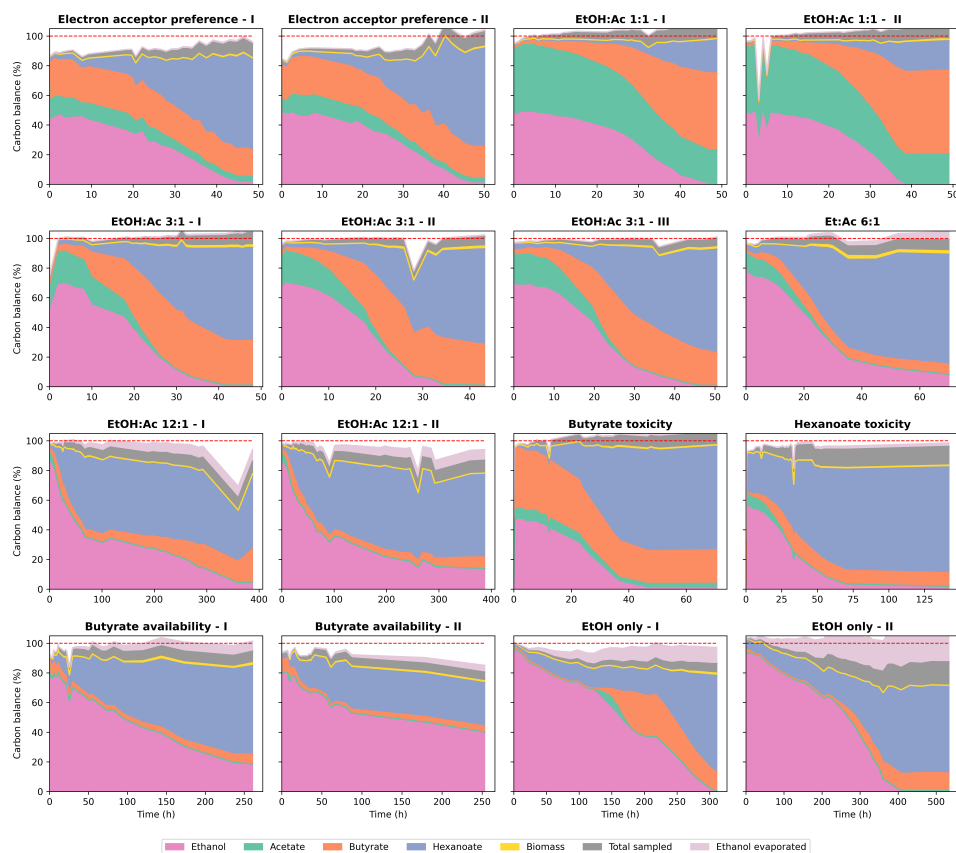
Figure S 6.1: Normalized carbon distribution. The carbon distribution was calculated and normalized considering the removal of substrates and products and the volume changes through sampling and acid/base addition. Ethanol evaporation was calculated using data from an abiotic ethanol evaporation test and the mass 15 signal data from the MS. The red dashed line is drawn at 100%, indicating a fully closed balance.

6.5.1. Transport mechanisms over the cell membrane

Different mechanisms are used by cells to to transport species over their cell membrane. For chain elongated products, most of the product will be in its charged form as both the intra- and extracellular pH are likely near-neutral. The direction in which the transport mechanism works, depends on the chemical gradient of the species, and on whether ATP is invested for transport or not. In fig. 6.3, the different transport mechanisms are depicted. Their impact on the energy balance of the microorganism will be discussed below.
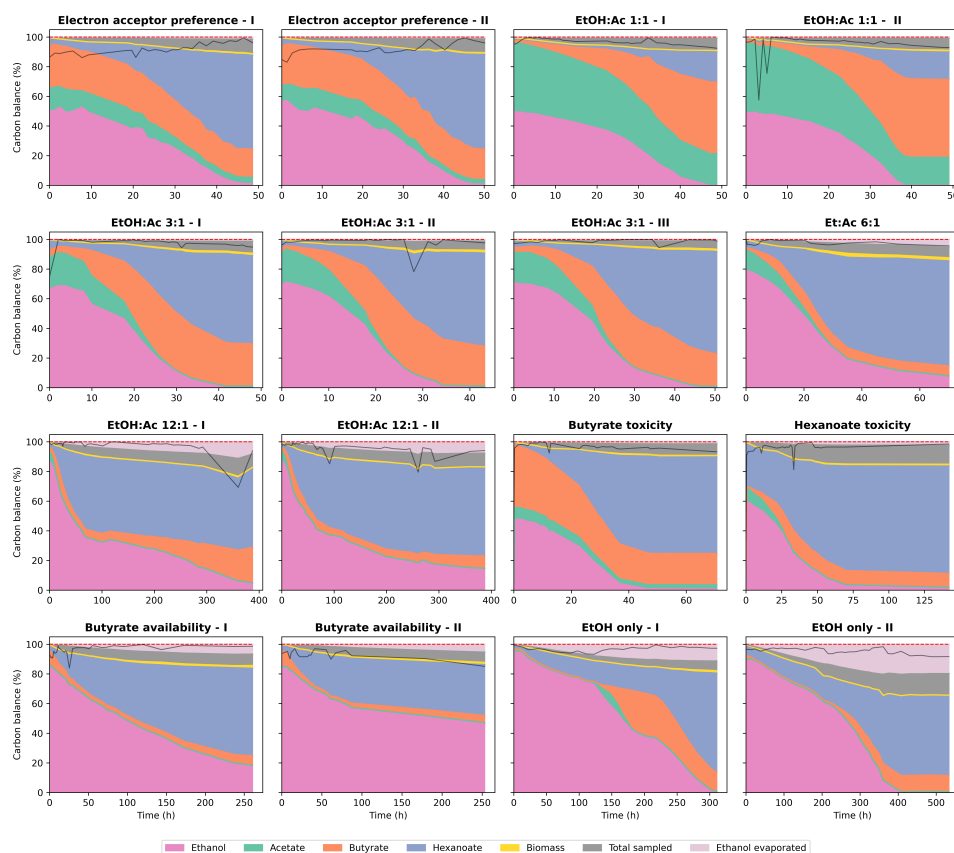
Figure S 6.2: Reconciled carbon distribution. The carbon distribution was rescaled to get a 100% closed electron balance after correcting for aberrant H_2 profiles. The red dashed line is drawn at 100%, indicating a fully closed balance. The black solid line indicates the confidence of the data at each reconciled measurement point. Points where outliers used to be have a lower confidence, whereas points that had a carbon balance close to 100% before data reconciliation have a high confidence.

Passive transport does not require energy, but only occurs in the direction of the concentration gradient of the associated acid. In experiments where, for example, the hexanoate extracellular concentration is higher than the intracellular concentration, and around neutral pH, any net passive transport of hexanoic acid will be directed into the cell. Active transport happens at the expense of ATP for the extrusion of compounds against their concentration gradient, and can occur for associated and dissociated acids. Chain elongation yields less than 0.5 ATP per elongated acid, making it improbable that active transport is the mechanism for most of the product displaced over the membrane, although it can reach high concentration differences between the intracellular and extracellular compound concentrations.

In cases where a higher intracellular concentration than extracellular concentration for a compound exists, a cell can use a proton symporter to reduce its intracellular proton concentration. This leads to an increase of the proton gradient across the cell membrane, which results in a slight increase in the proton motive force (pmf). Depending on compound concentrations (i.e. when the extracellular concentration is high), the proton symport can be directed into the cell (analogous to passive transport), leading to a decrease in pmf, which needs to be compensated by, likely, the transmembrane gradient that is produced by the Rnf complex, which decreases the available energy for ATP harvesting.

In a genome-scale model of *C. kluyveri* a proton antiport is assumed for acetate and butyrate transport over the membrane, but this is not based on annotated transporters found in the genome [26]. Therefore, alternative transport mechanisms can be considered.

An acid/acid antiporter, for example exchanging hexanoate for acetate, would be a feasible mechanism for the export of chain elongated acids. The charge balance is maintained, as two monovalent acids are interchanged. This means that no additional proton transport is required. As the pmf thereby remains unaffected, this mechanism does not require ATP investment, but is able to exchange one acid against a concentration gradient in favor of the other acid down its gradient. From an energy point of view, it therefore seems most plausible that acid/acid antiporters are used for substrate/product import/export. This would explain the clear preference of the microorganisms to grow in the presence of electron accepting SCFAs, as this export mechanism becomes unfeasible when no SCFAs are available. Potentially, this explains why butyrate is not consumed completely in the experiments performed in this thesis, as it is required for the export of hexanoate formed from only ethanol against its concentration gradient.

6

$A^-_{out} > A^-_{in}$

$$\frac{A^-_{2,in}}{A^-_{2,out}} > \frac{A^-_{1,out}}{A^-_{1,in}}$$

A_1^-

Out

In

n ATP | ADP, P_i m ATP | ADP, P_i

HA   H$^+$ A$^-$ H$^+$ A$^-$ H$^+$ A$^-$ A_2^-

Passive transport   *Proton antiport*   *Proton symport*   *Active transport*   *Acid/acid antiport*
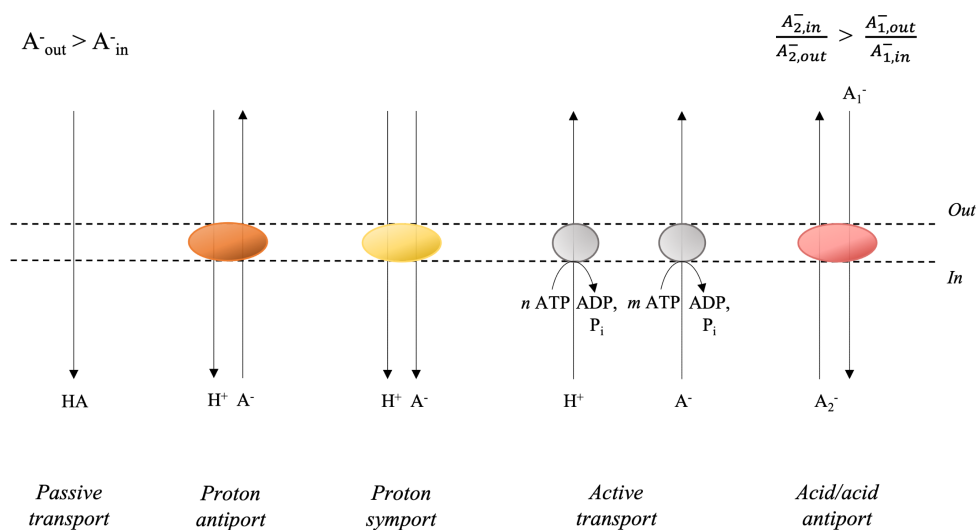
Figure S 6.3: Transport mechanisms of chain elongated products. Schematic representation of the different potential transport mechanisms of the chain elongated products out of the cell, where A- refers to either acetate, butyrate or hexanoate. In the acid/acid antiport, one of the organic acids is exchanged for a different acid.

7

OUTLOOK

Tʜɪs thesis, like many others, I believe, started with a question, and ended up with answers to this and to entirely different questions. Additionally, a whole heap of new questions have arisen that open opportunities for exciting future research. The research performed in this thesis was focused on the production of medium-chain fatty acids from syngas via microbial consortia of acetogens and chain elongators. More specifically, we aimed to *'increase the fundamental understanding of acetogens and chain-elongating microbes to pave the way towards their full-scale application in the bioconversion of syngas to biochemical building blocks'*. With this goal to guide us, we have continued to scratch the surface of all there is to know about carbon monoxide consuming microbes and their potential chain-elongating partners. Some important takeaways from this thesis are:

- Overflow metabolism is a functional trait of acetogens to deal with CO toxicity, and understanding of this mechanism can be used to direct the product spectrum of syngas fermentation by controlling the operational conditions **(Chapter 2)**

- Specifically, the mass transfer rate of CO can be manipulated, for example via the CO content of the feed gas, to trigger overflow metabolism and produce ethanol at the expense of acetate. Additionally, temporary increases in the CO content of a chemostat bioreactor give insight in the substrate uptake kinetics of CO consuming microbes **(Chapter 3)**

- The production of medium-chain carboxylic acids is not favorable at mildly acidic pH, but not impossible either **(Chapter 4)**

- Chain-elongating microbes have a highly flexible metabolism, which provides interesting avenues for simplifying chain elongation to a single-substrate and single-product process **(Chapter 5)**

- Capturing the metabolic flexibility of chain-elongating microbes in a kinetic model is not trivial, and specific care must be taken on how the data is handled to prevent confusing measurement inaccuracies for microbial activity **(Chapter 6)**

Even though our understanding of the microbial team players in C_1-to-C_6 conversion has increased with the work in this thesis, many more questions have arisen in the study of these fascinating microorganisms. These questions revolve around three main themes: the internal world of our microbes of choice, microbial ecology, and process optimization, which will be discussed separately in the sections to follow. However, I believe that these themes are communicating vessels: discoveries and observations in one of them can change our perception in the others, too.

7.1. THE INTERNAL WORLD OF OUR MICROBES

The experimental work presented in this thesis, but also the experiments that did not work out and the times that the microbes refused to grow led me to contemplate the smallest pieces of machinery that make cells work. While doing this, it became clear to me that the internal world of the microbes we study is actually not so well known to us yet (fig. 7.1).
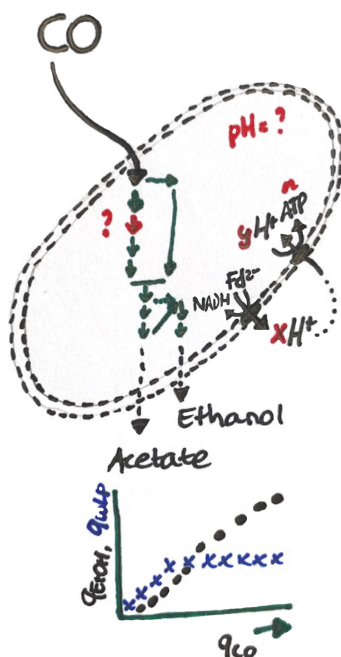
Figure 7.1: Schematic representation of a CO-consuming acetogen. In this thesis, the mechanism of dealing with increased CO fluxes by increasing the ethanol production flux and not, after a certain treshold, the flux through central carbon metabolism (q_{WLP}) was identified. Still, many of the other inner workings of CO consumers remain to be verified, quantified and uncovered. These include the internal pH, the stoichiometries of the Rnf and ATPase membrane complexes and the rate-limiting step in the WLP, all indicated in red.

7.1.1. SMALL DIFFERENCES, LARGE IMPLICATIONS

C. autoethanogenum and other acetogenic species are microorganisms that have specialized in living in stringent conditions. Their substrates are toxic and/or have a low energy content, which makes the formation of enough ATP to stay alive a tricky business. Still, they survive and thrive and many authors including myself have marvelled over this. The trick that these organisms use to keep life on the rails is a tight regulation of their internal affairs. This is precisely the domain where many scientists (again, including myself) have so far assumed rather than experimentally verified the values of crucial parameters. It is time to make a change.

137

For example, *C. autoethanogenum* grows between pH 4.5 and 6.5 with an optimum of 5.8 - 6.0 [1]. Because of this slightly acidic optimal pH, it has been assumed [2, 3] that the internal pH is matched to the environment and close to 6 instead of the biochemical standard value of 7. This has, however, never been verified. Different methods that could also be applied to cultures of *C. autoethanogenum* have been reported [4–6]. Specifically, weak acids or bases like 5,5-dimethyl-oxazolidine dione or methylamine can be used. The calculation of the intracellular pH is then done from the established equilibrium between the intra- and extracellular concentrations of the indicator compound, and depends on an accurate estimation of cell volume. Ideally, this measurement would therefore be done for example in a microfluidics device that can be observed under the microscope. Microfluidic devices that are suitable for working with anaerobes are currently under development (*Martijn Diender, personal communication*). Then, the cell volume can be calculated as precisely as possible and the extracellular equilibrium concentration can be measured from the liquid stream exiting the microfluidics device. Other options include the use of ^{31}P NMR, where the resonance frequency of ^{31}P is pH-dependent, and radio- or fluorescently labelled probe molecules. Fluorescence often depends on the presence of oxygen, so suitable fluorescent dyes for anaerobic systems must be used [7]. An accurate measurement of the intracellular pH would help verify previously performed thermodynamic calculations [3, 8, 9], aid future theoretical analyses of intracellular metabolite concentrations [10], give perspective to the available data on WLP enzyme kinetics [2, 11] and provide targets for optimization of the conditions in such assays and shed light on which transport mechanisms are likely to be used and on the actual potential for energy harvesting. Once the internal pH is known, the free energy change of the bifurcating Rnf complex can be recalculated as done in [8] to re-assess the H^+/e^- stoichiometry of the complex. Combining this with a detailed study of the ATPase rotor architecture [12] would allow for much more accurate estimations of the ATP yield on substrate of syngas metabolisms. Even more accurate estimates could be made if the ratio between reduced and oxidized ferredoxin could be measured *in vivo*, for which a method has not been developed to date.

7.1.2. Enzymatics of acetogens

Other questions that remain to be answered are related to the machinery required for catabolism and growth, and how they are linked. In experiments with *C. autoethanogenum* grown on fructose as only carbon- and electron source, the success of reactor startup appeared to be correlated with the flowrate at which nitrogen was sparged (data not shown). At a relatively high sparging rate (100 mL N_2 min^{-1}) we observed long lag-phases or no growth at all, whereas growth did occur at a lower sparging rate (10 mL N_2 min^{-1}). Catabolizing fructose leads to the formation of acetate, ethanol, H_2 and CO_2, of which H_2 and CO_2 are removed with sparging. Theoretically, this should not influence the growth of the organisms, as glycolysis can proceed independently of the WLP. The obstruction of growth at high sparging rate, however, indicates that glycolysis and the WLP might be biochemically linked. Whether this is the case and what the molecular basis of this coupling would be, is

a captivating avenue for future research.

Furthermore, it would be interesting to identify which enzyme in the WLP is rate-limiting. This is, however, not trivial. Enzymatic assays with purified enzymes might give a good indication, but potentially provide a skewed image as the conditions in the cell are not comparable to the conditions in an enzymatic assay. Identifying the rate-limiting step provides fundamental insight in the metabolism, as well as new avenues for metabolic engineering. This enzyme could for example be knocked down to show whether overflow metabolism is triggered already at lower q_{CO}, to confirm that a limited WLP capacity ultimately underlies the occurence of overflow metabolism. In that case, engineered microbes with a lower WLP capacity might provide an interesting phenotype for industry, as these microbes will convert more of the substrate to ethanol.

7.1.3. ACETOGENS AND THEIR ENVIRONMENT

Open questions concerning the interactions between the microbe and its environment are even more difficult to pinpoint. When cultivating *C. autoethanogenum*, reducing agents are routinely used [1, 13–15] and the redox potential of the cultivation broth drops once the organism starts to grow. This indicates that the 'electron activity' of the cultivation medium is altered upon microbial growth [16], which could be related to the formation of catabolic products. Taking this notion to the extreme, one[1] could imagine that the organisms might even use the medium as a kind of extracellular battery. As the redox potential of the medium is important for and influenced by *C. autoethanogenum*, and surely also its acetogenic relatives, getting a better understanding of how the interaction between microbe and medium works might even reveal the ecological role of this organism in defining its habitat properties. Maybe it could even be elucidated if and how it communicates with its co-habitants.

7.1.4. A CLOSER LOOK AT CHAIN-ELONGATING ORGANISMS

Also for chain-elongating organisms various questions are left to be answered about the inner workings of their cells, as well as their metabolism and its control. Similar as for *C. autoethanogenum*, the stoichiometries of the Rnf complex and ATPase of chain-elongating microbes are largely based on assumptions. Furthermore, it has not been elucidated yet whether the proton gradient generated through the Rnf complex is, as is assumed now, fully used for ATP generation, or whether it is also being used for facilitating the transport of molecules over the cell membrane. Knowledge on such fundamental mechanisms might help us to understand why RBO has, to date, not been observed to happen independently of EO (**Chapter 6**), despite this being the catabolic strategy with the highest (even though not by much) theoretical ATP yield per mol of ethanol [17]. On the other end of the spectrum lies the theoretical possibility of EO as the sole catabolic process in a chain-elongating microbe, given that the hydrogen partial pressure is maintained low enough [18]. Verifying that this can happen *in vivo* likely requires the use of defined co-cultures of chain elongators and hydrogenotrophic methanogens. Ideally, the biochemical conversion profiles as

---

[1]Certainly not anyone, but my talented student Stef Broenink did

well as the transcriptome and proteome of these cultures would be monitored for extended periods of time. This might even shed light on the evolutionary origin of chain-elongating microbes.

Additionally, it remains elusive whether the different cycles of reversed β-oxidation are catalyzed by the same sets of enzymes or not. The presence of two different genes for each step of the reversed β-oxidation and three different thiolases in the genome of *C. kluyveri* leaves room for imagination [19], but ideally a combination of enzymatic assays with purified enzymes and *in vivo* growth studies with strains with different knock-outs should be used to resolve this question. In order to do this, a genetic toolbox for *C. kluyveri* is required. Then, it should be identified whether the expression of these genes is subject to some kind of regulation. It has already been hypothesized that redox-sensing transcriptional regulator Rex could have a significant role in directing the carbon flux in *C. kluyveri*, but also that complex, multilayered transcriptional regulation could be at play in this bacterium [20]. The putative reversal of the Rnf complex (**Chapter 5**) might also be controlled by regulatory mechanisms, either transcriptional or (post-)translational.

7.2. MICROBIAL ECOLOGY

In the previous section, and in the rest of this thesis, we have seen that the behavior of microorganisms is irreversibly linked to the environment they reside in. In natural ecosystems, the environment is not only manipulated by a single microorganism. This is why it is important to consider microbial ecology and the (potentially uncovered) interactions (fig. 7.2) that can take place both in engineered and in natural environments.

7.2.1. SHARING COMMODITIES

In **Chapter 2** the role of acetate as electron sink in acetogen overflow metabolism was identified. To verify that CO conversion capacity and acetate availability are interlinked, pulse experiments (like in **Chapter 3**) should also be performed in a medium with limited acetate availability. This could, for example, be done in a bioreactor with cell retention and a high liquid dilution rate. It would also be highly interesting to replace acetate with other organic acids, such as propionate, butyrate, valerate or hexanoate in this system, as acetogens often share their ecological niche with organisms that produce (some of) these acids [21–23]. The capacity of acetogens to reduce other organic acids to their corresponding alcohols has already been demonstrated [9], but it remains elusive whether their availability can boost CO uptake capacity, if different acids lead to different CO uptake capacities and if both pure- and mixed cultures of syngas fermenters exhibit this functional trait. Additionally, it remains unclear whether acetogen overflow metabolism has a beneficial effect on the organic acid producers.

In **Chapter 4** we enriched a chain-elongating microbial community at different pH. Independent of the pH, we saw a side-population of hydrogenotrophic methanogens develop, which coincided with a relative decrease in hexanoate productivity at neutral pH. In the systems operated here, methanogens were then chemically

inhibited to solely study chain elongators, leaving unresolved whether the shift in product spectrum was merely a transient observation, or due to interactions between chain elongators and methanogens. It has been proposed that H_2 co-feeding can aid the hexanoate-specificity during chain elongation [24], but no clear mechanistic explanation has been proposed yet. The potential synergies between chain elongators and their H_2-consuming counterparts are understudied thus far [25] and can be further explored either in synthetic co-cultures or in enrichment cultures with conditions tuned to the target microorganisms. Not only hydrogenotrophic methanogens, but also homoacetogens and sulfate reducers should be considered in such studies (fig. 7.2).

7.2.2. Competing for substrate

When considering the use of open mixed cultures in a single-stage process for integrated syngas fermentation and chain elongation, even more potential community members should be taken into account. Especially due to the presence of organic acids, which can serve as carbon source for anabolic reactions, the enrichment of hydrogenogenic and methanogenic carboxydotrophs as well as (CO-dependent) sulfate reducers will become possible [26]. Consumption of CO or the products of CO fermentation by sulfate reducers can be minimized by limiting the sulfate supply. Curbing H_2 formation from CO is likely easy, as it has the lowest ATP yield of the anoxic carboxydotrophic pathways. Furthermore, hydrogenogenic metabolisms are most prevalent under thermophilic conditions. These organisms can therefore likely be outcompeted in mesophilic systems with a selective pressure for high biomass yields. However, since H_2 is also a suitable electron donor for the WLP and feeding with high-H_2 streams can even improve the ethanol selectivity of syngas fermentation [27], it is debatable whether the presence of hydrogenogenic carboxydotrophs would be detrimental to the process at all. Carboxydotrophic methanogens, on the other hand, have a similar amount of Gibbs free energy available as acetogens [26], indicating that a tight competition for substrate could take place. Some enrichment studies on CO show that methane production originates from indirect routes, such as acetoclastic methanogenesis [28–30], but direct conversion of CO to CH_4 is also possible [31–33]. Even thought methanogens appear to be more sensitive to CO toxicity, it cannot be excluded that they will prevail in CO-converting microbial communities. Whether they convert CO or CO-derived compounds, methane formation implies losing carbon and electrons that should end up in higher-value products and must therefore be prevented. To understand how to prevent substrate losses to methane formation, enrichment cultures should be used to comprehend the competitive strategies of carboxydotrophic (and hydrogenotrophic) methanogens and acetogens. Analyzing the differences in microbial community structure and product spectrum in bioreactors with continuous versus pulsed CO feeding, at a dilution rate high enough to prevent acetoclastic methanogens, provides an interesting avenue for this type of study. For process control in large-scale reactors, chemical inhibition might still be required. Ethylene, one of the impurities that can be present in syngas originating from biomass gasification, actually proved to be an effective inhibitor of methanogenesis [34–36], showing that methanogen inhibition might even come at

no additional costs.
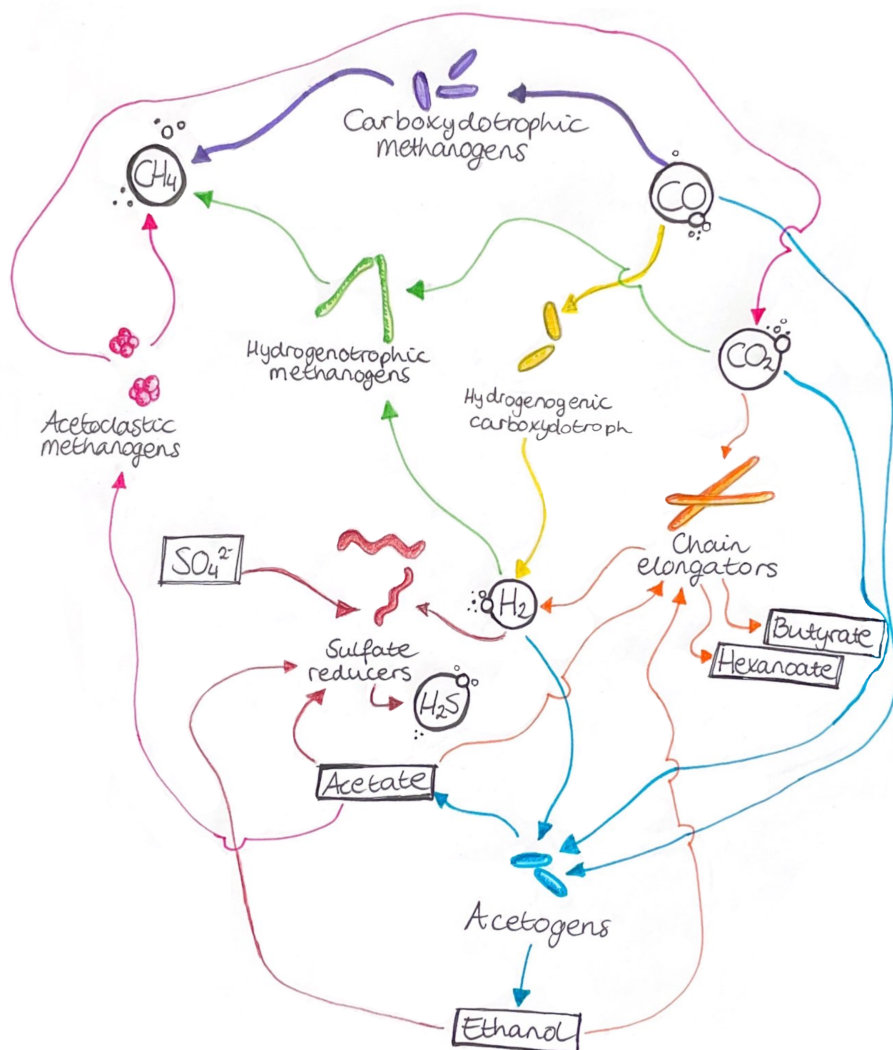
Figure 7.2: The CO-to-C6 anaerobic foodweb. This foodweb represents the key players and organisms to avoid in the bioconversion of syngas to chain-elongated organic acids. The interconversion of organic acids into their corresponding alcohols is not taken into account here, but complicates the food web even further.

7.3. PROCESS OPTIMIZATION

7.3.1. SYNGAS FERMENTATION AND CHAIN ELONGATION AT SCALE

To move towards a circular economy we must make waste-to-product conversions possible at large scale. Luckily, the efforts to get there are being made by many scientists inside and outside of academia. The company LanzaTech has made the production of ethanol from syngas possible at full scale. They are using metabolic engineering strategies to achieve a plug-and-play library of microbial catalysts for the production of various chemicals, including chain-elongated acids and their corresponding alcohols [37–39]. Yet, the achieved concentrations of chain-elongated products achieved with engineered acetogens is orders of magnitude lower than what has been achieved in mixed- and defined consortia to date [14, 40]. This stresses the importance of continued efforts to optimize the use of microbial consortia as well. ChainCraft, a company situated in the port of Amsterdam, turns food waste into chain-elongated acids at pilot scale. At both these companies the expertise and experience is generated to bring the C_1-to-C_6 process to large scale.

7.3.2. PROCESS INTEGRATION - A ONE-POT WONDER?

One of the key questions in scale-up is whether syngas fermentation and chain elongation should also be integrated in a single bioreactor or not. One-stage systems are feasible, but their operation is certainly not trivial. Differences in pH optima can, for example, lead to loss of chain-elongating activity in mixed cultures. This could be circumvented by using synthetic co-cultures, but the product concentrations and -specificities reached with both mixed and- synthetic consortia leave room for improvement [14, 31, 40, 41]. A factor that might hamper reaching the full potential of chain elongators in integrated processes is the inherent low concentration of substrates for chain elongation. Another challenge that should be overcome in an integrated bioreactor is that the product spectrum of both syngas fermentation and chain elongation must be controlled simultaneously. The high ethanol-to-acetate ratios required for optimal hexanoate production [42–46] can potentially be achieved in bioreactors with CO pulse feeding, via periodically changing the gas compositions or the mass transfer capacity (i.e. via stirring, gas flow, recirculation) of the bioreactor. This would provide an alternative to the use of pH shocks that exploit acid toxicity as a driving force for further reduction to ethanol [47], which is incompatible with simultaneous chain elongation. The feasibility of pulse feeding for increasing the ethanol-to-acetate ratio should be assessed. If this is successful, it also remains to be evaluated whether the chain-elongating organisms can cope with these fluctuations, either in mixed cultures or in synthetic co-cultures.

7.3.3. GRANULATION AND *in situ* PRODUCT REMOVAL FOR PROCESS INTENSIFICATION

An interesting avenue for further process intensification would be the use of granular biomass or other types of cell retention. The advantage of a gaseous substrate is that the gas- and liquid retention times are not coupled, which theoretically simplifies

7

the buildup of high biomass concentrations. Granulation in chain-elongating systems has been observed, but maintaining robust granules is not a given [48, 49]. Still, the use of granular biomass could significantly improve the process rate of ethanol-only chain elongation to hexanoate. Another potential advantage is that, when syngas fermentation and chain elongation are integrated in a single granule, chain elongators will be protected from CO toxicity. The CO consuming microbes will likely form the outer layer of the granule, shielding the chain elongators from CO. Yet, CO consumers will only survive in a biofilm if the liquid concentration of CO (an off-the shelf probe for its direct measurement would significantly advance the field!) is sufficiently high to establish a CO gradient over the biofilm depth. High liquid concentrations of CO can only be attained in bioreactor systems with enhanced gas/liquid mass transfer capacities, which is also an important area of future study [50, 51].

Even if granulation is attained, granules do not always develop as expected [52] and the formation, structure and performance of granules of acetogen-chain elongator consortia provide an interesting avenue for further study. It must be considered, though, that systems with high biomass concentrations also accumulate high product concentrations. These can be detrimental for both cell activity and viability (**Chapter 4)** and granulation potential. This can be mitigated through the use of *in situ* product removal, where the chain-elongated products are removed continuously from the fermentation broth. Various researchers have observed that the use of *in situ* product removal unlocks the potential to also produce the C_8-compound octanoate with chain-elongating microbial communities [42, 45, 53]. Octanoate is significantly more toxic than its C_6-counterpart, making its production to significant concentrations unfeasible in systems without *in situ* product removal. Yet, it is easier to separate, has a higher market value and has a less pungent odour [45]. The trade-off between C_6 and C_8 production should be made based on the dynamic market demand for either product. With the increasing body of knowledge on chain-elongating communities and how to control them, tuning the operational parameters of an industrial-scale system to select for the required product will become an easy task in the future.

7.4. BIOTECHNOLOGY AND SOCIETY

Potential new technologies are being conceived all the time. Some of them are born from the minds of scientists that have long believed something to be possible and finally break through all the barriers in their way towards their big discovery. Others start with a frustrated scientist, because their experiments don't show the results that they need to prove their hypothesis. Until they look again, or ruminate for a long time, or both, and find out that something entirely different, unexpected and truly fascinating is happening. Independent of how they get to the point where they think 'wow, this is really something', they are by now convinced that their discovery will change the world.

One little problem. Nobody knows about it yet.

144

Sure, maybe the research team does. A small group of other researchers in another university that accidentally fell down the same rabbit hole. But the general public? Policy makers? No, sir. So a struggle begins, where stiff scientific language has to be translated into something that is understandable to, well, most people. And when they do understand it, they probably still don't *care* about it.

Okay, that might be a little bit of a grim scenario. If we tell them that we can cure a disease, they will probably find it interesting. They still don't care about the details, but they'll just tune out during the explanation of the molecular mechanism and tune back in when we tell them how much money they can make with it. Hitting the ground running in the development of a biotechnological process almost exclusively happens when it promises a lot of cash, and soon.

This thesis revolves around the production of chemicals from waste. Chemicals that we are already used to, like ethanol, and chemicals for which market development is also one of the key steps towards success, like hexanoic acid. Neither of these products promise large revenue streams within the blink of an eye. This is a huge problem that I decided to ignore while I was studying my microbes because:

1. My goal was to let myself be amazed, to learn a bit more about all that we cannot see (or actually, an unimaginably small part of that) and to enjoy this process of learning more about life in the broadest sense. Focusing on this seemed like a smart idea, because:

2. I think I would continuously be disappointed if I allowed myself to focus too much on how hard it is to actually change the world

But now that we are at the end of this journey, I think it is time for me to tap into that disappointment just for a little while to see if we can do something about it. Let me start with explicitly stating that the big problem is that we, producers of renewable bulk chemicals, are competing with fossil fuel prices. This is understandable, because renewable chemicals are supposed to replace fossil ones. But when you think about it a bit longer, it is quite ridiculous. Fossil fuels are free. They can now also be extracted from the Earth basically for free, because we have been optimizing the technology to do so for close to two centuries. Admittedly, we have to pay for crude oil refining, but beside that we mainly pay for sustaining international conflicts and to compensate for people selling stuff that is not actually theirs.

Things need to change [54]. For starters, new renewable chemical prices should not be compared to the prices of their fossil equivalent. Reallocating fossil fuel subsidies to the development of more sustainable alternatives would also greatly help new technologies to take off. But let's not externalize all the blame here. Process engineers should take responsibility for identifying the real bottlenecks for getting a process to the market in an early stage, to make sure that efforts are focused on the right goal. For chain elongation, for example, it is likely that the main bottleneck is the recovery of the product. Luckily, excellent researchers are already working

7

on integrating fermentation and product recovery to clear the path to large-scale implementation [42, 44, 53, 55, 56].

Maybe even more importantly, scientists have the responsibility to communicate what they do and what is going on in the scientific world to people outside their research bubble. Changing the world is hard, but if we can spark interest in more people, more people will start to care. We should start by explaining to each other what we are doing in a language we all understand. I believe that scientists have the tendency to overestimate each other and overcomplicate their stories. Let's stop doing that. Let's start at the beginning of the story and get more comfortable with explaining the basics before we dive into the content. Let's just choose a single message to convey. Let's not always explain the nitty-gritty of our methods (all the more reason to interact afterwards with the people that do want to know!). And let's be bold and make a joke once in a while. Even when we are explaining to our colleagues what we do. And especially in group seminars and at conferences! Repeating the background knowledge to someone that already knows is so much better than losing 80% of our audience after the first two minutes of the talk. This will allow us to better explain our work, but also the discoveries of our fellow scientist, to our friends and family. If each of us aims to do that, we will already greatly amplify our effective reach. Then we can also expand our circle of impact by looking for opportunities to talk about science on for example the radio, in a TedTalk, on a podcast, on social media, in the news(paper) or at schools. Let's spread the word about science together.

7

BIBLIOGRAPHY

[1]   J. Abrini, H. Naveau, and E.-J. Nyns. "*Clostridium autoethanogenum*, sp. nov., an anaerobic bacterium that produces ethanol from carbon monoxide". In: *Archives of Microbiology* 161 (1993).

[2]   J. Mock, Y. Zheng, A. P. Mueller, S. Ly, L. Tran, S. Segovia, S. Nagaraju, M. Köpke, P. Dürre, and R. K. Thauer. "Energy Conservation Associated with Ethanol Formation from H_2 and CO_2 in *Clostridium autoethanogenum* Involving Electron Bifurcation". In: *Journal of Bacteriology* 197.18 (Sept. 2015). Ed. by W. W. Metcalf, pp. 2965–2980. DOI: 10.1128/JB.00399-15.

[3]   V. Mahamkali, K. Valgepea, R. De Souza Pinto Lemgruber, M. Plan, R. Tappel, M. Köpke, S. D. Simpson, L. K. Nielsen, and E. Marcellin. "Redox controls metabolic robustness in the gas-fermenting acetogen *Clostridium autoethanogenum*". In: *Proceedings of the National Academy of Sciences* 117.23 (June 2020), pp. 13168–13175. DOI: 10.1073/pnas.1919531117.

[4]   I. R. Booth. "Regulation of Cytoplasmic pH in Bacteria". In: *MICROBIOL. REV.* 49 (1985).

[5]   G. M. Cook. "The intracellular pH of the thermophilic bacterium *Thermoanaerobacter wiegelii* during growth and production of fermentation acids". In: *Extremophiles* 4.5 (Oct. 2000), pp. 279–284. DOI: 10.1007/s007920070014.

[6]   A. Kurkdjian and J. Guern. "Intracellular pH: Measurement and Importance in Cell Activity". In: *Annual Review of Plant Physiology and Plant Molecular Biology* 40 (1989).

[7]   M. Flaiz, T. Baur, J. Gaibler, C. Kröly, and P. Dürre. "Establishment of Green- and Red-Fluorescent Reporter Proteins Based on the Fluorescence-Activating and Absorption-Shifting Tag for Use in Acetogenic and Solventogenic Anaerobes". In: *ACS Synthetic Biology* 11.2 (Feb. 2022), pp. 953–967. DOI: 10.1021/acssynbio.1c00554.

[8]   K. Schuchmann and V. Müller. "Autotrophy at the thermodynamic limit of life: a model for energy conservation in acetogenic bacteria". In: *Nature Reviews Microbiology* 12.12 (Dec. 2014), pp. 809–821. DOI: 10.1038/nrmicro3365.

[9]   J. M. Perez, H. Richter, S. E. Loftus, and L. T. Angenent. "Biocatalytic reduction of short-chain carboxylic acids into their corresponding alcohols with syngas fermentation". In: *Biotechnology and Bioengineering* 110.4 (Apr. 2013), pp. 1066–1077. DOI: 10.1002/bit.24786.

[10]   R. González-Cabaleiro, J. M. Lema, J. Rodríguez, and R. Kleerebezem. "Linking thermodynamics and kinetics to assess pathway reversibility in anaerobic bioprocesses". In: *Energy & Environmental Science* 6.12 (2013), p. 3780. DOI: 10.1039/c3ee42754d.

[11]   S. Wang, H. Huang, J. Kahnt, A. P. Mueller, M. Köpke, and R. K. Thauer. "NADP-Specific Electron-Bifurcating [FeFe]-Hydrogenase in a Functional Complex with Formate Dehydrogenase in *Clostridium autoethanogenum* Grown on CO". In: *Journal of Bacteriology* 195.19 (Oct. 2013), pp. 4373–4386. DOI: 10.1128/JB.00678-13.

[12]   R. O. Norman, T. Millat, K. Winzer, N. P. Minton, and C. Hodgman. "Progress towards platform chemical production using *Clostridium autoethanogenum*". In: *Biochemical Society Transactions* 46.3 (June 2018), pp. 523–535. DOI: 10.1042/BST20170259.

[13]   K. Valgepea, R. De Souza Pinto Lemgruber, K. Meaghan, R. W. Palfreyman, T. Abdalla, B. D. Heijstra, J. B. Behrendorff, R. Tappel, M. Köpke, S. D. Simpson, L. K. Nielsen, and E. Marcellin. "Maintenance of ATP Homeostasis Triggers Metabolic Shifts in Gas-Fermenting Acetogens". In: *Cell Systems* 4.5 (May 2017), 505–515.e5. DOI: 10.1016/j.cels.2017.04.008.

[14]   M. Diender, I. Parera Olm, M. Gelderloos, J. J. Koehorst, P. J. Schaap, A. J. M. Stams, and D. Z. Sousa. "Metabolic shift induced by synthetic co-cultivation promotes high yield of chain elongated acids from syngas". In: *Scientific Reports* 9.1 (Dec. 2019), p. 18081. DOI: 10.1038/s41598-019-54445-y.

[15]   J. L. Cotter, M. S. Chinn, and A. M. Grunden. "Influence of process parameters on growth of *Clostridium ljungdahlii* and *Clostridium autoethanogenum* on synthesis gas". In: *Enzyme and Microbial Technology* 44.5 (May 2009), pp. 281–288. DOI: 10.1016/j.enzmictec.2008.11.002.

[16]   L. Kjaergaard. "The redox potential: Its use and control in biotechnology". In: *Advances in Biochemical Engineering, Volume 7.* Vol. 7. Series Title: Advances in Biochemical Engineering. Berlin/Heidelberg: Springer-Verlag, 1977, pp. 131–150. DOI: 10.1007/BFb0048444.

[17]   L. T. Angenent, H. Richter, W. Buckel, C. M. Spirito, K. J. J. Steinbusch, C. M. Plugge, D. P. B. T. B. Strik, T. I. M. Grootscholten, C. J. N. Buisman, and H. V. M. Hamelers. "Chain Elongation with Reactor Microbiomes: Open-Culture Biotechnology To Produce Biochemicals". In: *Environmental Science & Technology* 50.6 (Mar. 2016), pp. 2796–2810. DOI: 10.1021/acs.est.5b04847.

[18]   H.-J. Seitz, B. Schink, and R. Conrad. "Thermodynamics of hydrogen metabolism in methanogenic cocultures degrading ethanol or lactate". en. In: *FEMS Microbiology Letters* 55.2 (Oct. 1988), pp. 119–124. DOI: 10.1111/j.1574-6968.1988.tb13918.x.

[19]   H. Seedorf, W. F. Fricke, B. Veith, H. Brüggemann, H. Liesegang, A. Strittmatter, M. Miethke, W. Buckel, J. Hinderberger, F. Li, C. Hagemeier, R. K. Thauer, and G. Gottschalk. "The genome of *Clostridium kluyveri*, a strict anaerobe with unique metabolic features". In: *Proceedings of the National Academy of Sciences* 105.6 (Feb. 2008), pp. 2128–2133. DOI: 10.1073/pnas.0711093105.

[20]   L. Hu, H. Huang, H. Yuan, F. Tao, H. Xie, and S. Wang. "Rex in *Clostridium kluyveri* is a global redox-sensing transcriptional regulator". In: *Journal of Biotechnology* 233 (Sept. 2016), pp. 17–25. DOI: 10.1016/j.jbiotec.2016.06.024.

[21]   H. A. Barker, M. D. Kamen, and B. T. Bornstein. "The Synthesis of Butyric and Caproic Acids from Ethanol and Acetic Acid by *Clostridium kluyveri*". In: *Proceedings of the National Academy of Sciences* 31.12 (Dec. 1945), pp. 373–381. DOI: 10.1073/pnas.31.12.373.

[22]   S. Joshi, A. Robles, S. Aguiar, and A. G. Delgado. "The occurrence and ecology of microbial chain elongation of carboxylates in soils". In: *The ISME Journal* 15.7 (July 2021), pp. 1907–1918. DOI: 10.1038/s41396-021-00893-2.

[23]   B. Schink. "Diversity, Ecology, and Isolation of Acetogenic Bacteria". In: *Acetogenesis.* Ed. by H. L. Drake. Boston, MA: Springer US, 1994, pp. 197–235. DOI: 10.1007/978-1-4615-1777-1_7.

7

[24] F. C. F. Baleeiro, S. Kleinsteuber, and H. Sträuber. "Hydrogen as a Co-electron Donor for Chain Elongation With Complex Communities". In: *Frontiers in Bioengineering and Biotechnology* 9 (Mar. 2021), p. 650631. DOI: 10.3389/fbioe.2021.650631.

[25] P. Candry and R. Ganigué. "Chain elongators, friends, and foes". In: *Current Opinion in Biotechnology* 67 (Feb. 2021), pp. 99–110. DOI: 10.1016/j.copbio.2021.01.005.

[26] M. Diender, A. J. M. Stams, and D. Z. Sousa. "Pathways and Bioenergetics of Anaerobic Carbon Monoxide Fermentation". In: *Frontiers in Microbiology* 6 (Nov. 2015). DOI: 10.3389/fmicb.2015.01275.

[27] K. Valgepea, R. De Souza Pinto Lemgruber, T. Abdalla, S. Binos, N. Takemori, A. Takemori, Y. Tanaka, R. Tappel, M. Köpke, S. D. Simpson, L. K. Nielsen, and E. Marcellin. "H2 drives metabolic rearrangements in gas-fermenting *Clostridium autoethanogenum*". In: *Biotechnology for Biofuels* 11.1 (Dec. 2018), p. 55. DOI: 10.1186/s13068-018-1052-9.

[28] J. I. Alves, A. J. Stams, C. M. Plugge, M. Madalena Alves, and D. Z. Sousa. "Enrichment of anaerobic syngas-converting bacteria from thermophilic bioreactor sludge". In: *FEMS Microbiology Ecology* 86.3 (Dec. 2013), pp. 590–597. DOI: 10.1111/1574-6941.12185.

[29] A. L. Arantes, J. I. Alves, A. J. M. Stams, M. M. Alves, and D. Z. Sousa. "Enrichment of syngas-converting communities from a multi-orifice baffled bioreactor". In: *Microbial Biotechnology* 11.4 (July 2018), pp. 639–646. DOI: 10.1111/1751-7915.12864.

[30] S. Sancho Navarro, R. Cimpoia, G. Bruant, and S. R. Guiot. "Biomethanation of Syngas Using Anaerobic Sludge: Shift in the Catabolic Routes with the CO Partial Pressure Increase". In: *Frontiers in Microbiology* 7 (Aug. 2016). DOI: 10.3389/fmicb.2016.01188.

[31] M. Diender, A. J. M. Stams, and D. Z. Sousa. "Production of medium-chain fatty acids and higher alcohols by a synthetic co-culture grown on carbon monoxide or syngas". In: *Biotechnology for Biofuels* 9.1 (Dec. 2016), p. 82. DOI: 10.1186/s13068-016-0495-0.

[32] L. Daniels, G. Fuchs, R. K. Thauer, and J. G. Zeikus. "Carbon Monoxide Oxidation by Methanogenic Bacteria". In: *Journal of Bacteriology* 132.1 (Oct. 1977), pp. 118–126. DOI: 10.1128/jb.132.1.118-126.1977.

[33] D. J. Lessner, L. Li, Q. Li, T. Rejtar, V. P. Andreev, M. Reichlen, K. Hill, J. J. Moran, B. L. Karger, and J. G. Ferry. "An unconventional pathway for reduction of CO_2 to methane in CO-grown *Methanosarcina acetivorans* revealed by proteomics". In: *Proceedings of the National Academy of Sciences* 103.47 (Nov. 2006), pp. 17921–17926. DOI: 10.1073/pnas.0608833103.

[34] D. Xu, D. R. Tree, and R. S. Lewis. "The effects of syngas impurities on syngas fermentation to liquid fuels". In: *Biomass and Bioenergy* 35.7 (July 2011), pp. 2690–2696. DOI: 10.1016/j.biombioe.2011.03.005.

[35] F. C. F. Baleeiro, S. Kleinsteuber, and H. Sträuber. "Recirculation of H_2, CO_2, and Ethylene Improves Carbon Fixation and Carboxylate Yields in Anaerobic Fermentation". In: *ACS Sustainable Chemistry & Engineering* 10.13 (Apr. 2022), pp. 4073–4081. DOI: 10.1021/acssuschemeng.1c05133.

[36] F. C. F. Baleeiro, L. Varchmin, S. Kleinsteuber, H. Sträuber, and A. Neumann. "Formate-induced CO tolerance and methanogenesis inhibition in fermentation of syngas and plant biomass for carboxylate production". In: *Biotechnology for Biofuels and Bioproducts* 16.1 (Feb. 2023), p. 26. DOI: 10.1186/s13068-023-02271-w.

7

[37] F. E. Liew, R. Nogle, T. Abdalla, B. J. Rasor, C. Canter, R. O. Jensen, L. Wang, J. Strutz, P. Chirania, S. De Tissera, A. P. Mueller, Z. Ruan, A. Gao, L. Tran, N. L. Engle, J. C. Bromley, J. Daniell, R. Conrado, T. J. Tschaplinski, R. J. Giannone, R. L. Hettich, A. S. Karim, S. D. Simpson, S. D. Brown, C. Leang, M. C. Jewett, and M. Köpke. "Carbon-negative production of acetone and isopropanol by gas fermentation at industrial pilot scale". In: *Nature Biotechnology* 40.3 (Mar. 2022), pp. 335–344. DOI: 10.1038/s41587-021-01195-w.

[38] N. Fackler, B. D. Heijstra, B. J. Rasor, H. Brown, J. Martin, Z. Ni, K. M. Shebek, R. R. Rosin, S. D. Simpson, K. E. Tyo, R. J. Giannone, R. L. Hettich, T. J. Tschaplinski, C. Leang, S. D. Brown, M. C. Jewett, and M. Köpke. "Stepping on the Gas to a Circular Economy: Accelerating Development of Carbon-Negative Chemical Production from Gas Fermentation". en. In: *Annual Review of Chemical and Biomolecular Engineering* 12.1 (June 2021), pp. 439–470. DOI: 10.1146/annurev-chembioeng-120120-021122.

[39] B. Vögeli, L. Schulz, S. Garg, K. Tarasava, J. M. Clomburg, S. H. Lee, A. Gonnot, E. H. Moully, B. R. Kimmel, L. Tran, H. Zeleznik, S. D. Brown, S. D. Simpson, M. Mrksich, A. S. Karim, R. Gonzalez, M. Köpke, and M. C. Jewett. "Cell-free prototyping enables implementation of optimized reverse β-oxidation pathways in heterotrophic and autotrophic bacteria". In: *Nature Communications* 13.1 (June 2022), p. 3058. DOI: 10.1038/s41467-022-30571-6.

[40] R. Ganigué, P. Sánchez-Paredes, L. Bañeras, and J. Colprim. "Low Fermentation pH Is a Trigger to Alcohol Production, but a Killer to Chain Elongation". In: *Frontiers in Microbiology* 7 (May 2016). DOI: 10.3389/fmicb.2016.00702.

[41] H. Richter, B. Molitor, M. Diender, D. Z. Sousa, and L. T. Angenent. "A Narrow pH Range Supports Butanol, Hexanol, and Octanol Production from Syngas in a Continuous Co-culture of *Clostridium ljungdahlii* and *Clostridium kluyveri* with In-Line Product Extraction". In: *Frontiers in Microbiology* 7 (Nov. 2016). DOI: 10.3389/fmicb.2016.01773.

[42] C. M. Spirito, A. M. Marzilli, and L. T. Angenent. "Higher Substrate Ratios of Ethanol to Acetate Steered Chain Elongation toward *n*-Caprylate in a Bioreactor with Product Extraction". In: *Environmental Science & Technology* 52.22 (Nov. 2018), pp. 13438–13447. DOI: 10.1021/acs.est.8b03856.

[43] M. T. Agler, C. M. Spirito, J. G. Usack, J. J. Werner, and L. T. Angenent. "Development of a highly specific and productive process for n-caproic acid production: applying lessons from methanogenic microbiomes". In: *Water Science and Technology* 69.1 (Jan. 2014), pp. 62–68. DOI: 10.2166/wst.2013.549.

[44] S. Ge, J. G. Usack, C. M. Spirito, and L. T. Angenent. "Long-Term *n*-Caproic Acid Production from Yeast-Fermentation Beer in an Anaerobic Bioreactor with Continuous Product Extraction". In: *Environmental Science & Technology* 49.13 (July 2015), pp. 8012–8021. DOI: 10.1021/acs.est.5b00238.

[45] L. A. Kucek, C. M. Spirito, and L. T. Angenent. "High n-caprylate productivities and specificities from dilute ethanol and acetate: chain elongation with microbiomes to upgrade products from syngas fermentation". In: *Energy & Environmental Science* 9.11 (2016), pp. 3482–3494. DOI: 10.1039/C6EE01487A.

[46] Y. Liu, F. Lü, L. Shao, and P. He. "Alcohol-to-acid ratio and substrate concentration affect product structure in chain elongation reactions initiated by unacclimatized inoculum". In: *Bioresource Technology* 218 (Oct. 2016), pp. 1140–1150. DOI: 10.1016/j.biortech.2016.07.067.

7

[47] H. Richter, M. Martin, and L. Angenent. "A Two-Stage Continuous Fermentation System for Conversion of Syngas into Ethanol". In: *Energies* 6.8 (Aug. 2013), pp. 3987–4000. DOI: 10.3390/en6083987.

[48] Q. Mariën, B. Ulčar, J. Verleyen, B. Vanthuyne, and R. Ganigué. "High-rate conversion of lactic acid-rich streams to caproic acid in a fermentative granular system". In: *Bioresource Technology* 355 (July 2022), p. 127250. DOI: 10.1016/j.biortech.2022.127250.

[49] M. Roghair, D. P. Strik, K. J. Steinbusch, R. A. Weusthuis, M. E. Bruins, and C. J. Buisman. "Granular sludge formation and characterization in a chain elongation process". In: *Process Biochemistry* 51.10 (Oct. 2016), pp. 1594–1598. DOI: 10.1016/j.procbio.2016.06.012.

[50] M. P. Elisiário, H. De Wever, W. Van Hecke, H. Noorman, and A. J. J. Straathof. "Membrane bioreactors for syngas permeation and fermentation". en. In: *Critical Reviews in Biotechnology* 42.6 (Aug. 2022), pp. 856–872. DOI: 10.1080/07388551.2021.1965952.

[51] C. J. W. Hop. "Rotor-Stator Spinning Disc Reactor". PhD thesis. Eindhoven: TU Eindhoven, June 2023.

[52] D. Batstone, J. Keller, and L. Blackall. "The influence of substrate kinetics on the microbial community structure in granular anaerobic biomass". In: *Water Research* 38.6 (Mar. 2004), pp. 1390–1404. DOI: 10.1016/j.watres.2003.12.003.

[53] R. Palomo-Briones, J. Xu, C. M. Spirito, J. G. Usack, L. H. Trondsen, J. J. L. Guzman, and L. T. Angenent. "Near-neutral pH increased n-caprylate production in a microbiome with product inhibition of methanogenesis". In: *Chemical Engineering Journal* 446.3 (2022). DOI: https://doi.org/10.1016/j.cej.2022.137170.

[54] COGEM and Gezondheidsraad. *Trendanalyse Biotechnologie: Tijd voor een integrale visie*. Tech. rep. Bilthoven: COGEM, 2023, p. 36.

[55] J. M. Carvajal-Arroyo, S. J. Andersen, R. Ganigué, R. A. Rozendal, L. T. Angenent, and K. Rabaey. "Production and extraction of medium chain carboxylic acids at a semi-pilot scale". In: *Chemical Engineering Journal* 416 (July 2021), p. 127886. DOI: 10.1016/j.cej.2020.127886.

[56] J. Xu, B. Bian, L. T. Angenent, and P. E. Saikaly. "Long-Term Continuous Extraction of Medium-Chain Carboxylates by Pertraction With Submerged Hollow-Fiber Membranes". In: *Frontiers in Bioengineering and Biotechnology* 9 (Aug. 2021), p. 726946. DOI: 10.3389/fbioe.2021.726946.

7

Nomenclature

Chemical species		
CO	Carbon monoxide	(-)
CO_2	Carbon dioxide	(-)
H_2	Hydrogen	(-)
CH_4	Methane	(-)
N_2	Nitrogen	(-)
Ac	Acetate	(-)
EtOH	Ethanol	(-)
But	Butyrate	(-)
Hex	Hexanoate	(-)
X	Biomass	(-)

Metabolism		
WLP	Wood-Ljungdahl pathway	(-)
RBO	Reversed β-oxidation pathway	(-)
RBO1	Reversed β-oxidation cycle 1 - acetate to butyrate	(-)
RBO2	Reversed β-oxidation cycle 2 - butyrate to hexanoate	(-)
EO	Ethanol oxidation	(-)
ATP	Adenosine triphosphate	(-)
NAD/NADH	Oxidized/reduced nicotinamide adenine dinucleotide	(-)
Fd/Fd^{2-}	Oxidized/reduced ferredoxin	(-)
CODH	Carbon monoxide dehydrogenase	(-)
MTHRF	Methylene tetrahydrofolate reductase	(-)
Rnf	Rhodobacter nitrogen fixation enzyme complex	(-)
AOR	Acetaldehyde oxidoreductase	(-)
Nfn	Electron confurcating complex	(-)
FDH	Formate dehydrogenase	(-)
CODH/ACS	CO dehydrogenase/Acetyl-CoA synthase	(-)
ALDH	Acetaldehyde dehydrogenase	(-)
ADH	Alcohol dehydrogenase	(-)
MTHFD	Methylene tetrahydrofolate dehydrogenase	(-)
ACK	Acetate kinase enzyme	(-)

Other symbols		
γ	Degree of reduction	(-)
μ	Biomass-specific growth rate	(h^{-1})
SCFA	Short-chain fatty acid	(-)

MCFA	Medium-chain fatty acid	(-)
F	Gas- or liquid flow	$(mol \cdot h^{-1})$
N	Amount of a gaseous species	(mol)
M	Amount of a dissolved species	(mol)
C_i	Concentration of compound i	$(mol \cdot L^{-1})$
T	Temperature	(K)
T_N	Gas/liquid transfer term	$(mol \cdot h^{-1})$
V	Volume	(L)
q	Biomass-specific rate	$(mmol \cdot g_x \cdot h^{-1})$
v	Flux	$(mmol \cdot h^{-1}$

Curriculum Vitae

Maximilienne Toetie ALLAART

Maxim was born on the 18th of January, 1995 in Amsterdam, where she attended Het Amsterdams Lyceum for her high school education. Chemistry was her favorite subject and Amsterdam her favorite city in the Netherlands, so choosing a BSc programme seemed a job already done... But then a very excited Life Science and Technology student talked about her programme in an obligatory open day, and Maxim was sold. She moved to Leiden to follow the joint-degree Delft/Leiden LST programme and did her BSc thesis in the Industrial Microbiology section in Delft on the ancient parent of brewers' yeast. Enamoured with the microbial world and all its potential, she chose to follow the Biochemical Engineering track of the LST masters' programme at the TU Delft. As she started to follow her first courses of the masters, she also represented the students of the Faculty of Science of Leiden University and pushed for a more sustainable university as a board member in the Faculty Board. During her master thesis, she studied the competitive advantage of lactic acid bacteria in the Environmental Biotechnology section, under daily supervision of Jules Rombouts. Still enamoured with the microbial world, but now also with the atmosphere of EBT, she decided to pursue a PhD in the group of Robbert Kleerebezem on syngas fermentation. Before starting her PhD, she did an internship in Biopolis S.L. in Valencia where she worked on organic waste conversion to bioproducts, learning lab vocabulary (and much more!) in Spanish and mastering her serve on the beach volley court. Maxim has a passion for communicating about science and connecting (with) people, which she brought to use in the organization of the first 'Emerging Microbial Technologies' conference in Delft in May 2022, which was funded by FEMS and co-organized with her colleagues Jules Rombouts and Martijn Diender. In her spare time she likes to cook, ideally without recipes, go on walks and hikes in the mountains, read and eat delicious food.

LIST OF PUBLICATIONS

5. M. T. Allaart, C. Korkontzelos, D. Z. Sousa, R. Kleerebezem, "A novel experimental method to determine substrate uptake kinetics of gaseous substrates applied to carbon monoxide-fermenting *Clostridium autoethanogenum*". *Submitted for publication in Biotechnology and Bioengineering in May 2023*

4. M. T. Allaart, B. B. Fox, I. H. M. S. Nettersheim, D. Z. Sousa, R. Kleerebezem, "Chain elongating microorganisms metabolize ethanol in the absence of short-chain fatty acids". *Submitted for publication in Scientific Reports in May 2023*

3. M. T. Allaart, M. Diender, D. Z. Sousa, and R. Kleerebezem. "Overflow metabolism at the thermodynamic limit of life: How carboxydotrophic acetogens mitigate carbon monoxide toxicity". In: *Microbial Biotechnology* 16.4 (Apr. 2023), pp. 697–705. DOI: 10.1111/1751-7915.14212

2. M. T. Allaart, G. R. Stouten, D. Z. Sousa, and R. Kleerebezem. "Product Inhibition and pH Affect Stoichiometry and Kinetics of Chain Elongating Microbial Communities in Sequencing Batch Bioreactors". In: *Frontiers in Bioengineering and Biotechnology* 9 (June 2021), p. 693030. DOI: 10.3389/fbioe.2021.693030

1. J. L. Rombouts, M. C. M. van Loosdrecht, R. Kleerebezem, D. G. Weissbrodt, G. R. Stouten, M. T. Allaart, "High yield lactic acid production using mixed cultures". *Patent with number WO2020229370A2, filed May 8, 2020, and issued November 19, 2020.*

CONFERENCE CONTRIBUTIONS

Presenting author is <u>underlined</u>.

8. <u>Allaart, M.T.</u>, Diender, M., Sousa, D.Z., Kleerebezem, R. 'Overflow metabolism at the thermodynamic limit of life: how carboxydotrophic acetogens mitigate carbon monoxide toxicity', **VAAM Annual Conference 2023**, Göttingen, Germany (September 2023). Oral presentation.

7. <u>Allaart, M.T.</u>, Diender, M., Sousa, D.Z., Kleerebezem, R. 'Getting a grip on the product spectum of CO fermentation: On how rate influences metabolic strategy', **Scientific Spring Meeting KNVM NVVM**, Papendal, The Netherlands (April 2023). Poster presentation.

6. <u>Allaart, M.T.</u>, Fox, B.B., Nettersheim, I.H.M.S, Sousa, D.Z., Kleerebezem, R. 'Controlling the product spectrum of chain elongating microbial communities: direct conversion of ethanol to hexanoate', **2nd International Chain Elongation Conference**, Bad Boll, Germany (November 2022). Oral presentation. *Best presentation award*

5. Allaart, M.T., Remeijer, M., Fox, B.B., Sousa, D.Z., <u>Kleerebezem, R.</u> 'Translating a mechanistic understanding of chain elongating microorganisms into a kinetic modelling framework', **17th IWA World Conference on Anaerobic Digestion**, Ann Arbour, USA (June 2022). Oral presentation.

4. <u>Allaart, M.T.</u>, Kerstjens, M., Sousa, D.Z., Kleerebezem, R. 'Competing, Collaborating or Coexisting: the Effect of Methanogens on Chain Elongation', **4th International Conference on Biogas Microbiology**, Braga, Portugal (May 2022). Oral presentation. *Best presentation award*

3. <u>Allaart, M.T.</u>, Fox, B.B., Nettersheim, I.H.M.S, Sousa, D.Z., Kleerebezem, R. 'Brewery wastewater to value: direct microbial conversion of ethanol to caproate', **IWA Young Water Professionals Conference**, Delft, The Netherlands (April 2022). Oral presentation. *Best presentation award*

2. <u>Allaart, M.T.</u>, Stouten, G.R., Sousa, D.Z., Kleerebezem, R. 'Product Spectrum and pH Influence Stoichiometry and Kinetics of Chain Elongating Communities in Sequencing Batch Bioreactors, **Resource Recovery & Biorefineries**, Aveiro, Portugal (September 2021). Poster presentation.

1. <u>Allaart, M.T.</u> 'Microbial teamwork for syngas conversion to medium-chain carboxylic acids', **CLIB C1 PhD symposium** (April 2021, virtual). Oral presentation.